NASA/TM-2001-209976

SIMBIOS Project 2000 Annual Report

Giulietta S. Fargion, SAIC General Sciences Corporation, Beltsville, Maryland
Charles R. McClain, Goddard Space Flight Center, Greenbelt, Maryland

National Aeronautics and
Space Administration

Goddard Space Flight Center
Greenbelt, Maryland 20771

Preface

The purpose of this technical report is to provide current documentation of the the Sensor Intercomparison and Merger for Biological and Interdisciplinary Oceanic Studies (SIMBIOS) Project activities, NASA Research Announcement (NRA) research status, satellite data processing, data product validation, and field calibration. This documentation is necessary to ensure that critical information is related to the scientific community and NASA management. This critical information includes the technical difficulties and challenges of validating and combining ocean color data from an array of independent satellite systems to form consistent and accurate global bio-optical time series products. This technical report is not meant as a substitute for scientific literature. Instead, it will provide a ready and responsive vehicle for the multitude of technical reports issued by an operational project.

The SIMBIOS Science Team Principal Investigators (PIs) original contributions to this report are in chapters four and above. The purpose of these contributions is to describe the current research status of the SIMBIOS-NRA-96 funded research. The contributions are published as submitted, with the exception of minor edits to correct obvious grammatical or clerical errors.

Table of Contents

Chapter 1

An Overview of SIMBIOS Project Activities and Accomplishments During FY00

Charles R. McClain
NASA Goddard Space Flight Center, Greenbelt, Maryland

Giulietta S. Fargion
SAIC General Sciences Corporation, Beltsville, Maryland

In FY00, the SIMBIOS Project brought a number of activities to fruition and laid the groundwork for new initiatives in FY01. Of particular importance was ensuring that the SIMBIOS program was renewed and a new science team selected in FY00. With SeaWiFS continuing to perform well, the Terra platform and MODIS being launched in December 1999, and several other global missions scheduled for launch (e.g., the Aqua platform with a second MODIS (2001), the ENVISAT mission with MERIS (2001), and ADEOS-II with GLI and POLDER) the first real opportunties to merge global data sets can be pursued. NASA HQ did approve a three-year continuation of the science team under an NRA and the Project Office. As it is taking some time for the MODIS team to work through the initial on-orbit processing issues, merger activities within the Project Office have been a low priority with most of the emphasis being on other program objectives which will provide a broader foundation and capabilities for working with multiple global data sets in the future. These activities and accomplishments are described below.

1. SIMBIOS Science Team Support

a. A science team meeting was held in Annapolis in late 1999, but no team meeting was held 2000. It was decided that the second science team meeting should occur in January 2001 when the new science team would be officially in place.
b. Under a SIMBIOS NRA released in late 1999, a new science team was selected. The new team consists of 19 U.S. and 12 international investigations with addition international investigations to be added as post-NRA proposals are received and accepted. The Project Office negotiated the revised statements of work and budgets required for the agreements (contracts, memoranda of understandings, etc., depending on whether the organization was a university or a government agency) with each member of the new science team. In cases of reselected investigations, bridging arrangements were executed and contract close-out procedures were executed for all contracts of the first science team. Agreements with the international team members are being initiated by NASA/HQ.
c. In June, the SIMBIOS Project management conducted team performance evaluation of all investigations. Formal evaluations of investigations funded through contracts are required by the NASA Procurement Office.
d. The Project Office provided cruise support (satellite coverage information, near-realtime data products, etc.) to 52 experiments (not all by Science Team members).

2. Satellite Data Analyses

a. Reception, processing, distribution of IRS-P3 MOS data continued operationally. The data is realtime broadcast as captured at Wallops Flight Facility using a subsystem purchased from a firm in India. Therefore, the coverage is the western North Atlantic and eastern continental U.S. and Canada. When the spacecraft is configured for MOS data collection (periods of space data collection using another instrument precludes MOS operations), the data is captured, networked to the Project Office, processed, and distributed on-line via a browse capability.
b. The calibration of the OCTS and POLDER using MOBY comparisons and the SeaWiFS atmospheric correction scheme was completed. The analyses provide consistent data products from the two instruments using common match-up and regional average value comparisons.
c. The SIMBIOS science team and Project staff played a major role in defining the algorithm improvements incorporated into the SeaWiFS reprocessing #3 (McClain et al., 2000a,b and O'Reilly et al., 2000). The SeaWiFS Project held workshops and algorithm round robins in preparation for the reprocessing in which science

team members and Project staff actively participated.

d. In October, the Korean Aerospace Research Institute (KARI) solicited the Project's assistance in calibrating the KOMPSAT/OSMI. The Project is currently working with the KOMPSAT program to gain better insight into the instrument characteristics and to obtain coverage over MOBY.
e. In November, the Project was approached by NASDA about assisting in a reprocessing of the entire OCTS GAC data set based on the SeaWiFS data quality. The Project has accepted this invitation to collaborate and is working on logistical matters with NASDA.

3. Sunphotometer Data Acquisition

a. Project supported AERONET coastal and island CIMEL sites were added at Oahu (Hawaii), the Azores, Turkey, and Argentina. Another site in Australia will be instrumented in early 2001.
b. A consistent end-to-end data processing procedure was developed for the suite of sun photometers that provide data to the Project. The different instruments include the Microtops hand-held instrument, CIMEL, the Brookhaven shadow-band radiometer, SIMBAD, and PREDE. The analysis procedures include calibration, derived product generation, quality control, archival in SeaBASS, and satellite match up analyses. The procedures are being documented in a NASA technical memorandum which will be published in early 2001.
c. The Project has two PREDE systems, one of which has a shipboard stabilizer. The Project purchased a second stabilizer so that both systems could be ship-deployed. The Project has also worked with the manufacturer on some design problems that have been encountered.

4. Bio-Optical Data Evaluation And Synthesis

a. The SeaBASS data volume continues to grow steadily as Science Team members and others submit new data sets. The sun photometer data from the coastal CIMEL sites and the shipboard observations is also being ingested into the archive. Data quality control tests are being refined and automated in order to keep up with the increasing volume of new data. In order to make SeaBASS more efficient and easier to use, the archive was redesigned and rebuilt over the past year.
b. The in situ measurement protocols were updated, expanded, and published (Fargion and Mueller, 2000). The format of this protocol manual was changed so that specific topics were included as chapters with different groups of authors for each chapter.
c. The SeaWiFS and SIMBIOS Projects have invested heavily in activities focused on the improvement of in situ radiometric data. However, questions regarding the accuracy of the pigment measurements had not been adequately addressed until this year. The SeaWiFS field program under Stan Hooker conducted a limited pigment round robin between international laboratories he has been working with. The SIMBIOS Project also conducted a joint round robin with the Office of Naval Research that included a number of U.S. laboratories. The round robin was conducted by the University of Maryland/Horn Point Environmental Laboratory. The results of both round robins have been finalized and summarized in chapter 22 and will be followed by a more detailed NASA TM publication in early 2001. The results of the SeaWiFS round robin were quite satisfactory, but the SIMBIOS round robin showed sizable errors in some pigment analyses. Thus, the SIMBIOS round robin results support the strategy implemented under the SIMBIOS NRA of having one laboratory process all the Science Team's pigment data using the latest HPLC technology.

5. Radiometric Data Quality Assurance

a. In order to monitor field instrument performance between calibrations and reduce the cost of frequent calibrations, the SeaWiFS Project commissioned NIST to design a stable field deployable source. The NIST source, the SeaWiFS Quality Monitor (SQM; Johnson et al., 1998), has proven to be extremely reliable through extensive field testing in programs such as the Atlantic Meridional Transect (AMT; Hooker and Aiken, 1998) cruises. Seed funding of commercial versions of the SQM was provided in 1996 to two companies by the SIMBIOS Project. This year, the Project purchased one system and has worked with the other company in product evaluation testing. Ultimately, the Project plans to provide funds to U.S. science team members who collect bio-optical data to purchase an SQM.
b. The SeaWiFS Project also had NIST design a portable transfer radiometer, the SeaWiFS Transfer Radiometer (SXR; Johnson et al., 1998), to be used in calibration round robins and in satellite instrument calibrations. The original SXR proved to very accurate and has been used extensively by the SeaWiFS Project. The SIMBIOS Project has assumed the responsibility of continuing the calibration round robin activity and has published the results of one experiment (Riley and Bailey, 1998). The SIMBIOS Project

purchased a copy of the SXR for future round robins, but the instrument has suffered stability problems. With much testing and interaction with the manufacturer, the problems have been resolved and the instrument has been recalibrated at NIST. This sets the stage for the next round robin experiment.

6. Outreach

a. Project staff provided technical support for MOS and OCTS processing in the SeaWiFS Data Analysis System (SeaDAS). The SIMBIOS and SeaWiFS Projects also provided system administration, software maintenance, and hardware upgrade support to the SeaDAS program.
b. From September 1999 through December 2000, the SeaWiFS and SIMBIOS Projects sent representatives to 28 national and international conferences and workshops, in addition to several SeaWiFS and MODIS workshops. In most cases, presentations were made and the SeaWiFS/SIMBIOS booth was manned at eight of the conferences.

With these accomplishments, the SIMBIOS Project is well positioned to undertake a number of new initiatives in 2001. These include, but are not limited to, the following:

- Collaborate with NASDA on the reprocessing of the OCTS GAC data set,
- Assist the KARI in the calibration and processing of the KOMPSAT/OSMI data,
- Work with the MOS science team on the use of MOS for linking the SeaWiFS with the ADEOS-I OCTS and POLDER time series,
- Assist the SeaDAS group on incorporating POLDER processing capabilities into SeaDAS,
- Work with the MODIS oceans team and Science Team members on SeaWiFS-MODIS data merger,
- Continue the development of a diagnostic ocean color data set, a recommended by members of the IOCCG,
- Design and execute the next calibration round robin experiment with the new Science Team, and
- Begin preparations for the ENVISAT/MERIS (2001) and ADEOS-II/GLI (2002) missions. The Project hosted a NASDA representative for two months in late 2000 to assist in the GLI preparations.

Finally, in September 2000, the SeaWiFS Project Office, working with other scientists and engineers at GSFC (which also hosts the SIMBIOS Project), assumed new responsibilities in assisting NASA HQ to develop a long-term program for global carbon cycle research. As a result, the Project Office has been reorganized somewhat to allow Chuck McClain to focus on the carbon initiative. Gene Feldman and Giulietta Fargion assumed additional management responsibilities for SeaWiFS and SIMBIOS, respectively, as shown in Figure 1.1. Figure 1.2 and table 1.1 provides a more detailed organization chart of the SIMBIOS Project. The SIMBIOS and SeaWiFS Projects are largely staffed by on-site contractors. The ocean color support contract under which these personnel work expired in 2000. Beginning in late 1998, Project civil service staff worked on a new procurement package for support services that was released and competed for in early 2000. As a result of the solicitation and bidding competition, with the incumbent, SAIC/General Sciences Corporation, was selected as the prime contractor. The contract is for five years, that will provide continuity of effort beyond the renewed SIMBIOS three-year program.

REFERENCES

Fargion, G. S., and J. L. Mueller, 2000: Ocean Optics for Satellite Ocean Color Sensor Validation, Revision 2, NASA/TM-2000-209966, NASA Goddard Space Flight Center, Greenbelt, MD, 184 pp.

Johnson, B. C., P.-S. Shaw, S. B. Hooker, and D. Lynch, 1998: Radiometric and engineering performance of the SeaWiFS quality monitor (SQM): a portable light source for field radiometers, *J. Atmos. Oceanic Technol.*, 5(4), 1008-1022.

Johnson, B. C., J. B. Fowler, and C. L. Cromer, 1998: The SeaWiFS Transfer Radiometer (SQM), NASA/TM-1998-206892, Vol. 1, S. B. Hooker and E. R. Firestone, eds., NASA Goddard Space Flight Center, Greenbelt, MD, 58 pp.

Hooker, S. B., and J. Aiken, 1998: Calibration evaluation and radiometric testing of field radiometers with the SeaWiFS quality monitor (SQM), *J. Atmos. Oceanic Technol.*, 5(4), 995-1007.

McClain, C. R. and others, 2000a: SeaWiFS Postlaunch Calibration and Validation Analyses, Part 1, NASA/TM-2000-206892, Vol. 9., S. B. Hooker and E. R. Firestone (eds.), NASA Goddard Space Flight Center, Greenbelt, Maryland, 82 pp.

McClain, C. R. and others, 2000b: SeaWiFS Postlaunch Calibration and Validation Analyses, Part 2, NASA/TM-2000-206892, Vol. 10., S. B. Hooker and E. R. Firestone (eds.), NASA Goddard Space Flight Center, Greenbelt, Maryland, 57 pp.

O'Reilly, J. E. and others, 2000: SeaWiFS Postlaunch Calibration and Validation Analyses, Part 3, NASA/TM-2000-206892, Vol. 11, S. B. Hooker and E. R. Firestone (eds.), NASA Goddard Space Flight Center, Greenbelt, Maryland, 49 pp.

Riley, T., and S. Bailey, 1998: The sixth SeaWiFS/SIMBIOS intercalibration round robin experiment (SIRREX-6), August-December 1997, NASA/TM-1998-206878, NASA Goddard Space Flight Center, Greenbelt, Maryland, 26 pp.

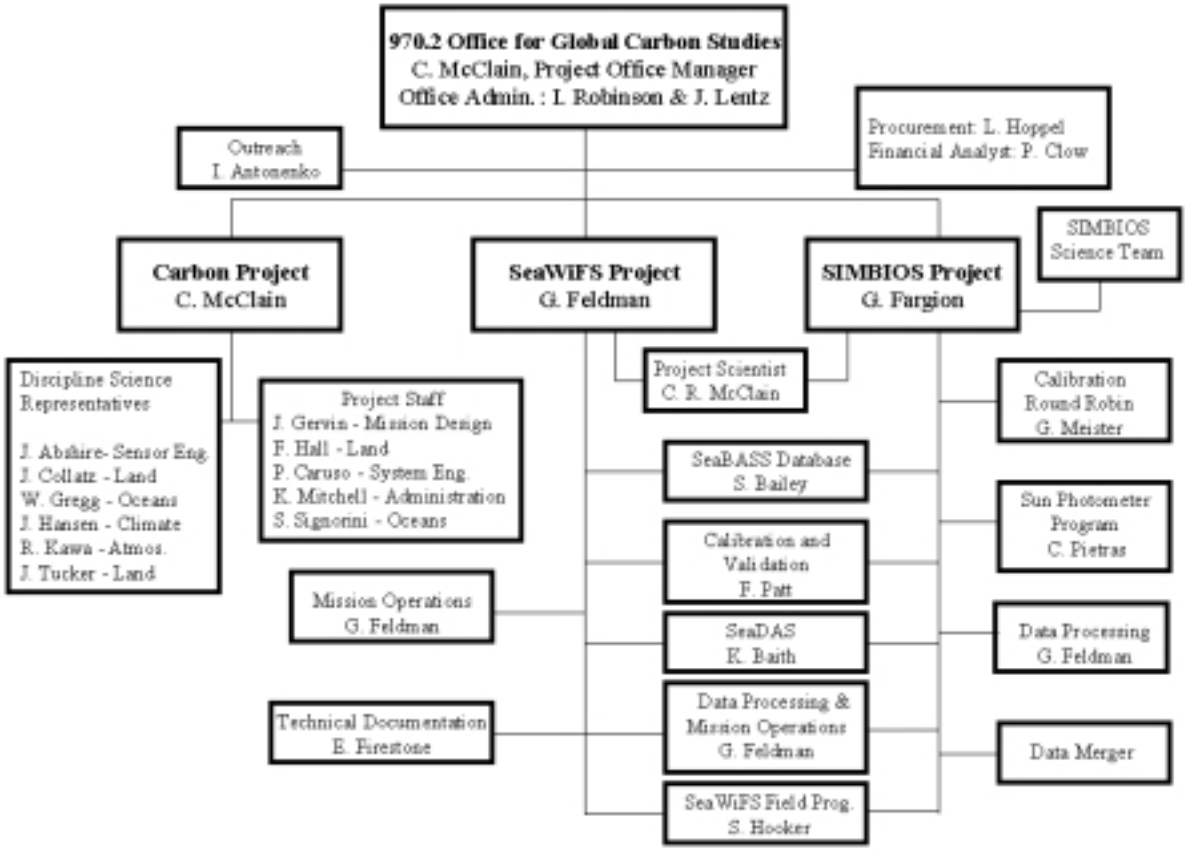

Figure 1.1 Organization chart of the Office for Global Carbon Studies.

Table 1.1 SIMBIOS Project Personnel

Ewa Ainsworth	SAIC General Sciences Corporation
Irene Antonenko*	SAIC General Sciences Corporation
Sean Bailey*	FutureTech Corporation
Robert Barnes *	SAIC General Sciences Corporation
Patty Clow *	NASA
Giulietta Fargion	SAIC General Sciences Corporation
Gene Feldman *	NASA
Bryan Franz *	SAIC General Sciences Corporation
Joel Gales*	FutureTech Corporation
Lynne Hoppel *	NASA
Kirk Knobelspiesse*	SSAI Corporation
Sung Lee *	SAIC General Sciences Corporation
Kathy Lingerfelt*	NASA
Charles McClain *	NASA
Gerhard Meister	FutureTech Corporation
Kevin Miller*	FutureTech Corporation
Fred Patt *	SAIC General Sciences Corporation
Christophe Pietras	SAIC General Sciences Corporation
India Robinson *	NASA
Paul Smith *	SAIC General Sciences Corporation
Judy Stubblefield*	SAIC General Sciences Corporation
Tamara Tucker *	SAIC General Sciences Corporation
Jeremy Werdell*	SSAI Corporation
Bill Woodford*	FutureTech Corporation

* shared with SeaWiFS Project

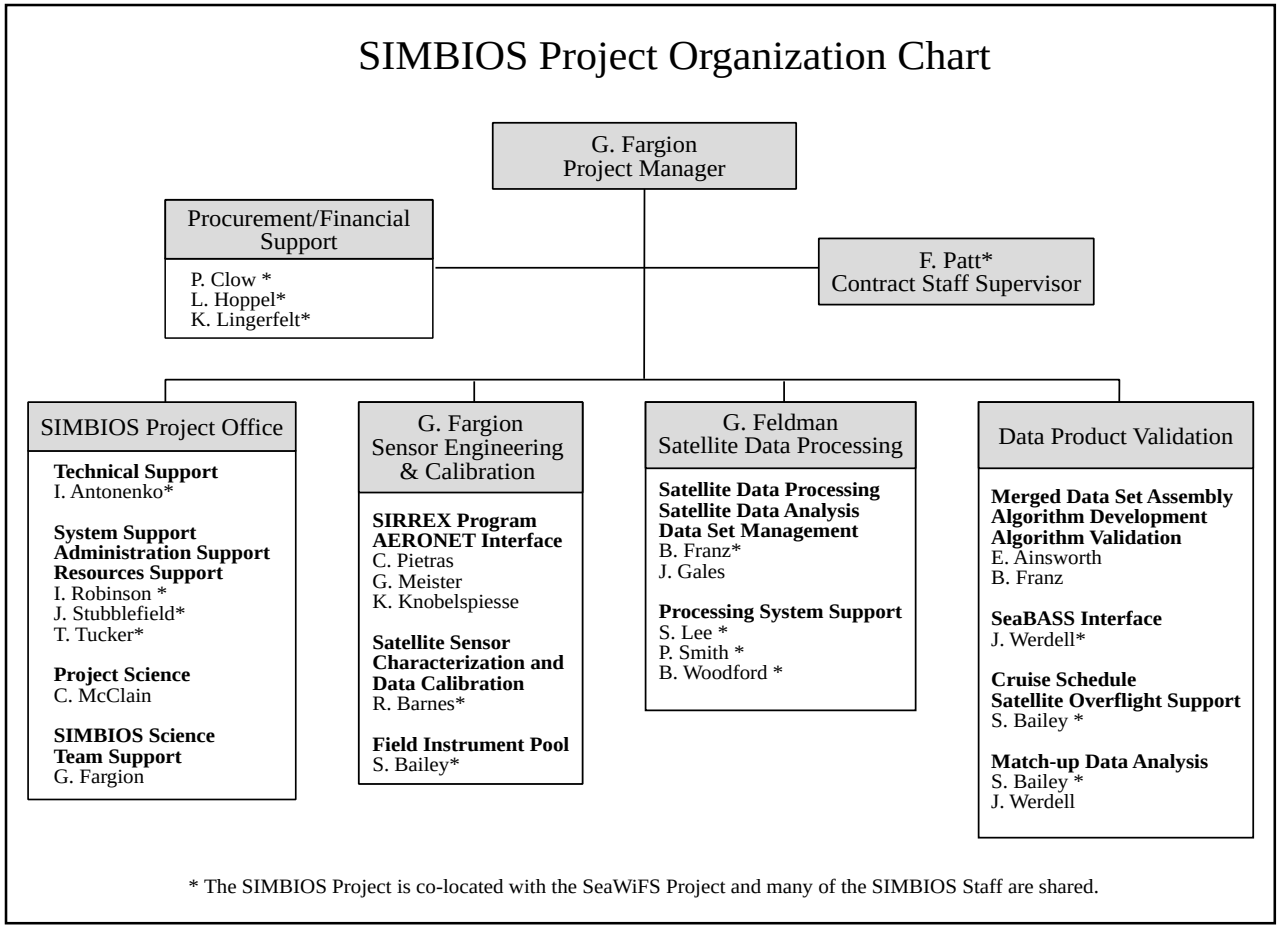

Figure 1.2 SIMBIOS Project organization chart

Chapter 2

SIMBIOS: Science Team and Contracts

Giulietta S. Fargion

SAIC General Sciences Corporation, Beltsville, Maryland

2.1 SCIENCE TEAM

The Science Team is selected through NASA Research Announcement (NRA). Presently NASA has had two NRA's, in 1996 and 1999. NASA HQ manages the process of team selection, but the Goddard Space Flight Center (GSFC) NASA Procurement Office handles the team contracts, work statements and, if necessary, budget negotiations. The Project funds numerous US investigators and collaborates with several international investigators, space agencies (e.g., NASDA, CNES, KARI, etc.) and international organizations (e.g., IOCCG, JRC). US investigators under contract provide *in situ* atmospheric and bio-optical data sets, and develop algorithms and methodologies for data merger schemes. NASA GSFC Procurement requires formal evaluations for all contracts at the end of each contract year. These evaluations are to go into a database and are shared with the PI's institution or upper management.

The locations of specific SIMBIOS team investigations (i.e., NRA-96 and NRA-99) are shown in Figures 2.1 and 2.2. The international ocean color community response for the NRA-99 was overwhelming, with a total of 75 PI's attempting to collaborate with the Project group in twelve proposals. The twelve international proposals cover topics ranging from protocols, calibration-validation activities, atmospheric-biological algorithms, and data merging.

The SIMBIOS Science Team (NRA-96) meetings were held in August 1997 at Solomons Island (Maryland), in September 1998 at La Jolla (California) and in September 1999 at Annapolis (Maryland). Meanwhile, the SIMBIOS Science Team's (NRA-99) first meeting will be held in January 2001 at GSFC in Greenbelt, Maryland.

In general, all Science Team members, US and international, were in attendance or were represented by one of their staff. Also, the IOCCG and MODIS Teams were invited, and most attended or sent representatives. During each year the Project Office has fostered international collaborations by hosting visiting scientists at GSFC. These visits lasted from one week to several months. For international participants, the Project provided partial or as-needed travel support to team meetings or to collaborate with the project on specific topics such as calibration, and product evaluations. Chapters 4 to 23 contain the individual PI's contributions of the first SIMBIOS team (i.e., NRA-96) and describe the funded research topics, field studies activities, and results of concluded research. These chapters are reproduced as submitted with minimal editing by thr Project Office.

2.2 CONTRACT OVERVIEW

The third-year SIMBIOS NRA-96 contracts ended in the July-September 2000 time frame. Close-out procedures were executed for all contracts of the first science team (NRA-96). The Project granted no-cost extensions to all the PIs that requested it.

Due to NASA HQ funding changes for the new SIMBIOS Science Team (NRA-99), the Project Office had to renegotiate all the statements of work and prepare new budgets for each member of the new science team. The renegotiated agreements where then formalized in contracts or memoranda of understanding, depending on whether the organization was a university or a government agency, respectively. In cases where the reselected investigations needed bridging arrangements, the Procurement Office executed contract modifications. The SIMBIOS Project provided bridging funds from the end date of the previous contract to the start date of the new contract (projected date was December 2000). SIMBIOS key contract and project personnel to work on contracts are shown in Table 2.1.

Agreements with the international team members have being initiated by NASA HQ and are presently administered by Dr. John Marra, Program Manager for Ocean Biogeochemistry. These agreements should be in place by Spring 2001.

Table 2.1 Contract evaluation key personnel

Contracting Officer:	Lynne Hoppel
Contracting Assistant:	Kathy Lingerfelt
Resource/Financial Officer:	Patty Clow
Manager , SIMBIOS Project:	Giulietta Fargion
Manager, Office for Global Carbon Studies:	Charles McClain

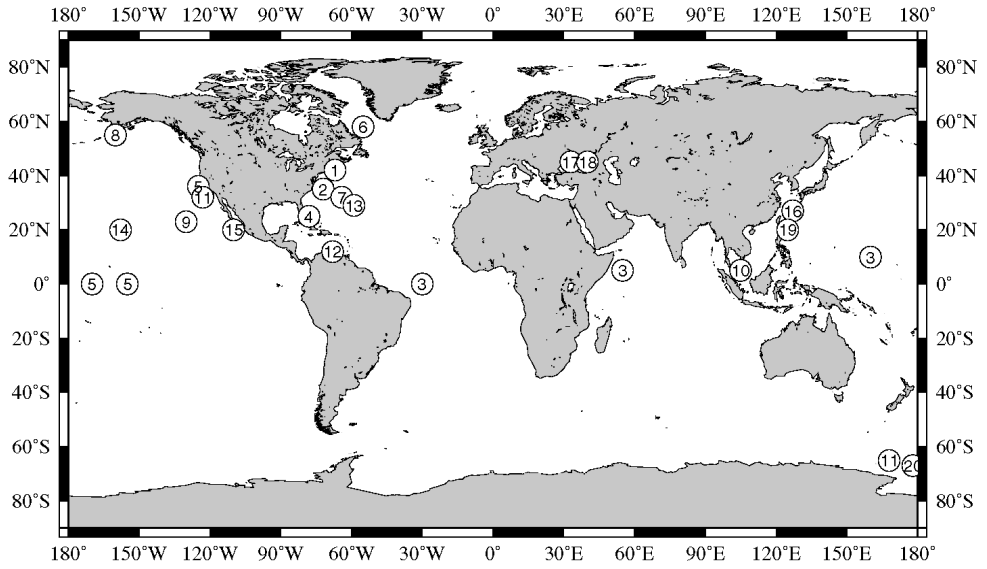

Figure 2.1. Global distribution of the NRA-96 selected SIMBIOS studies. United States (field): (1) Balch; (2) Brown/Brock; (3) Capone/Carpenter/Subramaniam and Miller; (4) Carder and Green; (5) Chavez; (6) Cota; (7) Dickey; (8) Eslinger; (9) Frouin; (10) Miller; (11) Mitchell and Green; (12) Müller-Karger; (13) Siegel; (14) Porter (15) Zaneveld and Mueller. United States (theoretical): Flatau; Siegel and Stamnes/Chen. International: He; Korotaev; Kopelevich; and Li.

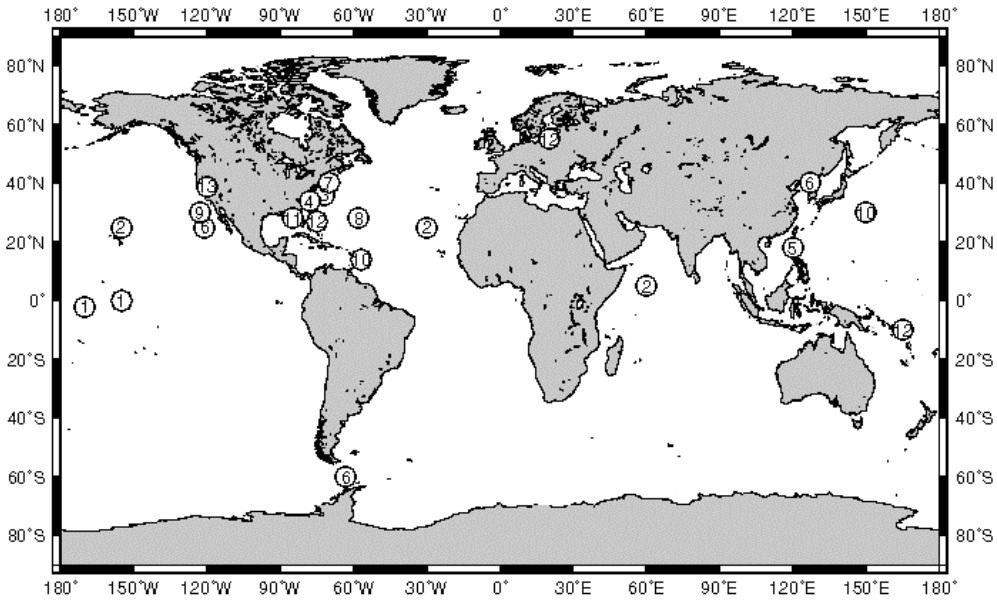

Figure 2.2. Global distribution of the NRA-99 selected SIMBIOS studies. United States (field): (1) Chavez; (2) Frouin; (3) Gao; (4) Harding; (5) Miller; (6) Mitchell; (7) Morrison; (8) Nelson; (9) Siegel; (10) Spinhirne; (11) Stumpf; (12) Subramaniam; (13) Zalewski. United States (theoretical, protocols, or team support): Gregg; Hooker; Maritorena; Mueller; Trees and Wang. International: Bohm; Zibordi; Fougnie; Deschamps; Antoine; Kopelevich; Ishizaka; Fukushima; Chen; Li; He and Tang.

Chapter 3

SIMBIOS Project Data Processing and Analysis Results

Ewa Ainsworth, Giulietta Fargion, Bryan Franz, Christophe Pietras and Paul Smith
SAIC General Sciences Corporation, Beltsville, Maryland

Sean Bailey, Joel Gales and Gerhard Meister
FutureTech Corporation, Greenbelt, Maryland

Kirk Knobelspiesse and Jeremy Werdell
Science Systems and Applications Inc., Greenbelt, Maryland

Menghua Wang
University of Maryland Baltimore County, Baltimore, Maryland

Charles McClain and Gene Feldman
NASA Goddard Space Flight Center, Greenbelt, Maryland

3.1 INTRODUCTION

The SIMBIOS Project is concerned with ocean color satellite sensor data intercomparison and merger for biological and interdisciplinary studies of the global oceans. Imagery from different ocean color sensors can now be processed by a single software package using the same algorithms, adjusted by different sensor spectral characteristics, and the same ancillary meteorological and environmental data. This enables cross-comparison and validation of the data derived from satellite sensors and, consequently, creates continuity in ocean color information on both the temporal and spatial scale. The next step in this process is the integration of *in situ* ocean and atmospheric parameters to enable cross-validation and further refinement of the ocean color methodology. The SIMBIOS Project Office accomplishments during 2000 year are summarized under (a) satellite data processing, (b) data product validation, (c) SeaBASS database, (d) supporting services, (e) sun photometers and calibration activities and (f) calibration round robins. These accomplishments are described below.

3.2 SATELLITE DATA PROCESSING

3.2.1 MOS: Data Collection, Processing, and Distribution

Since February 1999, the SIMBIOS project has been operating a receiving station at NASA's Wallops Flight Facility (WFF) to acquire data from the German Modular Optoelectronic Scanner (MOS) onboard the Indian IRS-P3 spacecraft. When a pass is acquired at Wallops, the raw files are transferred to the SIMBIOS project at NASA's GSFC via an automated FTP process. The raw files are then converted to Level-0 format through a software package provided by the Indian Space Research Organization (ISRO). The resulting Level-0 files are made available to German Remote Sensing Data Centre (DLR-DFD) for archive and distribution. In addition, the SIMBIOS project processes the data through Level-1B using the standard software provided by the German Institute for Space Sensor Technology (DLR-ISST) (Neumann et al., 1995). All data processed by the SIMBIOS project is made available through the MOS browse system at SIMBIOS web page. The Level-1B data can be processed to Level-2 using a SIMBIOS-developed software tool that applies the standard SeaWiFS algorithms of Gordon and Wang (1994). This Multi-Sensor Level-1 to Level-2 software (MSL12) is currently capable of processing data from SeaWiFS, MOS, OCTS, and POLDER using identical algorithms, and it has been applied in previous studies of MOS-SeaWiFS cross-calibration (Wang and Franz, 1999).

MOS Intercomparison with SeaWiFS

The SIMBIOS project has recently developed a prototype application to automate the sensor-to-sensor intercomparison process using the online archive of MOS data from Wallops and the SeaWiFS HRPT data from the GSFC groundstation. MOS scenes are first reprocessed to

Level-1B to ensure the latest calibration has been applied, and then the meta-data of each 200 x 200 km scene segment is examined to determine the observation time, geographic area, and percentage of visible ocean pixels. If the scene segment contains at least 80% ocean pixels and no more than 20% cloud pixels, the process proceeds to perform a database search for potential SeaWiFS file matchups. Once a valid SeaWiFS match is located, the area corresponding to the MOS scene segment is identified in terms of pixel and scan limits within the SeaWiFS scene, and both subscenes are processed to Level-2 using MSl12. Some sample results from this automated analysis are shown in Figure 3.1. The histograms show the distribution of SeaWiFS (solid line) and MOS (dashed line) water-leaving reflectance within each match-up scene, for the spectral channels near 443, 490, and 510 nm. The selected scenes represent various locations off the U.S. East Coast, for various times throughout years 1999 and 2000. These results demonstrate that the Gordan and Wang (1994) atmospheric correction scheme, in conjunction with a sensor cross-calibration, can provide comparable water-leaving reflectance retrievals from two independent observations from different sensors at different times of day. With the recent catastrophic failure of the MOS onboard calibrator unit, the SIMBIOS Project's ability to monitor the relative calibration with SeaWiFS may prove to be of value for future MOS calibration control.

Future Activities

We have already studied the relative differences between MOS and SeaWiFS AOP retrievals when applying standard Gordon and Wang techniques to both sensors (Wang and Franz, 1999), and we used those results to develop a relative calibration for MOS. Since that study, we have used our archive of SeaWiFS and MOS data from Wallops to monitor the relative stability of the AOP retrievals between the two sensors, and they are generally in good agreement. The SeaWiFS calibration is tied to the *in situ* data from the MOBY bouy (Eplee et al., 2000). Using the same techniques and the same atmospheric correction algorithms, we have also developed a vicarious calibration between OCTS and MOBY. We now plan to complete the circle and determine the relative agreement between OCTS and MOS, thereby placing some confidence level on the relative comparability of OCTS and SeaWiFS. This information is important to temporally merge the two global missions.

3.2.2. OCTS

At the request of, and in collaboration with NASDA, we expect to acquire and process the entire OCTS GAC archive from Level-1A through Level-3. Level-2 processing will be performed using MSl12, with algorithms and output formats nearly identical to standard SeaWiFS processing, and Level-3 processing will be performed using standard SeaWiFS space and time binning software. Most of the science processing software has already been updated and generalized for this purpose, and verification of the Level-1A to Level-1B GAC processing is in progress. Negotiations are underway with the Goddard DAAC to archive and distribute the OCTS GAC products.

3.2.3 Data Processing

Both OCTS and POLDER Level-1B data can now be processed to Level-2 oceanic and atmospheric products using the MSL12 software. In addition, SIMBIOS project has developed a capability in MSL12 to process the OCTS Level-0 to Level-1B data. The OCTS Level-1B data processed with the MSL12 are usually in good agreement with the NASDA standard Level-1B product. However, there are some differences between satellite navigation algorithms used in the two data processing protocols. For OCTS bands 1-8, the radiance differences in a pixel by pixel comparison between the two data processing protocols are typically 0.54%, 0.53%, 0.54%, 0.85%, 1.00%, 1.62%, 2.20%, and 2.67%, respectively. These differences are primarily due to improved navigation routines used in the MSL12. Based on a study by Wang (1999), the MSL12 software is the implementation of the same standard SeaWiFS atmospheric correction algorithm (Gordon and Wang, 1994b) applyed to the OCTS, POLDER, and other ocean color sensors (e.g., MOS). There are some major improvements in MSL12 for the OCTS and POLDER data processing concurrent with changes in processing algorithms for the SeaWiFS 3rd data reprocessing in May 2000 (Wang, 2000b). Some specific atmospheric correction algorithm improvements include:

- Improved Rayleigh lookup tables, in which the Rayleigh (air molecule) scattering radiance is a function of the sea surface wind speed, were generated and implemented in the data processing system (Wang, 2000a) for OCTS, POLDER, and MOS.
- A sun glint contamination correction algorithm was developed and implemented in MSL12 (Wang and Bailey, 2000).
- An iterative correction algorithm accounting for ocean radiance contributions at wavelengths 765 and 865 nm was developed and implemented in the data processing step (Siegel et al., 2000).
- A correction algorithm for the sensor spectral band-pass effects on the derived water-leaving radiances for SeaWiFS (Wang et al., 2001) was developed. Similar algorithms for both OCTS and POLDER were also implemented in MSL12. Corrections of the sensor spectral band-pass effects are necessary in order to have meaningful Level-2 product comparisons derived from two different sensors, e.g., OCTS and POLDER.
- Correction of the ocean whitecap radiance contributions (Gordon and Wang, 1994a) has been updated (Wang, 2000b) with some current in situ measurements (Frouin et al., 1996; Moore et al., 1998; Moore et al., 2000).

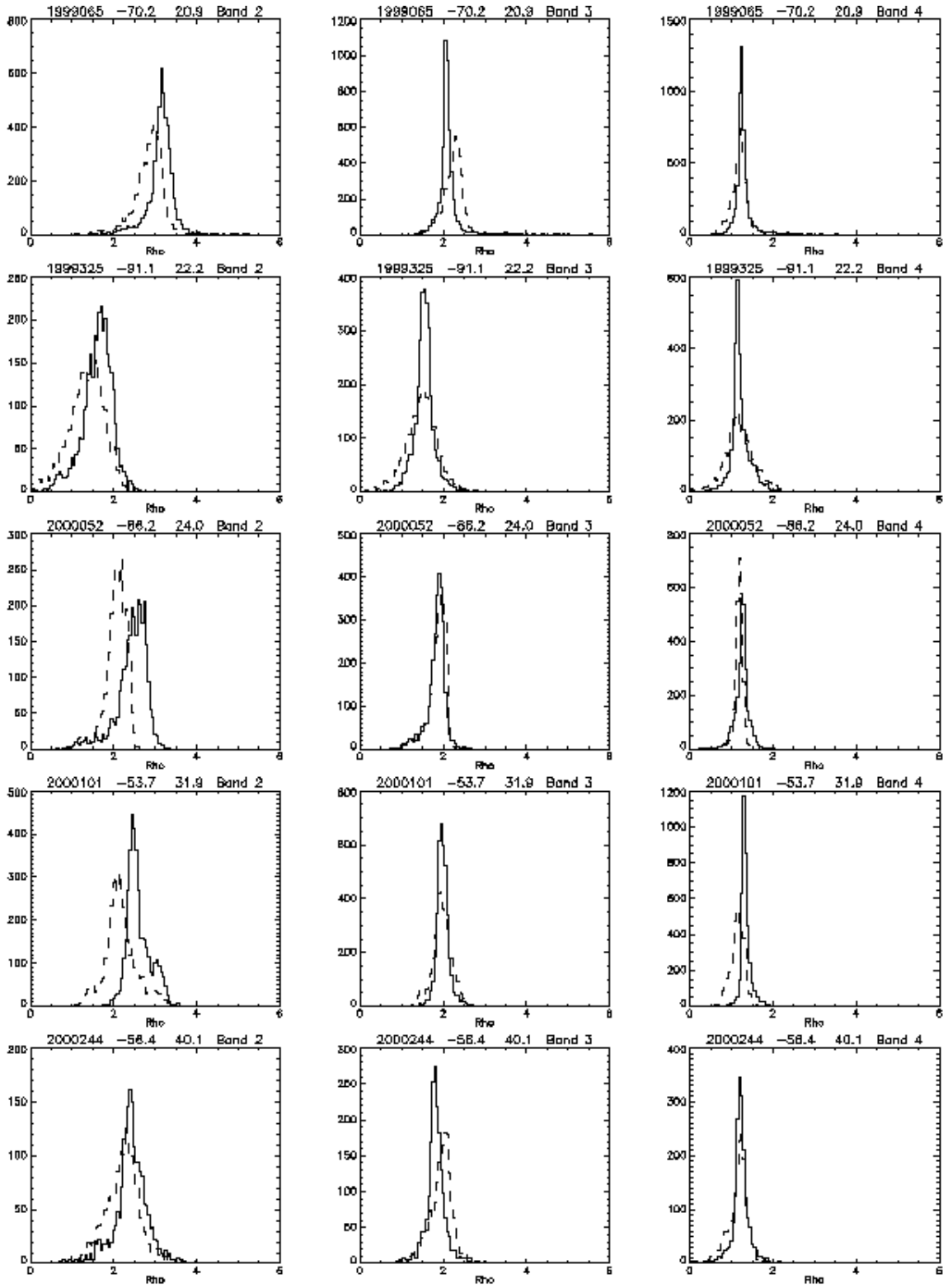

Figure 3.1. Frequency distributions of percentage water leaving reflectance retrieved for both SeaWiFS (solid line) and MOS (dashed line). Panel titles indicate year, day, longitude, latitude, and SeaWiFS band number.

- The current 12 aerosol models used in the atmospheric correction are: Oceanic RH=99%, Maritime RH=50%, 70%, 90%, and 99%, Coastal RH=50%, 70%, 90%, and 99%, and Tropospheric RH=50%, 90%, and 99% (Wang, 2000b).

The updated MSL12 software significantly improves derived ocean and atmospheric products.

3.3 PRODUCT VALIDATION

We are continuing our efforts in comparing and analyzing ocean optical property data derived from both OCTS and POLDER. One of the main objectives with this effort is to understand and develop methodologies for meaningful comparison and possible merging of data products from multiple ocean color missions. In this section, we briefly outline some major improvements in the OCTS and POLDER data processing, the procedure of the sensor vicarious calibration applied to both OCTS and POLDER using the in situ MOBY data, and present and discuss some comparison results derived from OCTS and POLDER measurements.

Sensor Vicarious Calibration

It is well known that, for ocean color remote sensing, an on-orbit vicarious calibration of sensor and algorithms is necessary (Gordon, 1995). The vicarious calibration technique has been successfully applied to SeaWiFS (Eplee and McClain, 2000; Robinson and Wang, 2000) as well as for the MOS and SeaWiFS product comparisons (Wang and Franz, 2000). A vicarious calibration for OCTS and POLDER using the *in situ* measurements from the Marine Optical Bouy (MOBY) (Clark et al., 1997) was carried out. First, 765 nm band vicarious calibration for OCTS and POLDER was conducted using a similar method as that applied to SeaWiFS (Robinson and Wang, 2000). Next, with the derived 765 nm gain coefficient, the MOBY *in situ* measurements were used for the calibration of visible bands (Eplee and McClain, 2000). This coefficient is used to calibrate the OCTS and POLDER visible bands such that the derived normalized water-leaving radainces are equivalent to the *in situ* measurements. The MOBY site has stable clear-ocean waters and is usually prevailed with maritime aerosols and clear atmosphere. The MOBY program has therefore been providing consistently high quality, clear-ocean optical data. Five *in situ* measurements on Nov. 26, 1996, Jan. 13, 1997, Jan. 17, 1997, Feb. 16, 1997, and Feb. 23, 1997 were used. Table 3.1 provides the derived gain coefficients (except 670 nm band) for OCTS and POLDER. We are currently in the process of finalizing the gain coefficients for the 670 nm band.

Matchup Analyses

Reprocessing of the OCTS *in situ* matchups to data taken from the SeaBASS database was performed. Matchup data from Wallops Level-0 data and from Level-1B data files supplied to the SIMBIOS Project by NASDA/EORC were processed to Level-2 using MSL12 and the vicarious gain coefficients used to process the Wallops data set. Therefore, there are two OCTS data sets processed to Level-2. Files in the GSFC Wallops archive that matched *in situ* data points were processed from Level-0 (to Level-1B) to Level-2, while Level-1B data files supplied to the SIMBIOS Project by NASDA/EORC were processed to Level-2. The calibration gain coefficients in Table 3.1 were used for both data sets. The CNES has kindly provided the SIMBIOS project with POLDER Level-1B data corresponding to the SeaBASS database. For a given location (scene), POLDER can acquire as many as fourteen near-contemporaneous measurements. With the POLDER gain coefficients as in Table 3.1, the normalized water-leaving radiances at the POLDER spectral bands were derived from Level-1B data using the MSL12.

Table 3.1. The derived vicarious gain coefficients for OCTS and POLDER spectral bands

Wavelength	**Vicarious Gain Coefficient**	
(nm)	OCTS	POLDER
412	1.12426	—
443	1.01539	1.06465
490	0.95084	1.02350
520	1.01784	—
565	1.03255	0.97541
765	0.92093	1.02946
865	0.89000	1.00000

However, it was noted that, for a given scene, the POLDER derived normalized water-leaving radiances sometimes have high variations with various POLDER viewing directions. Therefore, we used an averaging scheme to eliminate the high variation points. For a given location, the derived normalized water-leaving radiances from all possible POLDER viewing directions are first averaged. Data points which are within 50% variation in the first averaged value (i.e., 0.5-1.5 of the average value) are then used to derive the final mean value and considered as the POLDER derived normalized water-leaving radiances for the scene. Figure 3.2 (a)-(c) provide matchup results for the OCTS and POLDER. Fig. 3.2 (a) and 3.2 (b) are matchup results derived from OCTS NASDA Level-1B and Wallops Level-0 data, while Fig. 3.2 (d) shows results derived from POLDER CNES Level-1B data. Each plot also gives a linear fit coefficient of slope, intercept (Int), and the correlation coefficient (R). Note that the perfect match corresponds to value of slope of 1, intercept of 0, and the correlation coefficient of 1.

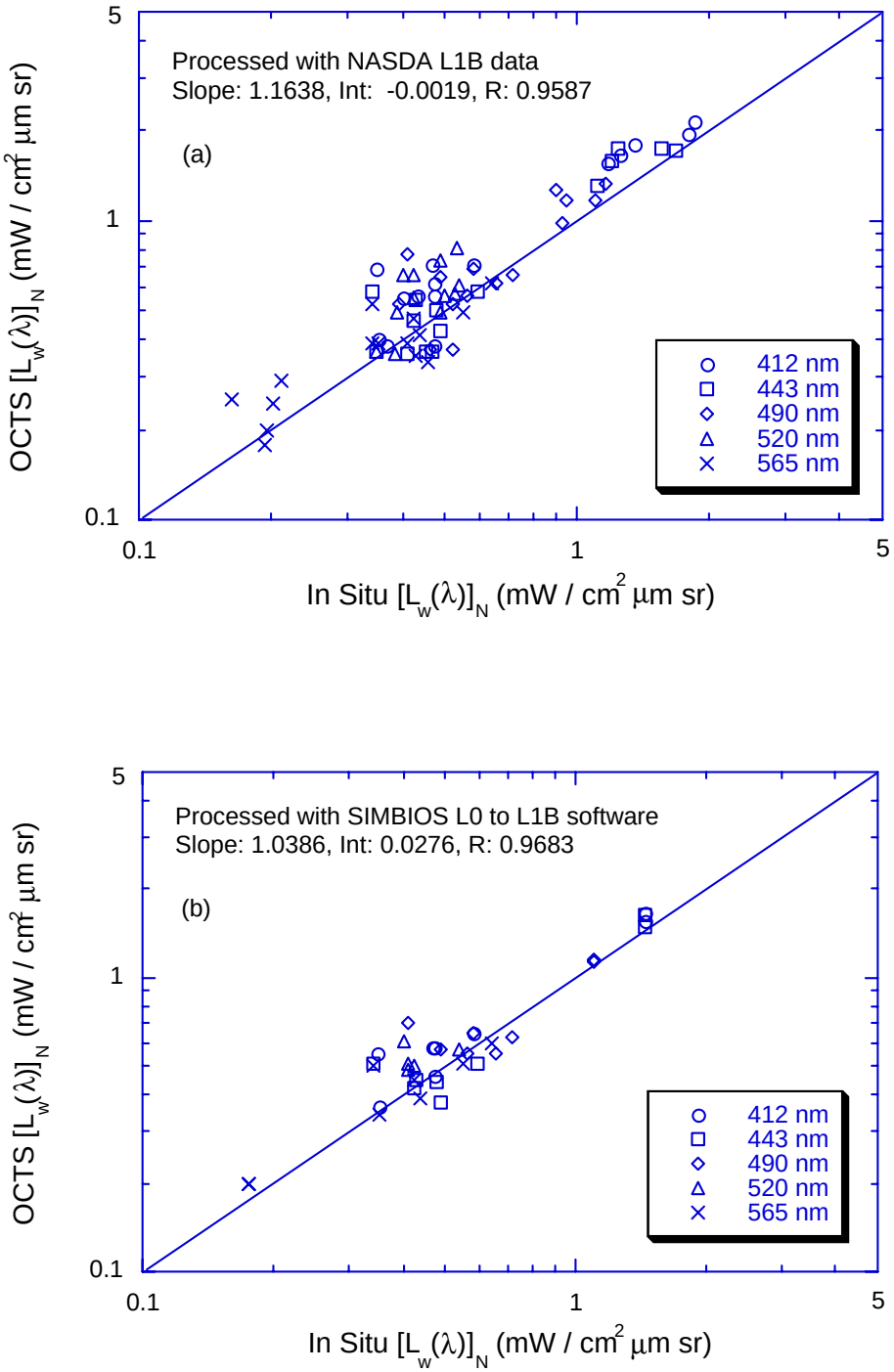

Figure 3.2 Sensor-derived normalized water-leaving radiances from (a) OCTS with NASDA Level-1B data; (b) OCTS with Wallops Level-0 data.

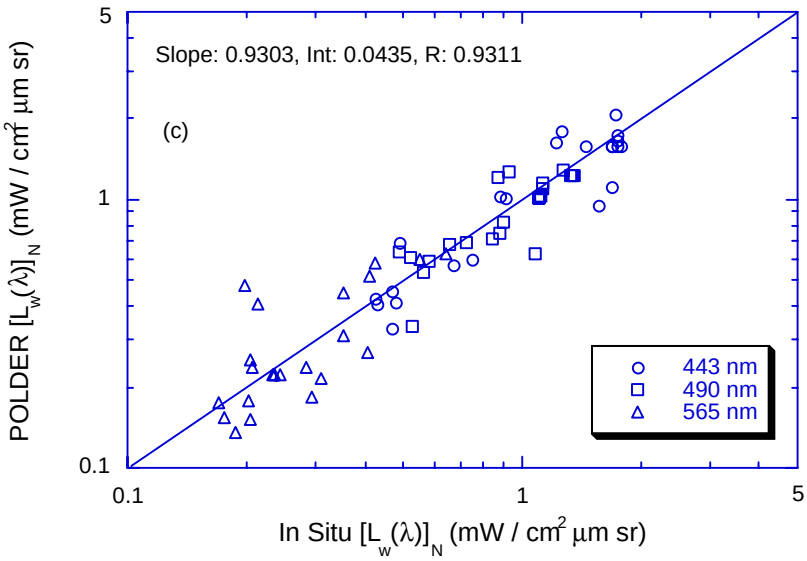

Figure 3.2 Sensor-derived normalized water-leaving radiances from (c) POLDER CNES Level-1B data compared with the in situ measurements.

3.4 SEABASS INTERFACE

The SIMBIOS Project maintains the SeaWiFS Bio-optical Archive and Storage System (SeaBASS) as an archive for *in situ* products used in scientific analyses (e.g. product verification and bio-optical algorithm development). Stored data include measurements of water-leaving radiance, chlorophyl *a*, and other related optical and pigment measurements collected on ships, moorings, and drifters. Additional information on SeaBASS is provided in Werdell et al. (2000) and Hooker et al. (1994). A current description of the SeaBASS system is also available via the World Wide Web at http://seabass.gsfc.nasa.gov.

SeaBASS contains data from over 500 cruises, encompassing more than 10,000 data files. Currently, data are archived as simple, flat (two-dimensional) ASCII text with standard metadata headers to fully define each file. The headers contain information on date, time, location, investigators involved, parameters collected, units, and other related descriptive information. The SIMBIOS Project designed the format to ensure that data files were simple, yet comprehensive, globally compatible among different computer platforms, and effortlessly ingested into the database. Specific information and examples of the data format may be referenced from the SeaBASS web site at http://seabass.gsfc.nasa.gov/seabass_submit.html.

The data format has not changed significantly during the past year of the SIMBIOS effort. Three metadata headers were added: (1) 'measurement_depth' is the depth at which discrete data were collected (e.g. bottle samples, and moored and buoy data); (2) 'water_depth' is the bottom depth at the site where data were collected; and (3) 'secchi_depth' is the secchi depth at the site where data were collected. Two metadata headers were made optional (i.e. they are no longer required): (1) 'parameters' and (2) 'original_file_name'. A list and description of each metadata header is available at http://seabass.gsfc.nasa.gov/seabass_header.html.

The most significant change to the data format was the standardization of the names and units used in the 'fields' and 'units' headers. Note that all data are accepted, but common data types (e.g. AOP's, IOP's, pigments) are now required to be abbreviated in a particular way and presented in specific units. For example, (1) a column of upwelling radiance data collected at 412.3 nm is required to be listed as 'Lu412.3' with units of 'uW/cm^2/nm/sr'; or, (2) a column of HPLC-derived chlorophyll *a* data is required to be listed as 'chl_a' with units of 'mg/m^3'. A current list of standard SeaBASS field names and units is available via the web at http://seabass.gsfc.nasa.gov/cgi-bin/stdfields.cgi.

Protocols for format checking and data submission have not been altered over the past year. The SIMBIOS Project currently uses a PERL script feedback program known as FCHECK to maintain the standard format for incoming data files. Contributing researchers may test their data for compatibility with SeaBASS from any platform by electronically mailing their files to fcheck@seabass.gsfc.nasa.gov. Once the data files meet SeaBASS format requirements, the contributor may send their data files and related documents (e.g. cruise reports and calibration files) to the SeaBASS Admistrator via file transfer protocol (FTP). The Administrator stores the files in their

appropriate location in the archive and ingests the files into the SeaBASS database. Password-secure web access to the data files, the database, and supporting documentation is available at the SeaBASS web site. For additional information on format checking and data security issues refer to the SIMBIOS Project 1998 Annual Report (McClain and Fargion, 1999) and the SeaBASS web site.

The procedures for water-leaving radiance, normalized water-leaving radiance, and chlorophyll *a* match-up analyses changed little during the past year of the SIMBIOS effort. Modifications were made to the processing software concurrently with the third reprocessing of SeaWiFS data. In particular, the Level 2 processing code was changed from ANLY (l2gen) to the Multisensor Level-1 to -2 (MSL12) program. Additional information on the match-up analysis and protocols may be found in the SeaWiFS Postlaunch Technical Report Series Volume 10 (Bailey et al., 2000).

The architecture of the SeaBASS system will continue to undergo major changes in the upcoming year. In the past year of the SIMBIOS effort, a new SeaBASS relational database was designed and built with the following modifications: (1) an increase in the the number of tables to improved data normalization; (2) a reconfigured system to take advantage of multiple processors and increased physical storage space; (3) the development of software for internal SIMBIOS Project Office accounting purposes; and (4) the ability to store all data and metadata in the relational database. The most visible change to the user community will be how SeaBASS handles queries via the World Wide Web. Currently, SeaBASS database queries return a list of files that contain data or metadata meeting the query criteria. Using the new database, users may query for not only a list of files, but also the physical data values meeting the query criteria. Search engines taking advantage of this feature will be available to the SeaBASS user community for pigment and atmospheric data in Spring 2001.

3.5 SUPPORT SERVICES

In an effort to improve the quality and quantity of calibration and validation data sets, the SIMBIOS Project offers several support services to field investigators. These services include; scheduling of on-board LAC recording for SeaWiFS; overflight predictions for operational sensors (currently SeaWiFS, OCTS, MOS-B, MODIS, OCI, and OCM); near real time SeaWiFS imagery for cruise locations; and sunphotometer instrumentation from a pool of project-owned instruments. These services may be requested via the World Wide Web at http://simbios.gsfc.nasa.gov. In return for these services, the SIMBIOS Project requests that the field investigators provide in situ validation data to the Project's bio-optical archive, SeaBASS. Since January of 2000, the SIMBIOS Project has supported 52 cruises (Table 3.2).

Scheduling SeaWiFS On-board LAC Recording

Since much of the world's oceans are not covered by a SeaWiFS HRPT station, high-resolution data may be recorded onboard the SeaWiFS sensor. As a service to the scientific community, the SIMBIOS Project in conjunction with the SeaWiFS Project can schedule SeaWiFS onboard LAC for cruises that occur outside HRPT coverage. SeaWiFS has the ability to record a maximum of 10 minutes of high-resolution data per downlink. Typically, a 30-second interval is allotted for LAC target, which corresponds to 180 scan lines or approximately 200 km along track at nadir. Detailed information on LAC scheduling is available on the SIMBIOS web site.

Overflight Predictions for Operational Sensors

For calibration and validation purposes, in situ measurements should be made as close to the sensor overflight time as is possible. To aid investigators in determining when sampling should occur, the SIMBIOS Project offers overflight predictions for all operational ocean color remote sensors. Currently, the sensors supported are SeaWiFS, MOS-B and OCI, MODIS, and OCM. Detailed information on overflight predictions is available on the SIMBIOS web site.

Near Real Time SeaWiFS Imagery

In addition to providing predictions for satellite overflight times, the SIMBIOS Project offers near real time imagery of the operational SeaWiFS products in JPEG or GIF format to cruises at sea. 'True color' images are in JPEG format, all other products are in GIF format. These images provide field investigators with additional information with which they may maximize *in situ* sampling of transient oceanographic features. The default specifications for the images provided include:

- available LAC, HRPT, and GAC;
- chlorophyll-a and pseudo-true color images;
- 2-degree box about a designated location or the entire designated region;
- image width of 600 pixels;
- minimum percent valid chlorophyll pixels: 5%;
- images may be customized to best accommodate individual investigator needs.

Detailed information on near real-time imagery is available on the SIMBIOS web site.

Table 3.2 SIMBIOS supported cruises with services provided.

Cruise	Principal Investigator	Begin Date	End Date	On-board LAC	Overflight Predictions	Near Real Time images	Instrument Pool
CalCOFI_0100	Greg Mitchell	1/6/00	1/28/00		•		
Southern_Ocean	Greg Mitchell	1/15/00	3/14/00		•	•	•
VOG_1	John N. Porter	1/23/00	1/30/00		•		
Bahamas_Experiment	Stanford Hooker	2/10/00	3/3/00	•	•	•	
AMLR_99_00	Mati Kahru	2/18/00	3/16/00		•		
NFRDI_0002	Mati Kahru	2/19/00	3/3/00		•		
Modycot	Jean-Noel Druon	2/22/00	3/11/00			•	
ChesLight2000	Glenn Cota	2/23/00	3/31/00		•		
EcoHab_FLT_GoM	Bob Swift	3/1/00	3/9/00		•		
Optics_Eilat	Emmanuel Boss	3/10/00	5/7/00		•	•	
MODIS_MAB_FLT	Bob Swift	3/10/00	3/24/00		•		
Venice_Tower_Mar00	Jean-Francois Berthon	3/13/00	3/24/00		•		
TC00_04	Carrie Leonard	3/20/00	4/29/00			•	
Florida_Coast	Stanford Hooker	3/20/00	4/30/00		•	•	
MODIS_SAB_FLT	Bob Swift	3/25/00	3/27/00		•		
Projeto_Revizee	Aurea Ciotti	3/27/00	5/7/00	•	•		
AOL_GoM_Val_Flt	Bob Swift	3/27/00	4/21/00		•		
GOM2000	Richard Miller	4/2/00	4/15/00		•	•	•
RV Revelle_ASIAEX	Michael Caruso	4/12/00	5/5/00			•	
Scotia_Prince_Ferry	William Balch	4/12/00	10/24/00		•	•	•
TC00_04	Carrie Leonard	4/14/00	4/30/00		•		
Belgica_2000_11	Kevin Ruddick	4/17/00	4/19/00		•		
TOTO_3	Robert Steward	4/19/00	5/2/00		•		•
HarmBloom	Steve Groom	4/28/00	5/6/00			•	
LabradorSea	Glenn Cota	5/1/00	6/10/00	•	•	•	
Terengganu	Tadris Ahmad	5/2/00	6/16/00		•		
COBOP	Robert Steward	5/10/00	6/6/00				•
NFR0005	Mati Kahru	5/22/00	6/1/00		•		
Windy_CoOP	Raphael Kudela	5/23/00	8/1/00			•	
GlobecCCSMeso2000	Andrew Barnard	5/26/00	6/19/00		•	•	
Belgica_2000_15	Kevin Ruddick	6/5/00	6/7/00		•		
Mucillagine	Vittorio Barale	6/6/00	10/1/00		•	•	
Vattern_June_2000	Peter Land	6/7/00	6/8/00		•		
Gulf_of_Oman	Rick Miller	6/12/00	7/13/00	•	•		
KA_00_05	Francisco Chavez	6/19/00	7/9/00	•	•		
Adriatic	Stan Hooker	6/23/00	7/24/00			•	
Gulf_of_Maine_Class	Bruce Monger	6/28/00	7/1/00		•	•	
LEO-15_Experiment	Bob Arnone	7/1/00	7/31/00		•		
SW_Florida	Robert Steward	7/7/00	7/21/00				•
SSS	Stephan Howden	7/10/00	9/1/00			•	
METEOR_M48	Christian Schaefer-Neth	7/19/00	10/11/00			•	
GLOBEC_Oregon	Andrew Barnard	7/28/00	8/18/00	•	•	•	
Chukchi_Sea	Glenn Cota	8/1/00	8/31/00	•	•	•	
OCE97_11168	Bruce Bowler	8/4/00	8/13/00		•		
SeineSat2	Francis Gohin	8/30/00	9/25/00			•	
Eastern_Mediterranean	Sukru Besiktepe	9/15/00	9/30/00			•	

Belgica_2000_24	Kevin Ruddick	10/2/00	10/6/00		•		
R_V_Meteor	Ray Barlow	10/12/00	10/31/00	•	•	•	
MiRIR_2	Richard Miller	10/20/00	11/3/00		•	•	
Michoacan2000	Mati Kahru	11/6/00	11/20/00		•		
Big_Eye_Oceanog	Carrie Leonard	11/7/00	11/21/00		•	•	
Venice_Tower_No	J.F. Berthmore on	11/13/00	12/1/00		•		

3.6 SIMBIOS SUNPHOTOMETERS AND CALIBRATIONS

Atmospheric correction of satellite radiances and, in particular, estimation of aerosol effects on the upwelling radiance at the top of the atmosphere is one of the most difficult aspects of satellite remote sensing. Merging of aerosol properties obtained from *in situ* observations with these derived by sensor algorithms creates exceptional opportunities to validate and improve the atmospheric correction. There are many uncertainties associated with *in situ* measurements themselves. These uncertainties include sun photometer or radiometer calibration and operational problems, inadequate manual handling, and cloud contamination. When matching against atmospheric properties obtained by a satellite sensor, additional uncertainties come into play. These uncertainties may be caused by different satellite and surface instrument viewing angles and by observation acquisition time discrepancies. In the case of the atmosphere, these uncertainties are considerable. Therefore, exact calibration of sun photometers and radiometers is essential, as well as the best possible (and uniform from instrument to instrument) correction of obtained measurements. Finally, in order to cross-validate the quality of *in situ* data, as well as extract measurements of high stability and confidence, and compare them against satellite sensor estimates with the largest degree of certainty, having multiple observations from different sun photometers and radiometers is essential.

3.6.1 Instrument Pool

The SIMBIOS Project provided funding to several of the NRA-96 science team members for the purchase of *in situ* ocean optical instrumentation. The funding was provided with the stipulation that these instruments would be part of a Project Office instrument pool for three years (1997-2000). These instruments are to be returned to the science team members and will not be part of the instrument pool after the year 2000. The SIMBIOS Project has a sun photometer instrument pool available for the new science team (NRA-99). This pool currently consists of 12 MicroTops hand-held sun photometers, 2 PREDE sun photometers (Japan), 2 SIMBAD and 2 SIMBADA sun photometers, developed by the Laboratoire d'Optique Atmospherique (LOA, France), as well as 1 micro-pulse Lidar.

In addition to the sun photometer instrument pool, the SIMBIOS Project takes advantage of the existing Aerosol Robotic Network (AERONET), which is dedicated to monitoring aerosol optical thickness around the globe. Because most of the sun photometers used within the AERONET project are in continental zones, the SIMBIOS group enhanced this network with island and coastal stations.

Ten SIMBIOS CIMEL sites have been confirmed and delivered so far and include Coconut Island (Hawaii--replacing Lanai for management reasons) Ascension Island, Bahrain, Papeete (Tahiti), Wallops Island (Virginia, USA), Chinae (South Korea), Erdemli (Turkey), Puerto Madryn (Argentina), and Horta (Azores). The implementation of the site of Perth (Australia) has been delayed due to customs authorization but is expected soon. The remaining two SIMBIOS CIMELs are presently at Goddard Space Flight Center. One instrument is a back up for Hawaii, the second one is a back up for the other sites. Cruise experiments handled by various SIMBIOS investigators allow for the collection of *in situ* measurements from hand-held and shipboard sun photometers. These measurements, with the augmented AERONET network, provide the Project with global data sets.

Sun Photometer Calibration: Non-Polarized Channels

The calibration of the sun photometers was described in McClain and Fargion (1999). Details on the sunphotometers' operations, calibrations and theoretical principles are posted at http://simbios.gsfc.nasa.gov/Sunphotometers/calibration.html. Twelve Microtops, two SIMBAD and two PREDE instruments are calibrated before and after every cruise deployment. The processing code is common to all sun photometers. This code allows for inter-calibration with a CIMEL as the reference instrument and is based on the time to time voltage ratios. The first and last calibration for the Microtops #3773, the SIMBAD #972306 and the PREDE #PS090063 are shown in Table 3.3. With the V0 are displayed the standard deviation $\Delta V0$ corresponding to the atmosphere variation during the calibration or due to the time difference with the CIMEL reference. Clear days are selected as "calibration" days if they have a variation $\Delta V0/V0$ less than 1% (Table 3.3). We have found that the optics and filters of the instrument can change dramatically after one year of use. In the case of the PREDE #PS090064 the variation reached 5%. Several factors lead to the degradation of the calibration and the effect strongly depends on the wavelength. Thus the Project recommends a frequent schedule of calibrations for

each field experiment in order to retrieve the most accurate AOT.

Sun Photometer Calibration: Polarized Channels

The calibration of the polarized version of the CIMEL sun photometers was described in McClain and Fargion (1999). The first polarized sun photometer (#191) of the SIMBIOS Project was deployed in Erdemli (Turkey) and worked since November 1999. The second polarized sun photometer (#162) was deployed in Wallops (USA) in June 2000.

Above Water Radiometer Calibration

The SIMBAD radiometer is also an above water radiometer (in addition to being a sun photometer). The optics and filters are the same but the electronic gain is different. The calibration is performed using a 6" integrated sphere at GSFC. SIMBAD instruments were calibrated since August 1999. Table 3.4 shows the reflectance per count obtained using six lamps. The 6" integrated sphere is maintained and calibrated monthly by the Calibration Facility group at Goddard (http://spectral.gsfc.nasa.gov).

3.6.2 Extraction of in situ AOTs

The Project has recently implemented its own correction strategy for instrument voltages corresponding to AOTs. The approach ensures a uniform AOT processing for all instruments making the AOTs comparable amongst the instruments and between instruments and satellite sensor AOTs derived by means of the atmospheric correction (see chapter 6 and 11 in Fargion and Mueller, 2000). Also, the method uses a consistent set of tuning variables, such as ancillary data, concurrently applied for the correction of satellite radiances. Therefore, some stages of the satellite and *in situ* data processing are identical, contributing to increased confidence in the match-ups.

SeaWiFS Data Acquisition

The SeaWiFS aerosol optical thickness (AOT) data were obtained by spatially co-locating a 25x25 pixel grid box around the pixel containing the ground-based measurement station, thereby providing a maximum of 625 SeaWiFS retrievals in each matchup. A spatial homogeneity (uniformity) test in the retrieved $\tau_a(865)$ was then conducted to screen thin cirrus and high altitude aerosol contamination because the *in situ* and satellite measurements are often looking through different atmosphere paths. Only those satellite data sets that passed the spatial homogeneity test were used for the matchup analyses.

In Situ Data Acquisition from Cimel

A select group of the ground stations from AERONET were chosen for the matchup analyses. These instruments were located at either coastal or island stations and were operational for a reasonable length of time after SeaWiFS went into operation. Table 3.5 provides the AERONET station name, location (latitude and longitude), and the corresponding responsible AERONET PIs. Currently, efforts are underway to include additional AERONET stations. The retrieval of data from AERONET has been automated to facilitate the matchup analyses. Once per month, a script is automatically run to access the AERONET database and retrieve τ_a data for the predetermined sites. For the matchup purpose, the ground-based measurements from AERONET were first reduced to include only those records that fall ±3 hr of the SeaWiFS overpass for a given station. These records include the aerosol optical thickness measured at the four spectral wavelengths (440, 500, 670, and 870 nm).

Table 3.3. Top of Atmosphere (TOA) signals and standard deviations for the sun photometers determined by transfer calibration from a calibrated CIMEL at GSFC between August 1998 and September 2000.

Microtops #3773	**440nm**	**500nm**	**675nm**	**870nm**	**940nm**
08-20-1998	1238±7	988±4	1219±5	825±3	1929±11
06-09-1999	1238±4	987±4	1198±3	827±2	2178±13
09-20-2000	1242±5	984±4	1194±4	817±2	1958±21
SIMBAD #97206	**443nm**	**490nm**	**560nm**	**670nm**	**870nm**
08-20-1998	391290±719	477288±2026	404124±165	420995±2039	305421±414
09-23-1999	376205±2369	464224±815	391526±854	416182±933	300000±2204
03-06-2000	382815±2311	465574±2362	382168±1231	408538±961	301005±469
PREDE #PS090064	**440nm**	**500nm**	**675nm**	**870nm**	**940nm**
10-16-1998	1.36±0.003E-04	2.79±0.02E-04	3.52±0.02E-04	2.77±0.01E-04	2.61±0.01E-04
09-23-1999	1.30±0.002E-04	2.72±0.005E-04	3.40±0.01E-04	2.67±0.004E-04	2.67±0.02E-04

Table 3.4. Calibration coefficient for SIMBAD # 06 and 09 between 1999 and 2000.

SIMBAD #972306	**440nm**	**490nm**	**560nm**	**675nm**	**870nm**
08-12-1999	3.818±0.006	2.192±0.0015	2.432±0.002	4.229±0.002	8.029±0.002
01-14-2000	3.7650±0.0007	2.1339±0.001	2.3894±0.002	4.1096±0.002	7.6506±0.008
03-06-2000	3.6442±0.0025	2.1186±0.0010	2.4042±0.0016	4.1324±0.0024	7.7366±0.0044
08-18-2000	3.7942±0.0049	2.2376±0.0017	2.5963±0.0031	4.3958±0.0055	8.2380±0.0123
SIMBAD #972309					
08-12-1999	4.931±0.003	2.425±0.002	2.695±0.003	4.312±0.004	8.277±0.0025
01-14-2000	5.0134±0.003	2.3451±0.0002	2.6511±0.0006	4.2599±0.0003	7.9370±0.004
03-06-2000	4.7363±0.0022	2.2771±0.0002	2.6234±0.0010	4.2219±0.0011	8.0104±0.0057

As an initial quality control step, the data were averaged and some variation parameters were computed to screen possible cloud contamination. Only those data sets that had low temporal variations (stable atmosphere) were then further reduced to ±1 hr of the SeaWiFS overpass and used for the matchup analyses. Usually, the CIMEL instruments routinely take one measurement every 15 min near local noon; therefore, for a given SeaWiFS file, there may be as many as eight AERONET measurements that qualify as a match for the 2 hr time window. The strategy in the validation study is not to compromise good data with bad data for the purpose of more matchups, i.e., it is preferred to screen out some good data to keep the high quality of data sets.

AOT Match-up Results

Match-ups between AOT data obtained from *in situ* observations and satellite-derived AOT levels are analyzed to: i) verify calibration of satellite sensor near-infrared bands and ii) establish the effectiveness of the applied suite of aerosol models. Match-ups have been obtained for the SeaWiFS-derived aerosol properties and AOT levels calculated from AERONET and SIMBIOS sun and sky radiometer data. AOT calculated from satellite sensor observations are a by-product of the atmospheric correction (Gordon, 1994). The match-up results are not conclusive.

Table 3.5 AERONET sites used for aerosol matchup analyses.

Station	**Latitude**	**Longitude**	**AERONET PI**
Bahrain	26.32	50.50	C. McClain*
Bermuda	32.37	-64.70	B. Holben
Dry Tortugas	24.60	-82.80	K. Voss & H. Gordon
Kaashidhoo	4.97	73.47	B. Holben
Lanai	20.83	-156.99	C. McClain*
SanNicolas	33.26	-119.49	R. Frouin

* SIMBIOS Project Office

Research into vicarious calibration of the SeaWiFS instrument using *in situ* AOT observations and validation of the atmospheric correction algorithm is continuing. The initial scheme for elimination of cloudy and erroneous AOT measurements was applied with CIMEL sun and sky radiometer data (Wang, 2000). This strategy was based on statistical estimates of AOT variations throughout a day and only used one spectral band (870nm) of the CIMEL radiometer to analyze those variations. Figure 3.3 illustrates the results of comparisons between SeaWiFS-obtained AOT values and *in situ* AOT data derived from CIMEL measurements in 1998 and 1999. Four CIMEL sites are included in the match-ups. *In situ* AOT results are converted into SeaWiFS spectral bands and only those bands are displayed which are the closest to the original CIMEL bands. The slope and intercept of the linear fit are given at each wavelength. AOT match-ups compare well for SeaWiFS and *in situ* measurements in the red (670nm) and (865nm) bands. The slope of the linear fit between the pairs of SeaWiFS and *in situ* measurements closely approaches 1 for the 865nm band match-ups. Therefore, the calibration of SeaWIFS in band 8 may be considered reasonable. Nevertheless, as the wavelength decreases towards the visible spectrum, the slope value for the match-ups decreased indicating that the SeaWiFS algorithm underestimates AOT relative to CIMEL observations. Two reasons for this underestimation are considered: the relative and absolute calibrations of the SeaWiFS near-infrared bands, and the SeaWiFS aerosol models used to extrapolate the extracted near-infrared AOT measures towards the visible spectra. Further studies are needed to draw more precise conclusions about sensor and atmospheric correction accuracies. Several investigations are presented. The spectral distributions of daily AOT CIMEL measurements obtained at the AERONET/SIMBIOS sites are compared with the corresponding distributions of SeaWiFS-derived AOT matchup points. In general, SeaWiFS AOT spectral distributions appear to be defined by much flatter curves than *in situ* AOT measures. This strongly contributes to the inaccuracies in AOT matchups.

AOT Cross Calibration Experiment

Several sun photometers were deployed in early 1999 during the INDOEX experiment (http://borneo.ucsd.edu/index.html). The instruments were

used onboard the R/V Ronald H Brown ship sailing in the Indian Ocean for more than 2 months. Aerosol optical thicknesses were collected concurently using MicroTops sun photometer, SIMBAD and shadowband radiometers. Cross comparison between aerosol optical thicknesses obtained with each radiometer are presented on Figure 3.4. AOT measured by SIMBAD and shadowband radiometers are plotted versus AOT measured by the MicroTops sun photometer. We have limited the comparison to the *in situ* AOT collected within ±3 hr of the SeaWiFS overpass window. We allowed the maximum difference of thirty minutes between AOT observation time of each instrument. The maximum spatial difference between geographical locations where each set of AOT measurements was obtained is 15km.

A good agreement is shown at 870nm and is reasonable at other channels. The channels of each instrument could be slightly different, and so taking into account the spectral dependance of AOT could result in a better comparison. Nonetheless, promising comparisons between SeaWiFS and the three sun photometers are expected.

3.7 CALIBRATION ROUND ROBIN

A new optical laboratory has been set up by the SIMBIOS project. Its main purpose is to monitor the temporal stability of the SeaWiFS Transfer Radiometer SXR-II. The light source is a SeaWiFS Quality Monitor SQM-II manufactured by Satlantic. The laboratory is especially setup for the SXR-II / SQM-II configuration, but can also be used with 2 SQMs installed simultaneously. The distance between light source and radiometer can be varied from 0.2 to 1.2 m. The area containing the SXR and the SQM is enclosed by black felt curtains. Thus, light emitted from the remote instruments (PC screens, temperature controller and voltmeter display) is blocked, and only light from the SQM will be measured by the SXR. Measurements of ambient light and SXR dark current showed negligible differences, proving the effectiveness of the light absorption by the felt curtains.

A study comparing two commercial SQM versions [one from Satlantic Inc., one from Yankee Environ. System (YES) Inc.] is currently underway in order to evaluate each intruments' stability. The study is based on data from the above laboratory, data taken by the SIMBIOS team at YES facilities and data from two previous SIMBIOS measurement campaigns. Several experiments showed that the sensitivity of the SXR-II shifted after undergoing shocks of a magnitude that can be expected during shipping procedures. A problem with the mirror fixtures inside the SXR was soon identified as the most likely cause. During two repair sessions at Reyer Corp., the mirror fixtures were fastened and epoxied. Afterwards the SXR sensitivity remained stable: after controlled shock treatments as well as regular shipping, the sensitivity changed by less than 0.3%. The SXR-II was calibrated using the Hardy-Sphere of NASA GSFC Code 920.1 Calibration Facility. The radiance of the SQM-II was measured with the Code 920.1 spectroradiometer Optronics 746 (which was also used to calibrate the Hardy-Sphere) at wavelength intervals of 10 nm from 410 nm to 1100 nm (10 nm bandwidth for each measurement). The SQM radiances are shown in Figure 3.5 for three different light levels as measured by the Optronics 746 in the Code 920.1 clean room, and as measured by the SXR-II in the SIMBIOS laboratory. The data from the different sensors agree well, with deviations ranging from 0 to 10%, depending on wavelength. The strong deviations of the spectra from the theoretical blackbody Planck spectrum (e.g. the dip around 600 nm) are due to the blue colored glass in front of the SQM-II, whose purpose is to reduce the radiance in the red wavelength range in order not to saturate underwater radiometers.

In November 2000, the SXR-II was sent to NIST for calibration using the newly developed SIRCUS (Spectral Irradiance and Radiance Calibrations with Uniform Sources) facilities, that use tunable lasers and integrating spheres. Results are expected to be available by the end of the year.

3.8 SIMBIOS COMPUTING RESOURSES

The SIMBIOS computing facility contains a variety of equipment types. The main goal of the facility is to provide computational support for the following areas:

- routine bulk data processing,
- large scale analysis and matchup between sensors,
- focused analysis on data subsets, and
- storage of large sensor data sets.

Co-location of the facility with the SeaWiFS Project continues to benefit the Project by making available other resources such as high-quality color printers, network equipment, and other supporting equipment. Large-scale tasks such as bulk data processing and large-scale analysis tasks are performed by two Silicon Graphics (SGI) Origin 2000 servers.

Each system has 6 processors and approximately 3 gigabytes (GB) of RAM. The influx of large data sets for additional sensors requires increasing amounts of disk space, especially when performing comparative analysis. The Data Processing server has 90 GB of disk space and the Data Analysis server has 374 GB of total disk space. Long-term storage of data sets is handled by the 6 TB tape library attached to the Data Analysis server. Silicon Graphics O2 workstations continue to be the system of choice for software development and focused analysis tasks. The sizing of the workstations varies with the task requirements.

SIMBIOS is connected to the Internet via a 100-megabit link, making network transfer of large data sets more feasible. Internal connections are also 100 megabit for rapid transfer of data between the servers and the workstations. Data ingest for SIMBIOS is also done via removable media including CD-ROM, 8 millimeter tape, 4 millimeter (DAT) tape, and DLT media up through DLT 7000. Off-line media storage space is shared with the SeaWiFS Project.

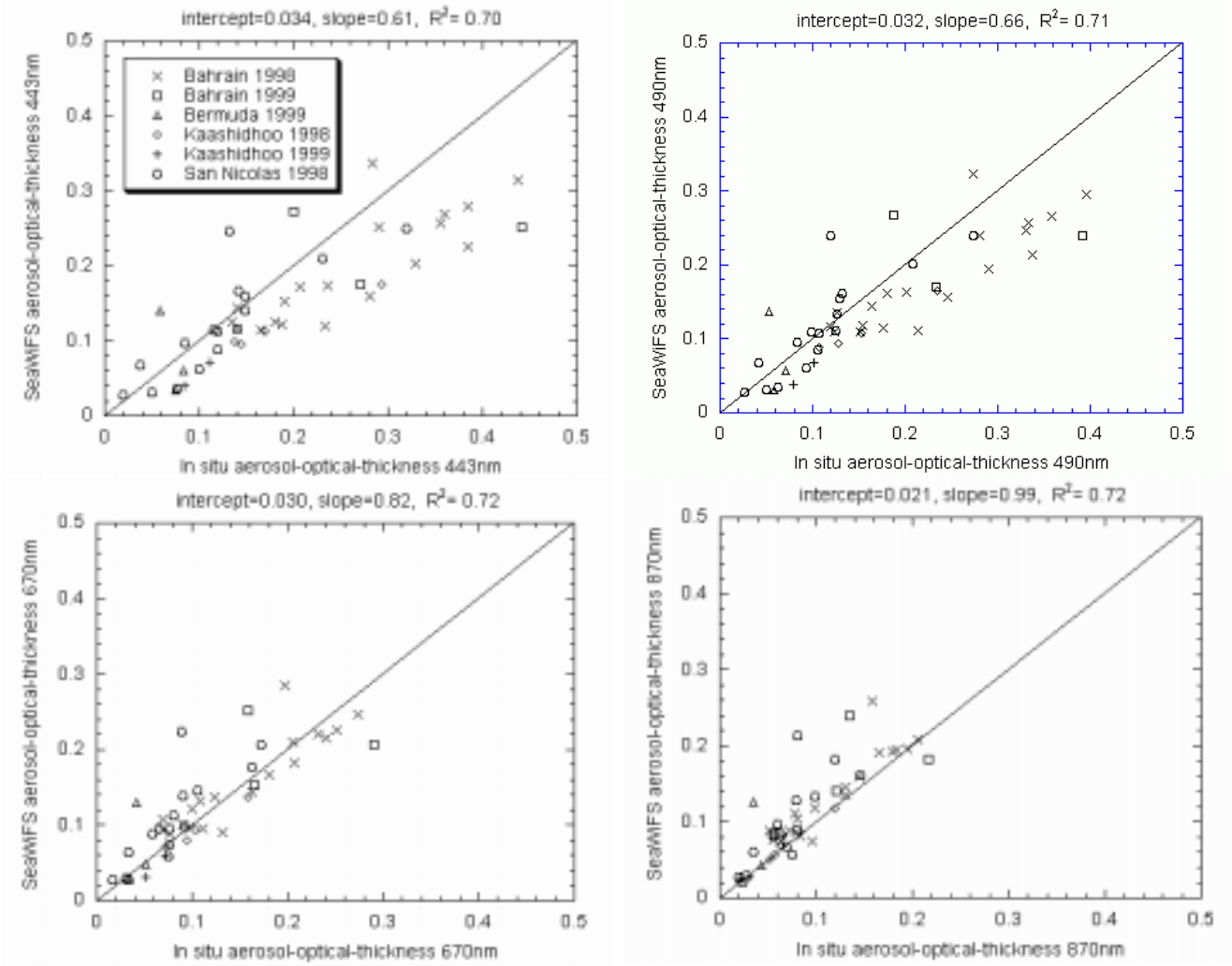

Figure 3.3. Match-up results between SeaWiFS-obtained AOT values and AOT measurements captured by different CIMEL sun photometers for a - 443, b – 490, c – 670 and d – 870 nanometers. Data collected in four sites were used: Bahrain, Bermuda, Kaashidhoo and San Nicolas Island.

The scope of the group's efforts expanded over the 1999 year, including the addition of the POLDER dataset, installation of a ground station at Wallops Flight Facility to receive MOS data downlinks, and routine processing of MOS data at the Greenbelt site. In support of these efforts, the facility has experienced moderate growth over the past year. A workstation was added to the Project, as well as additional local storage for the workstations and high capacity tape drives for local backup and archival capability.

Each server was upgraded with a FibreChannel interface. The new interface will allow the servers to participate in the SeaWiFS Project Storage Area Network (SAN). Connection to the SeaWiFS SAN will allow the SIMBIOS team to access SeaWiFS data products and ancillary data at a rate of up to 1 gigabit per second. Participation in the SeaWiFS high availability server cluster via Silicon Graphics (SGI) FailSafe software is planned for next fiscal year. Membership in the cluster will give the Project the capability of automatic failover of services from one server to another in the event of a server crash, maximizing resource availability.

REFERENCES

Bailey, S.W., C.R McClain, P.J. Werdell, B.D. Schieber, 2000: Normalized Water-Leaving Radiance and Chlorophyll *a* Match-Up Analyses. In SeaWiFS Postlaunch Technical Report Series, Volume 10, NASA Tech. Memo. 2000-206892, S.B. Hooker and E.R. Firestone, Eds. NASA Goddard Space Flight Center, Greenbelt, Maryland, 59 pp.

Clark D.K., H.R. Gordon, K.J. Voss, Y.Ge, W. Broenkow, and C. Trees, 1997: Validation of Atmospheric Correction Over Oceans. *J. Geophys. Res*., **102**, D14, 17,209-17,217.

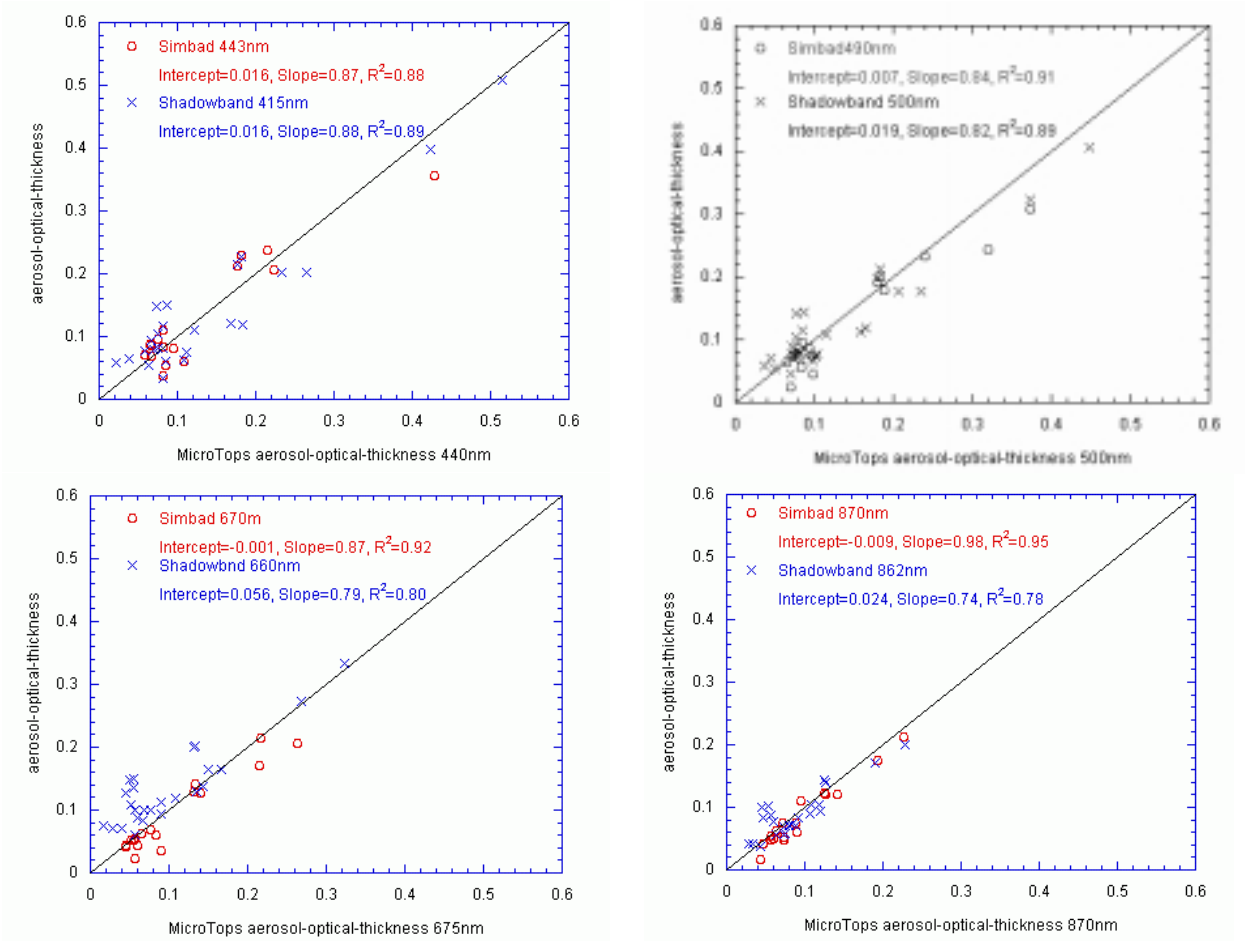

Figure 3.4. Cross comparison of AOT collected with MicroTops, SIMBAD and shadowband radiometers deployed onboard the R/V Ronald H Brown ship during INDOEX experiment (1999). Square symbols represent the data captured by SIMBAD and cross symbols represent AOT captured by shadowband radiometer. Comparisons are made for MicroTops channels: a - 440, b – 500, c – 675 and d – 870 nanometers.

Fargion, G. S., and J. L. Mueller, 2000: Ocean Optics for Satellite Ocean Color Sensor Validation, Revision 2, NASA/TM-2000-209966, NASA Goddard Space Flight Center, Greenbelt, MD, 184 pp.

Frouin, R., M. Schwindling, and P.Y. Deschamps 1996: Spectral reflectance of sea foam in the visible and near infrared: In situ measurements and remote sensing implications, *J. Geophys. Res.*, **101**, 14,361-14,371.

Gordon, H.R., 1995: Remote sensing of ocean color: a methodology for dealing with broad spectral bands and significant out-of-band response, *Appl. Opt.*, **34**, 8363-8374.

Gordon, H.R., and M. Wang, 1994a: Influence of oceanic whitecaps on atmospheric correction of ocean-color sensor, *Appl. Opt.*, **33**, 7754-7763.

Gordon, H.R., and M. Wang, 1994b: Retrieval of water-leaving radiance and aerosol optical thickness over the oceans with SeaWiFS: A preliminary algorithm, *Appl. Opt.*, **33**, 443-452.

Hooker, S.B., C.R. McClain, J.K. Firestone, T.L. Westphal, E-n. Yeh, and Y. Ge, 1994: The SeaWiFS Bio-Optical Archive and Storage System (SeaBASS), Part 1. In NASA Tech. Memo. 104566, Vol. 20, S.B. Hooker and E.R. Firestone, Eds., NASA Goddard Space Flight Center, Greenbelt, Maryland, 40 pp.

Eplee, Robert E. Jr., Wayne D. Robinson, Sean W. Bailey, Dennins K. Clark, P Jeremy Werdell, Menghua Wang, Robert A. Barnes, and Charles R. McClain, 2000: The Calibration of SeaWiFS, Part 2: Vicarious Techniques, Submitted to *Applied Optics*.

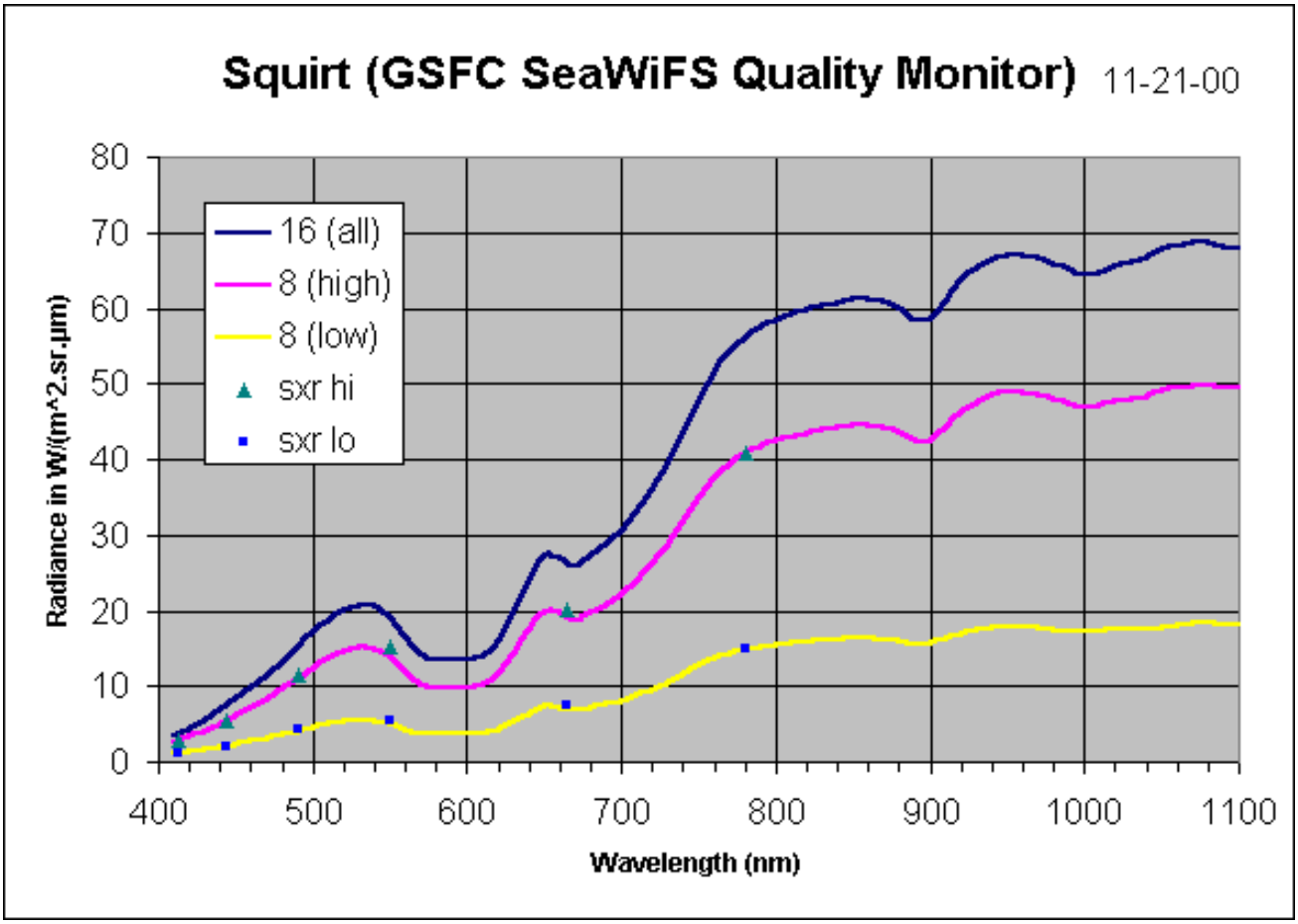

Figure 3.5. Radiances of the SeaWiFS Quality Monitor SQM-II (manufactured by Satlantic Inc.) for wavelengths from 410 nm to 1100 nm. The solid lines show data measured by the Optronics 746, the triangles and squares show data measured by the SXR-II. Figure produced by John Cooper of GSFC Code 920.1.

Eplee, Robert E. & C.R. McClain, 2000: MOBY Data Analysis for the Vicarious Calibration of SeaWiFS Bands 1-6, Vol. 9, In NASA Tech. Memo. 2000-206892, SeaWiFS Postlaunch Technical Report Series, S.B. Hooker and E.R. Firestone, Eds., NASA Goddard Space Flight Center, Greenbelt, Maryland, p43-50.

McClain, C.R,. and G.S. Fargion, 1999: SIMBIOS Project 1998 Annual Report, NASA Tech. Memo. 1999-208645, NASA Goddard Space Flight Center, Greenbelt, Maryland, 105 pp.

Moore, K.D., K.J. Voss, and H.R. Gordon 1998: Spectral reflectance of whitecaps: Instrumentation, calibration, and performance in coastal waters, *J. Atmos. Ocean. Tech.*, **15**, 496-509.

Moore, K.D., K.J. Voss, and H.R. Gordon, 2000: Spectral reflectance of whitecaps: Their contribution to water-leaving radiance, *J. of Geophys. Res.*, **105**, 6493-6499.

Neumann, A., Walzel, T., Tschentscher, C., Gerasch, B., Krawczyk, H, 1995: MOS-IRS Data Processing, Software and Data Products (Preliminary Documentation), DLR Institute for Space Sensor Technology.

Mueller, J.L., and R.W. Austin, 1995: Ocean Optics Protocols for Validation, Revision 1, NASA Tech. Memo. 104566, Vol. 25, S.B. Hooker, E. R. Firestone, and J. G. Acker, Eds., NASA Goddard Space Flight Center, Greenbelt, Maryland, 67 pp.

O'Reilly, J. E., S. Maritorena, B. G. Mitchell, D. A. Siegel, K. L. Carder, S. A. Garver, M. Kahru, and C. McClain, 1998: Ocean color chlorophyll algorithms for SeaWiFS, *J. Geophys. Res.*, **103**(C11), 24,937-24,953.

Robinson, W., and M. Wang, 2000: Vicarious calibration of the SeaWiFS band 7, In Vol. 9, NASA Tech. Memo. 2000-206892, SeaWiFS Postlaunch Technical Report Series, S.B. Hooker and E.R. Firestone, Eds., NASA Goddard Space Flight Center, Greenbelt, Maryland, p.38-42.

Siegel, D.A., M. Wang, S. Maritorena, and W. Robinson 2000: Atmospheric correction of satellite ocean color imagery: the black pixel assumption, *Appl. Opt.*, **39**, 3582-3591.

Wang, M. 1999: A sensitivity study of SeaWiFS atmospheric correction algorithm: Effects of spectral band variations, *Remote Sens. Environ.*, **67**, 348-359.

Wang, M., 2000a: Effects of the vicarious calibration on the SeaWiFS derived aerosol optical properties, Proceedings of Ocean Optics XV, Musée Océanographique, Monaco, October 16-20, 2000a.

Wang, M. 2000b: The SeaWiFS atmospheric correction algorithm updates, In Vol. 9, NASA Tech. Memo. 2000-206892, SeaWiFS Postlaunch Technical Report Series, S.B. Hooker and E.R. Firestone, Eds., NASA Goddard Space Flight Center, Greenbelt, Maryland, p.57-63.

Wang, M., and S. Bailey 2000: Correction of the sun glint contamination on the SeaWiFS aerosol optical thickness retrievals, In Vol. 9, NASA Tech. Memo. 2000-206892, SeaWiFS Postlaunch Technical Report Series, S.B. Hooker and E.R. Firestone, Eds., NASA Goddard Space Flight Center, Greenbelt, Maryland, p.64-68.

Wang, M., and B.A. Franz, 2000: Comparing the ocean color measurements between MOS and SeaWiFS: A vicarious intercalibration approach for MOS, *IEEE Trans. Geosci. Remote Sens.*, **38**, 184-197.

Wang, M., B.A. Franz, R.A. Barnes, and C.R. McClain, 2001: Effects of the SeaWiFS spectral band-pass on the retrieved ocean near-surface optical properties, *Appl. Opt.*, in press.

Wang M., S. Bailey, C. Pietras, C.R. McClain, and T. Riley, 2000: SeaWiFS Aerosol Optical Thickness Matchup Analysis, In SeaWiFS Post launch Tech. Memo. Series, Vol 10, 2000-206892, S.B. Hooker and E.R. Firestone, Eds, NASA Goddard Space Flight Center, Greenbelt, Maryland.

Werdell, P.J., S. Bailey, and G.S. Fargion, 2000: SeaBASS Data Protocols. In Ocean Optics Protocols for Satellite Ocean Color Sensor Validation, Revision 2, NASA Tech. Memo. 2000-209966, G.S. Fargion and J.L Mueller, Eds. NASA Goddard Space Flight Center, Greenbelt, Maryland, 184 pp.

This research was supported by the

SIMBIOS Project Office

PEER REVIEWED PUBLICATIONS

Barnes, R., R. E. Eplee, and F. S. Patt, 1998: SeaWiFS Measurements of the Moon. EurOpt Series, Sensors, Systems, and Next-Generation Satellites II, *SPIE*, **3498**, 311-324.

Barnes, R., R. E. Eplee, F. S. Patt, and C. R. McClain 1999: Changes in the Radiometric Sensitivity of SeaWiFS Determined from Lunar and Solar-based Measurements. *Applied Optics*, **38**, 4649-4669.

Fargion, G. S., C. R. McClain, H. Fukushima, J. M. Nicolas, and R. A. Barnes, 1999: Ocean color instrument intercomparisons and cross-calibrations by the SIMBIOS Project. *SPIE, **3870-68**,* 397-403.

Fargion, G. S., C. R. McClain, and R. A. Barnes, 2000: Ocean color instrument intercomparisons and cross-calibrations by the SIMBIOS Project (1999-2000). *SPIE*, **4135**, 411-420.

Mueller, J., C. McClain, R. Caffrey, and G. Feldman, 1998: The NASA SIMBIOS Program, *Backscatter*, May.

Siegel, D. A., M. Wang, S. Maritorena, and W. Robinson, 2000: Atmospheric correction of satellite ocean color imagery: the black pixel assumption, *Applied Optics* **39**, 3582-359.

Wang, M., 1999: A Sensitivity Study of SeaWiFS Atmospheric Correction Algorithm: Effects of Spectral Band Variations. *Remote Sens.Environm*., **67**, 348-359.

Wang, M., 1999: Atmospheric Correction of Ocean Color Sensors: Computing Atmospheric Diffuse Transmittance. *Applied Optics*, **38**, 451-455.

Wang, M., 1999: Validation study of the SeaWiFS oxygen A-band absorption correction: Comparing the retrieved cloud optical thicknesses from SeaWiFS measurements, *Appl. Opt.*, **38**, 937-944.

Wang, M. and B. A. Franz, 2000: Comparing the ocean color measurements between MOS and SeaWiFS: A vicarious intercalibration approach for MOS, *IEEE Trans. Geosci. Remote Sensing*, **38**, 184-197.

Wang, M., S. Bailey, and C. R. McClain, 2000: SeaWiFS Provides Unique Global Aerosol Optical Property Data, *Eos, Transaction, American Geophysical Union*, **81**, p197.

Wang, M., B.A. Franz, R.A. Barnes, and C.R. McClain, Effects of the SeaWiFS spectral band-pass on the retrieved ocean near-surface optical properties, *Applied Optics* (In press).

Accepted

Holben, B.N., et al., 2001: An emerging ground-based aerosol climatology: Aerosol Optical Depth from AERONET, *J. Geophys. Res.*

Porter J. N., M. Miller, C.Pietras, C. Motell: Ship Based Sun Photometer Measurement Using Microtops Sunphotometer, *J. Atmos. Oceanic. Technol.*

Wang, M. and S. W. Bailey, Correction of the Sun Glint Contamination on the SeaWiFS Ocean and Atmosphere Products, *Applied Optics*.

Submitted

Eplee Jr. R.E., W.D. Robinson, S.W. Bailey, D.K. Clark, P.J. Werdell, M. Wang, R.A. Barnes, and C.R. McClain, The Calibration of SeaWiFS, Part 2: Vicarious Techniques, *Applied Optics*.

Porter J. N., M. Miller, C.Pietras, C. Motell: Ship Based Sun Photometer Measurement Using Microtops Sunphotometer, *J. Atmos. Oceanic. Technol*.

Smirnov, A., B.N.Holben, O.Dubovik, N.T.O'Neill, T.F.Eck, D.L.Westphal, A.K.Goroch, C.Pietras, and I.Slutsker, Atmospheric aerosol optical properties in the Persian Gulf region, Geophys.Res.Lett.

OTHER PUBLICATIONS

Bailey S.W., C.R. McClain, P.J. Werdell, and B.D. Schieber, 2000: Normalized Water-leaving Radiance and Chlorophyll a Match-up Analyses. In SeaWiFS Postlaunch Technical Report Series, Vol. 10, NASA Tech. Memo. 2000-206892, S.B. Hooker and E.R. Firestone, NASA Goddard Space Flight Center, Greenbelt, Maryland.

Hsu N.C., W.D. Robinson, S.W. Bailey, and P.J. Werdell, 2000: The Description of the SeaWiFS Absorbing Aerosol Index. In SeaWiFS Postlaunch Technical Report Series, Vol. 10, NASA Tech. Memo. 2000-206892, S.B. Hooker and E.R. Firestone, NASA Goddard Space Flight Center, Greenbelt, Maryland.

McClain, C.R. and G.S. Fargion, 1999: SIMBIOS Project 1998 Annual Report, NASA Tech. Memo. 1999-208645, NASA Goddard Space Flight Center, Greenbelt, Maryland, 105 pp.

McClain, C.R. and G.S. Fargion, 1999: SIMBIOS Project 1999 Annual Report, NASA Tech. Memo. 1999-209486, NASA Goddard Space Flight Center, Greenbelt, Maryland, 128 pp.

Fargion, G.S. and J.L. Mueller 2000: Ocean Optics Protocols for Satellite Ocean Color Sensor Validation, Revision 2, NASA Tech. Memo. 2000-209966, NASA Goddard Space Flight Center, Greenbelt, Maryland, 183 pp.

Robinson, W. D. and M. Wang, 2000: Vicarious calibration of the SeaWiFS band 7, The SeaWiFS Postlaunch Technical Report Series, Vol. 9, NASA Tech. Memo. 2000-206892, S.B. Hooker and E.R. Firestone, Eds., NASA Goddard Space Flight Center, Greenbelt, Maryland, p.38-42.

Robinson W. D., G. M. Schmidt, C.R. McClain, and P.J. Werdell, 2000: Changes Made in the Operational SeaWiFS Processing, In SeaWiFS Postlaunch Technical Report Series, Vol. 10, NASA Tech. Memo. 2000-206892, S.B. Hooker and E.R. Firestone, NASA Goddard Space Flight Center, Greenbelt, Maryland.

Wang, M., 2000: The SeaWiFS atmospheric correction algorithm updates, In SeaWiFS Postlaunch Technical Report Series, Vol. 9, NASA Tech. Memo. 2000-206892, S.B. Hooker and E.R. Firestone, Eds., NASA Goddard Space Flight Center, Greenbelt, Maryland, p.57-63.

Wang, M., S. Bailey, C. Pietras, C. R. McClain, and T. Riley, 2000: SeaWiFS aerosol optical thickness matchup analyses, In SeaWiFS Postlaunch Technical Report

Series, Vol. 10, NASA Tech. Memo. 2000-206892, S.B. Hooker and E.R. Firestone, Eds., NASA Goddard Space Flight Center, Greenbelt, Maryland, p.39-44.

Wang, M., B. Franz, and R. Barnes, 2000: Analyses of the SeaWiFS spectral bandpass effects, *The SeaWiFS Postlaunch Technical Report Series*, Vol. 10, NASA Tech. Memo. 2000-206892, S.B. Hooker and E.R. Firestone, Eds., NASA Goddard Space Flight Center, Greenbelt, Maryland, p.6-11.

Wang, M. and S. Bailey, 2000: "Correction of the sun glint contamination on the SeaWiFS aerosol optical thickness retrievals," *The SeaWiFS Postlaunch Technical Report Series*, Vol. 9, NASA Tech. Memo. 2000-206892, S.B. Hooker and E.R. Firestone, Eds., NASA Goddard Space Flight Center, Greenbelt, Maryland, p64-68, 2000.

Werdell P.J., S.W. Bailey, and G.S. Fargion, 2000: SeaBASS Data Protocols and Policy. In Ocean Optics Protocols for Satellite Ocean Color Sensor Validation, Revision 2, G.S. Fargion and J.L. Mueller, NASA Tech. Memo.2000-209966, NASA Goddard Space Flight Center, Greenbelt, Maryland.

SIMBIOS PRESENTATIONS

Bailey S.W., P.J Werdell, C.R. McClain, and G.S. Fargion, 2000: Validation of SeaWiFS-derived Chlorophyll: Comparisons at Several Spatial and Temporal Scales, Oceanography from Space 2000, Venice, Italy,

Chou, M.D., P.K. Chan, and M. Wang, 1999: Global aerosol radiative forcing derived from SeaWiFS-inferred aerosol optical properties, to be presented at AGU Fall Meeting, Dec. 13-17, San Francisco, California.

Fargion, G. S., C. R. McClain, H. Fukushima, J. M. Nicolas, and R. A. Barnes, 1999: Ocean color instrument intercomparisons and cross-calibrations by the SIMBIOS Project. EOS/SPIE Symposium on Remote Sensing, Florence, Italy.

Fargion, G.S., 1999: An Overview of SIMBIOS Project. International Symposoium on Ocean color Remote Sensing and Carbon Flux by CERES and JUWOC, Chiba, Japan.

Fargion G. and C. McClain, 2000: NASA's Sensor Intercomparison and Merger for Biological and Interdisciplinary Ocean Studies (SIMBIOS) Program, SPRING AGU- Washington, DC

Fargion G. S., C. R. McClain and Robert A. Barnes, 2000: Ocean Color Instrument Intercomparisons and Cross-Calibrations by the SIMBIOS Project, Earth Observing System V, SPIE, San Diego.

Fargion G. S. and C. R. McClain, 2000: Three Years of Ocean Color Instrument Intercomparisons and Cross-Calibrations by the SIMBIOS Project (1997-2000), Conference on Remote Sensing of the Ocean and Sea Ice VI, Barcelona.

Pietras C. M, E. Ainsworth , S. Bailey, C. Hsu, M. Wang, Fargion G. and C McClain, 2000: Aerosol Properties from Field Measurements Using Hand-Held and Automatic Sun Photometers, Spring AGU, Washington DC.

Pietras C., E. Ainsworth, S.W. Baileyet al., 2000: Initial Results of Validation of Satellyte Sensor Derived Aerosol Optical Thickness Against In Situ Atmospheric Observations Collected by the SIMBIOS Project, to be presented at the Eighth International Symposium Physical Measurements and Signatures in Remote Sensing, Aussois, France, January 8-12, 2001.

Wang, M., 2000: Effects of the vicarious calibration on the SeaWiFS derived aerosol optical properties, *The AGU Spring Meeting*, Washington, DC.

Wang, M., 2000: Effects of the Sea Surface Wind Speed on the SeaWiFS Derived Ocean Color Optical Property Data, *Proc. the Ocean Optics XV*, Musée Océanographique, Monaco.

Chapter 4

Validation of Surface Bio-Optical Properties in the Gulf of Maine as a Means for Improving Satellite Primary Production Estimates

William M. Balch

Bigelow Laboratory for Ocean Sciences, West Boothbay Harbor, Maine

4.1 INTRODUCTION

One of the greatest challenges in providing sea-truth data for various ocean color sensors is climatology. This is particularly true in the Gulf of Maine since it is cloudy and foggy more than it is clear; the climatology shows on average, about 1 in 4-5 days has clear skies with clear days slightly more frequent in the late summer and early fall. Our strategy has been to use a ship of opportunity where one has choice of the sampling days. This provides much better flexibility to sample during clear periods with good satellite coverage. Our SIMBIOS contract has been to use the *M/S Scotia Prince* ferry as a ship of opportunity, running between Portland, Maine and Yarmouth, NS. Measurements include continuous, surface, along-track fluorescence, two independent measures of backscattering, total light scattering, absorption, beam attenuation, above-water remote sensing reflectance, calcite-dependent light scattering, temperature, and salinity. XBT drops allow acquisition of vertical temperature information, useful for defining isopycnal slope, which affects primary production. These data are comparable to a previous program from early 1982, where a ship of opportunity program (SOOP) was run on the truck ferry, *M/V Marine Evangeline*, which ran along the same transect (Boyd, 1985). These surface data were combined with satellite-derived sea surface temperature fields to examine the Maine coastal current (Bisagni et al., 1996). Unfortunately, this program stopped in 1982. The ongoing SIMBIOS results will dovetail nicely with the previous work (which also had CZCS coverage) for looking at any long-term changes in the Gulf of Maine hydrography, bio-optics, and biogeochemistry.

The Gulf of Maine is an ideal site for such a SOOP program. It is a semi-enclosed basin with an average depth of ~150m. Isopycnal slope (and productivity) appears to be strongly topographically driven, with the water column becoming isothermal at the 60m isobath around Georges Bank. The dynamic range of integrated productivity in the Gulf of Maine varies seasonally by a factor of 45X (0.1 to 4.4 gC m^{-2} d^{-1}; (O'Reilly and Busch, 1984; O'Reilly et al., 1987)), greater than in the California Current (only15X variability; 0.2-3.0 gC m^{-2} d^{-1}). The major east coast data set (MARMAP data set), also long in duration, unfortunately, cannot maintain measurements of pigments or inherent optical properties, thus this SIMBIOS project provides unique data for the region.

4.2 RESEARCH ACTIVITIES

We completed the following during the third year:

- May-October 2000 Twelve cruises aboard *M/S Scotia Prince* completed between Yarmouth, Nova Scotia and Portland, ME, as required by our contract.
- Initial data submissions to be followed by more results as discrete analyses of POC/PON, PIC, and cell counts are completed. The final cruise of this year was completed in 30 September, 2000; the following raw data are being worked up for distribution to the NASA SIMBIOS Project as soon as all post cruise calibrations are finished.

Our field measurements include surface flow-through bio-optics, and above-water optical measurements, hydrographic measurements, discrete samples for calibration.

The *M/S Scotia Prince* Ferry

The *M/S Scotia Prince* ferry is 472 ft long, it carries up to 1500 passengers and 220 cars, displaces 11,968 gross metric tons, and maintains18-20 kts speed in sea states up to Force 7. In order to use this ship, we call 2-3 d ahead of each targeted cruise date, when we see high pressure weather systems moving into the area. The ship operates between 15 May and 31 October, departing Portland, ME each day at 2100h EDT, and arriving in Yarmouth, NS at 0800 EDT, the next morning (11 h total steam). Following a 1 hour layover in Yarmouth, the ship departs at 0900h EDT, and returns to Portland by 2000h EDT, with another 1h layover before its next trip. The ferry company (Prince of Fundy Cruises Limited) installed a through-hull, non-toxic sample line for us to draw water. We park our mobile laboratory 30m aft of the sample pipe on the starboard side.

Typical Cruise Operation

After the ferry leaves Portland Harbor, it goes to Witch Rock, then takes a course of 87^o (true bearing), passing just north of Jeffreys Bank, then straight across Jordan Basin, to German Bank and Cape Forchu (Yarmouth entrance). During the evening leg to Yarmouth, we connect the many power, data, and antennae cables from the laboratory to the ship, ready the lab's air handling equipment, mount the radiometers, perform instrument calibrations, check seawater flow, and generally prepare for the return transit the next morning (plus a few hours sleep). Water flow is started ~ 1/4-1/2 hour after departure from Yarmouth and data collection begins at the Cape Forchu marker. The length of the transect is ~330 Km, with ~290-330 km of effective data collection.

Flow-Through System

Our flow-through system makes a suite of IOP measurements which are used to estimate the standing stock of POC and PIC continuously. A suite of AOP measurements from the bow allow direct verification of satellite radiance and chlorophyll estimates (the latter being directly compared to acetone extracts of chlorophyll). Data integration and logging are done by National Instruments LabVIEW software, run on three pentium processor computers. The system receives time and the ship's geographic position continually from a Garmin 220 global positioning system.

Sea water first enters a vortex de-bubbler (SUNY VDB1), then into a second 1.2m tall de-bubbler, equipped with a 1mm screen to keep the largest zooplankton and salps out of the optical instruments. (Entry of >1mm plankton into either one of the optical tubes of the ac-9 can cause poor data quality when comparing absorption and attenuation). Next, the flow enters an InterOcean TempSal thermal conductivity sensor. It measures salinity with an accuracy of +0.05 Practical Salinity Units and temperature to an accuracy of +/-0.1^{o}C. Temperature and salinity data also are used in the ac-9 post-cruise calibration. Next, the flow bifurcates into a Turner 10AU-005-CE fluorometer for monitoring underway chlorophyll fluorescence. The fluorometer is equipped with a daylight white F4T5D lamp, blue-violet excitation filter (peak excitation 438nm with half band pass of 340-500nm) and red emission filter (high pass >665nm interference filter). To insure against bio-fouling, the fluorometer is cleaned regularly.

The water then passes through a tertiary debubbler via metering pump, into a Wyatt Technologies Model Dawn F laser light scattering photometer for measurements of volume scattering. The flow-rate through this instrument is ~11-15 ml min^{-1}. The photometer operates with a10 mW Argon ion laser (514 nm) which is directed into the center of a flow-through cuvette, whereupon, sea water is viewed by 15 photodiodes arranged between 21.54^o and 158.14 ^{o}. Two additional photodiodes are for laser power monitoring (one in front of the viewing cuvette, and one after the cuvette). The laser beam has a 1/e^2 gaussian beam profile radius of 0.39 mm which makes the effective viewing volume of the light-scattering photometer 0.25 ml. All detectors are scanned at rates up to 400 HZ. For most flow-through applications, we slow the scanning rate to 200 HZ in order to not sample the same sea water volume twice, thus preventing pseudo-replication.

The LabVIEW software, which controls the Wyatt light scattering photometer, can be programmed to calculate averages and standard deviations of the sea water volume scattering function (VSF) over any desired time period. Backscattering of particulate and dissolved material ($b_{b\ p+g}$) is calculated by integrating the VSF in the backwards direction (Fig. 2C; see Balch et al.(1999)). For field applications, we typically average the data for ~50s (which represents an effective volume viewed of 9-12.5 ml). The statistics are highly informative for understanding the optical variability of different particle types. Values of $b_{b\ p+g}$ are well correlated to POC.

Because of our interest in suspended PIC from coccolithophores, we also measure volume scattering before and after dissolution of $CaCO_3$. Following the first 50s of measurements on raw sea water, another peristaltic pump is activated by the LabVIEW control system, which injects 0.5% glacial acetic acid into the flow stream and mixes it in a Teflon mixing coil. This drops the measured pH to ~5.8 to dissolve all $CaCO_3$. Once the pH stabilizes at the more acidic value, volume scattering is re-sampled and average backscattering re-calculated. The difference between the raw and acidified backscattering values represents the "acid-labile" backscattering (b_b'). Using field measurements, we have calibrated this acid-labile backscattering to atomic absorption estimates of suspended calcite concentration (r^2=0.83). The time for a complete acidification cycle can be adjusted, but we typically run one complete raw/acidification cycle every 4 min. This means that during any passage, we would be averaging data over ~2.2 km. For sea-truth measurements, this is adequate since typically a 3 pixel by 3 pixel area from SeaWiFS (10.9 km^2) is averaged for comparison with ship results.

Water next flows into an "ac-9" (Wet Labs, Oregon). This instrument simultaneously measures beam attenuation and absorption at nine wavelengths using a dual path optical scheme. The factory-stated accuracy of the attenuation and absorption measurements is +0.005m^{-1} with linearity error of +0.1%. Pure water values are subtracted in order to derive total particulate and dissolved attenuation (c_{p+g}) and absorption (a_{p+g}) which are then used to derive total particulate and dissolved scattering b_{p+g} (= c_{p+g} - a_{p+g}). An in-line solenoid valve system, upstream of the ac-9, directs flow through a filtration manifold every 2 min., which removes particulate matter bigger than 0.2µm. After another 2 minutes, flow reverts back to unfiltered sea water. Over each 4 minute segment of the voyage, the ac-9 measures the inherent optical properties (a, c and b) of total particulate and dissolved material, as well as just dissolved organic matter (Fig. 4.1

f,g,h). The difference between the two provides the IOPs of the particles only. This filtration manifold saved us from having to purchase and intercalibrate a second ac-9. As stated before, c_{p+g} and b_{p+g} are well correlated to POC.

Flow-through surface water then is viewed by a Hobi Labs HydroScat-2. This instrument is set to view an enclosed, 20-liter, sand-blasted, stainless steel container (painted flat black within). This vessel has a retractable brush inside to sweep bubbles from the viewing window. The instrument measures volume scattering at 140^o and extrapolates to backscattering using an assumed volume scattering function (Maffione and Dana, 1997). It estimates b_b (470 nm and 676 nm; Fig. 4.2b) plus chlorophyll fluorescence, and allows estimation of the wavelength dependence of b_b.

The water finally is run through a FlowCAM (Sieracki et al., 1998) which directs particles through an optical sensing volume (several µl), where it measures chlorophyll and phycoerythrin fluorescence of each particle and particle silhouette (using frame grabbing technology). The image analysis software then uses the particle silhouette to estimate equivalent spherical diameter. Data for each triggering particle are stored for later analysis. FlowCAM derived particle concentrations are within 25% of manual count methods and plots of manual vs. FlowCAM counts have an r^2 of 0.96. Flow CAM particle sizes are highly correlated (r^2=0.996) to manual particle size estimates and derived particle sizes of beads are generally within 2% of the nominal bead size (Sieracki et al., 1998) with resolution down to ~5µm diameter. This instrument provides major advances in our understanding of the size spectrum of particles, as well as the specific species that dominate the algal community along the ferry track, all in real time. A FlowCAM is in constant operation off the Bigelow Laboratory dock. Real-time image data can be viewed at http://www.bigelow.org/flowcam/. Particle volume is well correlated to cellular POC content.

Apparent optical properties

Water-leaving radiance and downwelling irradiance (for calculating remote sensing reflectance) is measured from the *M/S Scotia Prince* ferry using a Satlantic SeaWiFS Aircraft Simulator (SAS). This consists of a down-looking radiance sensor and a sky-viewing radiance sensor, both mounted on the bow (Fig. 4.1d,f). An irradiance sensor is mounted on the compass deck, aft of the bridge, far from any potentially shading structures. The radiance detector views the water at 40^o from nadir as recommended by the NASA SeaBOARR-98 report (Hooker et al., 1999). The distance of the sensor to the water is ~8m. The water radiance sensor can view over an azimuth range of ~200^o and nadir range of 0-90^o. The direction of the sensor is changed manually, as the sun's position changes, so the sensor is viewing the water 90 ^{o} from the sun's azimuth, to minimize sun glint. Protocols for operation and plaque calibration are made according to SeaWiFS Technical Memorandum #25 (Mueller and Austin, 1995) and the NASA SeaWiFS SEABOARR Experiment (Hooker et al., 1999). All data are logged at 16Hz. Before 1000h and after 1400h, data quality is poorer as the solar zenith angle increases. Post-cruise, the 16Hz data are filtered to remove as much residual white cap and glint as possible (we accept the lowest 5% of the data). These data are in good agreement with the SeaWiFS normalized water-leaving radiances Fig.4.2d and i). In addition, we also take Microtops sun photometer measurements when the sun is visible, in order to estimate aerosol optical depth.

Hydrographic Information

Temperature and salinity of the surface flow stream is measured with an InterOcean thermal conductivity sensor. It measures salinity with an accuracy of +0.05 Practical Salinity Units and temperature to an accuracy of +0.1^{o}C. (Fig. 4.2a)Hourly XBT profiles are used to construct one temperature section per trip from which we can calculate isotherm slope (strongly related to gradients in integrated primary production and chlorophyll).

Calibration

Calibration of the Satlantic radiance sensors is done annually. We also check the calibration of the radiance sensors using a 1.8% reflectance Spectralon plaque. Typical variability of the plaque values was ~+/- 0.2-0.3%. The ac-9 was given a dry calibration at the beginning of each cruise, a wet calibration (using 0.2µm filtered, de-ionized water) at the beginning and end of each cruise, as well as annual factory calibrations. These data showed that the absorption calibrations were good to ~0.005 m^{-1} and the c calibrations were good to ~0.01-0.02 $m^{-1.}$ The Wyatt light scattering photometer calibration was checked before and after each cruise with 0.02µm pore-size filtered HPLC-grade distilled water. The water backscattering calibrations were good to within +/-1 x 10^{-4} m^{-1}. Absolute calibrations of the 90^o detector were performed with methanol and the calibration of the remaining detectors was done (relative to the 90^o detector) using Dextran solution, which scatters isotropically. Comparison of pre- and post-cruise calibrations of the ac-9 and Wyatt light scattering photometer allowed us to account for instrument bio-fouling. The Hobi Labs Hydroscat 2 received annual factory calibrations.

Discrete Samples

Hourly, a surface water sample is taken for suspended $CaCO_3$, particulate organic carbon, chlorophyll, and microscope counts. The technique of Fernandez et al. (1993) is used to measure $CaCO_3$ concentrations. Briefly, 100 ml samples are filtered onto 0.4µm pore-size polycarbonate filters and rinsed first with filtered sea water, then borate buffer (pH=8) to remove sea water calcium chloride. Later, filters are placed in trace metal free centrifuge tubes with 5 ml 0.5% Optima grade nitric acid and the Ca concentration is measured

using an inductively-coupled plasma optical emission spectrometer (Scripps Inst. of Oceanography Analytical Facility). Chlorophyll and particulate organic carbon samples are filtered through H/A and baked GF/F filters, respectively, and measured according to the JGOFS protocols (JGOFS, 1996). We participated in the SIMBIOS-sponsored round robin on pigment measurements. A sampling of SeaWiFS-derived chlorophyll *a* versus ship-derived chlorophyll *a* for Gulf of Maine samples is shown in Fig. 4.2i. The OC-4 algorithm(O'Reilly et al., 1998) has made a dramatic improvement over the OC-2 algorithm in accuracy of chlorophyll predictions, but there is still a general overestimate by SeaWiFS (Fig. 4.1e).

Microscope enumeration of coccolithophores and coccoliths is done by filtering a 50ml water sample through a Millipore HA filter, rinsed with borate buffer, and frozen in a petri dish until counted (Haidar and Thierstein, unpublished-a; Haidar and Thierstein, unpublished-b). The filter is placed on a glass microscope slide, and 60°C Canada Balsam is placed on top of the filter, followed by a cover slip. The clarified filter is examined with an Olympus BH2 microscope equipped with polarization optics. Birefringent coccoliths and plated coccolithophores can then be counted. For statistical reasons, 200 coccoliths or cells are counted from each sample, when available.

Data manipulation

The types of continuous underway data collected during the Gulf of Maine SIMBIOS program are summarized in Table 4.1 with their appropriate units:

Table 4.1- Summary list of variables collected from the proposed Gulf of Maine test-site data set.

Underway Variable	*Unit*	*Details*
time		decimal calendar day (EDT and GMT)
latitude, longitude	°N, °W	Logged on GPS
temperature	°C	
salinity	PSU	
total upwelling radiance	$\mu W\ cm^{-2}\ nm^{-1}\ sr^{-1}$	412, 443, 490, 510, 555, 670 & 685 nm
downwelling irradiance	$\mu W\ cm^{-2}\ nm^{-1}$	412, 443, 490, 510, 555, 670 & 685nm
sky radiance	$\mu W\ cm^{-2}\ nm^{-1}$	412, 443, 490, 510, 555, 670 & 685nm
fluorescence	mg chl a m^{-3}	calibrated to hourly discrete chlorophyll samples;
absorption	m^{-1}	412, 440, 488, 510, 555, 630, 650, 676 and 715 nm; partic & dissolved
attenuation	m^{-1}	412, 440, 488, 510, 555, 630, 650, 676 and 715 nm; partic & dissolved
scattering(derived)	m^{-1}	412, 440, 488, 510, 555, 630, 650, 676 and 715nm; partic & dissolved
backscattering (total/acid-labile)	m^{-1};	total b_b at 470, 514 and 676 nm; acid labile backscattering at 514nm.
particle size spectrum	µm	size histogram and slope, calculated each 1/2h of cruise
particle image files		particle collages available for each 1/2h of cruise
Hourly Depth Profiles		
Temperature	°C	XBT profiles

Maintenance of Public Database:

All of our data from the previous year have been released to SEABASS. The data from the 2000 ferry trips are being finalized now, with final checks of vicarious calibrations. They will be released to SEABASS shortly. A summary of the number of data points and satellite match-ups are given in Table 4.2.

4.3 CONCLUSIONS

We exceeded our cruise requirements outlined in our original contract (performing 42 days of validation work, not 40). The additional two trips were funded by NOAA-NESDIS. We anticipate no problems in timely data work-up and submission as our processing software is well streamlined for post-cruise calibrations. We requested a no-cost extension in order to complete all the post-cruise calibration checks. Moreover, with three years of sampling completed, we will begin the summary publications about our findings. We will ship the Microtops radiometer back to Goddard soon, now that our third, and final field season is completed. The personnel of the Prince of Fundy, Ltd ferry company have been superb to work with; none of this work could have been accomplished without their exemplary "can-do" attitude. They installed a non-toxic, stainless steel pipe off of their sea chest, so we did not have to install our sampling arm during year three (the sample arm performed well for 30 trips, or ~9 thousand km with only one failure). This streamlined our operation *significantly* in the last year. Over the 42 trips, we achieved an average of ~83% success rate in sampling under clear skies. In all, we provided ocean color sea-truth data over 13,230 km, with over 3,600 satellite match-ups (Table 4.3).

Table 4.2 Summary of Gulf of Maine data taken from *M/S Scotia Prince*, over 3 years of Balch NASA SIMBIOS contract. Each measurement of optical properties, hydrography, or chlorophyll represents an average over ~2.2 kilometers of horizontal distance.

Activity	**1998**	**1999**	**2000***	**Total**
# cruises	10	20	12	42
#Lw,Ed SAS	867	3116	1440	5423
#ac-9	1388	2917	1440	5745
#bb(Wyatt)	1460	3290	1440	6190
#bb (HS-II)	0	3290	1440	4730
#Temp/Sal	1460	3290	1440	6190
#XBT Profiles(1/h)	85	171	96	352
#chl's	1421	3290	1440	6151
# chl Match-ups (+/-6h) with SeaWiFS**	**760**	**1779**	**1080**	**3619**

Note: *Data values for 2000 are best estimates (final calibration checks and data quality checks are being done over the next few months); ** Includes only SeaWiFS match-ups. Does not include MODIS match-ups, which may double the 2000 value.

Table 4.3 List of cruises and deliverables for FY'00 Balch SIMBIOS contract.

Cruise Location	Ferry Cruise #	Date (2000)	Fluorescence	Backscattering Wyatt&Hobi Labs	Calcite-dependent backscattering	Absorption	Scattering	Temperature	Microtops sun photometer	Stations	Suspended CaCO3	Chlorophyll	POC/PON	Conc. Coccoliths & Coccolithophores	Flow Cam (spp & size)	XBT's	Lt, Lsky, Ed, & nLw (Satlantic SAS)
Portland, Maine and Yarmouth (NS)	1	4 June	✓	✓*	✓	✓	✓	✓	✓	8	✓	✓	✓	✓	✓	✓	✓
Portland, Maine and Yarmouth (NS)	2	13 June	✓	✓	✓	✓	✓	✓	✓	8	✓	✓	✓	✓	✓	✓	✓
Portland, Maine and Yarmouth (NS)	3	20 June	✓	✓	✓	✓	✓	✓	✓	10	✓	✓	✓	✓	✓	✓	✓
Portland, Maine and Yarmouth (NS)	4	21 June	✓	✓	✓	✓	✓	✓	✓	8	✓	✓	✓	✓	✓	✓	✓
Portland, Maine and Yarmouth (NS)	5	24 June	✓	✓	✓	✓	✓	✓	✓	9	✓	✓	✓	✓	✓	✓	✓
Portland, Maine and Yarmouth (NS)	6	2 July	✓	✓	✓	✓	✓	✓	✓	10	✓	✓	✓	✓	✓	✓	✓
Portland, Maine and Yarmouth (NS)	7	11 July	✓	✓	✓	✓	✓	✓	✓	10	✓	✓	✓	✓	✓	✓	✓
Portland, Maine and Yarmouth (NS)	8	12 July	✓	✓	✓	✓	✓	✓	✓	9	✓	✓	✓	✓	✓	✓	✓
Portland, Maine and Yarmouth (NS)	9	22 Aug	✓	✓	✓	✓	✓	✓	✓	9	✓	✓	✓	✓	✓	✓	✓
Portland, Maine and Yarmouth (NS)	10	29 Aug	✓	✓	✓	✓	✓	✓	✓	9	✓	✓	✓	✓	✓	✓	✓
Portland, Maine and Yarmouth (NS)	11	14 Sept	✓	✓	✓	✓	✓	✓	✓	9	✓	✓	✓	✓	✓	✓	✓
Portland, Maine and Yarmouth (NS)	12	30 Sept	✓	✓	✓	✓	✓	✓	✓	8	✓	✓	✓	✓	✓	✓	✓
Total Stations										107							

✶Data from the Wyatt light scattering photometer are available but the Hobi Lab Hydroscat II was not functioning cruise.

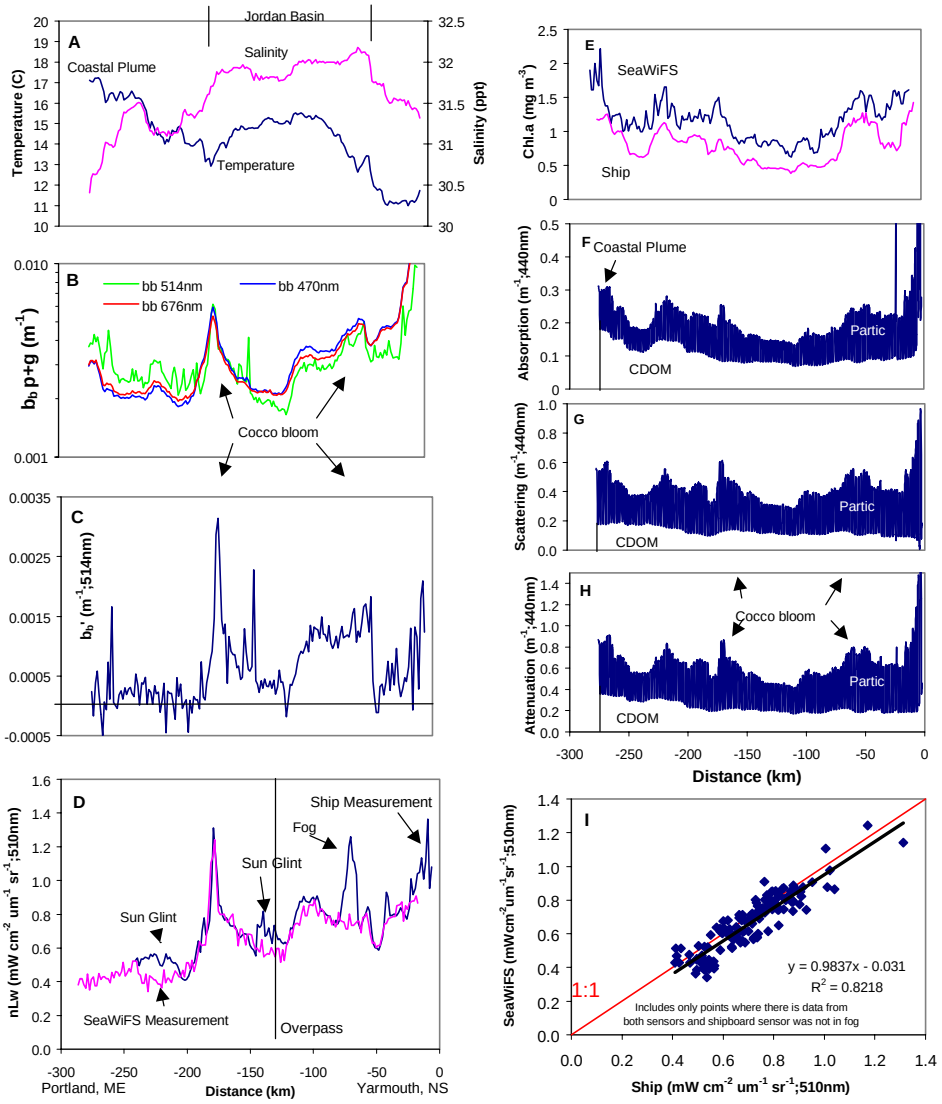

Figure 4.1 Representative data taken from July 2, 2000 transect through Gulf of Maine coccolithophore bloom. Distance from Yarmouth, NS is on the X axis for panels A-H. A) Surface temperature and salinity. The eastern Maine coastal current and Jordan Basin water are indicated. B) Backscattering measured by the Wyatt light scattering photometer (514nm; based on 15 point volume scattering functions) and Hydroscat II (470 and 676nm; based on volume scattering at one angle). Water values have been subtracted, thus b_b values are from particulate and dissolved material. It can be seen that the Wyatt data show higher frequency variability than the HSII, which is due to the smaller viewed volume (9ml vs 20L!). Moreover, both instruments clearly show similar trends, but their relative values vary, possibly due to changing shape of the VSF (which is not taken into consideration with the HSII, but is with the Wyatt). The coccolithophore bloom is plainly visible on either side of the stratified Jordan Basin (60 and 170km). C) Acid-labile backscattering (b_b'; measured with the Wyatt instrument), due to calcium carbonate. Values in coastal current are not significantly different from zero (FlowCAM showed the algal assemblage consisted of diatoms and dinoflagellates, with few coccolithophores. The ship moves 1.2 km during each 4' acidification cycle. Occasional negative b_b' values can result if phytoplankton b_b values *increase* (due to horizontal variability) during an acidification cycle (when b_b values should *decrease* due to $CaCO_3$ dissolution). In the coccolithophore bloom, calcite b_b' represented ~50% of the total backscattering (compare with panel C). D) Satlantic radiometer data for normalized water-leaving radiance compared with SeaWiFS values. At 60km, the ship passed through a fog bank, causing higher nLw values.

Significantly increased nLw in the coccolithophore bloom was evident. E) Fluorescence- and SeaWiFS-derived (OC4) chlorophyll concentrations. One can see that the OC4 algorithm generally overestimates chlorophyll by ~0.25µg l^{-1} in the Gulf of Maine. F,G,H) IOP data on absorption, scattering, and attenuation taken with ac-9. Pure water values subtracted. The blue region represents particle IOPs (>=0.2µm filterred), and the white region below represents the cDOM IOPs (< 0.2µm diameter). One can see the increased cDOM a, b, and c in the Eastern Maine coastal current. Also apparent in Jordan Basin, 1/2 of the absorption, and 1/3 of the scattering is from cDOM. Scattering and absorption peaks clearly evident in the coccolithophore bloom. I) SeaWiFS vs Ship measured nLw 440nm. Least-squares fit to the data has a slope which is not significantly different from 1.0.

REFERENCES

Balch, W.M., Drapeau, D.T., Cucci, T.L., Vaillancourt, R.D., Ki4patrick, K.A. and Fritz, J.J., 1999: Optical backscattering by calcifying algae--Separating the contribution by particulate inorganic and organic carbon fractions. *Journal of Geophysical Research* **104**, 1541-1558.

Bisagni, J.J., Gifford, D.J. and Ruhsam, C.M., 1996: The spatial and temporal distribution of the Maine Coastal Current during 1982. *Continental Shelf Research*, 1-24.

Femindez, E., Boyd, P., Holligan, P.M. and Harbour, D.S., 1993: Production of organic and inorganic carbon within a large scale coccolithophore bloom in the northeast Atlantic Ocean. *Marine Ecology Progress Series*, **97**, 271-285.

Haidar, A.T. and Thierstein, H.R., unpublished-a. Calcareous phytoplankton standing stocks, fluxes and accumulation in Holocene sediments off Ben-nuda (N. Atlantic). .

Haidar, A.T. and Thierstein, H.R., unpublished-b. Living calcareotis phytoplankton dynamics off Bermuda (N. Atlantic).

Hooker, S.B., Zibordi, G., Lazin, G. and McLean, S., 1999. The SeaBOARR-98 Field Campaign, SeaWiFS Postlaunch Technical Report Series, Vol. **3**. NASA, Greenbelt, MD, 40 pp.

JGOFS, 1996. Protocols for the Joint Global Ocean Flux Study (JGOFS) core measurements. Report no. 19 of the Joint Global Ocean Flux Study, Scientific Committee on Oceanic Research, International Council of Scientific Unions Intergovernmental Oceanographic Commission, Bergen, Norway, 170 pp.

Maffione, R.A. and Dana, D.R., 1997. Instruments and methods for measuring the backward-scattering coefficient of ocean waters. *Applied Optics* , **36**(24), 6057-6067.

Mueller, J.L. and Austin, R.W. (Eds.), 1995. Ocean optics protocols for SeaWiFS validation, Revision. 1, SeaWiFS Technical Report Series, Vol**. 25**. NASA Goddard Space Flight Center, Greenbelt, MD, 67 pp.

O'Reilly, J.E. and Busch, D.A., 1984: Phytoplankton primary production on the northwestern Atlantic shelf. Rapp. P. -v. R6un. Cons. int. *Explor. Mer*, **183**, 255-268.

O'Reilly, J.E., Evans-Zetlin, C. and Busch, D.A., 1987: Primary production. In: Backus, R.H., Bourne, D.W. (Eds.), Georges Bank, Massachusetts Institute of Technology, Boston, pp. 220-233.

O'Reilly, J.E., Maritorena, S., Mitchell, B.G., Siegel, D.A., Carder, K.L., Garver, S.A., Kahru, M. and McClain, C., 1998: Ocean color chlorophyll algorithms for SeaWiFS. *Journal of Geophysical Research*, **103**(Cl 1), 24937-24953.

Sieracki, C.K., Sieracki, M.E. and Yentsch, C.S., 1998: An imaging-in-flow system for automated analysis of marine microplankton. *Marine Ecology Progress Series***, 168**, 285-296.

This research was supported by the

SIMBIOS NASA contract # 97268

PEER REVIEWED PUBLICATION

Balch, William M., David T. et al. 1999: Optical backscattering by calcifying algae-Separating the contribution by particulate inorganic and organic carbon fractions *J. Geophys. Res*. 104: 1541-1558.

Gordon, Howard R., G. Chris Boynton, William M. Balch, Stephen B. Groom, Derek S. Harbour , and Tim J. Smyth. 2000: Retrieval of Coccolithophore Calcite Concentration from SeaWiFS Imagery. Geophysical Research Letters (in press).

PRESENTATIONS

Balch, B., D.T. Drapeau, et al. 1998: Backscattering of Light by Calcium Carbonae and Organic Matter in the Sea. EOS, Trans AGU, 79:OS7.

Balch, W. M., Drapeau, D. T., Bowler, B., Ashe, A., Vaillancourt, R., Dunford, S., and Graziano, 1999: Backscattering probability and calcite-dependent backscattering in the Gulf of Maine. Proceedings of the ASLO Meeting, Santa Fe.

Balch, W.B., H. R. Gordon, D. T. Drapeau, B. C. Bowler, A. L. Ashe, J. I. Goes, and H. M. Gomes, 1999: PIC:POC and the Remote Sensing of Biogenic Carbon in the Sea. In press Trans. AGU.

Balch, W., D. Drapeau, B. Bowler, A. Ashe, J. Goes, E. Scally. 2000. Anatomy of a coccolithophore bloom. Presented at "Oceans from Space, Venice, 2000", Venice, Italy, 9-13 Oct, 2000. European Communities, 2000. V. Barale, J. F. R. Gower, and L. Alberotanza Convenors.

Chapter 5

OCTS and SeaWiFS Bio-Optical Algorithm and Product Validation and Intercomparison in U.S. Coastal Waters

Christopher W. Brown
NOAA/NESDIS, Camp Springs, Maryland

Ajit Subramaniam
University of Maryland, College Park, Maryland

Mary Culver
NOAA Coastal Services Center, Charleston, South Carolina

John C. Brock
USGS Center for Coastal Geology, St. Petersburg, Florida

5.1 INTRODUCTION

Monitoring the health of U.S. coastal waters is an important goal of the National Oceanic and Atmospheric Administration (NOAA). Satellite sensors are capable of providing daily synoptic data of large expanses of the U.S. coast. Ocean color sensor, in particular, can be used to monitor the water quality of coastal waters on an operational basis. To appraise the validity of satellite-derived measurements, such as chlorophyll concentration, the bio-optical algorithms used to derive them must be evaluated in coastal environments. Towards this purpose, over 21 cruises in diverse U.S. coastal waters have been conducted (Subramaniam *et al.*, 1997a, 1997b, 1997c, 1998, 1999, 2000a, 2000b; Culver *et al.* 1998; Kiambo *et al.* 1999). Of these 21 cruises, 12 have been performed in conjunction with and under the auspices of the NASA/SIMBIOS Project. The primary goal of these cruises has been to obtain *in-situ* measurements of downwelling irradiance, upwelling radiance, and chlorophyll concentrations in order to evaluate bio-optical algorithms that estimate chlorophyll concentration.

In this Technical Memorandum, we evaluate the ability of five bio-optical algorithms, including the current SeaWiFS algorithm, to estimate chlorophyll concentration in surface waters of the South Atlantic Bight (SAB). The SAB consists of a variety of environments including coastal and continental shelf regimes, Gulf Stream waters, and the Sargasso Sea. The biological and optical characteristics of the region is complicated by temporal and spatial variability in phytoplankton composition, primary productivity, and the concentrations of colored dissolved organic matter (CDOM) and suspended sediment. As such, the SAB is an ideal location to test the robustness of algorithms for coastal use.

5.2 RESEARCH ACTIVITIES

Sampling Location and Collection Methods

Bio-optical measurements were collected at over 100 stations during nine cruises (Table 5.1) conducted in the South Atlantic Bight in order to evaluate and validate the five algorithms. The cruises were conducted from early spring to late fall in optically diverse waters ranging from the extremely shallow and turbid Pamlico Sound to the deep and clear Sargasso Sea (Figure 5.1). Optical instruments measured surface spectral downwelling irradiance, in-water spectral downwelling irradiance, and upwelling radiance.

Although sampling strategies and instrument packages varied between cruises, a Biospherical Instruments Profiling Reflectance Radiometer (PRR) cage was typically deployed off the stern of the vessel in conjunction with a reference surface unit with matching channels. Surface bucket samples were obtained for total suspended solids (TSS) concentration and for chlorophyll analysis by fluorometric and High-Pressure Liquid Chromatography (HPLC) techniques. Detailed descriptions of instruments and other ancillary measurements are presented in Subramaniam *et al.* (1997a, 1997b, 1997c, 1998, 1999, 2000a, 2000b) and Culver *et al.* (1998).

Table 5.1 Summary of cruise names, location, dates and sampling platforms.

Cruise	Dates	Number of Stations	Location	Vessel
FEB96LIT	22-23 Feb. 1996	7	Georgia Bight	*R/V Blue Fin*
APR96BF	3-5 Apr. 1996	18	Georgia Bight	*R/V Blue Fin*
APR96FER	22-25 Apr. 1996	16	Georgia Bight	*R/V Ferrel*
MAY97OB	5 May 1997 8 May 1997	5 4	Onslow Bay, NC, Pamlico Sound, NC	*R/V Onslow Bay, R/V Chipman*
SEP97SAB	5-24 Sept. 1997	11	South Atlantic Bight	*R/V Cape Hatteras*
NOV97SAR	4, 5 Nov. 1997	16	Saragasso Sea	*R/V Pametto*
APR98SAB	5-27 April 1998	23	South Atlantic Bight	*R/V Cape Hatteras*
NOV98SAB	27 Oct-23 Nov 1998	50	South Atlantic Bight	*R/V Cape Hatteras*
FEB99SAB	27 Jan–24 Feb 1999	11	South Atlantic Bight	*R/V Cape Hatteras*

Water Sample Analyses

Discrete water samples were collected following the PRR cast from the sea surface using a bucket or a Niskin bottle and filtered through glass fiber (GF/F) filters. The chlorophyll samples were cold extracted in 10 ml of 90% acetone (10% water) for 24 hours in the dark and the biomass was determined fluorometrically with a Turner Designs fluorometer as described in Subramaniam *et al.* (1998). The TSS concentration was measured as described by Parsons *et al.*, (1984). For cruises FEB96LIT, APR96BF, APR96FER, and NOV97SAR, chlorophyll *a* and other pigments were determined as described in Subramaniam *et al.* (1997). For the MAY97OB, SEP97SAB, APR98SAB and NOV98SAB cruises, chlorophyll *a* and other pigments were determined as described in Tester *et al.* (1995).

Quality Control

The PRR optical data were processed using the Bermuda Bio-Optics Project (BBOP) processing software (Siegel *et al.*, 1995). All optical profiles were graphed and examined. Profiles that exhibited evidence of surface perturbations, such as ship shadow, and the effects of passing clouds were excluded from further analysis. The *in-situ* downwelling irradiance (Ed-) was propagated through the water-air interface to Ed+ using a transmission loss of 4% (O'Reilly *et al.*, 1998). The *in-situ* upwelling radiance (Lu-) was propagated through water-air interface to water-leaving radiance (Lu+ or Lw) using a factor of 0.544 (O'Reilly *et al.*, 1998). The coefficient of variation (EsλErr) of the above-water downwelling irradiance Es (λ) measured by the reference sensor mounted on the ship was calculated as the ratio of the standard deviation to the mean of the Es(λ) measurements for the duration of the PRR600 profile. Es from profiles where EsλErr was greater than 10% (indicating either passing clouds or large ship roll) was not used in calculating remote sensing reflectance. The difference (dsλ) between the measured downwelling irradiance (Es) and the calculated downwelling irradiance (Ed+) was calculated and profiles with dsλ greater than 50% were excluded from analysis. Several other stations that possessed peculiar spectra were also eliminated. The remote sensing reflectance $R_{rs}(\lambda)$ and normalized water-leaving radiances nLw (λ) were calculated as

$$R_{rs}(\lambda) = 0.544 * \frac{L_u(0^-, \lambda)}{E_s(\lambda)}$$

and

$$nLw(\lambda) = F_0 * R_{rs}(\lambda)$$

Algorithm Evaluation

Optical profiles from a total of 88 stations were used to evaluate the five bio-optical algorithms developed to estimate surface chlorophyll concentration from satellite ocean color observations. These algorithms included the current SeaWiFS algorithm (OC4v4; O'Reilly *et al.*, 2000), the previous SeaWiFS algorithm and its improvement (OC2v4 and OC2v2; O'Reilly *et al.*, 1998), an algorithm proposed for the Southeastern United States (OCse; Stumpf *et al.*, 2000), and a semi-analytical algorithm based on Garver and Siegel's inverse model (UCSB; Garver and Siegel, 1997; Maritorena *et al.*, 2000). OCse is an empirical algorithm developed using data collected from highly absorbing waters of the Gulf of Mexico. The semi-analytical algorithm (UCSB) was selected because it explicitly estimates backscatter and CDOM absorption, in addition to chlorophyll concentration, and had the potential of reducing the error attributed to high concentrations of suspended sediments and riverine contribution of CDOM found in the South Atlantic Bight. The formulations used for each algorithm to calculate chlorophyll concentration were as follows:

$$(OC4v4)Chl = 10^{\left(0.336 - 3.067X + 1.930X^2 + 0.649X^3 - 1.532X^4\right)},$$

where $$X = \log\left(\frac{R_{rs}(443)}{R_{rs}(555)} > \frac{R_{rs}(490)}{R_{rs}(555)} > \frac{R_{rs}(510)}{R_{rs}(555)}\right).$$

$$\text{OC2v2Chl} = -0.0929 + 10^{\left(0.2974 - 2.2429X + 0.8358X^2 - 0.0077X^3\right)},$$

where $$X = \log\left(\frac{R_{rs}(490)}{R_{rs}(555)}\right).$$

$$\text{OC2v4Chl} = -0.071 + 10^{\left(0.319 - 2.336X + 0.879X^2 - 0.135X^3\right)},$$

where $$X = \log\left(\frac{R_{rs}(490)}{R_{rs}(555)}\right).$$

$$OCseChl = 10^{\left(-2.5\log\left(\frac{R_{rs}(490)}{R_{rs}(555)}\right)\right)}.$$

OCse is valid only in (coastal) regions of high chlorophyll concentration (Stumpf *et al.*, 2000). For regions possessing low chlorophyll concentrations, the OC4v4 algorithm was applied. For regions containing moderate chlorophyll concentrations, a log-transformed weighting was used to shift from OC4v4 (low chlorophyll waters) to OCse (high chlorophyll concentrations). The transform was applied based on the following criteria:

a) OCseChl < 0.1 mg/m^3, chlorophyll = OC4v4Chl (OC4v4Chl ~ 0.2 mg/m^3)

b) mg/m^3 < OCseChl < 0.5 mg/m^3, chlorophyll=

$$OCseChl = 10^{\left(\log(OCse)*\frac{\log(OCse)-\log(0.1)}{\log(0.5)-\log(0.1)}+\log(OC4v4)*\frac{\log(0.5)-\log(OCse)}{\log(0.5)-\log(0.1)}\right)}$$

c) OCseChl > 0.5 mg/m^3, chlorophyll = OCseChl

The logarithmic weighting was used as the OC4v4 and OCse algorithms are both in terms of log(Chl). The results remove the bias found between OC4v4 and the measured chlorophyll. A simple linear regression analysis between measured chlorophyll and algorithm chlorophyll in log space was performed to evaluate the algorithms. Only fluorometrically determined chlorophyll concentrations (ChlF) were employed in this evaluation. Typical measures of goodness-of-fit between *in-situ* chlorophyll concentrations and modeled retrievals, such as the coefficient of determiniation, r^2, were calculated and examined. In addition, an Algorithm Performance Index (API) was calculated as the log of the ratio of algorithm derived chlorophyll to measured chlorophyll. Consequently, an API value of 0 indicates that the algorithm predicted the measured chlorophyll concentration, a negative value indicates the algorithm underestimated chlorophyll, and a positive indicates the algorithm overestimated chlorophyll.

5.3 RESEARCH RESULT

Bottle Samples

In-situ chlorophyll (ChlF) values ranged from 0.16 to 5.20 μg/L with mean value of 1.51 μg/L and a median value of 1.03 μg/L. While many of the high chlorophyll stations lay along the coast and the low chlorophyll (0-1 μg/L) stations were situated along the outer shelf, no distinct spatial pattern was discernible in the *in-situ* chlorophyll concentrations (Figure 5.2). The absence of any obvious pattern in chlorophyll concentration is likely due to the temporal span over which the data were collected and the dynamic nature of phytoplankton biomass in the SAB. For example, surface chlorophyll concentration at a station located at the shelf break in September 1997 was 0.33 μg/L while a station occupied at the same position in November 1998 was 1.11 μg/L. This large variation could be attributable to interactions of the Gulf Stream with the shelf waters (McClain *et al.* 1984).

Algorithm Validation and Evaluation

Comparisons of measured and algorithm-derived estimates of chlorophyll concentration are illustrated in Figures 5.3 and 5.4. Figure 5.3 illustrates the frequency distribution of both measured and algorithm-derived values of chlorophyll concentration (ChlF) observed during our cruises in the South Atlantic Bight. In general, OC2v2 performed well at lower chlorophyll concentrations (up to 0.3 mg m^{-3}). As expected, OCse performed well in the high chlorophyll range (> 0.5 mg chl m^{-3}), with the shape of its cumulative frequency similar to that of in-situ chlorophyll concentration at values of 1 mg chl m^{-3} and greater. The overestimation in the 0.3 to 0.5 mg m^{-3} range is potentially due to the logarithmic weighting over this concentration interval. UCSB also exhibits roughly the same cumulative frequency shape as *in-situ* chlorophyll at higher chlorophyll concentrations, though it is less sigmoidal. Analysis of OC2v4, the "improved" version of OC2v2, performed substantially worse than its predecessor and was not presented.

Results of least-squares regression analysis are presented in Table 5.2. Of the five algorithms evaluated for the SAB, UCSB possessed the slope closest to 1.00 (slope = 1.036). All algorithms except OC4v4 displayed similar intercepts with a mean of 0.27 (n=4). The intercept of OC4v4 was almost twice as great (0.5). OC4v4, however, received the highest coefficient of determination (r^2 = 0.72), while UCSB received the lowest (r^2 = 0.52). The overall performance of UCSB was degraded by a few model retrievals that severely underestimated actual chlorophyll concentration (Fig. 5.4).

Table 5.2 Results of regression analysis for each algorithm.

Algorithm	OC2v2	OC2v4	OC4v4	OCse	UCSB
Slope	1.361	2.660	0.931	0.699	1.036
Intercept	0.288	0.299	0.503	0.236	0.269
r^2	0.693	0.644	0.721	0.695	0.523

Examining the Algorithm Performance Index (API) of the algorithms for all data indicated that OC2v2, OC2v4, and OC4v4 overestimated actual chlorophyll concentrations to

varying degrees, while OCse and UCSB underestimated them (Table 5.3). Average API values for UCSB suggest it performed very well. This result, however, was fortuitous. Close examination revealed that the "mean" value was achieved by averaging the overestimates and underestimates of individual measurements.

Dividing the data collected in "spring" (February-May) and "non-spring" (June-January) months indicated a seasonal component to algorithm performance (Table 5.3). Algorithms generally performed better, i.e. API approached 0, during the non-spring months. During the spring, all algorithms overestimated measured chlorophyll concentrations (Table 5.3). This overestimation is likely to result from increases in CDOM concentration (and absorption) caused by elevated river discharge into the SAB during the spring. The spatial distribution and number of stations in the spring and non-spring periods were similar, eliminating geographic bias.

5.4 CONCLUSIONS

We evaluated the performance of five chlorophyll *a* algorithm in the South Atlantic Bight by comparing radiometrically-derived chlorophyll concentrations and *in-situ* chlorophyll concentrations. The results indicate that biogeographical provinces alone do not improve algorithm performance in the SAB. Seasonal variation must be taken into account. The high variability observed in spring is likely due to the presence of high concentrations of CDOM in shelf waters. Consequently, we expected that an algorithm that accounts for CDOM is necessary to accurately estimate chlorophyll concentration in the South Atlantic Bight. It is therefore surprising that UCSB, the algorithm that explicitly solves for CDOM absorption, does not perform well in the SAB. It's poor performance may be due to several reasons. One, it requires accurate measurements from 412 to 555 nm. In waters containing high concentrations of CDOM, in which the signal at 412 and 443 nm are very low, small errors in the propagation of Lu through the surface may generate large errors in the estimated chlorophyll concentration. Two, the algorithm is driven by a statistical tuning that is based on a large number of pixels that may not be appropriately analyzed by individual measurements. OCse, the regional algorithm, worked reasonably well in the SAB and may be improved by changing the structure of its log-transformed weighting function over the chlorophyll concentration range of 0.3 - 0.5 mg m^{-3}.

ACKNOWLEDGEMENTS

In addition to funding provided by the NASA/SIMBIOS Project, this work was accomplished in partnership with many agencies and institutions, including the National Marine Fisheries Service Southeast Fisheries Science Center, Grice Marine Laboratory of the College of Charleston, Skidaway Institute of Oceanography. We sincerely thank Dr. P. Tester for the use of her data and her invaluable participation in all aspects of this project.

Table 5.3 Mean chl. concentration (ChlF) & Algorithm Performance Index (API) for each algorithm by cruise and season.

Cruise	ChlF	API OC2v2	API OC2v4	API OC4v4	API OCse	API UCSB
SEP97SAB	2.048	0.028	0.108	0.022	-0.176	0.039
MAY97OB	1.977	0.133	0.219	0.091	-0.049	-0.043
NOV97SAR	0.227	0.113	0.054	0.165	0.084	-0.040
NOV98SAB	1.042	-0.090	-0.097	-0.041	-0.227	-0.134
Non-Spring	1.314	-0.002	0.019	0.020	-0.129	-0.077
APR98SAB	1.619	0.348	0.507	0.278	0.077	0.041
APR96FER	1.943	0.218	0.349	0.151	-0.049	-0.008
FEB96LIT	1.134	0.531	0.622	0.527	0.249	0.552
FEB99SAB	0.784	0.129	0.162	0.073	-0.016	0.103
Spring	1.533	0.276	0.397	0.214	0.034	0.079
Total	1.421	0.132	0.202	0.114	-0.062	-0.003

REFERENCES

Culver, M.E., A. Subramaniam, J.C. Brock, M.E. Geesey, G.R. DiTullio, D. Jones, 1998: NOAA CSC/CRS Cruise NOV97SAR: Sargasso Sea Cruise. CSC Technical Report CSC/9-98/002. U.S. Department of Commerce, National Oceanic and Atmospheric Administration, Coastal Services Center, Charleston, SC.

Garver, S. A. and D. A. Siegel, 1997: Inherent optical property in version of ocean color spectra and its biogeochemical interpretation. 1. Time series from the Sargasso Sea.

Journal of Geophysical Research **102**(C8), 18,607-18,625.

Kiambo, R. W., M. E. Culver, P. A. Tester, R.P.Stumpf, A. Subramaniam, J. C. Brock and D. Eslinger, 1999: NOAA Cruise APR98SAB: South Atlantic Bight Cruise. CSC Technical Report. CSC/1-99/001. U.S. Department of Commerce, National Oceanic and Atmospheric Administration, Coastal Services Center, Charleston, SC.

McClain, C.R., L.J. Pietrafesa, and J.A. Yoder, 1984: Observations of Gulf Stream-induced and wind-driven upwelling in the Georgia Bight using ocean color and infrared imagery. *Journal of Geophysical Research* **89**: 3705-3723.

Maritorena, S., Siegel, D.A., Peterson, A.R. & Lorenzi-Kayser, M. 2000: Tuning of a pseudo-analytical ocean color algorithm for studies at global scales. Presented at the 2000 AGU Ocean Sciences Meeting (OS12M-05), San Antonio TX, 2000

O'Reilly, J. E., S. Maritorena, B. G. Mitchell, D. A. Siegel, K. L. Carder, S. A. Garver, M. Kahru and C. McClain, 1998: Ocean color chlorophyll algorithms for SeaWiFS." *Journal of Geophysical Research* **103** (C11): 24937-24953.

O'Reilly, J. E., and et al. , 2000: Ocean color chlorophyll *a* algorithms for SeaWiFS, OC2 and OC4: Version 4. SeaWiFS Postlaunch Calibration and Validation Analyses, part 3. NASA SeaWiFS technical report series. pp. 8 – 22.

Parsons, T. R., Y. Maita and C. M. Lalli , 1984: *A Manual For Chemical And Biological Methods For Seawater Analysis*, Pergamon Press.

Siegel, D.A., M.C. O'Brien, J.C. Sorensen, D.A. Konnoff and E. Fields, 1995: BBOP Data Processing and Sampling Procedures. Vol: 19, Institute for Computational Earth System Science, UC Santa Barbara, Santa Barbara, CA, 23pp.

Stumpf, R. P., R. A. Arnone, R. W. Gould, P. Martinolich, V. Ransibrahmanakul, P. A. Tester, R. G. Steward, A. Subramaniam, M. E. Culver and J. R. Pennock, 2000: SeaWiFS Ocean Color Data For U.S. Southeast Coastal Waters. Sixth International Conference on Remote Sensing for Marine and Coastal Environments, Charleston, SC, Veridian ERIM International.

Subramaniam, A., E.M. Armstrong, K.J. Waters, J.C. Brock, P.A. Tester, E.Haugen. 1997a: NOAA CSC/CRS Cruise MAR97OCC: OCTS Calibration Cruise. CSC Technical Report CSC/5-97/001. U.S. Department of Commerce, National Oceanic and Atmospheric Administration, Coastal Services Center, Charleston, SC.

Subramaniam, A., E.M. Armstrong, K.J. Waters, J.C. Brock, A.W. Meredith, R.O. Ranheim. 1997b: NOAA CSC/CRS Cruise MAY96NY: New Bight Apex Cruise. CSC Technical Report CSC/6-97/001. U.S. Department of Commerce, National Oceanic and Atmospheric Administration, Coastal Services Center, Charleston, SC.

Subramaniam, A., K.J. Waters, A.W. Meredith, E.M. Armstrong, R.M Bohne, W.G. Keull, J.R. Nelson, G.R. DiTullio, J.C. Brock. 1997c: NOAA CSC/CRS Cruise APR96FER: Gray's Reef Cruise. CSC Technical Report CSC/7-97/001. U.S. Department of Commerce, National Oceanic and Atmospheric Administration, Coastal Services Center, Charleston, SC.

Subramaniam, A., J.C. Brock, P.A. Tester, E. Haugen, R.P. Stumpf, 1998: NOAA NMFS Cruise MAY97OB: Onslow Bay and Pamlico Sound Cruise. CSC Technical Report CSC/2-98/001. U.S. Department of Commerce, National Oceanic and Atmospheric Administration, Coastal Services Center, Charleston, SC.

Subramaniam, A., M. Culver, D. Phinney, D. Phinney, J. Brown, B. Schieber, J. Brock, D. Eslinger, and C. Brown., 1999: NOAA Cruise JUL98NAN: Nantucket Shoals Cruise. NOAA CSC Technical Report, 99043-PUB. U.S. Department of Commerce, National Oceanic and Atmospheric Administration, Coastal Services Center, Charleston, SC.

Subramaniam, A., N. Blough, L. Harding, M. E. Geesey, C. W. Brown and M. E. Culver, 2000: NOAA Cruise OCT99MAB: Mid Atlantic Bight Cruise. Technical Report. CSC/20016-PUB. U.S. Department of Commerce, National Oceanic and Atmospheric Administration, Coastal Services Center, Charleston, SC.

Subramaniam, A., M. E. Culver and M. E. Geesey, 2000: NOAA Cruise APR00FWS: West Florida Shelf Cruise. CSC Technical Report. CSC/20018-PUB. U.S. Department of Commerce, National Oceanic and Atmospheric Administration, Coastal Services Center, Charleston, SC.

Tester, P.A., M.E. Geesey, C. Guo. H.W. Paerl and D.F. Millie, 1995: Evaluating phytoplankton dynamics in the Newport River estuary (North Carolina, USA) by HPLC-derived pigment profiles. *Mar. Ecol. Prog. Ser.* **124**, 237-245.

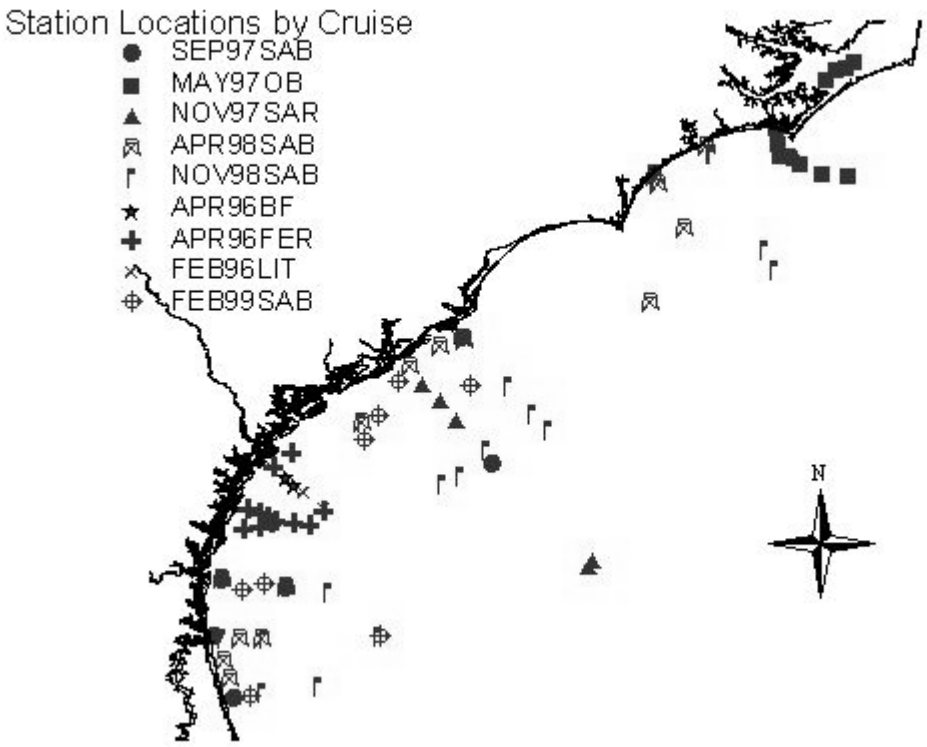

Figure 5.1 Location of stations.

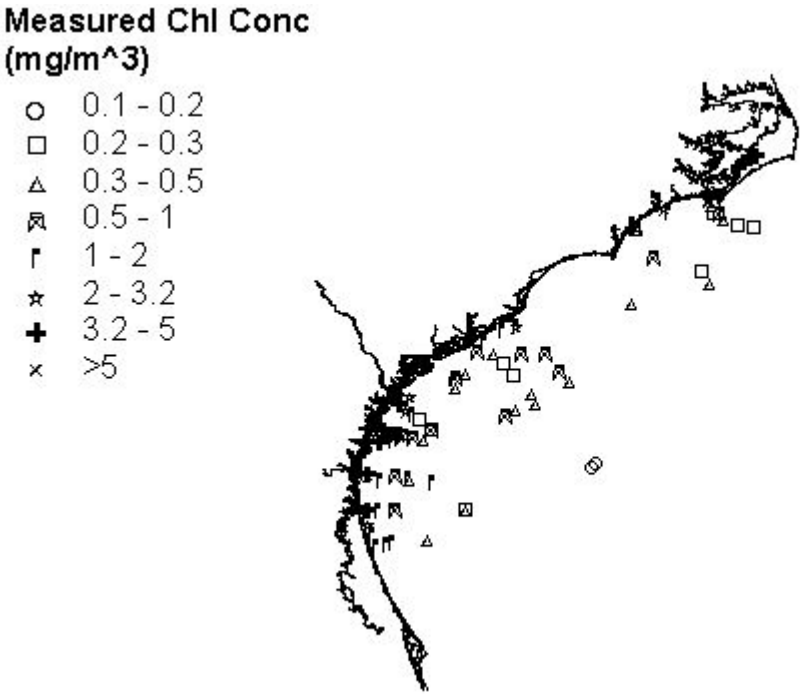

Figure 5.2 Spatial pattern of measured chlorophyll concentration in the South Atlantic Bight in this study.

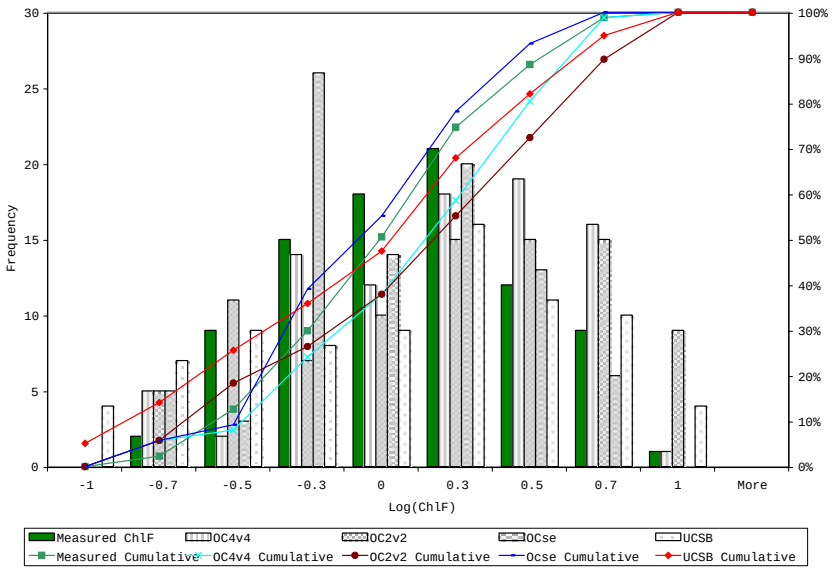

Figure 5.3 Histogram of measured and algorithm-derived chlorophyll concentrations.

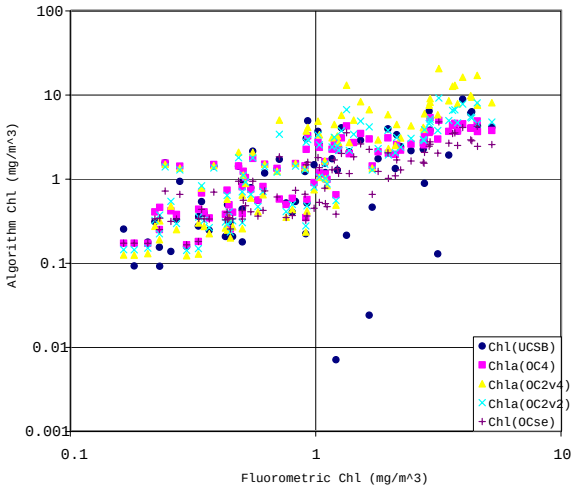

Figure 5.4 Scatter plot of measured and algorithm-derived chlorophyll concentration.

This research was supported by the

SIMBIOS NASA interagency agreement # 97879

OTHER PUBLICATIONS

Subramaniam, A., E.M. Armstrong et al., 1997a: NOAA CSC/CRS Cruise MAR97OCC: OCTS Calibration Cruise. *CSC Technical Report* CSC/5-97/001.

Subramaniam, A., E.M. Armstrong et al.,1997b: NOAA CSC/CRS Cruise MAY96NY: New York Bight Apex Cruise. *CSC Technical Report* CSC/6-97/001.

Subramaniam, A., K.J. Waters et al.,1997c: NOAA CSC/CRS Cruise APR96FER: Gray's Reef Cruise. *CSC Technical Report* CSC/7-97/001.

Subramaniam, A., J.C. Brock et al., 1998: NOAA NMFS Cruise MAY97OB: Onslow Bay and Pamlico Sound Cruise. *CSC Technical Report* CSC/2-98/001.

Subramaniam, A., C.W. Brown et al., 1999: Comparison of algorithms to determine chlorophyll concentration from satellite coean color in three regions: South Atlantic Bight. *CSC Technical Report* 99032-PUB.

PRESENTATIONS

Geesey, M. , M. Culver, A. Subramaniam, G. DiTullio, and J. Brock. 1998: Optical and biological variability in the South Atlantic Bight. Conference for Collaborative Research Activities in the South Atlantic Bight.

Culver, M. E., K. J. Waters, A. Subramaniam, D. A. Phinney, W. M. Balch, and D. T. Drapeau. 1998: Closure of inherent and apparent optical properties at a coastal station in the Gulf of Maine. Ocean Optics XIV.

Subramaniam, A. M.E. Culver, P.A. Tester, C.W. Brown, J.C. Brock. 1998: An Evaluation of the OC2 SeaWiFS Algorithm Performance in the South Atlantic Bight. Ocean Optics XIV.

Eslinger, D. L., M. E. Culver, D. Aurin, R. Swift, and F. Hoge. 1999: A Comparison of Active and Passive Ocean Color in Southeastern U.S. Coastal Waters. Estuarine Research Federation.

Chapter 6

Validation of Ocean Color Satellite Data Products in Under Sampled Marine Areas

Ajit Subramaniam
University of Maryland, College Park, Maryland

Raleigh R. Hood
University of Maryland Center for environmental Science, Maryland

Christopher W.Brown
NOAA/NESDIS, Camp Spring, Maryland

Edward J. Carpenter
SUNY at Stony Brook, New York

Douglas G. Capone
University of Southern California, California

6.1 INTRODUCTION

The planktonic marine cyanobacterium, *Trichodesmium* sp., is broadly distributed throughout the oligotrophic marine tropical and sub-tropical oceans (Capone *et al.*, 1997). *Trichodesmium*, which typically occurs in macroscopic bundles or colonies, is noteworthy for its ability to form large surface aggregations and to fix dinitrogen gas. The latter is important because primary production supported by N_2 fixation can result in a net export of carbon from the surface waters to deep ocean and may therefore play a significant role in the global carbon cycle (Hood *et al.* 2000). However, information on the distribution and density of *Trichodesmium* from shipboard measurements through the oligotrophic oceans is very sparse. Such estimates are required to quantitatively estimate total global rates of N_2 fixation. As a result current global rate estimates are highly uncertain (Hood *et al.* 2000). Thus in order to understand the broader biogeochemical importance of *Trichodesmium* and N_2 fixation in the oceans, we need better methods to estimate the global temporal and spatial variability of this organism. One approach that holds great promise is satellite remote sensing. Satellite ocean color sensors are ideal instruments for estimating global phytoplankton biomass, especially that due to episodic blooms, because they provide relatively high frequency synoptic information over large areas. *Trichodesmium* has a combination of specific ultrastructural and biochemical features that lend themselves to identification of this organism by remote sensing. Specifically, these features are high backscatter due to the presence of gas vesicles, and absorption and fluorescence of phycoerythrin. The resulting optical signature is relatively unique and should be detectable with satellite ocean color sensors such as SeaWiFS (Subramaniam *et al.* 1999b).

Surface aggregations of *Trichodesmium* have been noted in the Great Barrier Reef and northern Australian waters as early as 1770 (Furnas, 1992). Marshall (1933) noted that surface manifestations were highly aggregated and of short duration in his one year long study around the Low Isles, north of Cairns. Revelante and Gilmartin (1982) did a two year long study and found up to 40,000 trichomes/L off Townsville [assuming 200 trichomes/colony and 50 ng Chl/colony, (Carpenter, 1983)] - this gives a *Trichodesmium* specific chlorophyll concentration of 10 mg Chl/m^3. Kuchler and Jupp (1988) showed a dramatic space shuttle astronaut hand held camera photograph of a 150-km long *Trichodesmium* bloom in the Capricorn Channel in the southern end of the Great Barrier Reef. More recently, Glibert *et al.* (2000) reported a *Trichodesmium* bloom off Heron Island that ranged from 200 colonies/L to 5000 colonies/L (10-250 mg Chl/m^3).

Trichodesmium is also known to routinely occur along the southeastern coast of the United States off Florida, Georgia and South Carolina (Hulbert, 1967; Marshall, 1971). Dunstan and Hosford (1977) found that *Trichodesmium* was endemic to the continental shelf in the South Atlantic Bight and not necessarily contributed by the Gulf Stream or connected to

$$R_{rs}(\lambda) = 0.083 \frac{\left[b_{bw}(\lambda) + b_{bp}^{*}(\lambda) C_p + b_{bT}^{*}(\lambda) C_T + 0.30 C^{0.62} [0.02(0.5 - 0.25 \log C)(\frac{550}{\lambda})] C \right]}{\left[a_w(\lambda) + a_p^{*}(\lambda) C_p + a_T^{*}(\lambda) C_T + 0.05 e^{-0.02(\lambda - 412)} \right]} \quad (6.1)$$

sub-surface Gulf Stream intrusions. They found *Trichodesmium* all through the year in at least 36% of the stations (in December) to 76% of the stations (in July). The densest concentrations were usually at midshelf stations between the 20m and 200m isobaths. In July 1974, they encountered a shelf-wide bloom with 2000 (0.5 mg Chl/m^3) to 5600 (1.4 mg Chl/m^3) trichomes/L and a maximum of 36,000 trichomes/L (9 mg Chl/m^3 *Trichodesmium* specific chlorophyll).

It is apparent that these two marine areas, Capricorn Channel in the Southern Great Barrier Reef and the South Atlantic Bight, routinely experience high concentrations of *Trichodesmium*. We present here the development of a classification algorithm for *Trichodesmium*, based on a bloom observed by the SeaWiFS satellite in the Capricorn Channel and apply that algorithm to map another bloom encountered during a cruise in October 1998 in the South Atlantic Bight.

6.2 RESEARCH ACTIVITIES

The optical model used here (Eq. 6.1) parameterizes the expression for remote sensing reflectance (R_{rs}) presented by Kirk (1994). The parameterization is similar to that described by Subramaniam 1999(b), the major differences being that the present model is parameterized only for five wavelengths and uses coefficients relevant to the South Atlantic Bight.

To compute the reflectance spectra for varying concentrations of only *Trichodesmium*, the chlorophyll concentration of "other phytoplankton" was set to 0, and conversely to compute the reflectance spectra for varying concentrations of only "other phytoplankton", the chlorophyll concentration of *Trichodesmium* was set to 0. To study the effect of mixed populations, the reflectance spectra of a varying percentage of *Trichodesmium* to other phytoplankton for a total chlorophyll concentration of 1 mg Chl/m^3 was also computed.

Image Processing and Classification Development

A bright feature was noticed in a SeaWiFS true color image of the Capricorn Channel of July 16th 1998 by Norman Kuring at the SeaWiFS Project office and brought to our attention. We determined that *Trichodesmium* blooms were noted anecdotally from Heron Island during this period although no samples were taken (P. Bird personal communication). Weather observations taken there showed that the winds were light on the 14th (5-7 knots) and 15th (8-10 knots), and in general, conditions were favorable for a *Trichodesmium* bloom. The putative *Trichodesmium* bloom was seen as a bright feature (lighter blue) in the middle of the Capricorn Channel where the water depths are between 50 and 80 m. The shape of this bloom and its location is remarkably similar to the shape and location of a *Trichodesmium* bloom photographed from the space shuttle described by Kuchler and Jupp (1988).

High Resolution Picture Transmission (HRPT) SeaWiFS images for the Capricorn Channel and the South Atlantic Bight were obtained from the Goddard Distributed Active Archive Center and were processed from raw level 1b to level 2 using the l2gen procedure of SeaDAS (version 3.3, Fu *et al.*1998). Level 2 products included normalized water leaving radiance (nLw) at 412, 443, 490, 510, and 555 nm corresponding to bands 1 to 5 of the SeaWiFS sensor and chlorophyll concentration as calculated by the OC2 algorithm (O'Reilly *et al* 1998). Transects were taken through the bloom using the Rline procedure of SeaDAS to extract the chlorophyll concentration and the nLw values for the five bands.

The spectral characteristics along the transect showed that nLw443, nLw490, and nLw510 were relatively high inside the bloom (nLws > 1.6) with nLw490 being the highest, but rapidly fell outside the bloom (nLw < 1). Our optical model results described in detail in section 3.1 below, predicts that nLw 443, nLw490, nLw510 and nLw555 should be higher for *Trichodesmium* than for other phytoplankton at any chlorophyll concentration due to the high backscatter from gas vesicles found in *Trichodesmium*. The model also predicts that for *Trichodesmium* specific chlorophyll concentrations of between 0.5 and 1.5 mg Chl/m^3, nLw490 should have the highest magnitude. The magnitude of nLw510 was greater than that of nLw443 inside the transect of the bloom as predicted by the model. After analysis of various combinations of nLw443, nLw490, nLw555 from inside and outside the bloom, we found that the ratio of the difference between nLw490 and nLw443 to nLw490 and nLw555 best delineated the *Trichodesmium* bloom from the rest of the phytoplankton. The model results show that this "shape criteria" is not only valid for lower concentrations of *Trichodesmium* (<2 mg Chl/m^3), but is also valid for higher concentrations (2-4 mg Chl/m^3) of other phytoplankton as well. However, other phytoplankton did not have high nLws at these concentrations.

Based upon these model predictions and SeaWiFS observations, we developed a set of classification criteria to identify the presence of moderate concentrations (0.8-2 mg Chl/m^3) of *Trichodesmium* using SeaWiFS derived normalized water leaving radiances. A pixel is flagged as dominated by *Trichodesmium* if the following criteria are satisfied:

- nLw490 > 1.3 - absolute magnitude criteria
- nLw510 > nLw443 - relative magnitude criteria
- 0.4 > (nLw490 - nLw443)/(nLw490-nLw555) > 0.6 - shape criteria

Subramaniam *et al.* (1999a) showed that standard ocean color chlorophyll algorithms would underestimate *Trichodesmium* specific chlorophyll by a factor of at least 4 due to self-shading by the colonies (the "secondary packaging effect"). Therefore the chlorophyll concentrations derived by OC2 at pixels flagged as *Trichodesmium* dominated were multiplied by 4 to retrieve *Trichodesmium* specific chlorophyll concentrations.

On application of this classification to SeaWiFS data from various regions, we found that high water leaving radiance due to bottom reflectance from shallow waters and certain combinations of sediments and colored dissolved organic matter mimic the reflectance pattern of a *Trichodesmium* bloom. To avoid this, a 30m bathymetric mask was added to the classification scheme. We found that the spectral reflectance signature of *Phaeocystis* is very similar to *Trichodesmium* in magnitude and shape. However, *Phaeocystis* is predominantly a cold water species whereas *Trichodesmium* normally does not bloom in waters colder than 23°C and can be effectively screened by using a temperature criterion of 25°C. In order to avoid potential false positives from resuspended sediments and bright diatom blooms, we also exclude pixels where the wind speed is greater than 8 m/s.

6.3 RESEARCH RESULTS

Model results

Subramaniam *et al* (1999b) showed that *Trichodesmium* could not be distinguished from other phytoplankton at concentrations less than about 1.0 mg Chl/m^3. Here we model the normalized water leaving radiance (nLw) at 412, 443, 490, 510 and 555 nm corresponding to bands 1, 2, 3, 4, and 5 of SeaWiFS for *Trichodesmium* and other phytoplankton for chlorophyll concentrations ranging from 0.5-10 mg Chl/m^3. As expected, the model predicts that the nLw spectrum of *Trichodesmium* should be different from that of other phytoplankton, especially at high chlorophyll concentrations (Figure 6.1a, 6.1b). Even at 0.5 mg Chl/m^3, while the spectra of nLw for *Trichodesmium* and other phytoplankton are similar, the model predicts that the magnitude of nLw490, nLw510 and nLw555 should be higher for *Trichodesmium* due to the high backscatter contribution of its gas vacuoles. The model also predicts that the magnitude of nLw412 for *Trichodesmium* should always be lower than that of other phytoplankton due its higher chlorophyll specific absorption as described by Subramaniam *et al.* 1999a. At *Trichodesmium* chlorophyll specific concentrations greater than 0.5 mg Chl/m^3, the model predicts that the magnitude of nLw510 will be greater than nLw443.

However, comparison of the model predicted nLw spectra for pure *Trichodesmium* populations to nLw spectra derived from SeaWiFS imagery give ambiguous results (Figure 1c). A global search of the SeaWiFS imagery revealed very few pixels with the spectrum that closely resembled the spectrum that is generated by the model at high *Trichodesmium* concentrations, i.e. we could not find any dense *Trichodesmium* blooms in the ocean with the model predicted spectrum. This may be because the modeled spectra are for pure populations of *Trichodesmium*, whereas, in the field, one is more likely to find mixed populations. In order to examine the impact of mixed populations on the predicted spectra, the model was run for increasing proportions of other phytoplankton to *Trichodesmium* from 10% other phytoplankton to 90% other phytoplankton for a total chlorophyll concentration of 1 mg Chl/m^3 (Figure 6.1d). As anticipated, the reflectance at 490nm is highest for 10% other phytoplankton due to the high backscatter at this wavelength from *Trichodesmium* and lowest for 90% other phytoplankton where the influence of *Trichodesmium* on the spectrum is small. The spectral shape appears to flatten as the amount of *Trichodesmium* is reduced. The spectral shape and magnitude of the normalized water leaving radiance spectrum from a pixel in the middle of the Capricorn Channel bloom is very close to that of a mixture of 40% *Trichodesmium* and 60% other phytoplankton (Figure 6.1d) showing that the SeaWiFS observed spectra are that of a mixed population. Thus, the model-predicted spectra for mixed populations of *Trichodesmium* and other phytoplankton can be found in SeaWiFS imagery. In fact, even in cases of very dense, nearly monospecific blooms, the satellite will likely always see a mixture of *Trichodesmium* and other phytoplankton species because a SeaWiFS pixel is 1 km^2 while *Trichodesmium* blooms tend to occur in linear patches or striated patterns with width scales of 10s of meters. Thus, even the densest blooms extending 100s of km may never entirely fill a pixel and will therefore always include other optical influences such as other phytoplankton.

Mapping of Capricorn Channel Bloom.

The OC2 derived chlorophyll image (Figure 2a at http://www.usc.edu/dept/LAS/biosci/tricho/manuscripts/) shows four patches of apparently high chlorophyll concentrations (~0.7 mg chl/m^3). The apparently high chlorophyll concentration over the Great Barrier Reef (3) is probably an artifact of bottom reflection. While the high chlorophyll along the coast around Broad Sound (4) and off Frasier Island (6) maybe real, bottom reflection and sediments also probably contaminate those values. However, the high chlorophyll patch in the middle of Capricorn Channel has optical properties that are consistent with the presence of a *Trichodesmium* bloom. The adjacent Coral Sea region outside the Great Barrier Reef has chlorophyll values of 0.1 mg Chl/m^3. The apparent *Trichodesmium* bloom as mapped by the classification scheme (Figure 2b at

http://www.usc.edu/dept/LAS/biosci/tricho/manuscripts/) shows up as two patches. One is a larger patch in the middle of the Capricorn Channel; there is also a smaller patch off Cape Manifold. It is very likely that the classification rules are very conservative and do not map the entire *Trichodesmium* bloom. The scheme is a binary flag, where a pixel either satisfies a set criteria or fails, it cannot reproduce the gradual tail off that would likely be found in nature.

The normalized water leaving radiance values were extracted for each band along a transect through the bright feature (transect shown in Figure 2a, b at http://www.usc.edu/dept/LAS/biosci/tricho/manuscripts/). The spectral characteristics along the transect between 0 and 40 km are that of *Trichodesmium* (Figure 3 at http://www.usc.edu/dept/LAS/biosci/tricho/manuscripts/), i.e. nLw443, nLw490, and nLw510 are relatively high, (nLw > 1.6, 0-40 km). Beyond 40 km, the radiances decline rapidly (nLw < 1, 65-120 km). Between 40 and 60 km, the transect appears to pass through the edge of another filament of water dominated by *Trichodesmium* (at 51 km). The shape criteria (band3 - band2)/(band3-band5) is satisfied in the region 0 to 40 km and in the filament at 51 km but not elsewhere. But the chlorophyll values calculated by OC2 remains relatively high through most of the transect at about 0.6 mg Chl/m^3 inside the apparent *Trichodesmium* bloom and 0.4 mg Chl/m^3 along the rest of the transect. Thus, although *Trichodesmium* appears to dominate the optical properties in the center of the bloom, these waters are rich in other phytoplankton as well. As discussed above, the spectral shape and magnitude of a pixel from the center of the bloom very closely resembles the spectral shape and magnitude of the modeled spectrum for 1 mg Chl/m^3 chl with 40% *Trichodesmium* and 60% other phytoplankton (Figure 6.1d). As predicted by the model, nLw412remains relatively low inside the bright feature but is higher than nLw555 outside. However, nLw555 inside the apparent *Trichodesmium* bloom is much lower than the model prediction. The absolute magnitude criteria and the relative magnitude criteria are clearly associated with the shape criteria, indicating that the combination of these coherently describe a *Trichodesmium* induced optical feature at spatial scales of 10s of kilometers.

Application to South Atlantic Bight

During a cruise in the South Atlantic Bight in the fall of 1998, we encountered a *Trichodesmium* bloom along the 200 m isobath from about 33°N to 30°N. The bloom developed after a series of bright sunny and calm days beginning the 25th of October. As we traveled south from Beaufort NC, doing a series of transects across the shelf; we occasionally saw and sampled thin accumulations of *Trichodesmium* along the continental shelf edge. On the 30th of October, we encountered dense accumulations of *Trichodesmium* at the surface in the morning during a period of exceptionally calm weather, but these accumulations disappeared as the wind picked up after 11:00. On the 31st of October, we observed isolated accumulations a few meters wide, throughout the day as we traveled south about 200 km along the shelf break. On the 1st of November, there were dense blooms several 100 meters wide that turned the water greenish yellow in patches. By the morning of the 3rd of November, the winds had picked up and a low pressure front passed through the region on the night of the 5th of November accompanied by wind speeds of over 30 knots. After this no surface accumulations were observed for the next 10 days. The OC2 derived chlorophyll image (Figure 3 at http://www.usc.edu/dept/LAS/biosci/tricho/manuscripts/) shows the bottom reflection from the Little Bahamas Bank (2) as an apparent high chlorophyll feature. The shallow turbid coastal waters (4, 5) can also be seen as apparent high chlorophyll along the coast. The Gulf Stream (6) can be recognized by its low (0.1 mg Chl/m^3) chlorophyll concentration, while the continental shelf generally appears to have a higher chlorophyll concentration between 0.4 and 0.8 mg Chl/m^3. The turbid waters around Cape Canaveral (3) have a much higher apparent chlorophyll concentration of about 4 mg Chl/m^3.

The *Trichodesmium* bloom is seen separated from coastal turbid waters in the chlorophyll image (Figure 4a at http://www.usc.edu/dept/LAS/biosci/tricho/manuscripts/) by about 20 km. It appears to lie just inshore of the Gulf Stream edge, and along the continental shelf edge. Application of our classification scheme reveals the bloom as a linear feature 100 km long and 20 km wide with a scalloped eastern edge (Figure 4b). The latter characteristic may be due to low amplitude Gulf Stream meanders. There appears to be a small east-west gradient in chlorophyll concentration, with the *Trichodesmium* specific chlorophyll ranging from 1.5 to 2.5 mg Chl/m^3. A comparison of Figures 4a and 4b (at http://www.usc.edu/dept/LAS/biosci/tricho/manuscripts/) shows that *Trichodesmium* makes up only a small part of the total chlorophyll seen in this region. Bottom reflections in the Little Bahamas Bank also appear to satisfy the classification criteria as it too shows up in the classification image. Normally, bottom reflection effects would be masked out by the depth criteria in the classification scheme, but here it appears that parts of the bathymetric data are inaccurate, as only a part of the bank is masked.

Two transects, one east-west (Figure 5a and 5b at http://www.usc.edu/dept/LAS/biosci/tricho/manuscripts/) and the other north-south were taken through the 30 October SeaWiFS image of the bloom using the Rline procedure of SeaDAS. The east west transect very dramatically reveals the difference between *Trichodesmium* dominated water and other water types. The transect begins in the Gulf Stream (0-28 km) where chlorophyll concentration is low (~0.1 mg Chl/m^3), nLw443 and nLw412 are higher than the other bands, consistent with low *Trichodesmium* concentrations. Then as we move shoreward into the region between 30 and 45 km, the nLws increase in all bands except 412 and the chlorophyll concentration increases from 0.1 to about 0.5 mg Chl/m^3. The spectral shape and magnitudes of nLws in this region corresponds to that predicted for moderate concentrations of

Trichodesmium. Farther shoreward, between 45 and 60 km, all the nLw decrease in magnitude but the chlorophyll concentration remains about the same, between 0.5 and 0.7 mg Chl/m^3, consistent with the spectral shape of other phytoplankton. Finally, close to shore, nLw490, nLw510, and nLw555 as well as the calculated chlorophyll values increase indicating turbid, high chlorophyll waters. The spectral shape is almost the mirror image of the Gulf Stream waters with nLw555 being the highest followed by nLw510, nLw490, and nLw443. The second transect runs north-south (Figure at http://www.usc.edu/dept/LAS/biosci/tricho/manuscripts/), along the bright feature from near its northern edge to the south into nonbloom waters. As in the Coral Sea case, it appears that when the *Trichodesmium* concentration falls below a threshold, the magnitude of nLw510 gets lower than the magnitude of nLw443 and thus the classification criteria is no longer satisfied even though there is probably *Trichodesmium* present in the water (between 26 and 40 km in the transect). Thus, the classification tends to create artificially sharp boundaries.

Shipboard observations from the SAB

Two National Data Buoy Center weather buoys provided wind speed, direction, wave heights and atmospheric pressure in the region. Buoy 41008 is located at the Grays Reef National Marine Sanctuary (31.4N, 80.87W), 40 nautical miles southeast of Savannah. Buoy 41009 is located 20 nautical miles east of Cape Canaveral at 28.5N, 80.18 W. The initial patch originated almost exactly at the location of buoy 41009. The maximum water temperature measured at buoy 41009 was 27.6°C and the minimum was 25.3°C between 25 October and 6 November. The average temperature during this period was 26.6°C. On days when we saw visible accumulations of *Trichodesmium* at the surface, bucket samples were taken for enumeration using an epifluorescence microscope.

The first visible accumulation of *Trichodesmium* was observed on the morning of 30 October. At 9:45 AM, the patch was a few meters wide but stretched for many kilometers along the shelf break. A surface sample from the densest part had 6700 trichomes/L (Table 6.1). The water was glassy calm with less than 1-knot wind. *Trichodesmium* was extremely patchy as the total chlorophyll measured at this station from surface water outside the patch was only 0.37 mg Chl/m^3 – about 1/6th the calculated *Trichodesmium* specific chlorophyll. By the time the satellite overpass at 12:30, the wind had picked up to 7 knots. The *Trichodesmium* patches disappeared and the surface sample only had 13 trichomes/L. The classification did not show any evidence of *Trichodesmium* in the SeaWiFS image at this location. On the 31st, although we observed visible accumulations of *Trichodesmium* through the day while transiting along the shelf break, the surface sample at 16:40 coinciding with the SeaWiFS overpass contained only 740 trichomes/L. Still, the *Trichodesmium* specific chlorophyll made up 43% of the total chlorophyll measured at this station. On the 1st November, the seas were very calm from early morning through early afternoon and we observed large accumulations of *Trichodesmium* during this period. At 9:15 AM, we were in the middle of a very large accumulation and a surface bucket sample contained 12300 trichomes/L. Here, *Trichodesmium* specific chlorophyll was 71% of the total chlorophyll measured at the station. However, the skies clouded over before the SeaWiFS overpass and only a small section of one of the patches is visible in the SeaWiFS image.

6.4 DISCUSSION

Optical Model

Subramaniam *et al* 1(999b) showed that there were significant differences in the hyperspectral remote sensing reflectance spectra of *Trichodesmium* versus other phytoplankton at chlorophyll concentrations of 1 mg Chl/m^3 and above, and that the differences were very pronounced at high, bloom like concentrations of 10 mg Chl/m^3. The model that we present here was parameterized for five bands of 10 nm width matched to the SeaWiFS sensor. When the hyperspectral data was reduced to five bands, some of the obvious differences such as the pronounced reflectance peak around 470 and 530 nm and the trough around 510 nm disappeared due to the reduced spectral resolution. Other differences between the model of Subramaniam *et al.* (1999b) and the one presented here include a different parameterization of sky reflectance - here we have followed the method of Kirk (1994) rather than that of Carder and Steward (1985). Also, in the present model we have used an average of the CDOM "slope parameters" reported by Nelson and Gaurdia (1995) representative of the mid shelf in the South Atlantic Bight rather than the open ocean or extremely turbid waters end members used in Subramaniam *et al* (1999b). Finally, we restructured the model to take into account mixed populations of *Trichodesmium* and other phytoplankton. As discussed in section 4.2 below, considering mixed populations is extremely important at various spatial scales.

A comparison of the model predicted and satellite derived normalized water leaving radiances leads us to believe that the model may be over predicting nLw555. This could be because the model exaggerates the contribution of phycoerythrin fluorescence at chlorophyll concentrations of 1-2 mg chl/m^3. The backscatter+fluorescence spectra measurements detailed in Subramaniam *et al* (1999b) were made on a concentrated collection of colonies in a small volume (about 20 colonies/mL). This is the equivalent of a 100 mg Chl/m^3. The fluorescence observed at such high concentrations may not be linearly scalable to lower chlorophyll concentrations between 0.5 and 2 mg Chl/m^3. However, it should be noted that the hyperspectral model of Subramaniam *et al (*1999b) corresponds extremely well both in shape and in magnitude

with field measurements of a *Trichodesmium* bloom in the Caribbean Sea (Navarro, 1998).

Image Classification

Subramaniam et al (1999b) found that it would not be possible to distinguish between *Trichodesmium* and other phytoplankton based on optical characteristics alone at chlorophyll concentrations below about 0.8 mg Chl/m^3 (16 colonies/L). An algorithm developed from the optical model of Subramaniam et al (1999b) and applied to global level 3 (8 day, 9 km binned global area coverage, "quality controlled") data revealed very few "hits". This could be because the optical model predictions are wrong, because of incorrect atmospheric correction, or because the eight-day temporal binning and the nine km spatial binning smeared the *Trichodesmium* signal out. In addition, dense surface blooms of *Trichodesmium* would probably fail the standard quality control procedures and be eliminated from the level 3 data or could be misclassified as clouds.

Because the theory based optical model was not helpful in developing an algorithm, we tried to use an empirical image based approach. However, at present, we do not have ground truth data with chlorophyll measurements and cell counts for even one mid ocean *Trichodesmium* bloom with a coinciding SeaWiFS image. Hence, even though coastal waters are extremely complex, we had to use coastal scenes with putative *Trichodesmium* blooms to develop our classification scheme. The use of actual SeaWiFS imagery overcomes two problems with using a purely theoretical approach. The first problem is to apply the appropriate atmospheric correction scheme to correctly derive the normalized water leaving radiance from the satellite sensor measurement of total radiance. In turbid waters, the water leaving radiance in the red and near infrared is not negligible, and the incorrect atmospheric correction results in an underestimate of the water leaving radiance, especially in the blue bands. Waters containing significant accumulations of *Trichodesmium* are golden brown in color and would have a significant water leaving radiance in the red and near infrared resulting in an underestimate of the water leaving radiance in the blue and green bands. Considering that the most prominent signal that distinguishes *Trichodesmium* from other phytoplankton is its high backscatter, it is not surprising that we were not able to map *Trichodesmium* blooms using an algorithm derived from the optical model. We have observed that a surface cyanobacterial bloom in the Baltic Sea has enough signal at 865 nm that portions of the bloom was misidentified and masked as clouds.

The second problem that the empirical approach overcomes is that of mixed populations. The question of mixed populations can be discussed at various spatial scales ranging from a point measurement all the way to a 9-km2 level 3 pixel. As seen at the station occupied on 1 November in the South Atlantic Bight (Table 6.1), even during a significant *Trichodesmium* accumulation with 12700 trichomes/L, *Trichodesmium* only contributed 71% of the total chlorophyll in that bucket sample. Thus at a very local scale, mixed populations can be discussed in terms of number of cells from each species of phytoplankton present in a small volume of water. However, mixed populations in a remote sensing context can also be discussed in terms of spatial inhomogenity. We have observed that while on the one hand, small concentrations of *Trichodesmium* (say 1 colony/L or less) are homogeneously distributed in the water column, as the concentrations increase, *Trichodesmium* tends to accumulate in patches near the surface. Thus on 30 October, while there was 1.83 mg *Trichodesmium* specific chlorophyll per m^3 in the sample taken for cell counts, there was only 0.37 mg Chl/m^3 in a water sample taken a few minutes later, presumably outside the *Trichodesmium* patch. Thus, unlike most other phytoplankton that are homogeneously distributed in the near surface water column, buoyant cyanobacterial such as *Trichodesmium* have a very patchy horizontal distribution within a 1 km^2 SeaWiFS pixel and the issue of mixed populations should also be discussed in terms of subpixel variability - the percent area within a pixel that is covered by *Trichodesmium*. It is unclear to us how the SeaWiFS sensor responds to subpixel variability. Subpixel variability occurs when the satellite sensor's instantaneous field of view is partially filled with surface accumulations of *Trichodesmium* with intervening clear water. The reflectivity observed by the sensor is a combination of both the *Trichodesmium* and ocean water reflectances which are integrated by the sensor. The exact sensor response depends on the relative amounts of *Trichodesmium* and clear water, the distribution of both in the sensor's field of view, and the integrating aperture function of the sensor. Consequently, we get reflectance values for a pixel containing some *Trichodesmium* that has neither the characteristics of *Trichodesmium* nor other phytoplankton nor clear water. At the very best, the relationship between the multispectral data and the ocean water, phytoplankton biomass, and *Trichodesmium* biomass is complex and these three signals may not be separable by linear methods or simple band ratio type algorithms. In the empirical classification approach outlined above, we cannot mechanistically account for atmospheric correction or subpixel variability, but these are embedded into the data used.

6.5 CONCLUSIONS

It is generally thought that organism specific remote sensing is not possible except in the case of organisms with exceptional optical properties that set them apart. *Trichodesmium* is an excellent example of such an organism with a unique combination of absorption, scattering and fluorescence properties. In this paper, we have demonstrated that it is possible to identify *Trichodesmium* when it is present in sufficient quantities (i.e. > 15 colonies/L), even in optically complex coastal waters rich in CDOM and sediments.

The classification scheme discussed here may not be universally applicable, being relevant only to coastal shelf

waters. This is not surprising considering that the training pixels are from the shelf. The present classification scheme is tuned to mixed populations in which other phytoplankton and CDOM make a more significant contribution to the optical signal than would be found in a *Trichodesmium* bloom in the middle of the ocean. We are now working on an open ocean classification criteria as well as a more robust universal algorithm using the optimization/inverse modeling technique of Maritorena *et al.* (2000).

REFERENCES

Capone, D. G., J. P. Zehr, H.W. Paerl, B. Bergman, and E.J. Carpenter, 1997: *Trichodesmium*, a globally significant marine cyanobacterium. *Science* **276**, 1221-1229.

Carder, K. L. and R. G. Steward, 1985. A remote-sensing reflectance model of a red-tide dinoflagellate off West Florida. Limnology and Oceanography **30**(2), 286-298.

Carpenter, E. J. (1983). Physiology and ecology of marine planktonic *Oscillatoria (Trichodesmium)*. *Marine Biology Letters* **4**(2), 69-85.

Dunstan, W. M. and J. Hosford, 1977: The distribution of planktonic blue green algae related to the hydrography of the Georgia Bight. *Bulletin of Marine Science* **27**(4), 824-829.

Fu, G., K.S. Baith, and C.R. McClain, 1998: SeaDAS: The SeaWiFS Data Analysis System, Proceedings of The 4th Pacific Ocean Remote Sensing Conference, Qingdao, China, July 28-31, 73-79.

Furnas, M. J., 1992: Pelagic *Trichodesmium* (=*Oscillatoria*) in the Great Barrier Reef Region. In: E.J. Carpenter, D.G. Capone, and J.G. Rueter (Eds), Marine Pelagic Cyanobacteria: *Trichodesmium* and other Diazotrophs. Kluwer Academic Publishers, Dordrecht. pp 265-272.

Glibert, P. M., J.M. O'Neil, C.A. Heil, 2000: Stimulation of Dinoflagellate Blooms During and After Blooms of the Diazotrophic Cyanobacteria *Trichodesmium*. *EOS* **80**(49), OS170.

Hood, R.R., A.F. Michaels, D.G. Capone, 2000: Answers sought to the enigma of marine nitrogen fixation. *EOS* **81**(133), 138-139.

Hulbert, E. M., 1967: Some notes on the phytoplankton of the southeastern coast of the United States. Bulletin of Marine Science **17**, 330-337.

Kirk, J. T. O., 1994: Light and Photosynthesis in Aquatic Ecosystems, Cambridge University Press.

Kuchler, D. A. and D. L. B. Jupp, 1988: Shuttle photograph captures massive phytoplankton bloom in the Great Barrier Reef. *International Journal of Remote Sensing.* **9**(8): 1299-1301.

Marshall, S. M., 1933: The production of microplankton in the Great Barrier Reef region. In: Scientific Reports of the Great Barrier Reef Expedition, Vol **2**, pp 111-157.

Marshall, H. G., 1971: Composition of phytoplankton off the Southeastern coast of the United States. *Bulletin of Marine Science* **21**, 806-825.

Maritorena, S., Siegel, D.A., Peterson, A.R. & Lorenzi-Kayser, M. 2000: Tuning of a pseudo-analytical ocean color algorithm for studies at global scales. Presented at the 2000 AGU Ocean Sciences Meeting (OS12M-05), San Antonio TX.

Navarro Rodriguez, A. J.,1998: Optical Properties of Photosynthetic Pigments and Abundance of the Cyanobacterium Trichodesmium in the Eastern Caribbean Basin. Ph.D. Thesis, University of Puerto Rico, Mayaguez, Puerto Rico.

Nelson, J. R. and S. Guarda, 1995: Particulate and dissolved spectral absorption on the continental shelf of the southeastern United States. *Journal of Geophysical Research* **100** (C5), 8715-8732.

O'Reilly, J. E., S. Maritorena, B.G. Mitchell, D.A. Siegel, K.L. Carder, S.A. Garver, M. Kahru, C. R. McClain, 1998: Ocean color chlorophyll algorithms for SeaWiFS. *Journal of Geophysics* **103**(C11), 24937-24953.

Revelante, N. and M. Gilmartin, 1982: Dynamics of phytoplankton in the Great Barrier Reef lagoon. *Journal of Plankton Research* **4**, 47-76.

Subramaniam, A., E. J. Carpenter, D. Karentz, and P.G. Falkowski, 1999a: Optical Properties of the Marine Diazotrophic Cyanobacteria *Trichodesmium* spp.; I - Absorption and Spectral Photosynthetic Characteristics. *Limnology and Oceanography* **44**(3): 608-617.

Subramaniam, A., E. J. Carpenter, and P.G. Falkowski, 1999b: Optical Properties of the Marine Diazotrophic Cyanobacteria *Trichodesmium* spp.; II - A Reflectance Model for Remote-Sensing. *Limnology and Oceanography* **44**(3), 618-627.

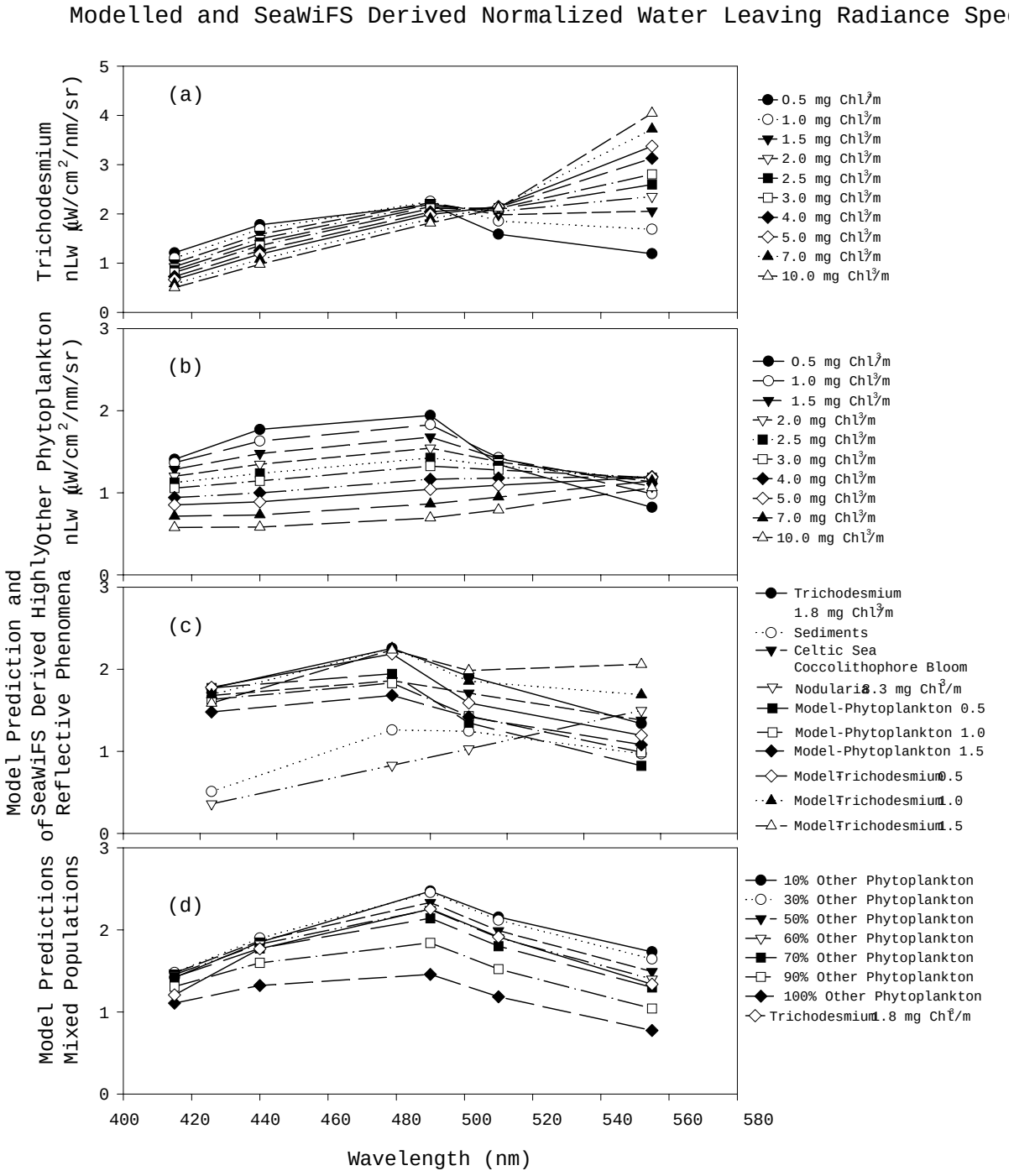

Figure 6. 1 A) Modeled remote sensing reflectance for “other phytoplankton”; B) Modeled remote sensing reflectance for Trichodesmium; C) Modeled and SeaWiFS measured Tricho and other phytoplankton, bright features; D) Modeled remote sensing reflectance for varying proportions of other phytoplankton to Trichodesmium when total chlorophyll is 1 mg Chl/m^3

Table 6.1 *In situ* measurements in the South Atlantic Bight

Date	Time GMT	Station Location		Wind speed (m/s)	Sea water Temp.	Trichodesmium Count (Trichomes/L)	Measured Total Clorophyll Mg Cl/m^3	SeaWiFS Derived Chlorophyll (mg Chl/$m^{3)}$
		Latitude	Longitude					
10/30	14:45	31.997	79.095	0.5	26.6	6700	0.366	-
10/30	17:30	31.772	79.313	3.5	26.6	13	0.426	0.303
10/30	19:40	31.700	79.460	3.5	26.7	155	0.906	-
10/31	16:40	30.009	80.500	5.5	25.4	740	0.435	
11/1	14:15	30.017	80.500	0.5	25.3	12300	4.318	-

This research was supported by the

SIMBIOS NASA contract # 97131

PEER REVIEWED PUBLICATIONS

Carpenter, E. J., J.P. Montoya, J. Burns, M. Mulholland, A.Subramaniam, D.G. Capone.1999. Extensive bloom of a N2 fixing symbiotic association in the tropical Atlantic Ocean. Mar. Ecol. Prog. Series. Vol.**185**, 273-283.

Capone, D.G., A. Subramaniam, J.P. Montoya, M. Voss, C. Humborg, F. Pollehne and E.J. Carpenter, 1998: An extensive bloom of the diazotrophic cyanobacterium, Trichodesmium erythraem, in the central Arabian Sea during the spring intermonsoon. *Marine Ecology Progress Series*. **172**, 281-292.

Zehr, J., E.J. Carpenter & T. Villareal. 2000. New perspectives on nitrogen-fixing microorganisms in tropical and subtropical oceans. *Trends in Microbiol*, 8, 68-73.

Accepted

Hood, R. R., A. Subramaniam, L. R. May, E. J. Carpenter and D. G. Capone, 2000: Remote Estimation of Nitrogen Fixation by Trichodesmium. *Deep-Sea Research* (1st Special Issue on the U.S. JGOFS SMP).

Subramaniam, A., R. R. Hood, C. W. Brown, E. J. Carpenter and D. G. Capone, 2000: Detecting Trichodesmium Blooms in SeaWiFS Imagery. *Deep-Sea Research.* (1st Special Issue on the U.S. JGOFS SMP).

PRESENTATIONS

Cota, G.F., W.G. Harrison, T. Platt, and S. Sathyendranth, 1998: OCTS ocean color and AVHRR observations in the Labrador Sea. Ocean Sciences Meeting, San Diego, *EOS* Transactions, **79**(1), Suppl: OS81.

Dupouy, C., J. Neveux, B. Fougnie, S. Colzy, and A. Subramaniam. 1999: Trichodesmium: an oceanic nitrogen fixer as detected by POLDER. Symposium ALPS'99, Colloque International et Ateliers, CNES, 18-23, January 1999, Meribel, France, Ocean Color P-01, pp. 1-5.

Dupouy, C., J. Neveux, A. Subramaniam, M. R. Mulholland, J. P. Montoya, L. Campbell, E. J. Carpenter and D. G. Capone, 2000: Satellite Captures Trichodesmium Blooms in the Southwestern Tropical Pacific. *EOS* **81**(2), 13-16.

Flatau, P., B. G. Mitchell, A. Subramaniam, J. Weldon, J. Wieland, K. Voss, R. Frouin, and J. Porter, 1999: Combined ocean color and atmospheric radiometeric measurements on R/V Ronald Brown ship during the Indian Ocean Experiment (INDOEX). 10th Conference on Atmospheric Radiation , 28th June - 2nd July 1999.

Subramaniam, A. and D.G. Capone, 2000: Global Occurrence of Trichodesmium During The 1997-1998 El Nino-La Nina Cylce. SOLAS Open Science Meeting, Damp Germany.

Subramaniam, A., J. Nolan, J. Wieland, M. Kahru, B.G. Mitchell, 2000: An Optical Bio-Geographical Description of the Indian Ocean During the 1999. Spring Intermonsoon Ocean Sciences 2000.

Subramaniam, A., S. Kratzer, E. J. Carpenter and E. Söderbäck, 2000: Remote sensing and optical in-water measurements of a cyanobacteria bloom in the Baltic Sea. Proceedings of the Sixth International Conference on Remote Sensing for Marine and Coastal Environments, Charleston, SC, Veridian ERIM International.

Chapter 7

Bio-Optical Measurements at Ocean Boundaries in Support of SIMBIOS

Francisco P. Chavez, Peter G. Strutton, and Brian M. Schlining
Monterey Bay Aquarium Research Institute, Moss Landing, California

7.1 INTRODUCTION

The equatorial Pacific is a major component of global biogeochemical cycles, due to upwelling that occurs from the coast of South America to beyond 180°. This upwelling has significant implications for global CO_2 fluxes (Tans *et al*., 1990; Takahashi *et al.*, 1997; Feely *et al.*, 1999), as well as primary and secondary production (Chavez and Barber, 1987; Chavez and Toggweiler, 1995; Chavez *et al*., 1996; Dugdale and Wilkerson, 1998; Chavez *et al*., 1999; Strutton and Chavez, in press). In addition, this region of the world's oceans represents a large oceanic province over which validation data for SeaWiFS are necessary. This project consists of a mooring program and supporting cruise-based measurements aimed at quantifying the spectrum of biological and chemical variability in the equatorial Pacific and obtaining validation data for SeaWiFS. The project has the following general objectives:

- to understand the relationships between physical forcing, primary production, nutrient supply and the exchange of carbon dioxide between ocean and atmosphere in the equatorial Pacific
- to describe the biological and chemical responses to climate and ocean variability
- to describe the spatial, seasonal and inter-annual variability in near surface plant pigments, primary production, carbon dioxide and nutrient distributions, and
- to obtain near real-time bio-optical measurements for validation of SeaWiFS and subsequent ocean color sensors.

7.2 RESEARCH ACTIVITIES

Moorings

Chavez *et al.* (1998; 1999; 2000) and McClain and Fargion (1999a, p.44) describe the configuration of the MBARI bio-optical and chemical instruments deployed at 0°, 155°W and 2°S, 170°W; two of the >70 moorings which form the Tropical Atmosphere Ocean (TAO) array. In addition, MBARI has also maintained smaller bio-optical packages at sites in the equatorial Pacific: 2°N, 180°; 2°S, 140°W, 2°N, 140°W and 2°N, 110°W (Strutton *et al*., submitted).

From 0°, 155°W and 2°S, 170°W, daily local noon (ie approximate time of SeaWiFS overpass) bio-optical and chemical data are transmitted via service ARGOS in near real time to MBARI, and then via automated FTP to the SeaBASS database, after processing and quality control. Higher frequency, publication-quality data (currently recorded at 15-minute intervals) are recovered at approximately six month intervals, and sent to the SeaBASS database after processing and quality control. Derived products, such as K_λ, OC2V4 chlorophyll, mean chlorophyll over the upper 20m of the water column (Morel, 1988), water leaving radiance (L_w), and remote sensing reflectance (Rrs) are included in these data files for validation efforts. In the past, L_w has been calculated via three different methods (McLain and Fargion, 1999b), but is currently calculated only as follows. The diffuse attenuation coefficient (K_λ) over the upper 20m of the water column is calculated using Ed_{3m+} and Ed_{20m}, then using this K_λ, Lu_{20m} is extrapolated back to just below the surface. This value (Lu_{0m-}) is then multiplied by 0.544 to account for transmission across the air-water interface, and hence derive Lu_{0m+}. Of the three methods previously used, this has been shown to be the most reliable, because the 3m+ and 20m instruments are less susceptible to fouling than the OCR-100s moored at ~1.5m.

Optical Profiling Measurements

On mooring maintenance cruises, optical profiles of the upper 100 to 200 m of the water column are performed, daily when possible, close to local noon. The instrument used is the Satlantic SeaWiFS Profiling Multispectral Radiometer (SPMR). Profile data are processed using Satlantic's ProSoft software, and a suite of derived products, including diffuse attenuation coefficients, water leaving radiances (Lwn) and light penetration depths. Parameters of interest (mostly Lwn) are provided to NASA post-cruise, and the profile data are archived at MBARI

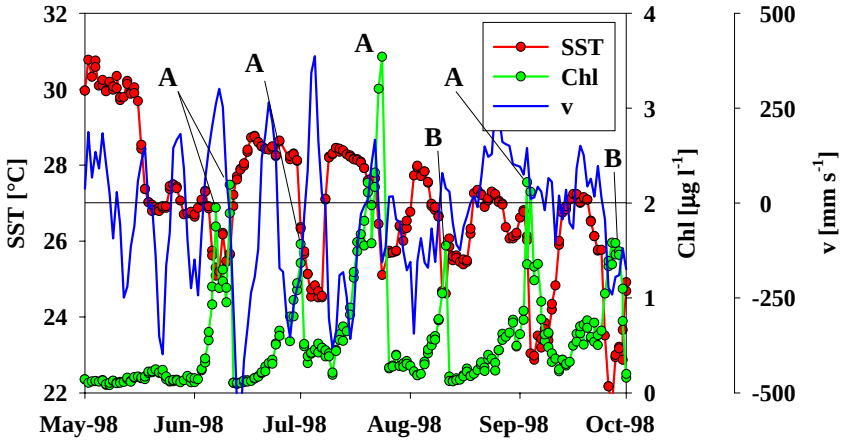

Figure 7.1 Time series of SST [°C] (—•—) and mooring-derived chlorophyll [µg l^{-1}] (—•—) at 2°N 110°W plotted with meridional velocity from 50 m ADCP data at 0° 110°W [mm s^{-1}] (———), May to September 1998. Extremely high chlorophyll concentrations are often observed at the leading or trailing edges of the cool SST anomaly (labeled A), or in the coolest sea surface waters associated with the core of the main equatorial upwelling bloom (labeled B). Positive values of v denote flow to the north at the equator, which should be indicative of northwards advection of cool, high-chlorophyll waters from the equatorial upwelling tongue.

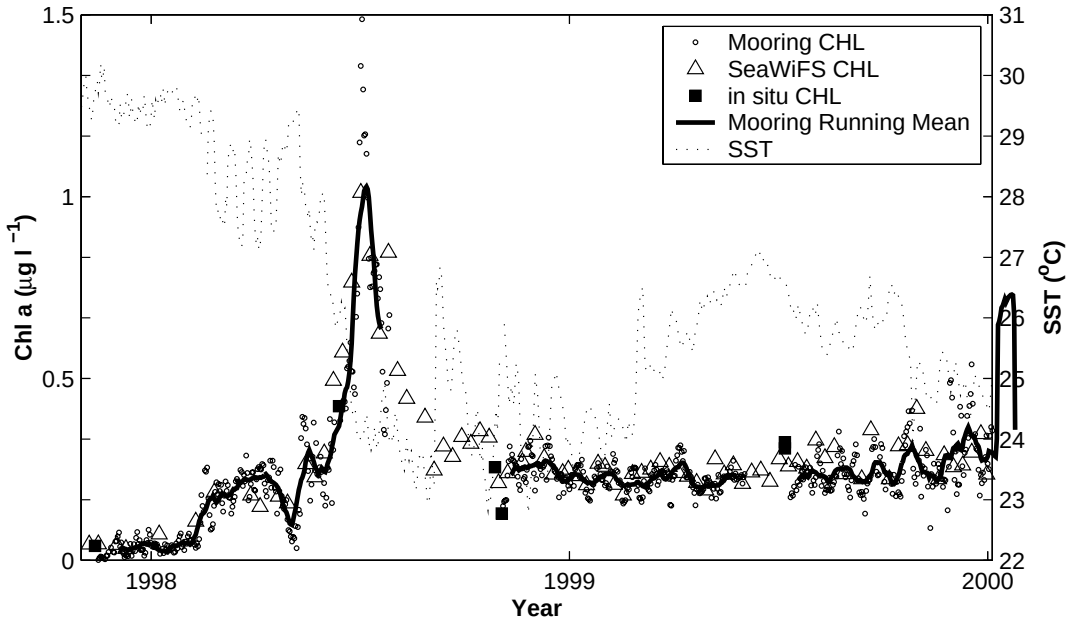

Figure 7.2 The time series of chlorophyll derived from the MBARI optical instruments on the TAO mooring at 0° 155°W (circles, solid line represents a moving average). For comparison, SeaWiFS chlorophyll for the mooring location is also plotted (triangles). The time series of SST indicates that the highest chlorophyll concentrations occurred during the retreat of the 1997-98 El Niño, in mid 1998. SeaWiFS and mooring chlorophyll exhibit relatively good agreement over more than an order of magnitude of chlorophyll concentrations.

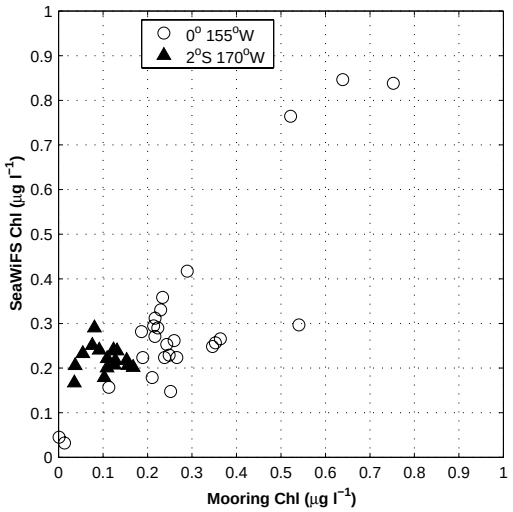

Figure 7.3 Comparison of SeaWiFS chlorophyll with mooring-derived chlorophyll for the MBARI instruments at 0° 155°W (circles) and 2°S 170°W (triangles). The data have been subject to the quality control described.

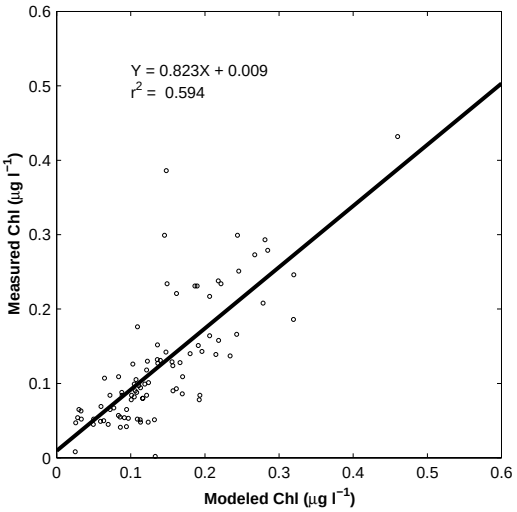

Figure 7.4 Comparison of surface chlorophyll concentrations obtained from SPMR optical cast data (x axis) with in-situ extracted chlorophyll (y axis).

along with existing optical profiles from almost every oceanic province.

In situ M*easurements*

Table 7.1 summarizes the cruises undertaken by MBARI thus far in support of SIMBIOS. Essentially, the cruise-based measurements consist of chlorophyll (using the fluorometric method described by Chavez *et al.* (1995)) and nutrient profiles (8 depths, 0-200m) obtained at CTD stations between 8°N and 8°S across the Pacific from 95°W to 165°E. On selected cruises (the 155°W and 170°W meridional transects), primary productivity (^{14}C) measurements are also performed. These data are archived at MBARI and the chlorophyll data provided to the SeaBASS database for algorithm development.

7.3 RESEARCH RESULTS

Biogeochemical Cycles

Several publications describing ecosystem variability in the equatorial Pacific have been produced under MBARI's SIMBIOS funding. Chavez *et al.* (1998) used mooring data from 0°, 155°W to describe the biological-physical coupling observed in the central equatorial Pacific during the onset of the 1997-98 El Niño. Chavez *et al*. (1999) combined the physical, biological and chemical data from moorings, ships and SeaWiFS to provide a comprehensive view of the ecosystem's response to the extreme physical forcings experienced during the 1997-98 El Niño. Strutton and Chavez (in press) summarized the *in situ* cruise measurements spanning the period from November 1996 to December 1998, and used these data to describe the perturbations to chlorophyll, nutrients and productivity during the same time period. Strutton *et al*. (submitted) used time series from the smaller Satlantic bio-optical packages (see above) and SeaWiFS imagery, to quantify the extreme anomalies in chlorophyll associated with the passage of tropical instability waves (TIWs) and the second half of 1998 and 1999. These data not only quantified the magnitude of the chlorophyll anomalies observed, but also helped to elucidate the mechanisms potentially responsible for the concentration of chlorophyll in association with TIWs. Figure 7.1 shows an example of the time series from 2°N 110°W where the relationship between TIWs and enhanced chlorophyll was particularly obvious between June and October 1998.

In addition to the manuscripts just described, Chavez *et al*. (2000) documented the design, and demonstrated efficacy of the shutter mechanism which protects the 20m radiometer on the moorings from fouling.

SeaWiFS Calibration/Validation

Figure 7.2 shows the time series collected thus far from the mooring at 0° 155°W. The two methods agree particularly well over a range of chlorophyll concentrations from ~0.05 to >1 μg l^{-1}. This agreement is further quantified in figure 7.3, which directly shows the comparison of the two methods for both the mooring at 0° 155°W and 2°S 170°W.

McClain and Fargion (1999b) showed matchup data derived from optical profiles of the SPMR in the equatorial Pacific. These data indicated excellent agreement between the satellite- and profile-derived water-leaving radiance values. Similarly, figure 7.4 compares the surface chlorophyll values obtained from SPMR casts with the extracted chlorophyll samples obtained at the same location.

7.4 CONCLUSIONS

Data collection will continue as for the period 1998-2000. The two major mooring installations at 0°, 155°W and 2°S, 170°W are now operating well and several improvements are planned for the next three year period of funding. These include the possible addition of hyperspectral instruments to better support validation efforts for future ocean color missions and increase the suite of biologically-relevant parameters that can be derived from the mooring data. The program of cruise-based measurements of chlorophyll, nutrients, primary productivity and bio-optical profiles will continue on up to eight equatorial Pacific cruises during 2000-2003, with scheduled SeaWiFS LAC where applicable, to enhance the probability of obtaining valid matchups.

During 1999 and 2000 our data processing and data provision capabilities have improved, & the majority of the mooring data can now be downloaded and plotted via the at: http:/bog.shore.mbari.org/servlet/NetcdfIndexServlet

During 2000 our quality control routines have been improved. The following quality control procedures are currently applied:

- Measured surface-incident irradiance (E_s) must be less than 1.15 times modeled E_s (Frouin, 1989).
- K_λ must be greater than that of pure water (Morel, 1988).
- Derive OC2 Chlorophyll for the Rrs ratios of 412/555, 443/555, 490/555, and 510/555. The coefficient of variance is calculated for each sample. Coefficients of variances less than 0.4 are acceptable.
- In coming years we hope to continue improvement of these criteria and use the results to perhaps modify mooring and instrument configurations.

REFERENCES

Chavez, F.P., and R.T. Barber, 1987: An estimate of new production in the equatorial Pacific, *Deep-Sea Research*, **34**, 1229-1243.

Chavez, F.P., K.R. Buck, R.R. Bidigare, D.M. Karl, D. Hebel, M. Latasa, L. Campbell and J. Newton, 1995: On the chlorophyll a retention properties of glass-fiber GF/F filters. *Limnology and Oceanography*, **40,** 428-433.

Chavez, F.P. and J. R. Toggweiler, 1995: in *Upwelling in the Ocean: Modern Processes and Ancient Records* C. P. Summerhayes, K. C. Emeis, M. V. Angel, R. L. Smith, B. Zeitzschel, Wiley & Sons, Chichester Eds., pp. 313-320.

Chavez, F.P., K.R. Buck, S.K. Service, J. Newton and R.T. Barber, 1996: Phytoplankton variability in the central and eastern tropical Pacific. *Deep-Sea Research*, ***43****(4-6)*, 835-870.

Chavez, F.P., P.G. Strutton, and M.J. McPhaden, 1998: Biological-physical coupling in the central equatorial Pacific during the onset of the 1997-98 El Niño. *Geophysical Research Letters*, **25***(19)*, 3543-3546.

Chavez, F.P., P.G Strutton, G.E. Friederich, R.A. Feely, G. Feldman, D. Foley and M.J. McPhaden, 1999: Biological and chemical response of the equatorial Pacific Ocean to the 1997-98 El Niño. *Science*, ***286,*** 2126-2131.

Chavez, F.P., D. Wright, R. Herlien, M. Kelley, F. Shane, and P.G. Strutton, 2000: A device for protecting moored spectroradiometers from bio-fouling. *Journal of Oceanic and Atmospheric Technology*. **17**, 215-219.

Dugdale, R.C. and F.P. Wilkerson, 1998: Silicate regulation of new production in the equatorial Pacific upwelling, *Nature****, 391***, 270-273.

Feely, R.A., R. Wanninkhof, T. Takahashi and P. Tans, 1999: Influence of El Niño on the equatorial Pacific contribution to atmospheric CO2 accumulation. *Nature*, **398**, 597-601.

Frouin, R., D.W. Ligner, and C. Gautier, 1989: A simple analytical formula to compute clear sky total and photosynthetically available solar irradiance at the ocean surface. *Journal of Geophysical Research*, **94,** 9731-9742.

McClain C.R. and G.S. Fargion, 1999a: SIMBIOS Project 1998 Annual Report. *NASA Tech. Memo. 1999-208645*, Eds., NASA Goddard Space Flight Center, Goddard, Maryland, 105pp.

McClain C.R. and G.S. Fargion, 1999b: SIMBIOS Project 1999 Annual Report. *NASA Tech. Memo. 1999-209486*, Eds., NASA Goddard Space Flight Center, Goddard, Maryland, 137pp.

Morel, A. 1988: Optical modeling of the upper ocean in relation to its biogenous matter content (Case I waters). *Journal of Geophysical Research*, ***93***, 10749-10768.

Strutton, P.G. and F.P. Chavez, 2000: Primary productivity in the equatorial Pacific during the 1997-98 El Niño. *J.Geophy. Research* (in press).

Tans, P.P., I. Y. Fung, T. Takahashi , 1990: Observational constraints on the global atmospheric CO_2 budget, *Science* **247,** 1431-1438.

Takahashi, T, R.A. Feely, R.F. Weiss, R. Wanninkhof, D.W. Chipman, S.C. Sutherland and Takahashi, 1997: Carbon dioxide and climate change. *Proceedings of the National Academy of Sciences*, **94**, 8314-8319.

Table 7.1. Summary of cruises during which *in situ* data have been obtained by MBARI in support of SIMBIOS. All cruises were undertaken aboard the NOAA ship *Ka'imimoana*, with the exception of cruise with ID ending in RB, which were aboard the NOAA ship *Ronald H. Brown*. Meridional transects indicate the lines occupied by the ship. Along each line, CTD stations were performed approximately every degree of latitude from 8°N to 8°S. Measurements consisted of extracted chlorophyll (Chl) plus nitrate, phosphate and silicate (Nutrients) at 8 depths between 0 and 200m. On selected cruises, primary productivity (PP) measurements were also made using ^{14}C incubation techniques, and daily optical profiles with the Satlantic Profiling Multispectral Radiometer (SPMR) were obtained. During GP7-98-KA, GP3-99-KA and GP7-99-KA, a SIMBAD radiometer was also used, on loan from the SIMBIOS instrument pool.

Cruise ID	Dates	Meridional transects	Measurements
GP6-97-KA	27-Sep-97 to 30-Oct-97	125°W and 140°W	Chl, PP, Nutrients, SPMR
GP7-97-KA	06-Nov-97 to 17-Dec-97	155°W, 170°W and 180°	Chl, PP, Nutrients, SPMR
GP1-98-KA	05-Feb-98 to 13-Mar-98	95°W and 110°W	Chl, Nutrients
GP2-98-KA	18-Apr-98 to 20-May-98	125°W and 140°W	Chl, Nutrients
GP3-98-KA	02-Jun-98 to 03-Jul-98	155°W and 170°W	Chl, PP, Nutrients, SPMR
GP4-98-KA	07-Jul-98 to 03-Aug-98	165°E and 180°	Chl, Nutrients
GP5-98-KA	05-Sep-98 to 09-Oct-98	125°W and 140°W	Chl, Nutrients
GP6-98-RB	11-Oct-98 to 13-Nov-98	95°W and 110°W	Chl, Nutrients
GP7-98-KA	19-Oct-98 to 13-Nov-98	155°W and 170°W	Chl, PP, Nutrients, SPMR
GP8-98-KA	18-Nov-98 to 12-Dec-98	180° and 170°W	Chl, Nutrients
GP1-99-KA	22-Jan-99 to 24-Feb-99	125°W and 140°W	Chl, Nutrients
GP2-99-KA	30-Apr-99 to 04-Jun-99	95°W and 110°W	Chl, Nutrients
GP3-99-KA	30-Jun-99 to 30-Jul-99	155°W and 170°W	Chl, PP, Nutrients, SPMR
GP4-99-KA	04-Aug-99 to 01-Sep-99	165°E and 180°	Chl, Nutrients
GP5-99-KA	09-Sep-99 to 14-Oct-99	125°W and 140°W	Chl, Nutrients
GP7-99-KA	20-Oct-99 to 14-Nov-99	155°W and 170°W	Chl, PP, Nutrients, SPMR
GP8-99-RB	1-Nov-99 to 10-Dec-99	95°W and 110°W	Chl, Nutrients
GP9-99-KA	18-Nov-99 to 12-Dec-99	180° and 170°W	Chl, Nutrients
GP1-00-KA	01-Feb-00 to 03-Mar-00	140°W and 125°W	Chl, Nutrients
GP2-00-KA	12-Apr-00 to 19-May-00	110° and 95°W	Chl, Nutrients
GP3-00-KA	15-Jun-00 to 12-Jul-00	155°W and 170°W	Chl, PP, Nutrients, SPMR
GP4-00-KA	17-Jul-00 to 14-Aug-00	165°E and 180°	Chl, Nutrients
GP5-00-KA	29-Aug-00 to 1-Oct-00	125°W and 140°W	Chl, Nutrients
GP6-00-KA	14-Oct-00 to 14-Nov-00	155°W and 170°W	Chl, PP, Nutrients, SPMR
GP7-00-RB	16-Oct-00 to 22-Nov-00	110°W and 95°W	Chl, Nutrients
GP8-00-KA	17-Nov-00 to 13-Dec-00	165°E and 180°	Chl, Nutrients

This research was supported by the

SIMBIOS NASA contract # 97134

PEER REVIEWED PUBLICATIONS

Chavez, F.P., Wright, D., Herlien, R., Kelley, M., Shane, F. and Strutton, P.G., 2000: A device for protecting moored spectroradiometers from bio-fouling. *Journal of Oceanic and Atmospheric Technology*. **17**, 215-219.

Chavez, F.P., Strutton, P.G., Friederich, G.E., Feely, R.A., Feldman, G.C., Foley, D.G. and McPhaden, M.J., 1999: Biological and chemical response of the equatorial Pacific Ocean to the 1997-98 El Niño. *Science*, **286**, 2126-2131.

Chavez, F.P., Strutton, P. G. and McPhaden, M. J., 1998: Biological-physical coupling in the equatorial Pacific during the onset of the 1997-98 El Niño. Geophysical Research Letters. **25**(19), 3543-3546.

Chavez, Francisco P., Peter G. Strutton and Michael J. McPhaden, 1998: Biological-physical coupling in the central equatorial Pacific during the onset of the 1997-98 El Niño. *Geophysical Research Letters*, **25**(19),3543-3546.

Accepted

Strutton, P.G. and Chavez, F.P. Primary productivity in the equatorial Pacific during the 1997-98 El Niño. *Journal of Geophyiscal Research*.

Submitted

Strutton, P.G., Ryan, J.P. and Chavez, F.P. Enhanced chlorophyll at tropical instability wave fronts in the equatorial Pacific. Geophysical Research Letters.

PRESENTATIONS

Chavez, Francisco, Gene Feldman, Michael McPhaden, David Foley and Peter Strutton, 1998: Remote Sensing of the Equatorial Pacific during 1997-98. AGU Fall Meeting, San Francisco, CA.

Friederich, Gernot, Francisco Chavez, Peter Strutton and Peter Walz, 1998: Bio-optical and Carbon Dioxide Time Series From Moorings in the Equatorial Pacific During 1997-1998. AGU Fall Meeting, San Francisco, CA.

Friederich, G E Walz, P M Strutton, P G Burczynski, M G Chavez, F P Seasurface pCO_2 Time Series from Moorings in Equatorial and Coastal Upwelling Systems. AGU Ocean Sciences meeting, San Antonio, Texas.

Strutton, P.G., Chavez, F.P. and McPhaden, M.J., 1998: In situ measurements of primary productivity in the equatorial Pacific during the 1997-98 El Niño. AGU Fall Meeting, San Francisco, CA.

Strutton, P.G., Ryan, J.P., Polito, P. and Chavez, F.P., 2000: High Chlorophyll in the Equatorial Pacific During 1998 Associated With Tropical Instability Wave Fronts. AGU Ocean Sciences meeting, San Antonio, TX.

Strutton, Peter G., Francisco P. Chavez and Michael J. McPhaden, 1998: Biological-physical coupling in the central equatorial Pacific during the 1997-98 El Niño. Ocean Optics XIV, Kailua-Kona, HI.

Strutton, Peter G., Francisco P. Chavez and Michael J. McPhaden, 1998: Primary productivity in the equatorial Pacific during the onset of the 1997-98 El Nino. AGU/ASLO Ocean Sciences Meeting, San Diego, CA.

Strutton, Peter G., Francisco P. Chavez and Michael J. McPhaden, 1998: Primary productivity in the equatorial Pacific during the onset of the 1997-98 El Nino. Pacific Climate Workshop, Catalina Island.

Strutton, Peter G., Francisco P. Chavez and Michael J. McPhaden, 1998: *In situ* measurements of primary productivity in the equatorial Pacific during the 1997-98 El Niño. AGU Fall Meeting, San Francisco, CA.

Strutton, Peter, Francisco Chavez, David Foley, Brian Schlining and Michael J. McPhaden, 1999: Remote Sensing of Biological-Physical Coupling in the Equatorial Pacific. ASLO Ocean Sciences Meeting, Santa Fe, NM.

Chapter 8

High Frequency, Long Time Series Measurements from the Bermuda Testbed Mooring in Support of SIMBIOS

Tommy Dickey, Laura Dobeck, David Sigurdson,

Sarah Zedler, Derek Manov and Xuri Yu

University of California at Santa Barbara, Santa Barbara, California

8.1 INTRODUCTION

It has been recognized that optical moorings are important platforms for the validation of SeaWiFS (Mueller and Austin, 1992). It was recommended that optical moorings be maintained in order to 1) provide long-term time series comparisons between in situ and SeaWiFS measurements of normalized water-leaving radiance (e.g., Gordon and Wang, 1994), 2) develop and test algorithms for pigment biomass and phytoplankton primary productivity, and 3) provide long-term, virtually continuous in situ observations which can be used to determine and optimize the accuracy of derived satellite products. These applications require the use of in situ radiometers for long periods of time to evaluate and correct for inherent satellite undersampling (aliasing and biasing) and degradation of satellite color sensors (e.g., drifts as experienced by CZCS).

The Bermuda Testbed Mooring program was initiated in 1994 at a site located about 80km southeast of Bermuda (31° 43' N, 64° 10' W) in waters of about 4530m depth (Dickey et al., 1997, 1998a, 2000). In August 1997 (i.e., BTM Deployment 8), with NASA's support, we started to provide the SIMBIOS program with large volumes of high frequency, long-term time-series bio-optical data from the BTM for SeaWiFS satellite ocean color groundtruthing and algorithm development. This NASA supported portion of the BTM activity spanned three years and covered five BTM deployments (No. 7 - 12). During these three years, the quality of radiometric data has improved dramatically. Excellent agreement between BTM moored data and both SeaWiFS and nearby ship profile radiometric data (e.g., Figures 8.1 and 8.2) demonstrate that technical advances in the moored optical observations have reduced the major difficulties that moored platforms face: biofouling and less frequent calibration.

8.2 RESEARCH ACTIVITIES

Key NASA supported BTM optical measurements have included: surface downwelling spectral irradiance (7 • 's, SeaWiFS matched: • = 412, 443, 490, 510, 555, 665, and 683nm;10nm bandwidth at half power) and subsurface downwelling spectral irradiance and upwelling spectral radiance (7 • 's for each, SeaWiFS matched). Data are collected at 6Hz for 45sec every hour during daylight and at midnight. In 1999, a 3-wavelength radiance sensor (• = 443, 490, and 555nm) at 7m and 7-wavelength radiance systems at 5 and 10m were deployed. These additional systems, with similar sampling schemes, significantly improve accuracy of the derived products such as water-leaving radiance (L_w) and spectral diffuse attenuation (K_d) which need vertical gradients of direct measurements for derivation. All the hourly averaged data have been submitted to the SIMBIOS office along with some high-resolution data with the original sampling rates. In addition, a telemetry system was used to provide near real-time BTM radiometric data to the UCSB Ocean Physics Laboratory for Deployments 11 and 12 (April - November 1999) and a software package was developed to make key data available to the SIMBIOS Project on a daily basis.

Products derived from the measured radiometric quantities include spectral attenuation coefficients, spectral reflectance ratios, and spectral water-leaving radiances. These data provide necessary links to and interpolation of radiometric data for remotely sensed observations of ocean color (e.g., SeaWiFS color imager), which can be used to estimate biomass and primary productivity globally. Spectral diffuse attenuation (K_d) at 490nm and water-leaving radiances (L_w) at 6 wavelengths (• = 412, 443, 490, 510, 555 and 665nm) were submitted to the SIMBIOS office. Time series of hourly averaged L_w at 412, 490 and 555nm and their comparison with the L_w from Bermuda Bio-optical Project (BBOP; e.g., Siegel et al. 1995) are shown in Figure 8.1 a and b. Intercomparison of near-noon L_w between BTM and SeaWiFS is shown in Figure 8.2.

The number of match-ups between BTM and SeaWiFS L_w is limited by the availability of SeaWiFS data. In addition to excellent agreement with both BBOP and SeaWiFS products, the BTM provides large volumes of virtually continuous data; continuity is certainly very important for studies on high-frequency variability.

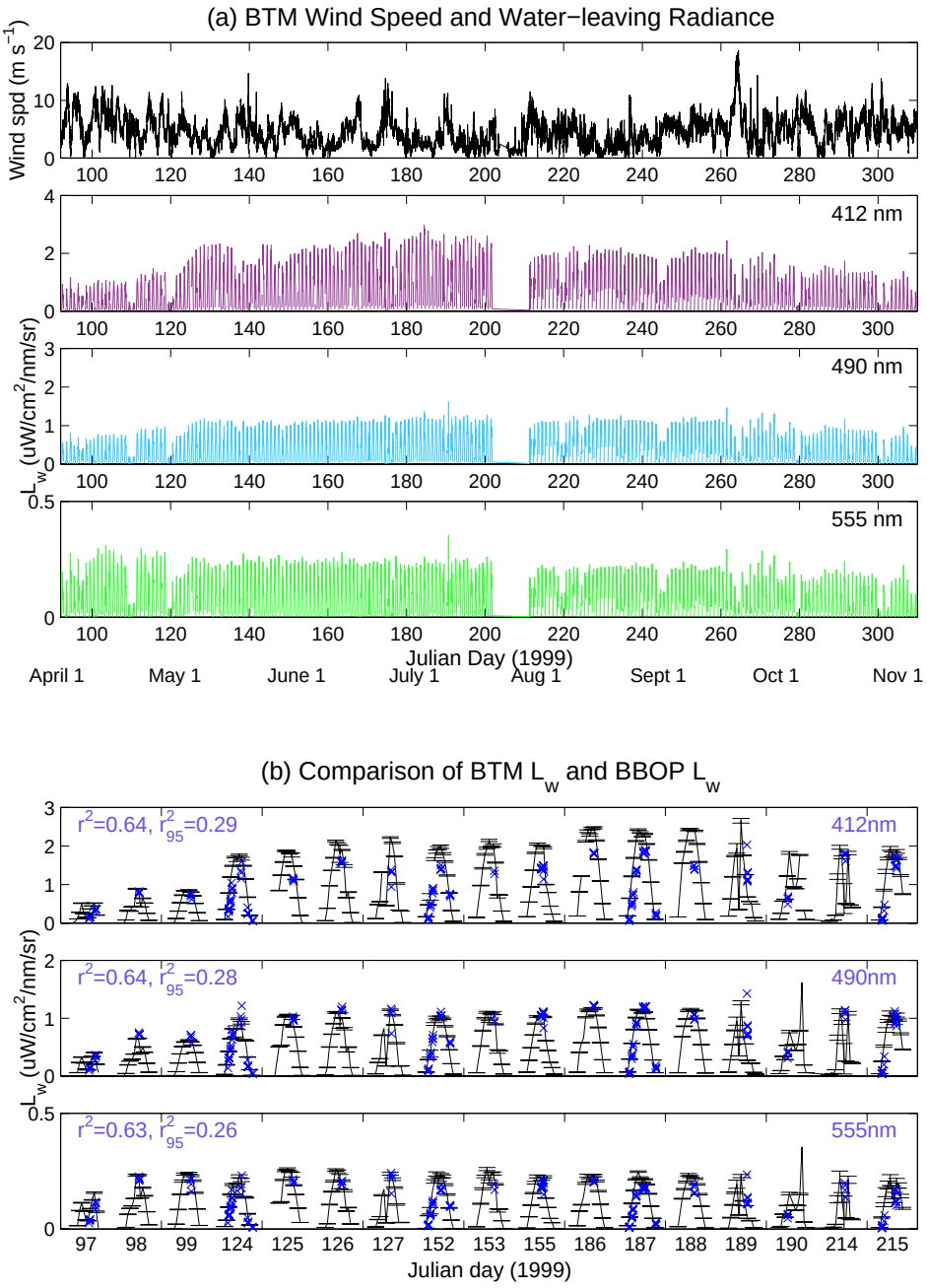

Figure 8.1. (a) Time series of surface wind speed (m s^{-1}) and water-leaving radiance L_w (•W cm^{-2} nm^{-1} sr^{-1}) for three selected wavelengths from BTM Deployments #11 and #12 (April 1 - November 6, 1999). Wavelengths are indicated in the upper-right corner of each panel.

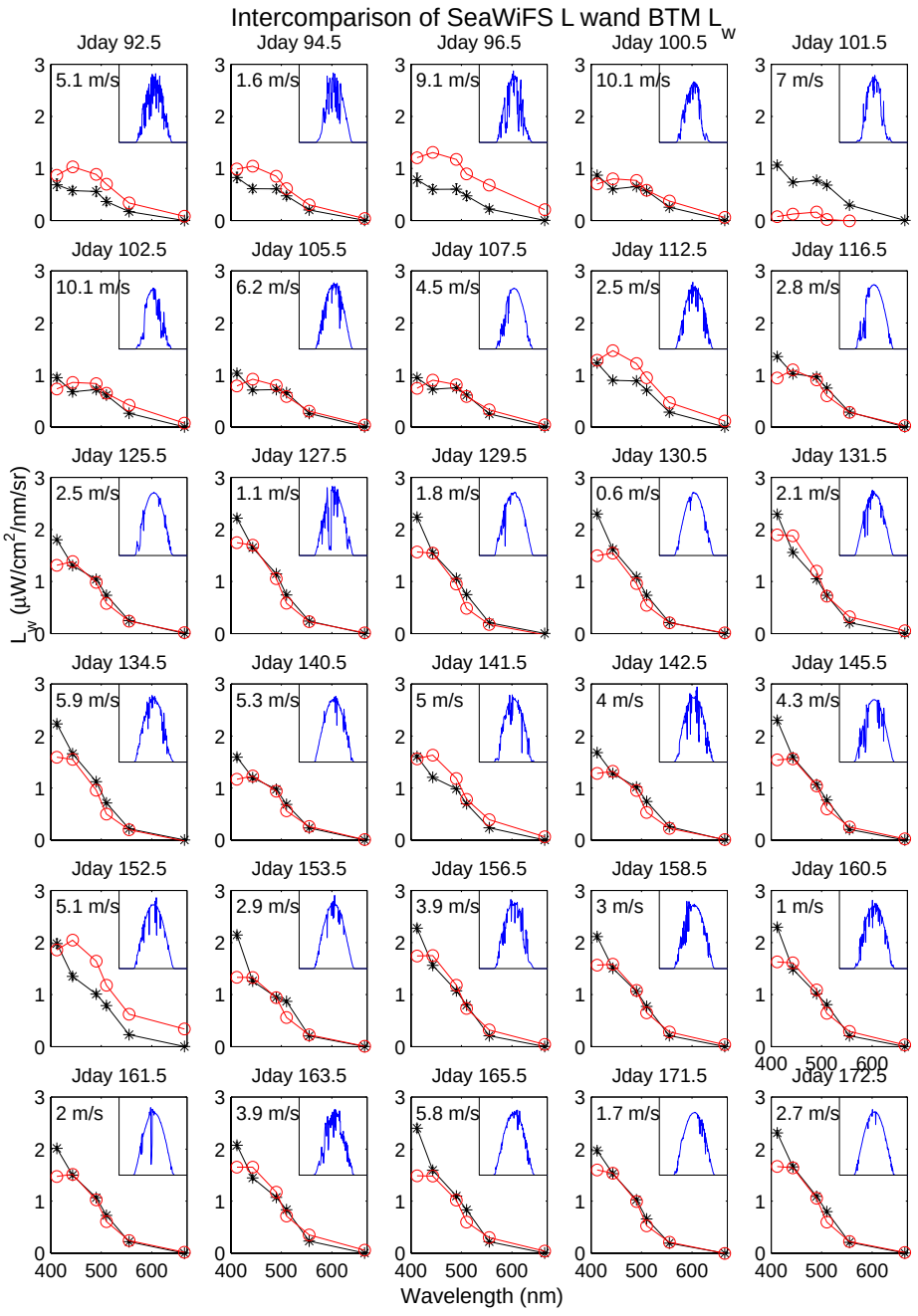

Figure 8.1. (b) Intercomparison between BTM L_w and BBOP L_w. Only those days when BBOP data are available are chosen. Circles are BTM data and asterixs are BBOP data. Vertical bars are 95% confidence intervals for hourly averaged BTM data. Squared cross-correlation coefficients and 95% significance levels are shown in the upper-left corner of each panel.

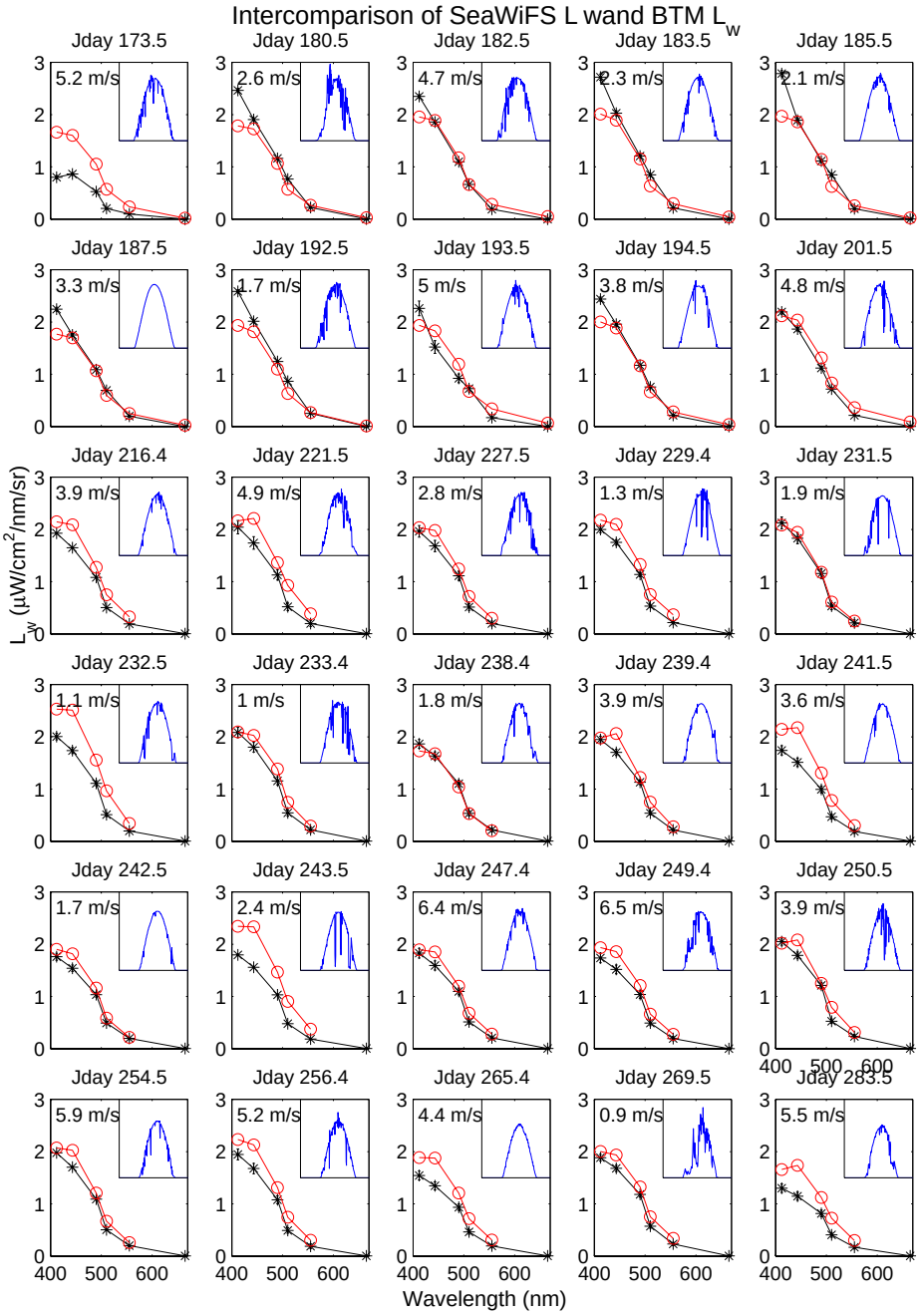

Figures 8.2. Spectral water-leaving radiance L_w derived from the BTM radiometers and from the SeaWiFS ocean color satellite for 60 days during Deployments #11 and #12 (April 1 - November 6, 1999). These panels show L_w values near noon on these 60 days (Julian day shown on the top of each panel). The circles indicate data from SeaWiFS and asterisks indicate BTM data. Noontime (1-h average) wind speed is indicated and the upper-right corner shows time series of the incident shortwave radiation for the day of interest. Cloudy days are evident.

8.3 RESEARCH RESULTS

Research activities are two-fold: technical improvements and scientific studies. Technically, moored optical platforms face two major issues: less frequent sensor calibration and biofouling. Continuous in situ calibration is not possible for moored instruments; therefore, BTM radiometric data are processed with pre-deployment and post-deployment factory calibrations. To deal with biofouling, copper shutters were recently installed adjacent to each optical window. The windows are open only during sampling. This technique is proving quite successful and extends the useful period of sampling. In addition, these data are compared with available concurrent BBOP shipboard profiling measurements and SeaWiFS data. We have applied a series of quality control and consistency tests, some of which were developed by Jay O'Reilly (Maritorena and O'Reilly, 2000), to the BTM data.

Scientifically, the radiometric data from the BTM have been used for a variety of studies. From these studies, several papers have been published (e.g., Dickey et al, 1998, 2000; Stramska and Dickey, 1998; McGillicuddy et al., 1998; McNeil et al., 1999). We are presently exploring the effects of wind speed, waves, solar altitudes and other atmospheric and oceanic conditions on radiometric properties. In addition, we have statistically analyzed intercomparison data between BTM, SeaWiFS and BBOP L_w, quantifying effects and biases arising from different undersampling methodologies by ships and satellites.

8.4 CONCLUSIONS

We have demonstrated that moorings-of-opportunity, such as the BTM, can provide large volumes of useful radiometric measurements for groundtruthing and algorithm development for ocean color satellite imagers. Further, it appears that BTM data sets will be quite useful for developing satellite correction algorithms for various environmental and undersampling effects. The BTM is a mature platform enabling the collection of large volumes of quality radiometric data for use with ocean color satellites. The concept of moorings-of-opportunity has been shown to be viable and in many ways superior to more traditional approaches. The next step is to implement optical measurements similar to those developed for the BTM SIMBIOS project using moorings in selected ocean regions as part of global ocean observatory programs.

ACKNOWLEDGMENTS

Data used for comparing ship-based and BTM data were shared by David Siegel and Margaret O'Brien. SeaWiFS data were provided for comparisons by the SIMBIOS Office, which also gave important input and suggestions for our study. The Bermuda Testbed Mooring program is supported by the NASA SIMBIOS program, the National Science Foundation, the Office of Naval Research, the National Ocean Partnership Program, and the University of California, Santa Barbara.

REFERENCES

Dickey, T.D., D. Frye, H.W. Jannasch, E. Boyle, and A.H. Knap, 1997: Bermuda sensor system testbed, *Sea Tech.*, 81-86.

Dickey, T., D. Frye, H. Jannasch, E. Boyle, D. Manov et al., 1998a: Initial results from the Bermuda Testbed Mooring Program, *Deep-Sea Res*. I, **45**, 771-794.

Dickey, T., D. Frye, J. McNeil, D. Manov, N. Nelson, D. Sigurdson, H. Jannasch, D. Siegel, A. Michaels, and R. Johnson, 1998b: Upper ocean temperature response to Hurricane Felix as measured by the Bermuda Testbed Mooring, *Mon. Wea. Rev*., **126**, 1195-1201.

Dickey, T., S. Zedler, X. Yu, S. Doney, D. Frye, H. Jannasch, D. Manov, D. Sigurdson, J.D. McNeil, L. Dobeck, T. Gilboy, 2000: Physical and biogeochemical variability from hours to years at the Bermuda Testbed Mooring: June 1994 – March 1998. *Deep-Sea Res*., (accepted).

Gordon, W.R. and M. Wang, 1994: Retrieval of water-leaving radiance and aerosol optical thickness over the oceans with SeaWiFS: a preliminary algorithm, *Appl. Optics*, **33**, 443-452.

Maritorena, S. and J. O'Reilly, 2000: Update on the operational SeaWiFS chlorophyll a algorithm. In SeaWiFS Postlaunch Calibration and Validation Analyses, Part 2, NASA Technical Memorandum 1999-206892, in press.

McGillicuddy, D.J., A.R. Robinson, D.A. Siegel, H.W. Jannasch, R. Johnson, T.D. Dickey, J.D. McNeil, A.F. Michaels, and A.H. Knap, 1998: New evidence for the impact of mesoscale eddies on biogeochemical cycling in the Sargasso Sea, *Nature*, **394**, 263-266.

McNeil, J. D., H. Jannasch, T. Dickey, D. McGillicuddy, M. Brzezinski, and C. M. Sakamoto, 1999: New chemical, bio-optical, and physical observations of upper ocean response to the passage of a mesoscale eddy, accepted, *J. Geophys. Res.*, **104**, 15,537-15,548.

Mueller, J.L. and R.W. Austin, 1992: Ocean Optics Protocols for SeaWiFS Validation, SeaWiFS Tech. Report Series, NASA Technical Memorandum 104566, Goddard Space Flight Center, Greenbelt, MD, 43pp.

Siegel, D.A., A.F. Michaels, J.C. Sorensen, M. O'Brien, and M.A. Hammer, 1995: Seasonal variability of light

availability and utilization in the Sargasso Sea, *J. Geophys. Res*., **100**, 8675 8713.

Stramska, M. and T. D. Dickey, 1998: Short term variability of the underwater light field in the oligotrophic ocean in response to surface waves and clouds. *Deep-Sea Res*. I, **45**, 1393-1410.

This research was supported by the

SIMBIOS NASA contract # 97127

PEER REVIEWED PUBLICATIONS

Dickey, T. D., D. Frye, H. W. Jannasch, E. Boyle and A. H. Knap, 1997: Bermuda sensor system testbed. *Sea Tech.*,, 81-86.

Dickey, T., D. Frye, H. Jannasch, E. Boyle, D. Manov, D. Sigurdson, J. McNeil, M. Stramska, A. Michaels, N. Nelson, D. Siegel, G. Chang, J. Wu, and A. Knap, 1998: Initial results from the Bermuda Testbed Mooring Program. *Deep-Sea Res. I*, **45**, 771-794.

Dickey, T., D. Frye, J. McNeil, D. Manov, N. Nelson, D. Sigurdson, H. Jannasch, D. Siegel, A. Michaels, and R. Johnson, 1998: Upper ocean temperature response to Hurricane Felix as measured by the Bermuda Testbed Mooring. *Mon. Wea. Rev*., **126**, 1195-1201.

Dickey, T., S. Zedler, X. Yu, S. Doney, D. Frye, H. Jannasch, D. Manov, D. Sigurdson, J.D. McNeil, L. Dobeck, T. Gilboy, 2000: Physical and biogeochemical variability from hours to years at the Bermuda Testbed Mooring: June 1994 – March 1998. *Deep-Sea Res*., in press.

Dickey, T., 2000: Instrumentation and new technologies, Chapter 6 in the book, Oceans 2020: *Science for Future Needs*, (in press).

Dickey, T., 2000: Sensors: inherent and apparent optical properties, in Encyclopedia of Ocean Science, eds. J. Steele, J. Thorpe, and K. Turekian, (in press).

Dickey, T., and P.G. Falkowski, 2000: Chapter 9. Solar energy and its biological-physical interactions in the sea. *The Sea*, (in press).

Glenn, S.M., W. Boicourt, B. Parker, and T.D. Dickey, 2000: Operational observation networks for ports, a large estuary, and an open shelf. *Oceanography*, **13**, 12-23.

McGillicuddy, D. J., A. R. Robinson, D. A. Siegel, H. W. Jannasch, R. Johnson, T. D. Dickey, J. D. McNeil, A. F. Michaels, and A. H. Knap, 1998: New evidence for the impact of mesoscale eddies on biogeochemical cycling in the Sargasso Sea. *Nature*, **394**, 263-266.

McNeil, J. D., H. Jannasch, T. Dickey, D. McGillicuddy, M. Brzezinski, and C. M. Sakamoto, 1999: New chemical, bio-optical, and physical observations of upper ocean response to the passage of a mesoscale eddy, *J. Geophys. Res*., **104,** 15,537-15,548.

Stramska, M. and T. D. Dickey, 1998: Short term variability of the underwater light field in the oligotrophic ocean in response to surface waves and clouds. *Deep-Sea Res. I*, **45**, 1393-1410.

PRESENTATIONS

Dickey, T., 1999: Recent Advances in Interdisciplinary Technologies and Their Potential Utilization in Ocean Observing Systems. Proceedings of the International Symposium: The Ocean Observing System, St. Raphael, France.

Dickey, T. D., X. Yu, L. Dobeck, S. Zedler, D. Sigurdson, and D. Manov, 2000: Optimal Utilization of Remotely-Sensed Color Data for Ocean Carbon Cycle Studies. *AGU/ASLO* Ocean Sciences Meeting, San Antonio, Texas.

Dickey, T., Emerging interdisciplinary technologies and their potential utilization in the Global Ocean Observing System, 2000: *Oceanology 2000*, Brighton, UK.

Dickey, T., 2000: The Bermuda Testbed Mooring: A mooring-of-opportunity for groundtruthing ocean color satellites, Oceans from Space, Venice, Italy.

Griffiths, G., R. Davis, C. Eriksen, D. Frye, P. Marchand, and T. Dickey, 1999: Towards new platform technology for sustained observations. Proceedings of the International Symposium: The Ocean Observing System, St. Raphael, France.

Manov, et al., 1998: Design of bio-optical and physical systems for moorings: Bermuda Testbed and Coastal Mixing and Optics. *AGU/ASLO*, San Diego.

McNeil ,et al., 1998: Bio-optical and chemical observations of the response of the upper ocean to the passage of a mesoscale eddy at the Bermuda Testbed Mooring. *AGU/ASLO*, San Diego.

Send, U., R. Weller, S. Cunningham, C. Eriksen, T. Dickey, M. Kawabe, R. Lukas, M. McCartney, S. Osterhuis, 1999: Oceanographic Time-series observations. Proceedings of the International Symposium*:* The Ocean Observing System, St. Raphael, France.

Sigurdson, et al., 1998: Design of a near real-time telemetry system for the Bermuda Testbed Mooring (BTM). *AGU/ASLO*, San Diego.

Sigurdson, D. E., D. V. Manov, T. D. Dickey, D. E. Frye, and J. Kemp, 2000: Results from the Near Real-Time Telemetry System on board the Bermuda Testbed Mooring (BTM). *AGU/ASLO* Ocean Sciences Meeting, San Antonio, Texas.

Zedler, et al., 1998: Time series observations and model simulations of Hurricane Felix, *AGU/ASLO*, San Diego.

Chapter 9

Remote Sensing of Ocean Color in the Arctic: Algorithm Development and Comparative Validation

Glenn F. Cota

Old Dominion University, Norfolk, Virginia

9.1 INTRODUCTION

The overall goal of this effort is to acquire a large bio-optical database, encompassing most environmental variability in the Arctic, to develop algorithms for phytoplankton biomass and production and other optically active constituents. A large suite of bio-optical and biogeochemical observations have been collected in a variety of high latitude ecosystems at different seasons.

The Ocean Research Consortium of the Arctic (ORCA) (www.ccpo.odu.edu/~orca/) is a collaborative effort between G.F. Cota of Old Dominion University (ODU), W.G. Harrison and T. Platt of the Bedford Institute of Oceanography (BIO), S. Sathyendranath of Dalhousie University and S. Saitoh of Hokkaido University. ORCA has now conducted 12 cruises and collected over 500 in-water optical profiles (Fig. 1A) plus a variety of ancillary data. Observational suites typically include apparent optical properties (AOPs), inherent optical property (IOPs), and a variety of ancillary observations including sun photometery, biogeochemical profiles and productivity measurements. All quality-assured data have been submitted to NASA's SeaBASS data archive. Our algorithm development efforts address most of the potential bio-optical data products for SeaWiFS, MODIS and GLI, and provides validation for a specific areas of concern, i.e. high latitudes and coastal waters.

9.2 RESEARCH ACTIVITIES

Two cruises on ships of opportunity were successfully completed. The first cruise in May-June, 2000 was on the CCG Hudson to the Labrador Sea. It was somewhat abbreviated by ship's mechanical problems, but still largely successful. The second cruise in August, 2000 was on the USCG Polar Star to the Chukchi and Beaufort Seas. This icebreaker cruise was highly successful with substantial collections of both AOPs and IOPs spanning a very wide range of environmental conditions.

Research efforts have focussed on data acquisition, processing and analysis, match-up analysis, and modeling and synthesis for publication. Our Labrador Sea data sets played a central role in NASA's and NASDA's validation efforts for OCTS, and have facilitated other lines of research (Pickart et al. 2000). Shareware PERL code has been developed to attach SeaBASS headers for common types of optical observations and is available on our web site. Additional ancillary data are also being submitted as they become available from our lab and collaborators.

Data sets have also been or are being made available to other investigators including Bernie Walters for detection of surface slicks with SAR, Jay O'Reilly for algorithm development of OC4 (O'Reilly et al. 2000) and spectral 1324 indices, Bob Pickart for time series analysis and feature identification in the Labrador Sea, planning of phase II field activities for NSF's Western Arctic Shelf Basin Interaction program, and others. The data sets are being made widely available via the web as our web site is expanded to include optical data, value-added products, a variety of ancillary information, and presentations. Cruise reports, station sheets, photos of sky and sea state, instrument specifications, calibration histories, etc. will be available.

9.3 RESEARCH RESULTS

High latitude ecosystems are often highly productive with a large range for biomass, which must be considered in algorithm development. Polar waters experience unique environmental conditions, and their bio-optical properties differ markedly from temperate data and models (e.g. Mitchell 1992, Sathyendranath et al. 2000). The current OC4V4 SeaWiFS algorithm shown in Figure 9.1 incorporates over half of our Arctic data (O'Reilly et al. 2000), and certainly is an improvement over previous SeaWiFS algorithms. However, compared to our tuned linear (OC4L) Arctic algorithm SeaWiFS OC4V4 underpredicts chlorophyll concentrations >1.5X across most of the range (Fig. 9.1B). Polynomial models (i.e. OC4P) may improve determination coefficients slightly, but there are no compelling bio-physical reasons to adopt them and they can be unreliable if extrapolated. Regional differences are evident in our Arctic datasets (Fig. 9.1A), but comparisons are confounded by different and limited ranges of biomass and environmental conditions.

Taxon-specific algorithms are attractive because of seasonal succession, regional dominance, and potential differences in taxon-specific productivity, export, or carbon cycling. Diatoms or prymnesiophytes often dominate polar phytoplankton assemblages, but are their optical signatures sufficiently distinct to discriminate between groups? Prymnesiophytes dominated reflectances signatures in the Labrador Sea (Fig. 9.2A), and had higher chlorophyll-specific absorption than diatoms (Cota et al. 2000a, Sathyendranath et al. 2000). Stations dominated by diatoms may have a distinct bio-optical relationship (Fig. 9.2A). However, taxon-specific algorithms seem premature given limited ranges, small sample sizes, and overlapping reflectance ratios.

There is a large degree of similarity between most algorithms developed at high latitude (Fig. 9.2B), where each algorithm is plotted over the approximate range of observations it was developed from. Our latest Arctic 2000 (Arc00) data extends the lower chlorophyll range, confirming a few low observations from the Gulf of Alaska and Bering Sea. Inclusion of these data changes the slope significantly from other regions like the Labrador Sea (Cota et al. 2000a). The latest Arctic OC4L lines now agrees better with the new OC4V4 SeaWiFS global algorithm except at low chlorophyll concentration (Figs. 9.1B & 9.2B). The most strikingly different algorithm is Arrigo et al.'s (1998) D+P for diatoms plus *Phaeocystis* (prymnesiophytes). Statistical differences between the slopes or intercepts for their algorithm were not reported, but their Table 4 and Figure 9 suggests their diatom, *Phaeocystis*, D+P, and all combined algorithms were very similar, perhaps indistinguishable. Mitchell's (1992) algorithms for the Arctic and Antarctic, Arrigo et al.'s (1998) for cryptophytes from the Ross Sea, Deirrsen and Smith's (in press) for the Antarctic Peninsula region and our Labrador Sea algorithm (not shown, Cota et al. 2000a) all display similar slopes. The range(s) of data used to develop algorithms can have a major influence on the slope of lines, and a broad range of environmental conditions is critical to develop robust algorithms. Mitchell's (1992) algorithms utilized radiance (not reflectance) ratios, slightly different spectral bands (488/560 nm), and included chlorophyll plus phaeopigments or "CZCS-pigment". Phaeopigments typically have a very minor influence on these relationships and should be excluded.

Remote sensing reflectance R_{rs} measurements made above-water have obvious utility, but are not widely accepted. Comparisons of select in-water and above-water R_{rs} ratios reveal a strong relationship in Figure 9.3 explaining about 92% of the variability. The slope is lower than unity in this limited data set. However, above-water reflectances appear to be slightly higher than in-water values, and more work is needed to clarify these differences and their variability.

Inherent optical properties hold the key to much of the regional variability. Relatively large diatom cells in high Arctic waters can be highly packaged (>90%) with very low chlorophyll-specific absorption compared with lower latitude ecosystems (Cota et al. 2000b). Specific absorption for diatoms at Resolute (Cota et al. 2000b) were about half those in the Labrador Sea (Cota et al. 2000a). Simulations with HydroLight (Mobley 1994) employing low, variable backscattering and the mean absorption spectra for phytoplankton and soluble materials reproduce the measured reflectance spectra except at lower biomass levels in the blue and green regions. Backscattering appears to be about twice as high at Resolute as in the Labrador Sea. Inclusion of scattering by nonpigmented particles should resolve discrepancies between observed and predicted reflectances. Absorption due to soluble matter also varies regionally with the highest values in our northernmost study site, the Canadian Arctic Archipelago near Resolute Bay, but nowhere have we found a good relationship with chlorophyll.

Several approaches for estimating primary production in the Arctic have been evaluated, but more recent results are being incorporated. Briefly, simple band-ratio algorithms explain about 80% and 50% of the observed variability between surface chlorophyll and integrated net daily production, respectively. Several production models were also tuned with our high latitude data for comparison Yoder's (pers. comm., Howard and Yoder 1997) MODIS production algorithm is a depth-integrated model employing satellite chlorophyll, daily PAR, SST, and climatologies for MLD. This model underestimated observed production with a slope of 0.74 and explained 42% of the variance. This discrepancy resulted primarily from melting ice, which made the observed MLD 3-10 times shallower than climatological estimates. Their estimated K_{PAR} would also be considerably higher than observed values at higher biomass levels. Another depth-integrated model by Behrenfeld and Falkowski (1997) utilizes similar environmental inputs and a temperature-dependent P_{opt} derived from productivity profiles. Their model also underpredicted production with a slope of 0.55, but explained 56% of the variance. Compound errors in satellite predicted chlorophyll and production would be ~two to fourfold underestimates. Performance deficiencies of various models are being explored.

9.4 CONCLUSIONS

Outstanding ancillary observations from our lab and international collaborators will be submitted as they become available. Additional publications are being prepared. Further improvements are being made to our web site.

ACKNOWLEDGEMENTS

Additional support was provided by Canada's Department of Fisheries and Oceans, Natural Resources Canada, and Japan's NASDA. The author thanks W.G. Harrison, T. Platt, S. Sathyendranath, V. Stuart, S. Saitoh, D.A. Ruble and J. Wang.

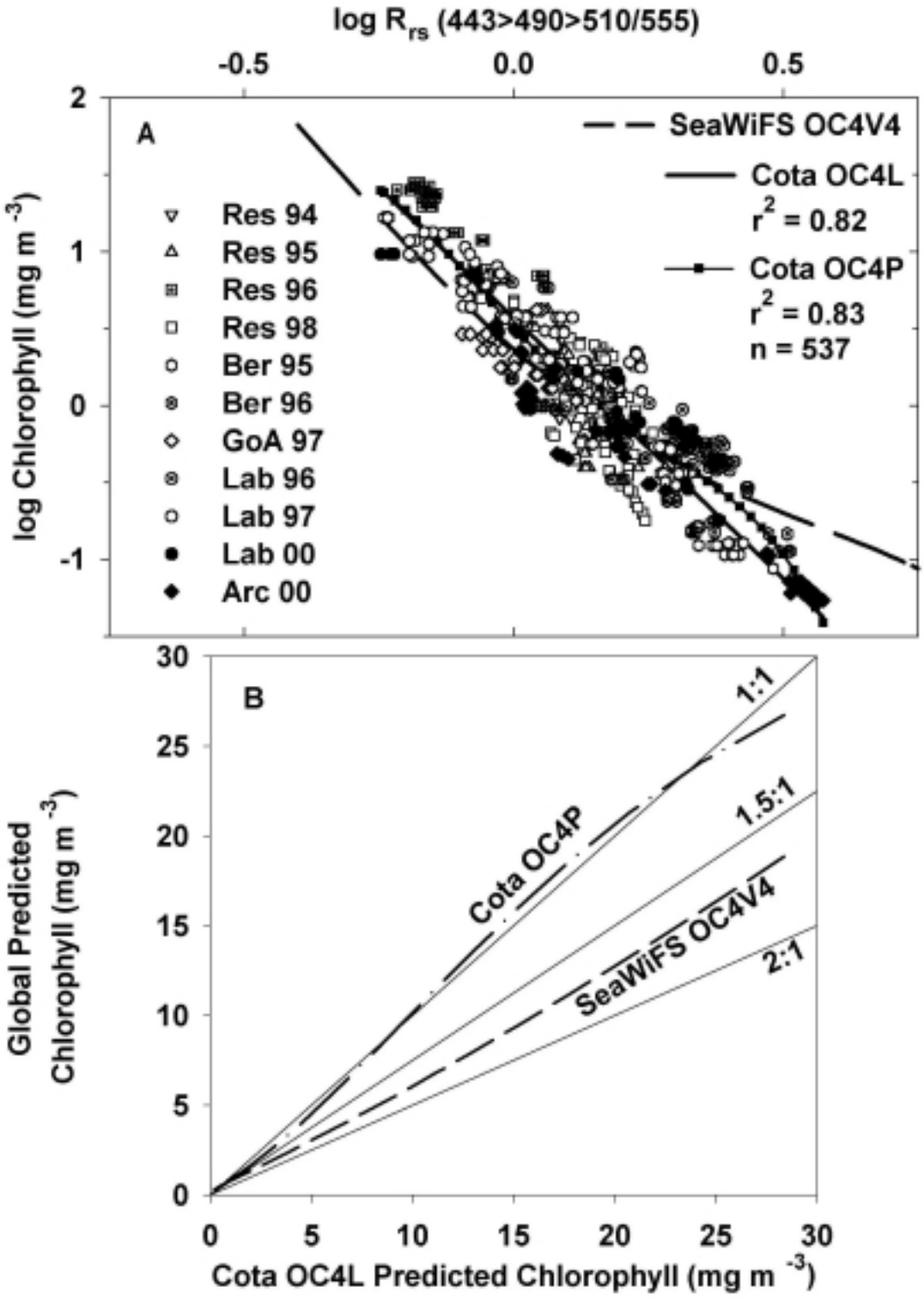

Figure 9.1. Tuned maximum-band chlorophyll algorithms for the Arctic and the OC4V4 SeaWiFS algorithm. **A**. Arctic algorithms are linear (OC4L) and 4th order polynomial (OC4P). **B**. Chlorophyll retrievals from OC4L compared to OC4P and SeaWiFS OC4V4.

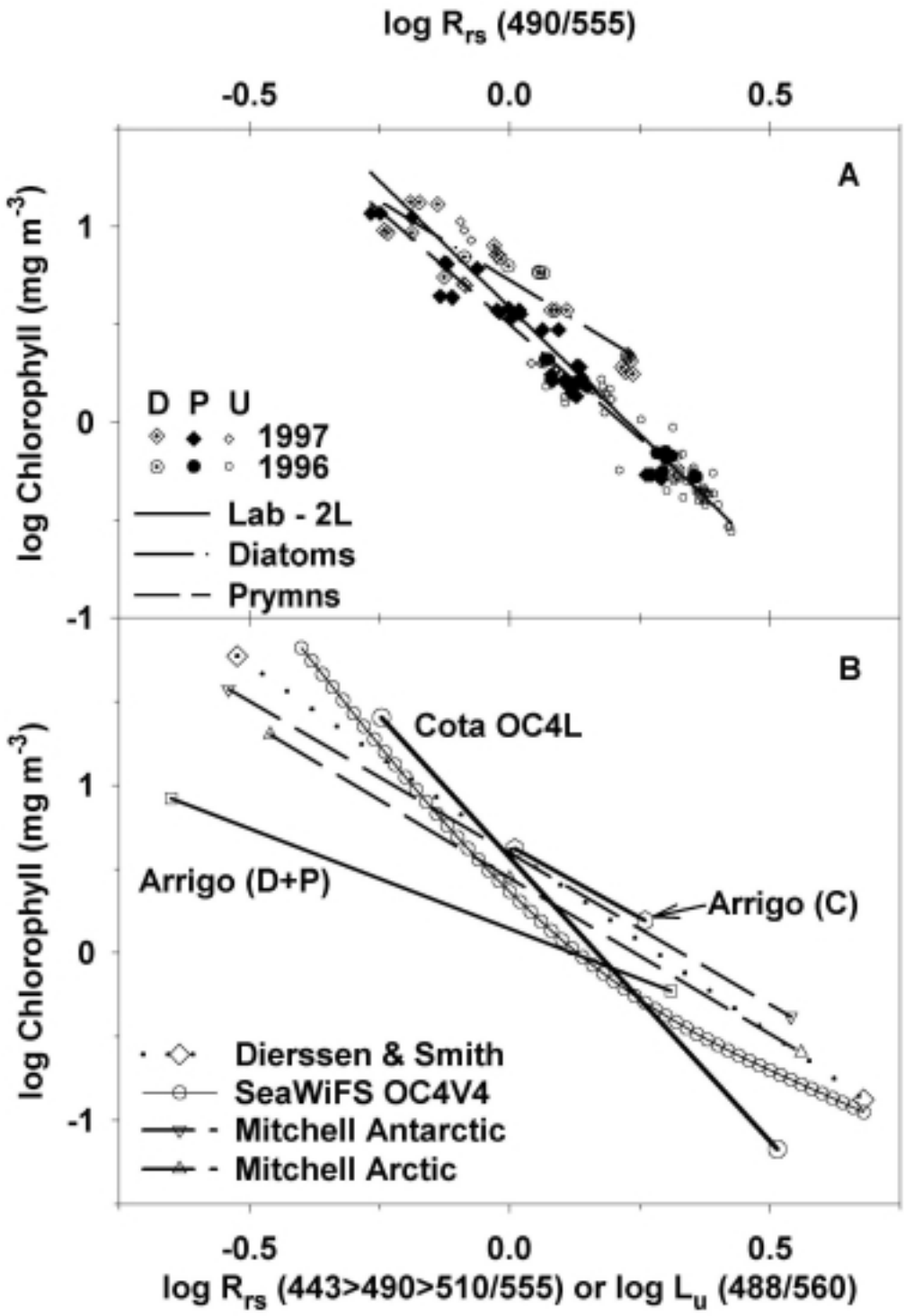

Figure 9.2. Taxon-specific algorithms and polar algorithm comparison. **A**. Two-band algorithms developed for the combined data sets from the Labrador Sea (Lab-2L), pigment groups diagnostic of diatoms (D, large filled symbols) and prymnesiophytes (P or Prymnes., large open symbols). Unidentified is U (small open symbols) and pigments were not available. **B**. The "global" SeaWiFS OC4V4 (O'Reilly et al. 2000) is included for reference with our composite Arctic OC4L algorithm and algorithms from the Antarctic peninsula region (Dierssen and Smith 2000), Ross Sea algorithms (Arrigo et al. 1998) for diatoms plus *Phaeocystis* (D+P) and crytophytes (C), and pigment (chlorophyll plus phaeopigments) algorithms for both polar regions (Mitchell 1992). Each algorithm is shown for the original range of values.

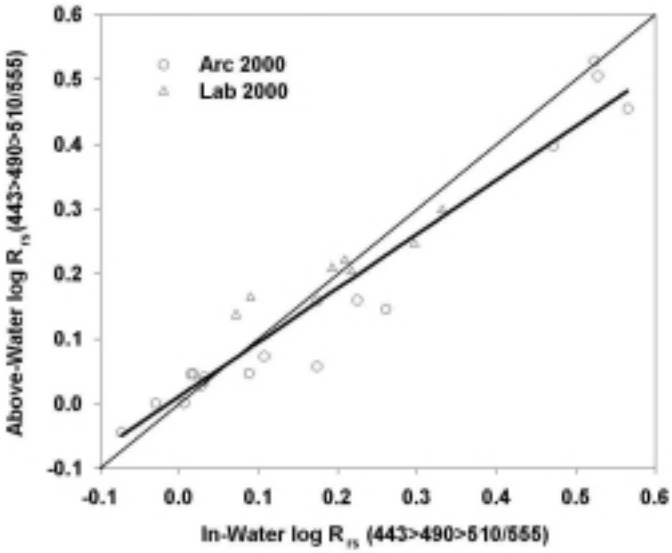

Figure 9.3. Reflectance ratios from in-water (SPMR) and above-water (SAS) optical measurements.

REFERENCES

Arrigo, K. R., D. H. Robinson, D. L. Worthen, B. Schieber, and M. P. Lizotte, 1998: Bio-optical properties of the southwestern Ross Sea, *J. Geophys. Res.*, ***103,*** 21683-21695.

Behrenfeld, M.J. and P.G. Falkowski, 1997: Photosynthetic rates derived from satellite-based chlorophyll concentration. *Limnol Oceanogr*. **42**, 1-20.

Cota, G.F., W.G. Harrison, T. Platt, S. Sathyendranath and V. Stuart, 2000a: Bio-optical properties of the Labrador Sea. *J. Geophys. Res.* (submitted).

Cota, G.F., D.A. Ruble, and J. Wang, 2000b: Bio-optical properties of high Canadian Arctic waters. *J. Geophys. Res.* (submitted).

Dierssen, H. M. and Smith, R. C. 2000: Bio-optical Properties and Remote Sensing Ocean Color Algorithms for Antarctic Coastal Waters. *J. Geophys. Res*. ***105***, 26,301-26,312.

Howard, K.L and J.A. Yoder, 1997: Contribution of the subtropical Oceans to global primary production. in: Liu, C.-T. (ed.) *Space Remote Sensing of Subtropical Oceans*, pp. 157-168, Pergamon, London.

Mitchell,B.G. 1992: Predictive bio-optical relationships for polar oceans and marginal ice zones. *J. Mar. Syst.* **3**,91-105.

Mobley, C. D. 1994: Light and Water: Radiative Transfer in Natural Waters. Academic Press, San Diego. 592pp.

O'Reilly, J. E., Maritorena, S., Siegel, D. A., O'Brien, M. C., Toole, D., Mitchell, B. G., Kahru, M., Chavez, F. P., Strutton, P., Cota, G. F., Hooker, S. B., McClain, C. R., Carder, K. L., et al. 2000: Ocean color chlorophyll *a* algorithms for SeaWiFS, OC2 and OC4: Version 4. Hooker, S. B. and Firestone, E. R. *NASA Tech. Memo. 2000-206892* , Vol. **11**, p. 9-23.

Pickart, R.S., D.J. Torres, R.A. Clarke and G.F. Cota, 2000: Hydrography of the Labrador Sea during active convection. *J. Phys. Oceanogr*. (in revision).

Sathyendranath, S., G. Cota, V. Stuart, H. Maass and T. Platt, 2000: Remote Sensing of phytoplankton pigments: A comparison of empirical and theoretical approaches. Intl. *J. Rem. Sens.* (in press).

Sathyendranath, S., T. Platt, V. Stuart, H. Maass and G. Cota, 1999: Remote sensing of phytoplankton biomass and primary production. *Aquabiology* **21**,17-22.

This research was supported by

the SIMBIOS NASA contract #97132

PEER REVIEWED PUBLICATIONS

Sathyendranath, S., G. Cota, V. Stuart, H. Maass and T. Platt, 2000: Remote Sensing of phytoplankton pigments: A comparison of empirical and theoretical approaches. *Intl. J. Rem. Sens*. (in press).

Sathyendranath, S., T. Platt, V. Stuart, H. Maass and G. Cota, 1999: Remote sensing of phytoplankton biomass and primary production. *Aquabiology* **21**, 17-22.

Submitted

Cota, G.F., W.G. Harrison, T. Platt, S. Sathyendranath and V. Stuart, 2000a. Bio-optical properties of the Labrador Sea. *J. Geophys. Res.* (submitted).

Cota, G.F., D.A. Ruble, and J. Wang, 2000b. Bio-optical properties of high Canadian Arctic waters. *J. Geophys. Res.* (submitted).

Pickart, R.S., D.J. Torres, R.A. Clarke and G.F. Cota, 2000. Hydrography of the Labrador Sea during active convection. *J. Phys. Oceanogr*. (in revision).

PRESENTATIONS

Cota, G.F., J.L. Anning, W.G. Harrison, T. Platt, D.A. Ruble, & S. Sathyendranath, 1999; Chlorophyll algorithms for the Labrador Sea. Global Line Imager ADEOS II Meeting, Kyoto, Japan.

Cota, G.F. and L.R. Pomeroy, 2000: Arctic shelf-basin production. Shelf-Basin Interactions pan Arctic meeting. Callaway Gardens, Georgia.

Cota, G.F., 2000: Bio-optical oceanography and ocean color. USCGC Polar Star.

Cota, G.F., D.A. Ruble, and J. Wang, 2000: Arctic bio-optical properties: Distinct differences. Global Line Imager ADEOS II meeting, Kanazawa, Japan.

Chapter 10

Satellite Ocean Color Validation Using Merchant Ships

Robert Frouin and David L. Cutchin,
Scripps Institution of Oceanography, University of California San Diego, California

Pierre-Yves Deschamps
Laboratoire d'Optique Atmospherique, Universite des Sciences et Technologies de Lille Villeneuve d'Ascq, France

10.1 INTRODUCTION

A collaborative measurement program for evaluating satellite-derived ocean color has been developed based on ships of opportunity (merchant, oceanographic) and specific instrumentation, the SIMBAD radiometer. The purpose of the measurement program is to complement, in a cost-effective way, dedicated evaluation experiments at sea, which are expensive, cannot be carried out over the full range of expected oceanic and atmospheric conditions, and generally provide a few match-ups. Ships participate in the program on a volunteer basis or at a very small cost, and measurement procedures do not interfere with other ship activities.

The SIMBAD radiometer is a portable, easy-to-operate instrument that measures the basic ocean color variables, namely aerosol optical thickness and water-leaving radiance, in typical spectral bands of ocean-color sensors, i.e., 443, 490, 560, 670, and 870 nm. Measuring these variables at the time of satellite overpass is usually sufficient to verify satellite-derived ocean color and to evaluate atmospheric correction algorithms (Schwindling et al., 1998). Any ordinary crew can learn quickly how to make measurements. Importantly, the ship is not required to stop, making it possible to collect data along regular routes traveled by merchant ships in the world's oceans.

Water-leaving radiance is measured by viewing the ocean surface from the side of the ship lit by the sun, outside the sun glint, at a nadir angle of 45 degrees and a relative azimuth angle of 135 degrees. A vertical polarizer reduces skylight reflected in the radiometer's field of view. Aerosol optical thickness is measured by viewing the sun, as done with classic sun photometers. The same optics, with a 2.5 degree field of view, and the same detectors with different gains are used in ocean- and sun-viewing modes. The radiometric measurements are made simultaneously in the instrument's five spectral bands, but the ocean and sun are viewed sequentially. Incident solar irradiance at the surface, a variable that must be known to normalize water-leaving radiance, is not measured but calculated, which can be done accurately when the sun is not obscured by clouds and cloud cover is less than 30%.

To achieve adequate sampling, a series of ten radiometers were built for use in two complementary networks, one operated by the Scripps Institution of oceanography (SIO), University of California San Diego, the other by the Laboratoire d'Optique Atmosphérique (LOA), University of Lille. Detailed information about the SIMBAD radiometer, measurement procedures and protocols, calibration history, processing software, and data are available at http://polaris.ucsd.edu/~simbad/ (SIO network) and http://www.loa.univ-lille1.fr/~simbad/ (LOA network).

10.2 RESEARCH ACTIVITIES

During the first year of the project efforts focused on finding suitable merchant ships (e.g., ships with the bridge forward), making arrangements with the ship owners and captains, and training officers to make SIMBAD measurements. Some of the selected ships, for example M/V Micronesian Navigator (SIO network) and M/V Toucan (LOA network) have proven reliable in providing data routinely. Arrangements were also made to collect data during research cruises, in particular the quarterly CalCOFI cruises off the California coast. During the second and third year of the project, as experience was gained and procedures became refined, the collection of SIMBAD data sets intensified. Some cruises allowed a verification of SIMBAD-measured water-leaving radiance. During October 1996-October 2000, 42 merchant ship voyages and research cruises were accomplished by the SIO network, providing more than 2,000 data sets of concomitant aerosol optical thickness and water-leaving radiance. The location of the data sets is displayed in Fig. 10.1. The major oceans were sampled, some data were collected at high latitudes, but most of the data were collected between latitudes of –40 and 40 degrees.

The SIMBAD data were used to verify the concept of the SIMBAD radiometer, perform comparisons with other instruments, calibrate vicariously the POLDER instrument,

and perform a first evaluation of SeaWiFS-derived water-leaving radiance. Activities also included verifying aerosol models for ocean color remote sensing, characterizing an extreme Asian dust event that reached the western United States, and analyzing OCTS radiance data for aerosol remote sensing. The main results of these activities are summarized in the next section.

10.3 RESARCH RESULTS

Direct atmospheric transmittance and sky radiance data collected during several years at the SIO pier in La Jolla were analyzed (Swindling et al., 1998). The objectives were (1) to verify whether the aerosol models selected for SeaWiFS are adapted to ocean color remote sensing from space, and (2) to identify what type of in situ atmospheric optics measurements should be performed to verify atmospheric correction algorithms. Aerosol optical thickness at 870 nm was generally low in La Jolla, with most values below 0.1 after correction for stratospheric aerosols. Two modes of variability characterized by Angström coefficients of 1.2 and 0.5 and corresponding to tropospheric and maritime models, respectively, were identified in the measurements. The SeaWiFS aerosol models allowed one to fit, within measurement inaccuracies, the derived values of the Angström coefficient and "pseudo" phase function (the product of single scattering albedo and phase function), key atmospheric correction variables. The study also showed that the "pseudo" phase function could be derived from the Angström coefficient, suggesting that sun photometer measurements at the time of satellite overpass may be sufficient, in most cases, to verify the atmospheric correction of ocean color.

The principle of the SIMBAD radiometer, in particular its ability to reduce reflected skylight, was justified theoretically and verified experimentally (Fougnie et al., 1999a). Theoretical calculations showed that, for a nadir angle of 45 degrees and a relative azimuth angle between solar and viewing directions of 135 degrees --the recommended geometry, reflected skylight is reduced to typically 10^{-3} in reflectance units at 443 nm (Fig. 10.2). This value represents 2 to 10% of the diffuse marine reflectance, the signal of interest. Furthermore, the effects of surface roughness on skylight reflection and, hence, uncertainties in sea state (wind speed) are minimized (smaller error bars in Fig. 10.2). Taking into account typical uncertainties in wind speed and geometry, the residual reflected skylight is correctable to a few 10^{-4} in reflectance units. For most oceanic waters, the resulting error on the diffuse marine reflectance in the blue and green is less than 1%. The theoretical results were verified experimentally at the SIO pier, by viewing the ocean surface with a scanning polarization radiometer (Fig. 10.3). The various angular and spectral effects predicted by theory have been evidenced in the measurements.

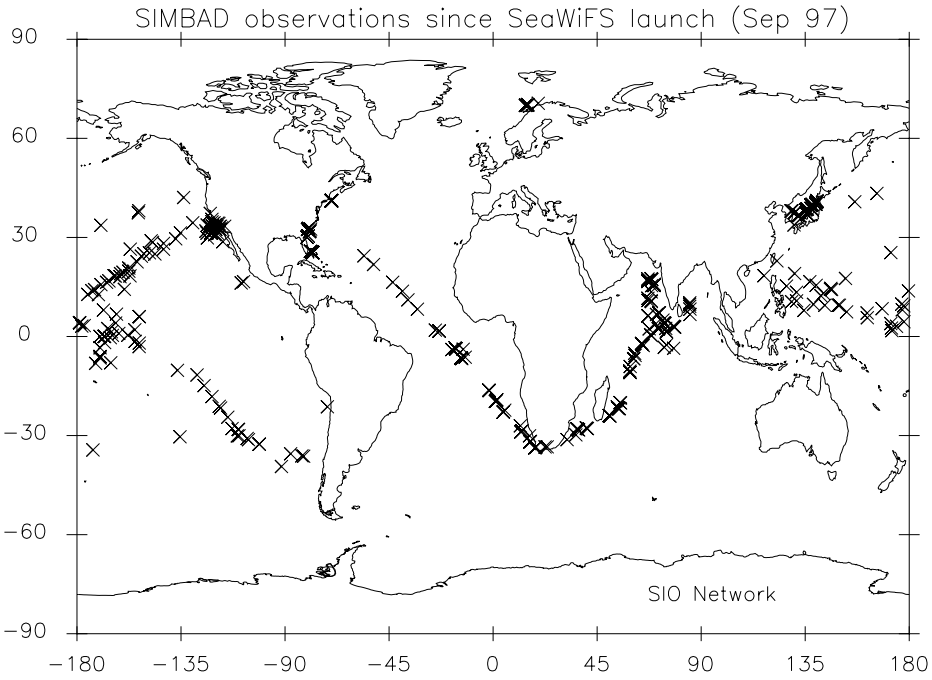

Figure 10.1. Location of the SIMBAD data sets collected by the SIO network.

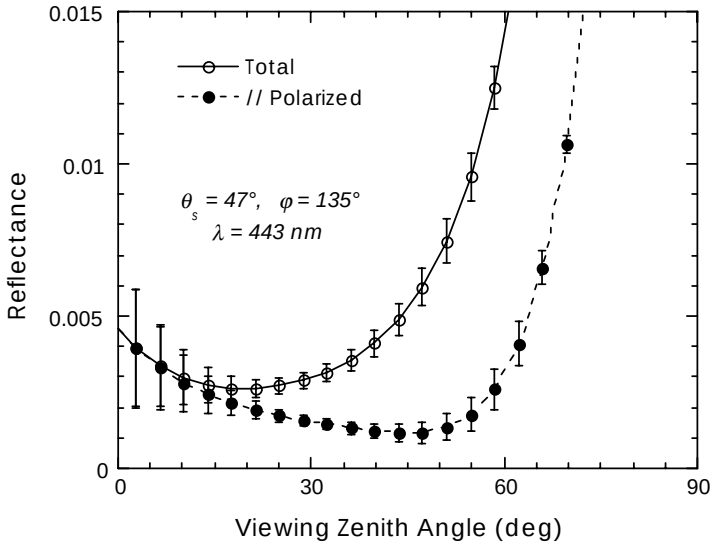

Figure 10.2. Simulated ocean reflectance at 443 nm as a function of viewing zenith angle. Sun zenith angle is 47 degrees and relative azimuth angle 135 degrees. The diffuse reflectance of the water body is equal to zero and the atmosphere only contains molecules. Error bars represent minimum and maximum values for varied wind speed from 2 to 12.5 ms^{-1}.

Since the water body polarizes incident, the measured polarized radiance differs from the total radiance. For the recommended geometry, the underwater scattering angle varies only between 148 and 158 degrees, and the maximum polarization factor varies between 0.83 and 0.92 (Fougnie et al., 1999a). Fig. 10.4 shows, for typical phytoplankton particles and a chlorophyll concentration of 0.1 mgm^{-3}, the ratio of parallel-polarized and total signals at 450 nm as a function of viewing zenith angle. The relative azimuth angle is 50.6 degrees. Various sun zenith angles are considered in the figure. For a sun not too close to zenith, one should be able to correct the polarization effects to within 5% relative inaccuracy, which compares with other errors, such as those due to bi-directional effects and radiometric calibration. The SIMBAD radiometer was evaluated at sea during various experiments, in particular CalCOFI in the southern California Bight and Aerosols-99 in the Atlantic and Indian Ocean. The diffuse marine reflectance measured by the radiometer was compared with that measured by an underwater MER optical system. The agreement between the two types of measurements is generally good, to within 10-15% (Fig. 10.5). Another comparison was performed with a surface-floating reflectance-meter in the Black Sea, and also showed good agreement (Fig. 10.6). Aerosol optical thickness measured by the SIMBAD radiometer also compared well with that measured by sun photometers during the October-November 1996 CalCOFI cruise (Nakajima et al., 1999) and during the Second Aerosol Characterization Experiment (ACE-II), as illustrated in Fig. 10.7. A more extensive comparison of aerosol optical thickness measurements made by SIMBAD and Microtops radiometers, shadow-band radiometer, and a lidar during Aerosols-99 further attested to the quality of the SIMBAD measurements (Voss et al., 2001). SIMBAD data were also used to evaluate airborne lidar measurements of aerosol optical thickness over the Atlantic Ocean during a European pollution outbreak (Flamant et al., 2000). The SIMBAD radiometer proved useful to check vicariously the radiometric sensitivity of the Polarization and Directionality of the Earth's Reflectance (POLDER) instrument onboard ADEOS (Fougnie et al., 1999b). The satellite radiance was compared with that computed for the same geometry using a radiation-transfer model. SIMBAD measurements of aerosol optical thickness and marine reflectance at the time of satellite overpass were used as input to the model. The accuracy of the

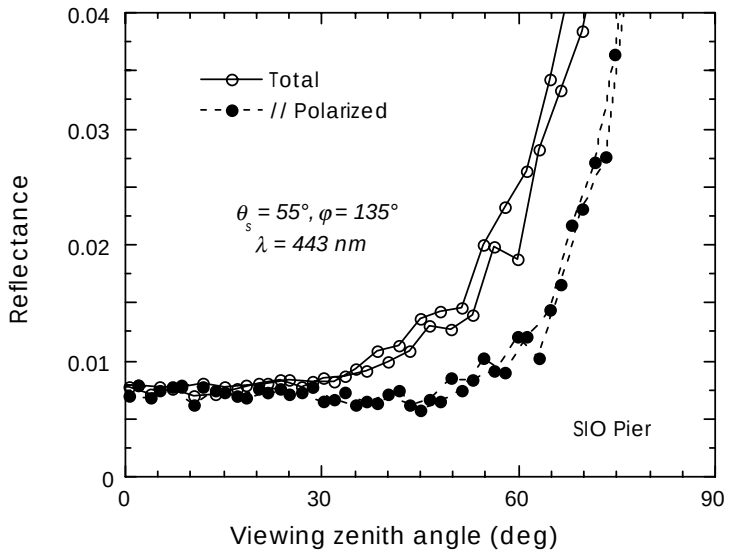

Figure 10.3. Measured ocean reflectance at 443 nm as a function of viewing zenith angle. Sun zenith angle is 55 degrees and relative azimuth angle 135 degrees.

vicarious calibration coefficients was estimated to be better than 3%. A large decrease of the POLDER instrument response was found in the blue, confirming the results previously obtained using alternative calibration techniques.

SIMBAD data were also used in an analysis of OCTS radiance for aerosol remote sensing (Nakajima et al., 1999). The study provided evidence that anthropogenic sulfate aerosols in mid-latitudes and biomass-burning aerosols in the sub-tropical regions are characterized by small particles (large Angström coefficient), whereas mineral dust particles from subtropical arid regions are characterized by small particles (small Angström coefficient).

A study of an extreme Asian dust episode, which reached the US Western Seaboard in April 1999, was also performed (Tratt et al., 2001). This event was observed at several in situ and remote sensing atmospheric instrument stations. Dramatic reductions in boundary layer visibility were recorded and the resultant peak backscatter coefficients exceeded upper-troposphere background conditions by at least two orders of magnitude. At San Nicolas island the measured and modeled aerosol optical thickness at 500 nm increased dramatically from 0.15 on April 25 to 0.52 on April 26-27 (Fig. 10.8). Volume size distribution on April 27 exhibited a prominent coarse mode at 1-2 µm radius and single scattering albedo was observed to increase from 0.90 in the blue to 0.93 in the near infrared. Concurrent lidar observations tracked the evolution of the plume vertical structure, which consisted of up to three well-defined layers distributed throughout the free troposphere.

SeaWiFS-derived marine reflectance was also evaluated against SIMBAD measurements. Sixty-two high-quality match-ups obtained in clear and turbid waters were analyzed (Fig. 10.9). The scatter between the two types of data is fairly large, but the agreement is generally good. A previous analysis of fifteen match-ups had indicated higher SeaWiFS values in the blue, but such overestimation is not apparent in Fig. 10.9, which might be explained in part by the re-processing of SeaWiFS data. Interpretation of the scatter in marine reflectance will require examining aerosol optical thickness retrievals and measurements. Thanks to the SIMBAD concept, aerosol measurements corresponding to the marine reflectance measurements are available for this analysis.

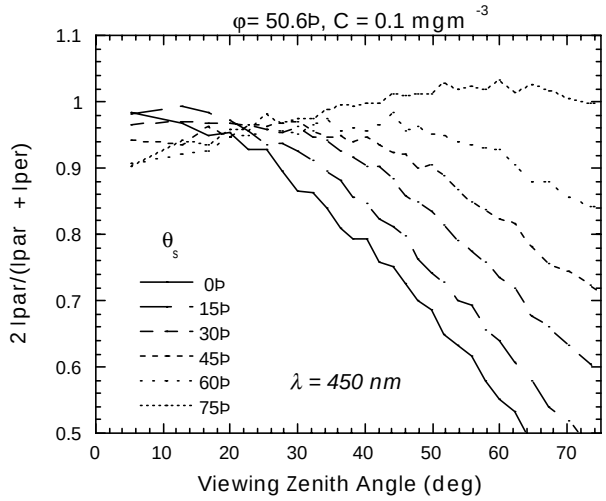

Figure 10.4. Monte Carlo simulations of the ratio of parallel-polarized and total reflectance of the ocean at 450 nm as a function of viewing zenith angle. Sun zenith angles are 0, 15, 30, 45, 60 and 75 degrees. The relative azimuth angle is 50.6 degrees. The ocean contains typical phytoplankton particles. Chlorophyll concentration is 0.1 mgm^{-3}.

ACKNOWDEGMENTS

The authors wish to thank all the officers and scientists that have collected SIMBAD data. They are grateful to J. McPherson for developing the SIMBAD processing code, S. Baily for adapting the code to PC and providing SeaWiFS match-up data, A. Poteau for processing SIMBAD data and maintaining the SIMBAD radiometers, and C. Pietras for helpful discussions. This work has been supported by the National Aeronautics and Space Administration under Contract NAS-97135 (to R. Frouin), the Centre National d'Etudes Spatiales, the Centre National de la Recherche Scientifique, and the Région Nord-Pas de Calais.

REFERENCES

Flamant, C., J. Pelon, P. Chazette, V. Trouillet, P. Quinn, R. Frouin, D. Bruneau, J.-F. Leon, T. Bates, J. Johnson, and J. Livingston, 2000: Airborne lidar measurements of aerosol spatial distribution and optical properties over the Atlantic Ocean during an European pollution outbreak of ACE-2. *Tellus*, **52B**, 652-677.

Fougnie, B., R. Frouin, P. Lecomte, and P.-Y Deschamps, 1999a: Reduction of skylight reflection effects in the above-water measurement of diffuse marine reflectance. *Appl. Optics*, **38**, 3844-3856.

Fougnie, B., P.-Y. Deschamps, and R. Frouin, 1999b: Vicarious Calibration of the POLDER ocean color spectral bands using in-situ measurements. *IEEE Trans. Geos. Rem. Sen.*, **37**, 1567-1574.

Nakajima, T., A. Higurashi , K. Aoki, T. Endoh, FH. Fukushima, M. Toratani, Y. Mitomi, B. G. Mitchell, and R. Frouin, 1999: Early phase analysis of OCTS radiance data for aerosol remote sensing. . *IEEE Trans. Geo. Rem. Sen.*, **37**, 1575-1585.

Tratt, D. M., R. Frouin, and D. L. Westphal, 2001: The April 1998 Asian Dust event: a Southern California perspective. *J. Geophysical Res.*, in press.

Schwindling, M. P.-Y. Deschamps, and R. Frouin, 1998: Verification of aerosol models for satellite ocean color remote sensing, *J. Geophys. Res.*, **103**, 24,919-24,935.

Voss, K. J., E. Welton, P. Quinn, R. Frouin, M. Reynolds, and M. Miller, 2001: Aerosol optical depth measurements during the Aerosols-99 experiment. J. Geophys. Res., in press.

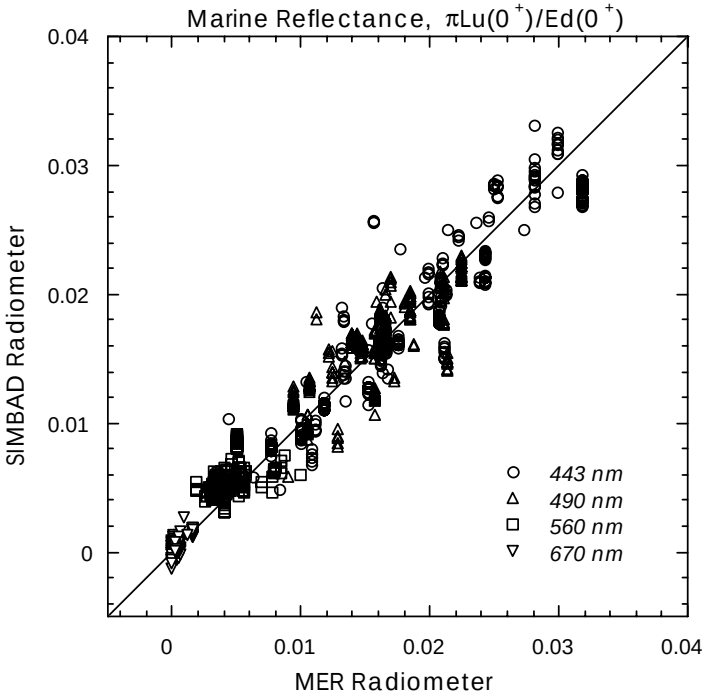

Figure 10.5. Comparison of marine reflectance measured by SIMBAD and MER radiometers during CalCOFI (southern California bight) and Aerosols-99 (Atlantic and Indian Oceans).

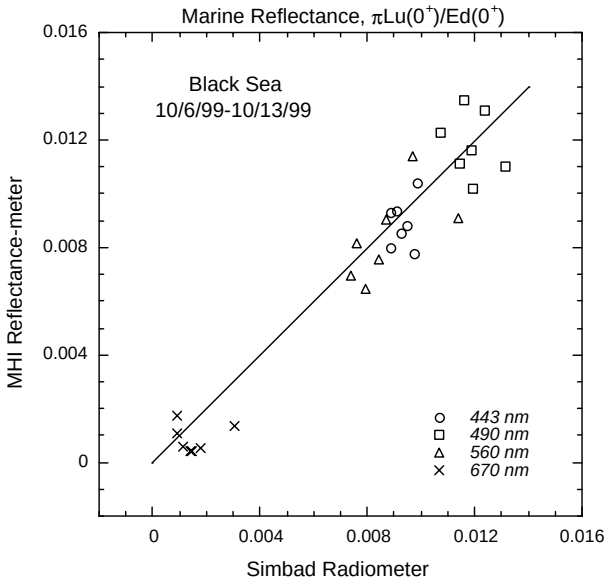

Figure 10.6. Comparison of marine reflectance measured by SIMBAD radiometer and Marine Hydrophysical Institute (MHI) reflectance-meter during the October 1999 R/V Bilim cruise in the Black Sea.

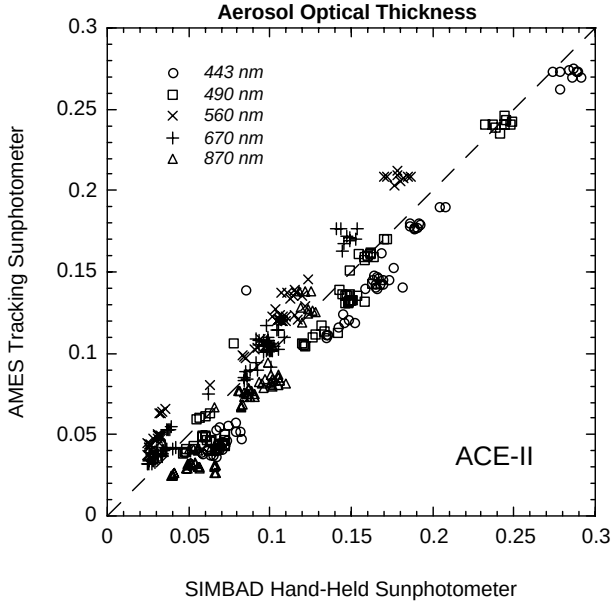

Figure 10.7. Comparison of aerosol optical thickness measured by SIMBAD radiometer and AMES tracking sun photometer during ACE-II (northeast Atlantic Ocean).

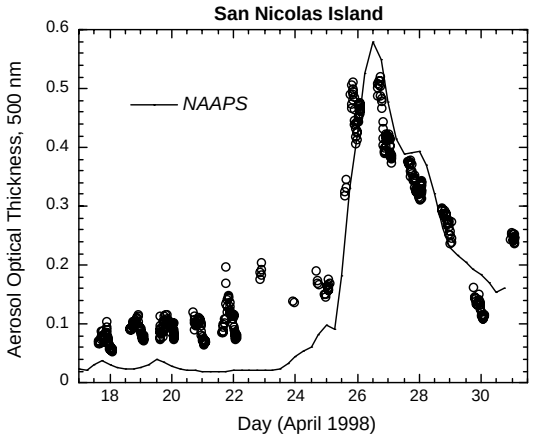

Figure 10.8. Time series of aerosol optical thickness at 500 nm at San Nicolas Island during April 18-May 1, 1998. Also shown is simulated is optical depth (x0.25) of dust and sulfate from the NRL Aerosol Analysis and Prediction System (NAAPS).

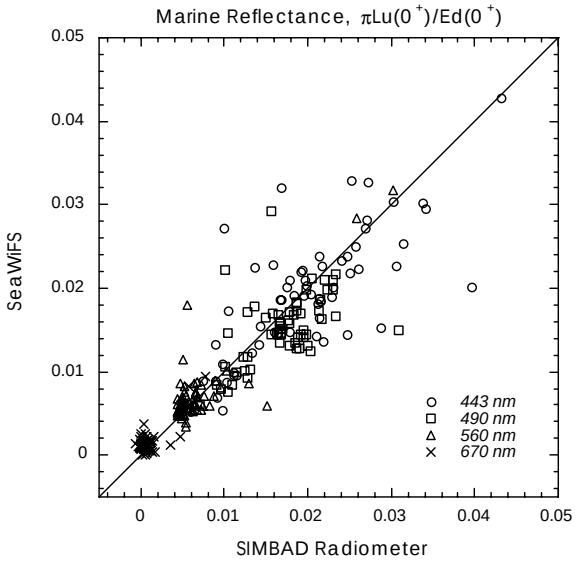

Figure 10.9. Comparison of marine reflectance derived by SeaWiFS and measured by the SIMBAD radiometer.

This research was supported by the

SIMBIOS NASA contract # 97135

PEER REVIEWED PUBLICATIONS

Fougnie, B., P.-Y. Deschamps, and R. Frouin, 1999: Vicarious Calibration of he POLDER ocean color spectral bands using *in situ* measurements. *IEEE Trans.Geos. Rem. Sen.,* **37**, 1567-1574.

Fougnie, B., R. Frouin, P. Lecomte, and P-Y. Deschamps, 1999: Reduction of kylight reflection effects in the above-water measurement of marine iffuse reflectance. *Appl. Optics*, **38**, 3844-3856.

Nakajima, T., A. Higurashi, K. Aoki, T. Endoh, H. Fukushima, M. Toratani,Y. Mitomi, B. G. Mitchell, and R. Frouin, 1999: Early phase analysis of CTS radiance data for Aerosol remote sensing. *IEEE Trans. Geo. Rem. Sen.*,**37**, 1575-1585.

Schwindling, M. P.-Y. Deschamps, and R. Frouin, 1998: Verification of erosol models for satellite ocean color remote sensing, *J. Geophys. Res.*,**103**, 24,919-24,935.

PRESENTATIONS

Fougnie, B., P.-Y. Deschamps, R. Frouin, B. G. Mitchell, 1998: Measuring water-leaving radiance with a polarization radiometer: theory and experimental verification. *EOS Trans*., **79**, No. 1, 99.

Frouin, R., P.-Y. Deschamps, B. G. Mitchell, and M. Kahru, 1998: The Normalized Difference Phytoplankton Index for satellite ocean color applications. *EOS Trans*., **79**, No. 1, 161.

Gross, L., R. Frouin, S. Thiria, and M. Crépon, 1998: Neural networks to retrieve phytoplankton pigment concentration from satellite-derived spectral ocean reflectance. *EOS Trans*., **79**, No. 1, 161.

Tratt, D. M., R. Frouin, and D. L. Westphal, 1999: A Southern California perspective of the April, 1998 trans-Pacific Asian dust event. Proceedings,10th Conference on Coherent Laser Radar, Mt. Hood, Oregon, June 28 – July 2, 1999, 137-140.

Chapter 11

High Altitude Measurements of Radiance at High Spectral and Spatial Resolution for SIMBIOS Sensor Calibration,Validation, and Intercomparisons

Robert O. Green, Betina Pavri and Thomas G. Chrien
NASA, Jet Propulsion Laboratory, Pasadena, California

11.1 INTRODUCTION

The successful combination of data from different ocean color sensors depends on the correct interpretation of signal from each of these sensors. Ideally, the sensor measured signals are calibrated to geophysical units of spectral radiance, and sensor artifacts are removed and corrected. The calibration process resamples the signal into a common radiometric data space so that subsequent ocean color algorithms that are applied to the data are based on physical processes and are inherently sensor independent. The objective of this project is to calibrate and validate the on orbit radiometric characteristics of SeaWIFS with underflights of NASA's calibrated Airborne Visible/Infrared Imaging Spectrometer (AVIRIS). This objective is feasible because AVIRIS measures the same spectral range as SeaWIFS at higher spectral resolution (Figure 11.1). In addition to satellite sensor underflights, the AVIRIS project has supported comparison and analysis of the radiometric calibration standards used for AVIRIS and SeaWIFS. To date, both the OCTS and SeaWIFS satellite sensors have been underflown by AVIRIS with matching spectral, spatial, geometric, radiometric, and temporal domains. The calibration and validation objective of this project is pursued for the following reasons: (1) Calibration is essential for the quantitative use of SeaWIFS and other SIMBIOS sensor data; (2) Calibration in the laboratory of spaceborne sensors is challenging; (3) Satellite sensors are subjected aging on the ground and to trauma during launch; (4) The Earth orbit environment is significantly different than the laboratory calibration environment; (5) Through years of effort AVIRIS has been demonstrated to be well calibrated; and (6) AVIRIS can match the spectral and spatial observation characteristics near the top of the atmosphere at the time of SeaWIFS measurements.

11.2 RESEARCH ACTIVITIES

The approach taken for the SIMBIOS Project has been to: (1) Determine the calibration accuracy of AVIRIS with high confidence in the laboratory, in flight, and on the runway before flight; (2) Underfly the SeaWIFS satellite sensor with AVIRIS matching observation geometry and addressing weather, satellite, aircraft, sensor, and location issues; (3) Correct AVIRIS spectral image data to the top of the atmosphere radiance; (4) Convolve AVIRIS spectral channels to SeaWIFS bands; (5) Determine and extract matching areas with correct observation geometry; (6) Compare and analyze the matchup data and repeat acquisitions for monitoring.
Matching the location, time, and illumination/observation angles of SeaWiFS is critical for comparison of radiometric data. The calibration of the SeaWiFS sensor presented special challenges due to the geometry of the sensor's observations. SeaWiFS scans cross-track at an angle 20° behind the satellite to avoid sunglint in the field of view. AVIRIS has a 15° scan angle. In order to match the >20° view angle of SeaWIFS, the AVIRIS ER-2 platform is banked at ~20°. This continuous bank results in a circular "flightline".

Conversion of AVIRIS data to top-of-the-atmosphere radiance is achieved through the use of the MODTRAN atmospheric modeling package. The stability and repeatability of AVIRIS calibration is validated through a series of inflight calibration experiments. With pre- and post-flight calibrations of AVIRIS, coupled with the on-board calibrator, calibration accuracy of better than 2% spectral, 3% radiometric and 3% spatial have been achieved.

11.3 RESEARCH RESULTS

AVIRIS data have been measured for the SIMBIOS Project on 970520, 971002, 990807, and 991001. Results from 1997 have been presented elsewhere, and the 991001 analysis is not yet complete, so only the 990807 results will be discussed here. On 7 August 1999, AVIRIS successfully underflew the SeaWIFS sensor off the east coast of the United States. AVIRIS is typically flown in two circles during the time of a SeaWIFS overpass, in order to span the time of the satellite overpass and ensure that some AVIRIS

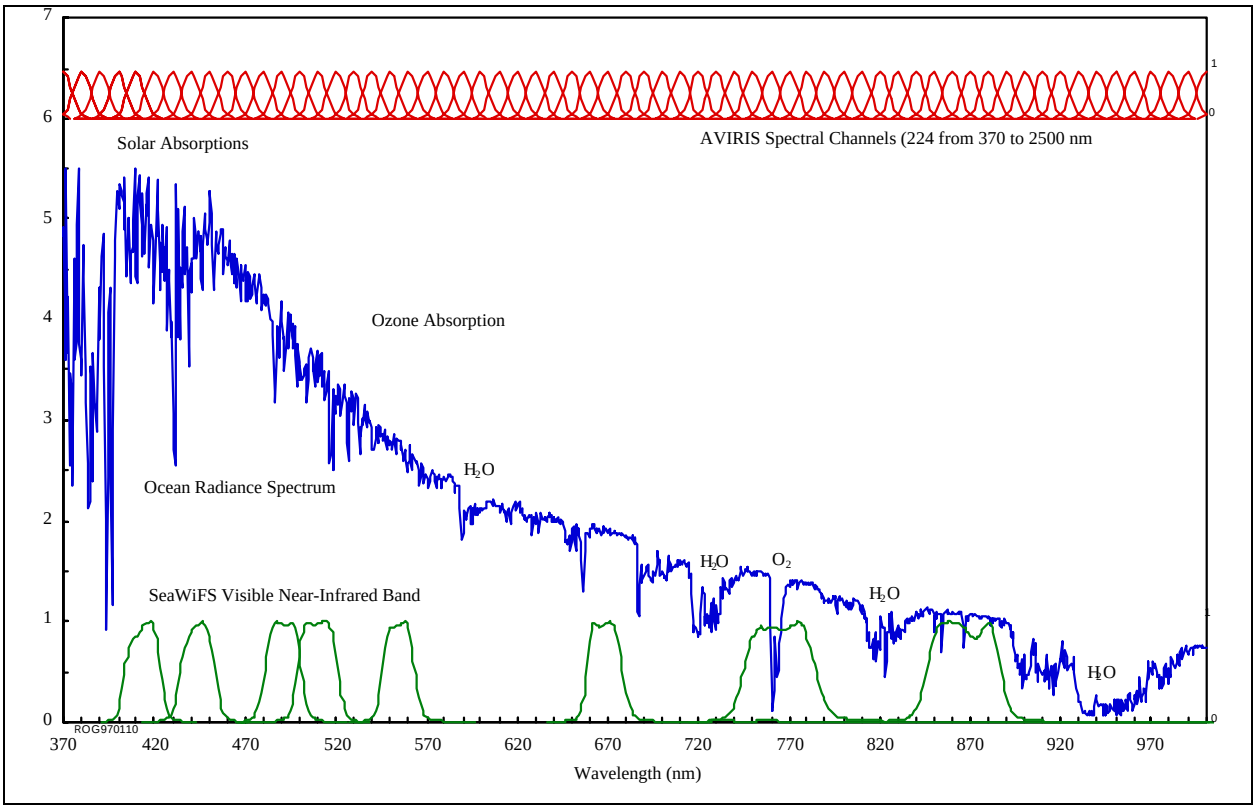

Figure 11.1. The eight SeaWIFS bands and the AVIRIS spectrally contiguous channels in the region from 370 to 1000 nm. A high spectral resolution modeled plot of the typical upwelling spectral radiance for an ocean target is shown in blue.

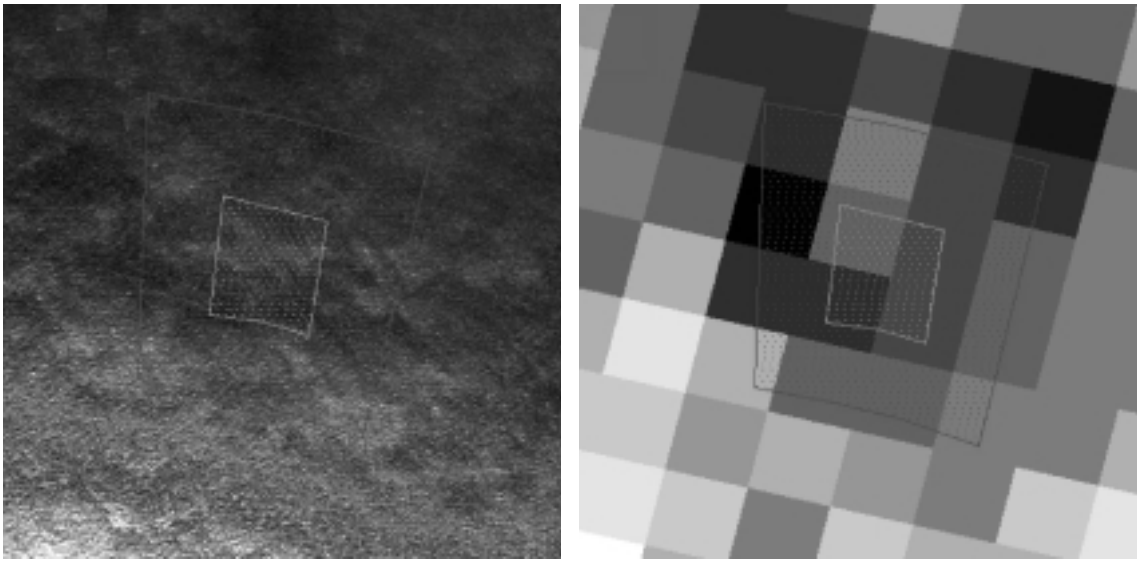

Figure 11.2. AVIRIS (left) and SeaWiFS (right) images of same region, taken contemporaneously. Regions of matching sun angle and look angle are shown. Pixels matching to within 5° are shown in red shading, while pixels matching to within 2° are marked with green.

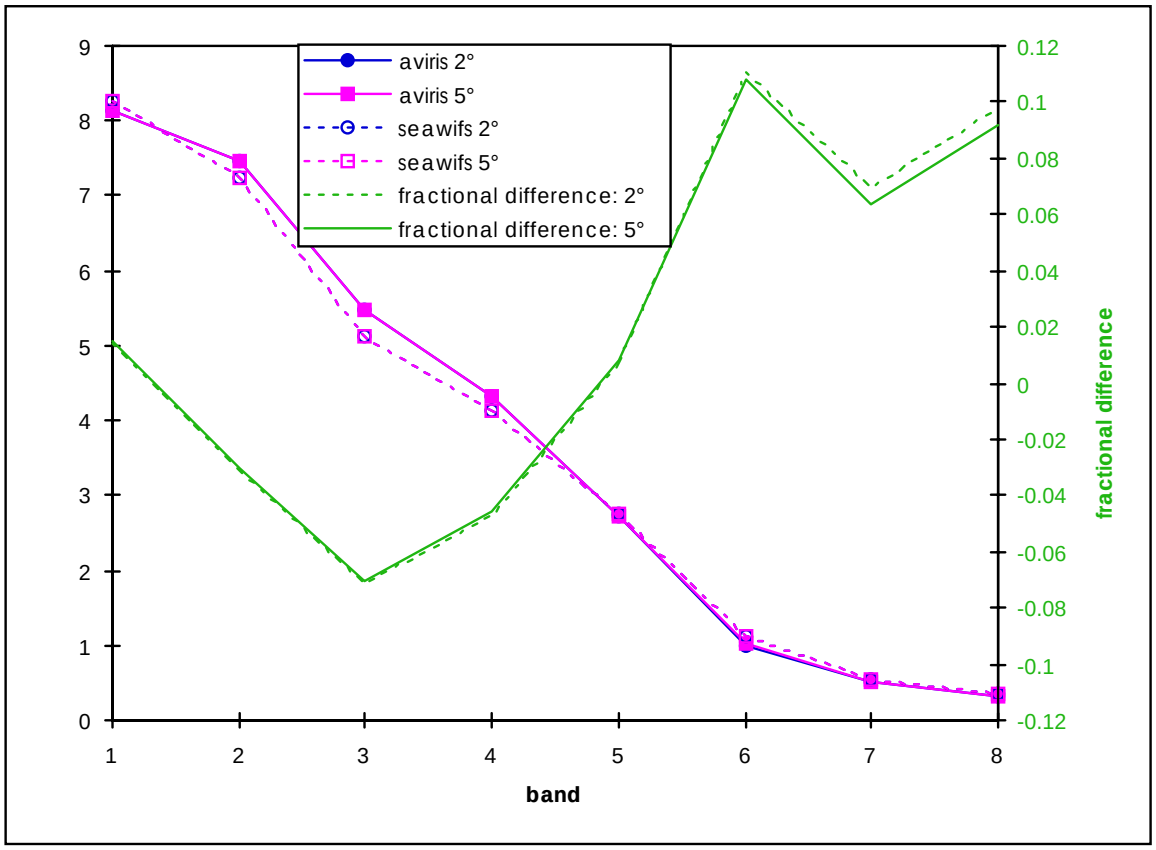

Figure 11.3. A plot of the SeaWIFS and AVIRIS radiance extracted for the overlapping observation geometry. The fractional differences are also plotted.

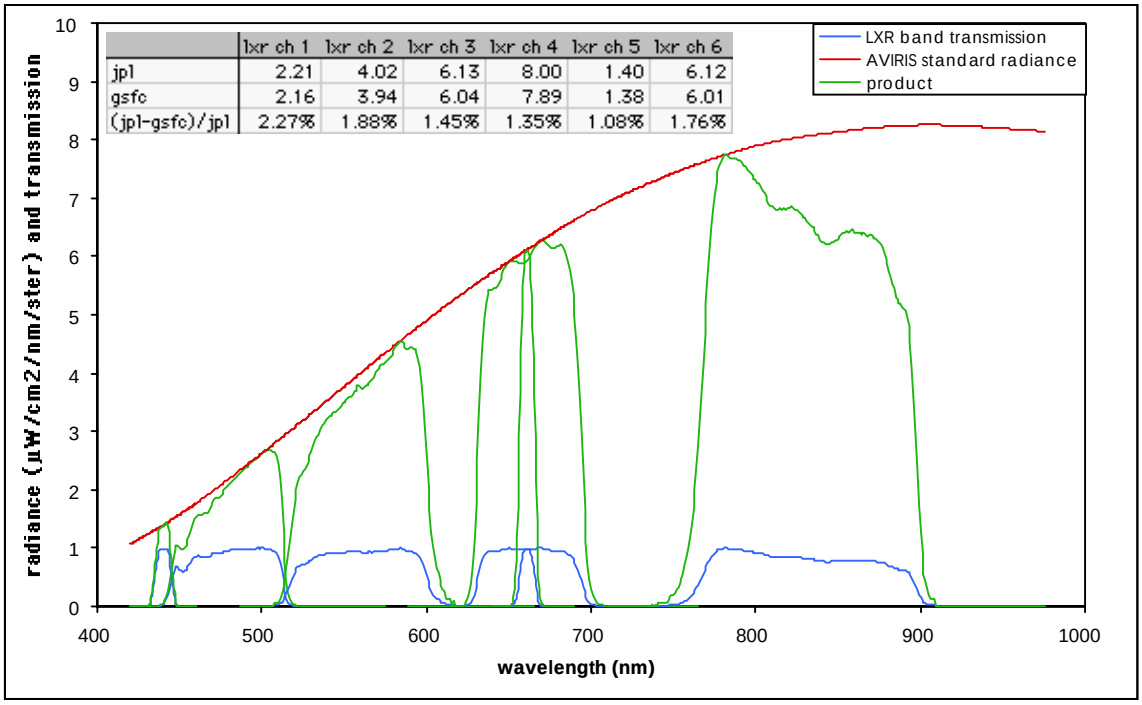

Figure 11.4. AVIRIS 1999 spectral radiometric calibration standard convolved and integrated to the Landsat Transfer Radiometer (LXR) bands.

data is taken during the acquisition window. The data from the flight are processed to calibrated radiance. Next, the data are corrected to top of the atmosphere radiance using the MODTRAN atmospheric model, supplimented with TOMS ozone mapper data. The AVIRIS data are then convolved to the reported SeaWiFS spectral response functions. To compare SeaWIFS and AVIRIS data, the data sets must be warped into the same geometric space, so that direct comparisons are available between pixels which match in space, time, illumination angle, and observation angle. Joe Boardman of AIG developed algorithms and software to enable us to use IDL/ENVI software to warp and analyze the unusual circular flightlines, and to produce observation and illumination angle from the AVIRIS navigation data. Using this new software, the datasets are co-registered. With the two data sets are projected into the same geometric space, the SeaWIFS and AVIRIS regions (Figure 11.2) with overlapping observation geometry can be selected, and the resulting radiance compared (Figure 11.3). The results for the 990807 AVIRIS underflight are presented in Table 1. Two cases are presented: matching illumination/observation angles to within 2°, and matching geometry to within 5°. Average radiance for matching geometry regions are shown, followed by the fractional differences between the AVIRIS and SeaWIFS-derived radiance. Agreement within 10% is achieved, with the exception of band 6. The magnitude of this discrepancy is larger than expected and can not be explained purely by AVIRIS radiometric uncertainty: The Landsat Transfer Radiometer (LXR) was able to view the AVIRIS radiometric calibration standard in June 1999. Analysis of the cross comparison of the LXR and AVIRIS 1999 radiometric standard was completed with good stability before and after the measurements. Results of this analysis are given in Figure 11.4. The LXR measurements show a maximum discrepancy of 2.5% between LXR measured and predicted radiance based on LXR reported spectral response functions and AVIRIS standard radiance. The results with the LXR are consistent with the expected uncertainty of 2% to 3% of the AVIRIS 1999 radiometric calibration standard in this spectral region.

11.4 CONCLUSIONS

Analysis of these data show radiometric calibration agreement ranging from 2% to 12% across the eight SeaWIFS bands. This discrepancy can not simply be explained by radiometric uncertainty within the AVIRIS calibration. Further, they are inconsistent with the results from the Landsat Transfer Radiometer experiment which show that the AVIRIS 1999 radiometric calibration standard agrees with the Goddard Space Flight Center LXR at the 2-3% level. Analysis of the SeaWiFS comparison is continuing in an attempt to understand the disagereement. Drifting SeaWiFS filter functions, a systematic error in SeaWiFS reported radiance, and the AVIRIS technique for convolving AVIRIS data with the SeaWiFS filter functions are all being considered as possible sources of the observed discrepancy. Several successful underflights of SeaWiFS were completed by AVIRIS in 2000, but analysis has been slowed by the reprocessing of the SeaWiFS data and a change in SeaWiFS L1B data format. Analysis of this data will proceed over the next several months. Comparison of these new results with those collected in the previous experiments will provide insight into the repeatability of the SeaWiFS sensor calibration.

ACKNOWLEDGMENTS

This research was carried out at the Jet Propulsion Laboratory / California Institute of Technology, Pasadena, California, under contract with the National Aeronautics and Space Administration. This research was funded as part of the SIMBIOS Project at the GSFC/NASA.

This research was supported by the

SIMBIOS NASA interagency agreement

PRESENTATION

Green, R.O., B. Pavri, and M. Shimada, 1998: On-Orbit Calibration of ADEOS OCTS with AVIRIS Underflight, Proc. Seventh Airborne Earth Science Workshop, Jet Propulsion Laboratory, JPL Pub. 97-21, Vol. 1, pp 205-212.

Green, R. O., B. Pavri, J. Faust, O. Williams, and C. Chovit, 1998: Inflight Validation of AVIRIS Calibration in 1996 and 1997. Summaries of the Seventh JPL Airborne Earth Science Workshop, Vol. 1.

Oaku, H., M. Shimada, and R. O. Green, 1998: OCTS Absolute Calibration Using AVIRIS. IGARSS, Seattle.

Pavri, B., T. G. Chrien, and R. O. Green, 1999: Intercomparison of Standards for Radiometric Calibration. Presented at the Eighth JPL AVIRIS Science and Applications Workshop.

Shimada, M., H. Oaku, Y. Mitomi, H. Murakami et al. 1999: Calibration of the Ocean Color and Temperature Scanner. IEEE Geoscience and Remote Sensing, a special issue of ADEOS.

Chapter 12

Merging Ocean Color Data from Multiple Missions

Watson W. Gregg
NASA/Goddard Space Flight Center, Greenbelt, Maryland

12.1 INTRODUCTION

Oceanic phytoplankton may play an important role in the cycling of carbon on the Earth, through the uptake of carbon dioxide in the process of photosynthesis. Although they are ubiquitous in the global oceans, their abundances and dynamics are difficult to estimate, primarily due to the vast spatial extent of the oceans and the short time scales over which their abundances can change. Consequently, the effects of oceanic phytoplankton on biogeochemical cycling, climate change, and fisheries are not well known.

In response to the potential importance of phytoplankton in the global carbon cycle and the lack of comprehensive data, the National Aeronautics and Space Administration (NASA) and the international community have established high priority satellite missions designed to acquire and produce high quality ocean color data. Seven of the missions are routine global observational missions: the Ocean Color and Temperature Sensor (OCTS), the Polarization and Directionality of the Earth's Reflectances sensor (POLDER), Sea-viewing Wide Field-of-view Sensor (SeaWiFS), Moderate Resolution Imaging Spectrometer-AM (MODIS-AM), Medium Resolution Imaging Spectrometer (MERIS), Global Imager (GLI), and MODIS-PM. In addition, there are several other missions capable of providing ocean color data on smaller scales. Most of these missions contain the spectral band complement considered necessary to derive oceanic pigment concentrations (i.e., phytoplankton abundance) and other related parameters. Many contain additional bands that can provide important ancillary information about the optical and biological state of the oceans.

Any individual ocean color mission is limited in ocean coverage due to sun glint and clouds. For example, one of the first proposed missions, the Sea-viewing Wide Field-of-view Sensor (SeaWiFS), can provide about 45% coverage of the global ocean in four days and only about 15% in one day (Gregg and Patt, 1993).

Objectives

We propose to investigate, develop, and test algorithms for merging ocean color data from multiple missions. We seek general algorithms that are applicable to any retrieved ocean color data products, and that maximize the amount of information available in the combination of data from multiple missions. Most importantly, we will investigate merging methods that produce the most complete coverage in the smallest amount of time, nominally, global daily coverage. We will also assess the ability to produce fuller coverage in larger time increments, including 4-day, 8-day (weekly), and monthly. We intend to develop methods that are not mission-specific, but take advantage of the unique characteristics of the missions as much as possible.

12.2 RESEARCH ACTIVITIES

Work has focused on 1) defining the problems and opportunities provided by the existence of multiple sensors, 2) analysis of past sensors to provide insights into the characteristics, drawbacks, and advantages of individual sensor responses in the context of merging, and 3) analysis, development, and testing of candidate merger algorithms.

Defining Problems and Opportunities of Multiple Missions

- First we assessed the global coverage improvements possible by the 6 global missions. These results show that significant scientific advantages can accrue from assembling and merging data from the multiple satellite platforms proposed for ocean color in the next decade. The principal advantages are increased ocean coverage in less time, and new observations of the daily dynamics of phytoplankton abundances, resulting from different observation times of co-located ocean areas. Data from three satellites can increase ocean coverage by 58% for one day, and 45% for four days. Additional satellites produce diminishing returns, however. This latter point is not necessarily an adverse finding, since each mission has a limited life expectancy and in-flight problems are, unfortunately, still not rare in the satellite business. Using observations from pairs of missions, as much as 14 hour time differences at co-located points can be realistically achieved at high latitudes, even considering the distribution of land masses and ice cover. Smaller time differences are observed at lower latitudes, but 5 to 7 hour differences are still available. Furthermore, massive numbers of these co-located pairs are available, suggesting that routine scientific studies of diel phytoplankton variability can be supported. These results

were published in the IEEE Transactions on Geoscience and Remote Sensing (Gregg et al., 1998).

- More detailed analyses emphasized seasonal and regional coverage improvements and was limited to the SeaWiFS/MODIS combination, since these are the two missions planned for launch next. The results showed that the launch of EOS AM-1 provides an opportunity to potentially improve ocean color observations by combining data from the SeaWiFS and MODIS missions. The sensors have different scanning characteristics and are flying on different platforms in different orbits. The results suggested that very large improvements in coverage frequency (daily to four-day) can be obtained by combining data from both sensors: 40-47% increases in global coverage over SeaWiFS alone in one day, and > 100% in areas near the solar declination. Four-day increases are slightly smaller for global coverage, 29-35%, but meridional percent increases are similar to the one-day case. These differences are due to reduced sun glint contamination obtained by tilting (SeaWiFS), and scanning away from the maximum glint region (MODIS), due to its 10:30 AM equator crossing time, and due to the large scan width of MODIS. The results show that SeaWiFS and MODIS are very complementary ocean color missions that can provide more complete observations of ocean processes at high frequency if data are combined. These results were published in the IEEE Transactions on Geoscience and Remote Sensing (Gregg and Woodward, 1998). A more detailed paper with more fully defined results was published as a NASA Technical Memorandum (Woodward and Gregg, 1998).

- Assessed potential capability for improving ocean color observations by selecting complementary mission orbits. Considering that observations are severely hampered by cloud cover and sun glint, a possibility exists for using multiple missions to improve the coverage of the oceans in shorter time scales. In fact, only about 10-18% of the oceans are observed in a single day, even by so-called global observational missions, due to these two ocean color contaminants. Analysis of a 7-day period of cloud cover from the International Satellite Cloud Climatology Project (ISCCP), show that 12% new surface area is available for viewing each day. This translates to an increase of about 0.5% per hour of separation in viewing times. Thus if the ocean could be viewed by 2 different satellites 4 hours apart, 2% more ocean area could be observed. This represents a coverage increase of about 13%. If 2 satellites were placed in Earth orbit with equator crossing times 4 hours apart, the improvement in coverage by these 2 satellites over a single one is about 60%.

- Furthermore, by managing the orbits of the 2 satellites, nearly complete sun glint avoidance can be achieved, further improving the ocean coverage. The best improvements can be made by 2 satellites in the same node, whose orbital positions are adjusted to view the sun glint contaminated areas of the other. If scan edges are useful for quantitative ocean color observations (the validity of which is unknown at this time), then only 2 polar-orbiting satellites are necessary. If not, a third satellite is necessary, preferably in a low inclination orbit where losses in coverage in the tropics by the polar orbiters can be best compensated (polar orbiters overlap coverage at high latitudes, and the scan edges are necessary only near the equator). However, the best configuration is 3 geostationary satellites, which provide complete global coverage routinely with a viewing time separation that can maximize cloud and sun glint avoidance, with a single polar orbiter to provide high latitude coverage. This option is considered expensive at the present time, however.

Analysis of Past Sensors

Investigations with OCTS began before the failure of ADEOS, in an effort to characterize its ocean color data for use with a merging activity with SeaWiFS. The loss of data from the sensor precludes its use in merging, but the similarity of some aspects of sensor design with MODIS suggests that significant understanding of the capabilities and deficiencies of MODIS data can be facilitated through a thorough analysis of OCTS data. In fact, we have found this to be true. Initial observations just after failure of OCTS suggested 6 problem areas: band registration, image striping, cloud noise, navigation, calibration, and bright target response (Gregg, 1997). Analysis of the first three led to solutions that improved imagery substantially (Gregg, 1998; Gregg, 1999). Particularly the methods for reducing image striping is a useful method for a problem expected to occur in MODIS imagery. Analysis of geolocation, radiometric stability and accuracy, and bright target responses were characterized (Gregg et al., 1999). The results here also have implications for MODIS.

Analysis of OCTS imagery indicated three areas of impairment for quantitative scientific research applications: 1) band misalignments, 2) image striping, and 3) image noise. These impairments are caused by 1) band offsets in the sensor design, 2) detector radiometric response variability, and 3) cloud contamination (primarily) and the band offset design (partially), respectively. The band offset design has potentially serious implication for ocean color research, given the presence of small scale variability, the requirement of multiple bands to produce ocean color geophysical outputs, and the sensitivity of the algorithms. A nearest neighbor band-to-band co-registration method produced the best results, with the least image noise, best cloud identification potential, and most accurate depiction of the actual full spectral suite at a given location. The offset design, however, still produced inconsistencies in a spectral understanding of each OCTS IFOV, and therefore provided a limitation on the sensor's ultimate capability. We found it effective to handle image striping by linearizing detector responses to the extent possible, and then applying a median filter to a quasi-

chlorophyll product to smooth out the individual detector responses (Fig. 12.1). Location of the total radiances used to produce the median filtered quasi-chlorophyll were retained and enable smoothing of the total radiances, after which a straightforward application of atmospheric correction can be performed. The net effect of both band co-registration and image striping reduction was to reduce the actual spatial resolution from < 1 km to about 5 km. A multi-step method for identifying and removing cloud effects was found to be a reasonably effective method.

The OCTS archive collected by NOAA and NASA over the US East Coast and Gulf of Mexico appeared to contain a geometric offset of 4 to 5 pixels in the along-track direction. Analyses of scan edges indicated that an adjustment to the tilt produces the most reliable agreement to a high resolution land data file. Analysis using an island matching algorithm confirmed that an adjustment to the tilt reduces the along-track bias: from about 5 pixels to 1.5 pixels for the tilted segment of operations Mar. 18, 1997 to end of mission, and from 2.6 to less than 0.3 pixels for the nadir pointing operations for Dec. 15, 1996 to Mar. 18, 1997.

OCTS appeared to exhibit near field scatter effects in its imagery (Fig. 12.2). These effects were substantial in magnitude, and had a spectral character, but were limited to approximately the dimensions of the focal plane (30 pixels wide by 10 pixels long). Not all bright targets exhibited these near field effects, nor did the effects always last the width of the focal plane. Most land features in the data set did not appear to produce effects as large as clouds, which was consistent with their relative brightness. Far field scatter effects were difficult to demonstrate conclusively, since haze or sub-saturating clouds could be ruled out. However, large cloud features nearly always produced successively decreasing reflectance far from their locations, and extending in all directions (Fig. 12.3). The effects also appeared to be non-spectral, which conformed to the effects of far field scatter. However, these effects, if they were in fact sensor-derived, were not large although long lasting, and did not necessarily produce adverse effects on ocean chlorophyll estimates because of the error-correcting nature of the atmospheric correction algorithms. Exceptions may occur in the presence of large amounts of tropospheric aerosols, whose scattering properties differ greatly from those of far field scatter and sub-saturating clouds. In any event, similar problems, e.g., sub-saturating clouds and thick haze, are encountered by all ocean color sensors, and probably do not have a large impact on the derivation of ocean properties.

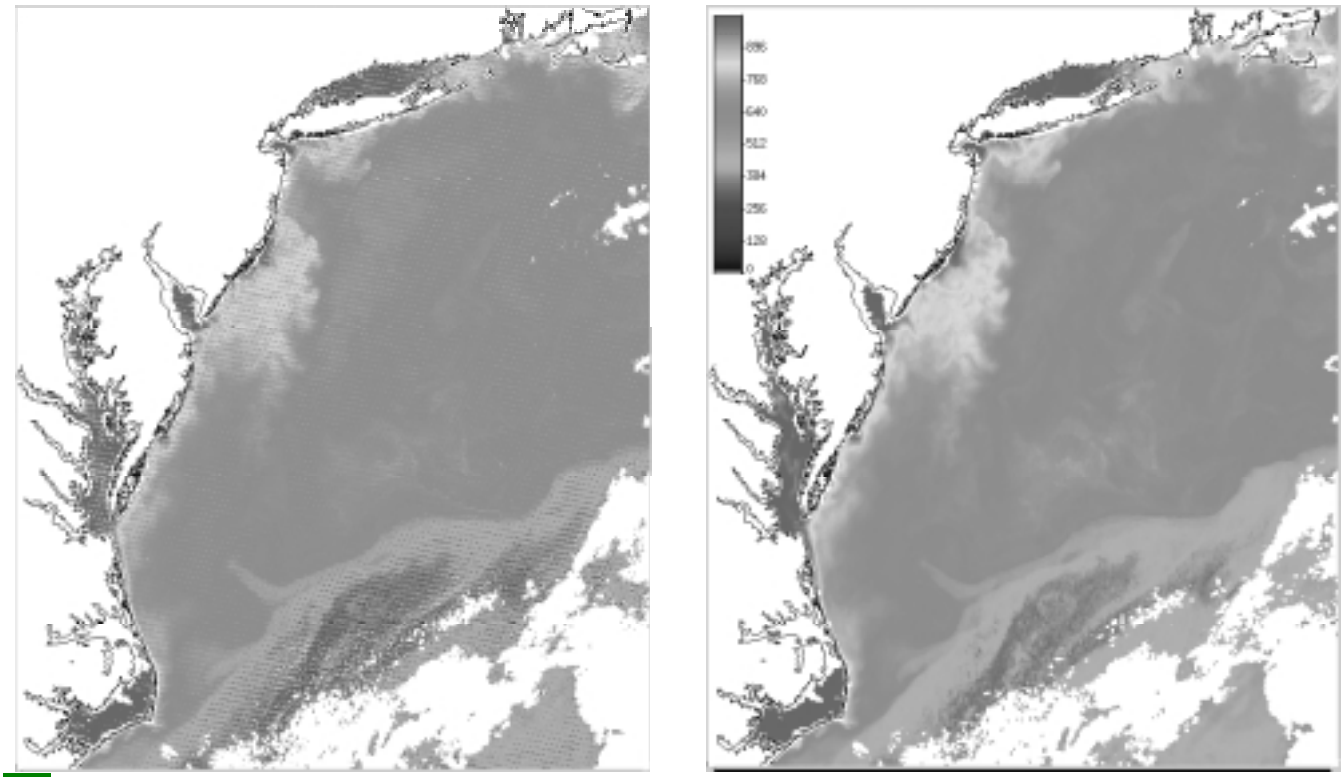

Figure 12.1. OCTS chlorophyll image of May 5, 1997 in the US Mid-Atlantic Bight, showing the reduction in image striping effects from uncorrected (a) to full striping corrections with a median filter applied (b). The reduction in image striping is dramatic, and the reduction in spatial resolution is small. Chlorophyll is logarithmically scaled for display, according to C(scaled) = $4\{[\log_{10}(C)+2]/0.012\}$. Thus, 128 scaled chlorophyll counts = 0.024 mg m^{-3}, 256 counts = 0.059 mg m^{-3}, 384 counts = 0.14 mg m^{-3}, 512 counts = 0.34 mg m^{-3}, 640 counts = 0.83 mg m^{-3}, 768 counts = 2.0 mg m^{-3}, and 896 counts = 4.9 mg m^{-3}.

However, these effects could impact aerosol analyses over the oceans. OCTS aerosol bands exhibited substantial short term variability, producing daily differences in aerosol reflectance ratios of 5 to >10%. Determination of longer term trends in the stability of the aerosol bands was inconclusive, because of the apparent long-term signal was much smaller than the short term variability, and because a complete seasonal cycle was not available due to the untimely loss of the mission after 9 months.

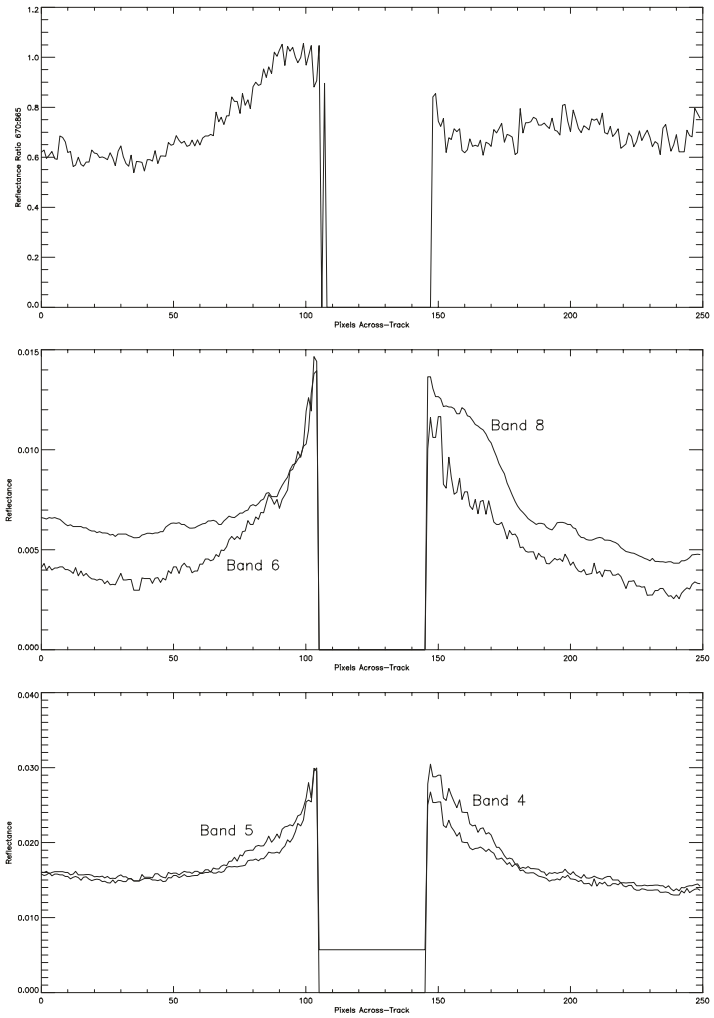

Figure 12.2 A transect through a north-south oriented cloud quantifies the apparent effects of bright targets on OCTS. The reflectance ratio of Band 6 to Band 8 increases as the scan approaches the cloud from the west, producing an elevated ratio to about 1.0 from a background value of 0.6 (these data utilize the pre-launch calibration of OCTS, and are not expected to produce a realistic ratio). A depression following the cloud produces the shadow that is apparent in the image. These Band 6 and 8 effects are due to different spectral responses of OCTS to bright targets due to the placement of the bands on the focal plane. Band 6 has a nearly symmetric response on both sides of the cloud since it in nearly on the optical axis. Band 8 exhibits a pronounced lingering effect on the east side of the cloud. The combination of these two effects produce the brightening/darkening effects seen in Fig. 3 when taken as a ratio. Bands 4 and 5 are at opposite ends of the focal plane, and exhibit expected behavior given their relative positions. Band 5 Rayleigh-corrected reflectance has been increased by 0.0057 to emphasize its effects relative to Band 4. Note that the major effects of near field scatter are limited to about 30 pixels.

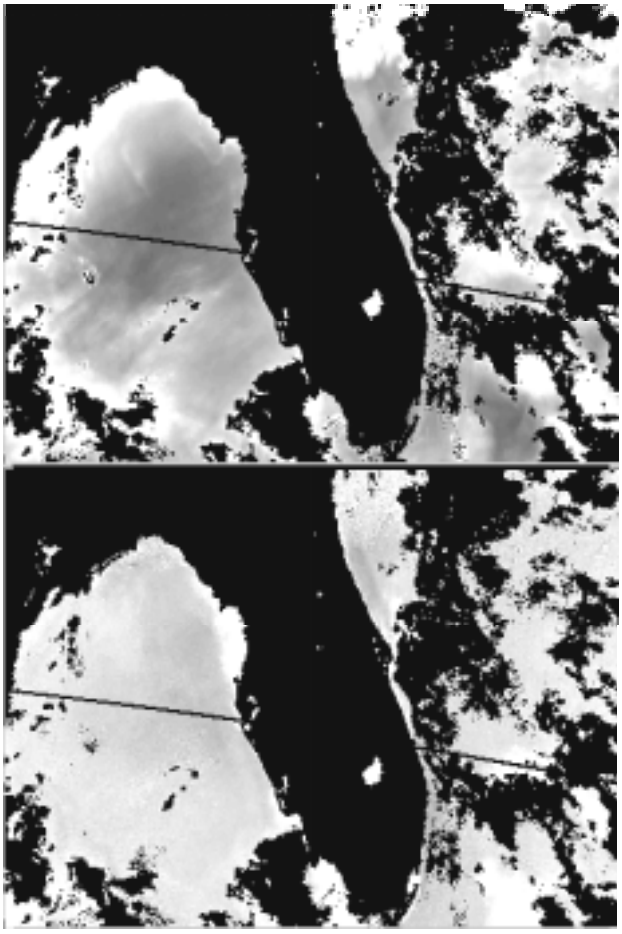

Figure 12.3. OCTS image of Florida and the eastern Gulf of Mexico on Jan. 24, 1997. Top: Band 8 aerosol reflectance. Bottom: Reflectance ratio of Band 6 to Band 8. The cloud bank in the Northern Gulf of Mexico produces bright target effects discussed before, but also appear to exhibit effects exceeding the 30 x 10 pixel dimensions of the focal plane. This may be due to far field scatter, which is less intense than near field scatter but may affect observations at quite large distances from bright targets. A key feature of far field scatter is its non-spectral nature. A concurrent view of the reflectance ratio shows no apparent effects from the cloud feature, suggesting spectral independence.

Atmospheric correction appeared to reduce the magnitude of this short term variability when observing normalized water-leaving radiances, which exhibited daily variability of only about 1-5%. Seasonal variability also appeared to exist, although observations in other areas of the oceans are necessary to conform that these are not sensor effects. Similarly, long-term trends of the sensitivity of OCTS Bands 1-5 were inconclusive because of these daily and seasonal effects, which exceeded the apparent mission lifetime effect. Comparison of calibration adjustment factors derived from 6 in-situ data sources with those obtained from an independent in-situ data set (Shimada et al., 1998) showed good agreement in the bands used to evaluate the optical state of water (Bands 1-5). Maximum differences in these bands were < 4%, and differences 1% or less were observed in Bands 1 and 2. Aerosol bands differed up to 5% in Bands 6 and 7 and 11% in Band 8, but were attributed to a measurement of Band 8 by an aircraft underflight by Shimada et al. (1998) , while Band 8 was assumed unadjusted from its pre-flight value here, due to our inability to evaluate it by any other means. However, the relative adjustments to Band 7 used here produced $\varepsilon(765,865)$ values in open ocean near 1, which are expected under most conditions, as opposed to about 1.15 using

the Shimada corrections, which is somewhat higher than expected.

Analysis and Development of Merging Algorithms

Efforts have begun on developing merging algorithms. We are investigating 4 possible approaches: 1) simple splicing/averaging, where data from 2 or more satellites are averaged where they coexist at grid points, and use of a single satellite in gaps where only one exists, 2) subjective analysis, where specific dependences and deficiencies are identified using knowledge about sensor environmental conditions and co-located observations are merged using different weighting functions for the sensors, 3) the Conditional Relaxation Analysis Method (CRAM), where the best data are selected as interior boundary conditions into a merged set using Poisson's equation, and 4) optimal interpolation, where merging occurs by weighting individual sensor data to minimize spatial covariance function. All forms have been implemented in software, and analysis of conceptual strengths and weaknesses has completed. Preliminary analysis of SeaWiFS and MODIS provided insight into operational aspects of the algorithms, but refined MODIS flight data are necessary to refine these conclusions.

REFERENCES

Gregg, W.W. and F.S. Patt, 1994. Assessment of tilt capability for spaceborne global ocean color sensors. IEEE Trans. *Geosci. Remote Sens.* **32**, 866-877.

Gregg, W.W., F.S. Patt, and R.H. Woodward, 1997. Development of a simulated data set for the SeaWiFS mission. IEEE Trans. *Geosci. Remote Sens.*, **35**, 421-435.

Reynolds, R.W., 1988. A real-time global sea surface temperature analysis. *J. Clim.*, **1**, 75-86.

Shimada, M. and others, 1998. Calibration and validation of the ocean color version-3 product from ADEOS OCTS. *J. Oceanogr.*, **54**, 401-416.

This research was supported by the

SIMBIOS NRA

PEER REVIEWED PUBLICATIONS

Gregg, Watson W., F.S. Patt and W.E. Esaias 1999: Initial Analysis of Ocean Color Data from the Ocean Color and Temperature Scanner. II. Geometric and Radiometric Analysis, *Applied Optics*, **38**, 5692-5702.

Gregg, Watson W., 1999: Initial Analysis of Ocean Color Data from OCTS. I. Imagery Analysis, *Applied Optics*, **38**, 476-485.

Gregg , Watson W. and R.H. Woodward 1998: Improvements in high frequency ocean color observations: Combining data from SeaWiFS and MODIS. *IEEE Transactions on Geoscience and Remote Sensing*, **36**, 1350-1353.

Gregg, Watson W., W.E. Esaias, G.C. Feldman, R. Frouin, S.B. Hooker, C.R. McClain, and R.H. Woodward., 1998: Coverage opportunities for global ocean color in a multi-mission era. *IEEE Transactions on Geoscience and Remote Sensing*, **36**, 1620-1627.

Woodward, Robert H. and W.W. Gregg 1988: An assessment of SeaWiFS and MODIS ocean coverage. NASA Technical Memorandum, 208607, 45 pp

PRESENTATIONS

Bontempi, Paula S., W.W. Gregg, and J.A. Yoder 1998: Initial observations of springtime surface chlorophyll-a in shelf waters off the southeastern United States by the Ocean Color and Temperature Sensor (OCTS). *EOS*, **79**, 28.

Conkright, M.E., W.W. Gregg, and C. Stephens, 1998: Historical chlorophyll data sets: Intercomparison of the NODC and NASA. *EOS*, **79**, 91.

Gregg, Watson W., 1998: Initial assessment of ocean color data from the OCTS mission. *EOS*, **79**, 28.

Gregg, W.W. and M.E. Conkright, 1998: Blended *in situ* and remotely-sensed ocean chlorophyll data sets. EOS, Transactions, American Geophysical Union.

Gregg, W.W. and M.E. Conkright, 1999: Initial results from a global blended ocean chlorophyll analysis. Proceedings of the 79th AMS annual meeting, 10th symposium on global change studies.

Gregg, Watson W., 1999: Considerations for Future Ocean Color Sensors. in Proceedings of the 8th Japan/US Working Group on Ocean Color (JUWOC), J. Ishizaka and J.

Campbell, eds., Earth Science and Technology Organization 98P0A1-D009, Shibaura, Minato-ku.

Gregg, W.W., 1999. Considerations for future ocean color sensors. Proceedings of the 8th Japan/US Working Group on Ocean Color (JUWOC), J. Ishizaka and J. Campbell, eds., Kona, Hawaii, Nov. 1998.

Chapter 13

Bio-Optical Measurement and Modeling of the California Current and Polar Oceans

B. Greg Mitchell

Scripps Institution of Oceanography, University of California San Diego, California

13.1 INTRODUCTION

This SIMBIOS project contract supports *in situ* ocean optical observations in the California Current, Southern Ocean, Indian Ocean as well as merger of other *in situ* data sets we have collected on various global cruises supported by separate grants or contracts. The principal goals of our research are to validate standard or experimental products through detailed bio-optical and biogeochemical measurements, and to combine ocean optical observations with advanced radiative transfer modeling to contribute to satellite vicarious radiometric calibration and advanced algorithm development.

In collaboration with major oceanographic ship-based observation programs funded by various agencies (CalCOFI, US JGOFS, NOAA AMLR, INDOEX and Japan/East Sea) our SIMBIOS effort has resulted in data from diverse bio-optical provinces. For these global deployments we generate a high-quality, methodologically consistent, data set encompassing a wide-range of oceanic conditions. Global data collected in recent years have been integrated with our on-going CalCOFI database and have been used to evaluate SeaWiFS algorithms and to carry out validation studies. The combined database we have assembled now comprises more than 700 stations and includes observations for the clearest oligotrophic waters, highly eutrophic blooms, red-tides and coastal case 2 conditions. The data has been used to validate water-leaving radiance estimated with SeaWiFS as well as bio-optical algorithms for chlorophyll pigments. The comprehensive data is utilized for development of experimental algorithms (e.g. high-low latitude pigment transition, phytoplankton absorption, and cDOM).

13.2 RESEARCH ACTIVITIES

A key element of our program includes on-going deployment on CalCOFI cruises to the California Current System (CCS) for which we have a 7-year time-series. This region experiences a large dynamic range of coastal and open ocean trophic structure and has experienced strong interannual forcing associated with the El Niño – La Niña cycle from 1997-2000 (Kahru and Mitchell, 2000; Kahru and Mitchell, in press). CalCOFI data provides an excellent reference for evaluating our other global data sets.

During the third year of our contract, we participated in 3 CalCOFI cruises, one cruise in collaboration with NOAA AMLR to the Southern Ocean, three cruises in East Asian marginal seas, and one cruise off the west coast of Mexico with colleagues from CICESE in Ensenada, Mexico. The global distribution of our present data set is shown in Figure 13.1. On all cruises, an integrated underwater profiling system was used to collect optical data and to characterize the water column. The system included an underwater radiometer (Biospherical Instruments MER-2040 or MER-2048) measuring depth, downwelling spectral irradiance (E_d) and upwelling radiance (L_u) in 13 spectral bands. A MER-2041 deck-mounted reference radiometer (Biospherical Instruments Inc) provided simultaneous measurements of above-surface downwelling irradiance. Details of the profiling procedures, characterization and calibration of the radiometers, data processing and quality control are described in Mitchell and Kahru (1998). The underwater radiometer was also interfaced with 25 cm transmissometers (SeaTech or WetLabs), a fluorometer, and SeaBird conductivity and temperature probes. When available, additional instrumentation integrated onto the profiling package included AC9 absorption and attenuation meters (WetLabs Inc.), and a Hydroscat-6 backscattering meter (HobiLabs).

In conjunction with *in situ* optical measurements, discrete water samples were collected from a CTD-Rosette immediately before or after each profile for additional optical and biogeochemical analyses. Pigment concentrations were determined fluorometrically and with HPLC. Spectral absorption coefficients (300-800 nm) of particulate material were estimated by scanning particles concentrated onto Whatman GF/F filters (Mitchell 1990) in a dual-beam spectrophotometer

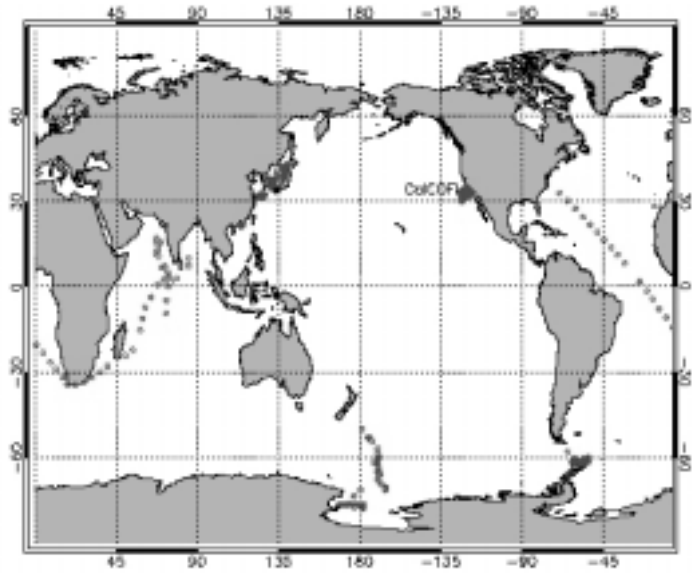

Figure 13.1. Distribution of *in situ* optical stations available for algorithm development.

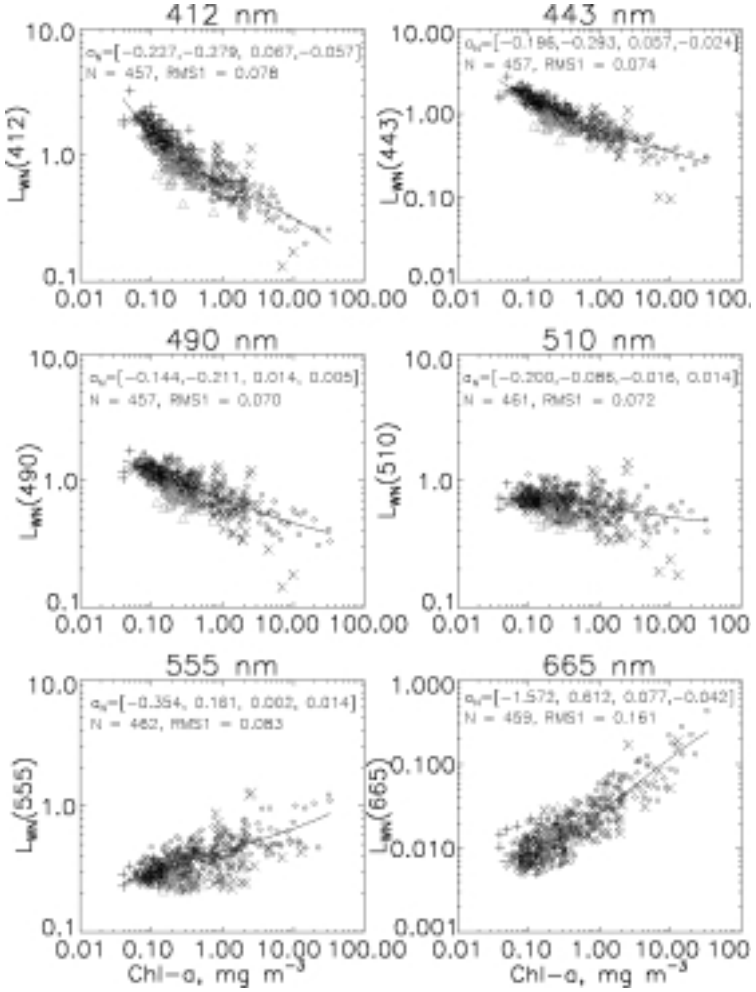

Figure 13.2. Normalized water leaving radiance at SeaWiFS bands plotted against chlorophyll for our global data set. Blue = CalCOFI, Green = Japan/East Sea; Black = INDOEX; Red = JGOFS Southern Ocean.

(Varian Cary 1). Absorption of soluble material was measured in 10 cm cuvettes after filtering seawater samples through 0.2 µm pore size polycarbonate filters. Absorption methods are described in more detail in Mitchell et al. (2000). We have also been collecting detailed measurements of other optical and phytoplankton properties including phycoerythrin pigment, size distribution using flow cytometry and a Coulter Multisizer, photosynthesis, and particulate organic matter (carbon and nitrogen).

13.3 RESEARCH RESULTS

Our normalized water leaving radiances (L_{wn}) at SeaWiFS bands for the global data set are plotted against surface chl-*a* in Figure 13.2. Our original CalCOFI data represented approximately 30% of the data used by O'Reilly et al. (1998) for development of the SeaWiFS OC2v2 and approximately 25% of the updated OC 4 algorithm (O'Reilly et al., 2000). Previously we used SeaDAS v3.0 to evaluate OC2v2 estimates of chl-*a* compared to a CalCOFI-specific regional algorithm (CAL-P6) using match-ups collected during CalCOFI cruises (Kahru and Mitchell, 1999). Here we compare retrievals for SeaDAS v4.0, which has updated atmospheric and bio-optical algorithms (Figures 13.3 and 13.4). Whereas OC2v2 in SeaDAS 3.0 tended to overestimate *in situ* chl-*a* at high values and underestimate at low values (Kahru and Mitchell, 1999), we find that OC4 in SeaDAS 4.0 tends to underestimate chl-*a* at high values, but is very good at low chlorophyll (Figure 13.3). Even after processing with the new atmospheric algorithm that eliminates the assumption that L_{wn} in the near infrared is zero (Siegel et al., 2000), SeaDAS v4.0 still has significant underestimates of L_{wn} at 412 for all our match-ups (chl-a range 0.1-10.0) with worse performance at high chl-*a* (Figure 13.4). Even L_{wn} 443 tends to be underestimated over most the range, but not as severely as L_{wn} 412. Continued effort is still required to improve the accuracy of L_{wn} if we are to be able to apply multi-wavelength bio-optical retrieval algorithms that require accurate estimates of L_{wn} at 412 and 443 (e.g. Garver and Siegel, 1997; Carder et al., 1999).

For the Southern Ocean data (red crosses in Figure 13.2), there is a strong deviation from our other global data sets, and much greater variance in the scatter plots. This region has been shown to have bio-optical algorithms that are different than low latitude regions such as CalCOFI (Mitchell and Holm-Hansen, 1991; Mitchell, 1992). The large variance in the L_{w}n-chl-a scatter plots may be attributable in part to very different community types (e.g. prymnesiophytes, diatoms, cryptophytes as discussed in Arrigo et al., 1998). Our results underscore the need for more data to serve as a basis for regional algorithms to improve estimates of chl-*a* from ocean color remote sensing. Regional algorithms will require procedures to allow transition from low latitude to high latitude without introducing errors at the lower latitudes. More data and advanced models are required to resolve issues regarding Southern Ocean bio-optical algorithms, and the causes of observed differentiation within the region as well as differences between the Southern Ocean and lower latitudes. For a better understanding, it is essential to determine not only reflectance and chlorophyll, but also inherent optical properties including absorption and backscattering as reported by Reynolds et al. (In press). Generally, there are few observations in the Southern Ocean, and even fewer with detailed observations including inherent optical properties. We lack combined pigment and optical observations in the extremely low chlorophyll regions that can be observed in the SeaWiFS images for the southern Pacific Ocean sector west of the Drake Passage, and the southern Indian Ocean sector west of Kerguelan Island. These two regions represent very low satellite-derived chlorophyll, which never exceed values of 0.2 mg chl-*a* m^{-3}.

A significant issue that has arisen within the SIMBIOS community is the fidelity of chl-a estimates using either HPLC or fluorometric methods. We have completed analysis and quality control for more than 800 samples taken from the same water sampling bottles during CalCOFI cruises (Figure 13.5). The fluorometric method is described in Venrick, et al., (1984) and the HPLC method is described in Goericke and Repeta (1993). We find that there is excellent overall agreement with a nearly 1:1 relationship, however individual samples routinely differ by up to30-40%. For the JGOFS Southern Ocean Polar Front cruises, the discrepancies were much larger and are still unresolved. A high priority for SIMBIOS should be to ensure the highest possible quality of pigment estimates, which will require consistent implementation of rigorous protocols. As a contribution to this effort, we participated in the SIMBIOS pigment round robin experiment during the past year.

15.4 CONCLUSIONS

With renewal of our SIMBIOS contract, we will continue our approach of acquiring detailed, high quality data sets at the global scale. We will continue to participate in CalCOFI cruises. In 2001 we will also

participate in the NOAA AMLR cruise to the Southern Ocean and the NOAA ACE-Asia cruise to the western sub-tropical Pacific, East China Sea, and Yellow Sea. A detailed set of spectral reflectance, absorption, backscattering, pigment, and particle size structure will be determined on most cruises. A new free-fall radiometer will be acquired with 19 channels (310-700 nm) for determining both downwelling and upwelling irradiance, and upwelling radiance for all spectral bands. We have shown that measuring these three radiometric geometries with our MER 2048 allowed us to retrieve backscatter and absorption coefficients (Stramska et al., 2000). We will continue our modeling efforts to improve our understanding of regional bio-optical properties and their relationship to biogeochemical parameters (e.g. Reynolds et al, in press; Loisel et al., submitted). Our goal is to develop appropriate regional parameterizations for semi-analytical inversion models for the retrieval of inherent optical properties as well as biogeochemical properties besides chl-*a* in addition to continuing our validation work for standard ocean color satellite algorithms.

REFERENCES

Arrigo, K.R., D.H. Robinson, D.L. Worthen, B. Schieber and M.P. Lizotte, 1998: Bio-optical properties of the southwestern Ross Sea. *Journal of Geophysical Research.* **103(C10)**, 21,683-21,695

Carder, K.L., F.R. Chen, Z.P. Lee and S.K. Hawes, 1999: Semianalytic moderate-resolution imaging spectrometer algorithms for chlorophyll *a* and absorption with bio-optical domains based on nitrate-depletion temperatures. *Journal of Geophysical Research.* **104(C3)**, 5,403-5,421

Garver, S.A. and D.A. Siegel, 1997: Inherent Optical Property Inversion of Ocean Color Spectra and its Biogeochemical Interpretation: 1. Time series from the Sargasso Sea. *Journal of Geophysical Research.* **102(C8)**, 18,607-18,625

Goericke, R. and D.J. Repeta, 1993: Chlorophylls a and b and divinyl chlorophylls a and b in the open subtropical North Atlantic Ocean. *Marine Ecology Progress Series.* **101**, 307-313

Kahru, M. and B.G. Mitchell, 1999: Empirical chlorophyll algorithm and preliminary SeaWiFS validation for the California Current. *International Journal of Remote Sensing.* **20(17) ,** 3,423-3,430

Kahru, M. and B.G. Mitchell, 2000: Influence of the 1997-98 El Niño on the surface chlorophyll in the California Current. *Geophysical Research Letters.* **27(18)**, 2,937-2,940

Kahru, M. and B.G. Mitchell, 2000: Seasonal and non-seasonal variability of satellite-derived chlorophyll and CDOM concentration in the California Current. *Journal of Geophysical Research*. (*in press*)

Loisel, H. and D. Stramski, 2000: Estimation of the inherent optical properties of natural waters from the irradiance attenuation coefficient and reflectance in the presence of Raman scattering. *Applied Optics.* **39(18)**, 3,001-3,011

Mitchell, B.G., 1990: Algorithms for determining the absorption coefficient of aquatic particulates using the quantitative filter technique (QFT). In: Spinrad, R., ed., Ocean Optics X, Bellingham, Washington, SPIE, pp. 137-148

Mitchell, B.G. (1992) Predictive bio-optical relationships for polar oceans and marginal ice zones. *Journal of Marine Systems,*. **3** ,91-105

Mitchell, B.G. and M. Kahru, 1998: Algorithms for SeaWiFS standard products developed with the CalCOFI bio-optical data set. *Cal.Coop.Ocean.Fish.Invest.R,*. **39**, 133-147

Mitchell, B.G. and O. Holm-Hansen, 1991: Bio-optical properties of Antarctic Peninsula waters: Differentiation from temperate ocean models. *Deep-Sea Research I.* **38(8/9)**, 1,009-1,028

Mitchell, B.G., A. Bricaud, K.L. Carder, J.S. Cleveland, G.M. Ferrari, R. Gould, M. Kahru, et al., 2000: Determination of spectral absorption coefficients of particles, dissolved material and phytoplankton for discrete water samples. *In**:** NASA, Ocean Optics Protocols for Satellite Ocean Color Sensor Validation*.

O'Reilly, J.E., S. Maritorena, B.G. Mitchell, D.A. Siegel, K.L. Carder, S.A. Garver, M. Kahru and C. McClain, 1998: Ocean color chlorophyll algorithms for SeaWiFS. *Journal of Geophysical Research.* **103(C11)** , 24,937-24,953

O'Reilly, J.E., S. Maritorena, D.A. Siegel, M.C. O'Brien, D.A. Toole, B.G. Mitchell, M. Kahru, et al., 2000: Ocean color chlorophyll *a* algorithms for SeaWiFS, OC2 and OC4: Version 4. In: NASA, SeaWiFS Postlaunch Calibration and Validation Analyses.

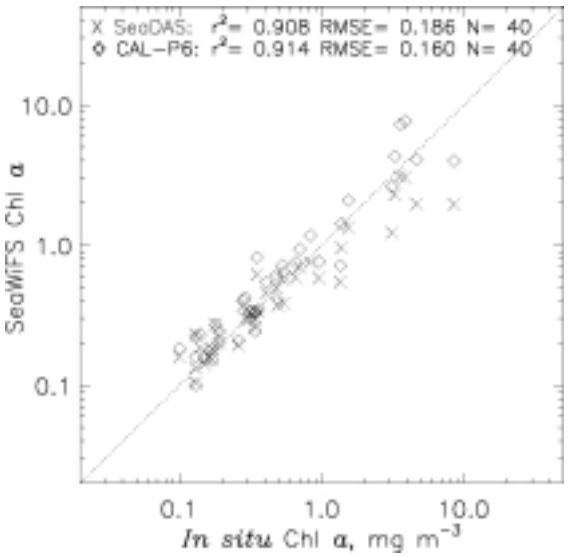

Figure 13.3. Chlorophyll-*a* estimates derived using SeaWiFS SeaDAS version 4.0 compared to in situ estimates of chlorophyll-*a* for NASA's global processing version 3.0 OC4 algorithm, and our CAL-P6 algorithm.

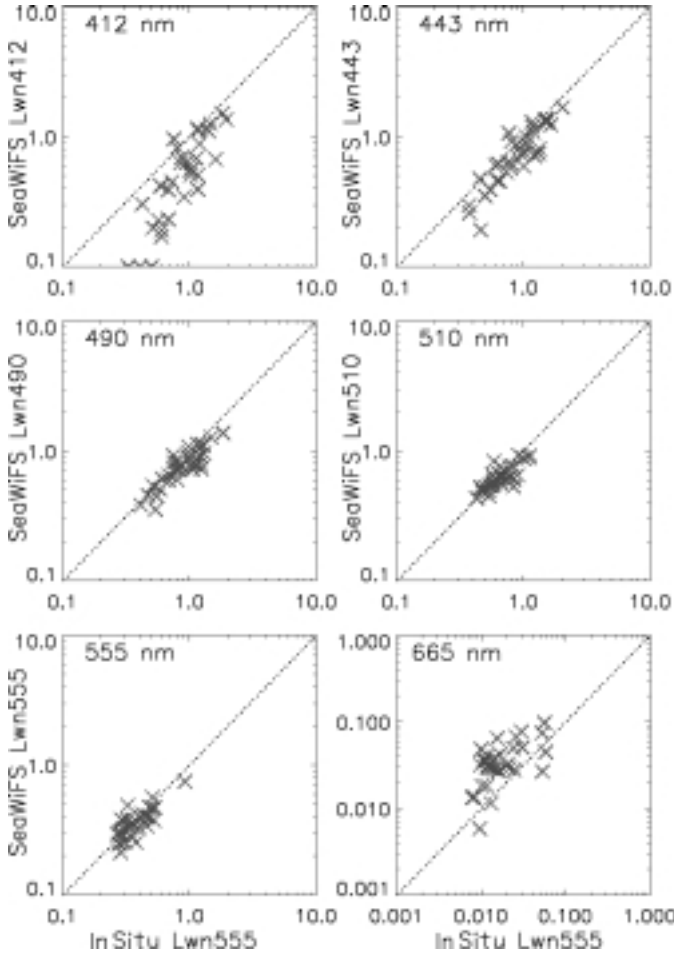

Figure 13.4. Normalized water leaving radiance derived from SeaWiFS SeaDAS version 4.0 processing compared to *in situ* measurements at the 6 visible bands of SeaWiFS.

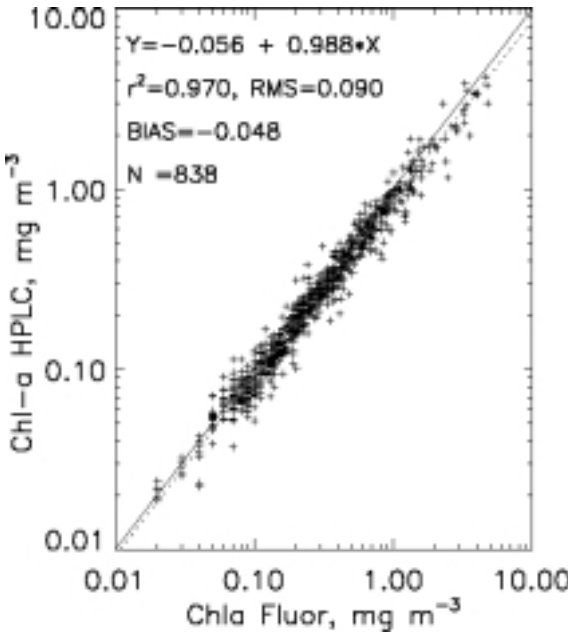

Figure 13.5. CalCOFI HPLC total chlorophyll-*a* (mono-vinyl and di-vinyl chl-*a*, and closely related derivates) plotted against fluorometric chlorophyll-*a*. The 1:1 and regression fits are indicated by the solid and dashed lines, respectively.

Reynolds, R.A., D. Stramski and B.G. Mitchell, 2000: A chlorophyll-dependent semi analytical reflectance model from derived from field measurements of absorption and back scattering coefficients within the Southern Ocean. *Journal of Geophysical Research*. (*In Press*)

Siegel, D.A., M. Wang, S. Maritorena and W. Robinson, 2000: Atmospheric correction of satellite ocean color imagery: The black pixel assumption. *Appl.Opt.* **39(21)** , 3,582-3,591

Stramska, M., D. Stramski, B.G. Mitchell and C.D. Mobley, 2000: Estimation of the absorption and backscattering coefficients from in-water radiometric measurements. *Limnology and Oceanography*. **45(3)**, 628-641

Venrick, E.L. and T.L. Hayward, 1984: Determining chlorophyll on the 1984 CalCOFI surveys. *CalCOFI Reports.*, **XXV**, 74-79

This research was supported by the

SIMBIOS NASA contract # 97130

PEER REVIEWED PUBLICATIONS

Gross, L., S. Thiria, R. Frouin, and B.G. Mitchell, 2000 Artificial neural networks for modeling the transfer function between marine reflectance and phytoplankton pigment concentration. *Journal of Geophysical Research*. **105**(C2), 3,483-3,495.

Kahru, M. and B.G. Mitchell, 1999: Empirical chlorophyll algorithm and preliminary SeaWiFS validation for the California Current, *International Journal of Remote Sensing* **20**(17), 3,423-3,429.

Kahru, M., and B.G. Mitchell, 2000. Seasonal and non-seasonal variability of satellite-derived chlorophyll and CDOM concentrations in the California Current. *Journal of Geophysical Research.* (*In Press*)

Mitchell, B.G. and M. Kahru, 1998: Algorithms for SeaWiFS standard products developed with the CalCOFI bio-optical data set. *CalCOFI Reports*, Vol. **39**: 133-147.

Nakajima, T., A. Higurashi, K. Aoki, T. Endoh, H. Fukushima, M. Toratani, Y. Mitomi, B.G. Mitchell and R. Frouin, 1999: Early phase analysis of OCTS radiance data for aerosol remote sensing, *IEEE Transactions*, **37**(3), 1,575-1,585.

O'Reilly, J.E., S. Maritorena, B.G. Mitchell, D.A. Siegel, K.L. Carder, S.A. Garver, M. Kahru, C. McClain, 1998: Ocean Color Chlorophyll Algorithms for SeaWiFS, *Journal of Geophysical Research*, **103**(C11), 24,937-24,953.

Reynolds, R.A., S. Stramski and B.G. Mitchell, 2000: A chlorophyll-dependent semianalytical reflectance model derived from field measurements of absorption and backscattering coefficient within the Southern Ocean. *Journal of Geophysical Research.* (*In Press*)

Stramska, M., D. Stramski, B.G. Mitchell and C.Mobley, 2000: Estimation of the absorption and backscattering coefficients from in-water radiometric measurements, *Limnology and Oceanography*, **45**(3), 628-641

Submitted

Loisel, H., D. Stramski, B.G. Mitchell, F. Fell, V. Fournier, B. Lemasle and M. Babin , 2000: Comparison of the ocean inherent optical properties obtained from measurements and inverse modeling. Submitted to *Applied Optics*.

Reynolds, R.A., S. Stramski and B.G. Mitchell, 1999: A chlorophyll-dependent semianalytical reflectance model derived from field measurements of absorption and backscattering coefficient within the Southern Ocean. Submitted to *Journal of Geophysical Research.*

Stramski, M., D. Stramski, B.G. Mitchell and C.Mobley, 1999: Estimation of the absorption and backscattering coefficients from in-water radiometric measurements, Submitted to *Limnology and Oceanography*.

PRESENTATIONS

Flatau, P.J., B. Bichnevicius, B.G. Mitchell, 1998:Vicarious calibration of the absorption and scattering measurements in the California Current, AGU Ocean Science Meeting, San Diego.

Fougnie, B., P.-Y. Deschamps, R. Frouin, and B.G. Mitchell, 1998: Measuring Water-Leaving Radiance with a Polarization Radiometer: Theory and Experimental Verification, AGU Conference, San Diego.

Frouin, R., P.-Y. Deschamps, B.G. Mitchell and M. Kahru, 1998: The Normalized Difference Phytoplankton Index for Satellite Ocean Color Applications, AGU Ocean Science Meeting, San Diego.

Kahru, M. and B.G. Mitchell, 1998: Empirical chlorophyll algorithm for the California Current, AGU,San Francisco.

Kahru, M. and B.G. Mitchell, 2000, Seasonal and non-seasonal variability of satellite-derived chlorophyll and CDOM concentration in the California Current. AGU Ocean Sciences Meeting, San Antonio, TX

Loisel, H., D. Stramski, M. Babin, F. Fell and B.G. Mitchell, 2000, An inverse model for the estimation of the inherent optical properties in presence of Raman scattering:

description and validation. AGU Ocean Sciences Meeting, San Antonio, TX

Mitchell, B.G., 2000, Global bio-optical algorithms and ocean color satellite validation for ocean color. August 21 - September 9, 2000. Satellite Oceanography 2000, Focus at the sea surface, Department of Physical Oceanography, CICESE, Ensenada B.C., MEXICO

Mitchell, B.G., M. Kahru, R. Reynolds, J. Wieland, D. Stramski 2000 Satellite Estimation Of Seasonal Variations In Organic Carbon To Chlorophyll-A Ratios In The Southern Ocean And Interpretation Of Carbon Flux Dynamics. AGU Ocean Sciences Meeting, San Antonio, TX

Mitchell, B.G., M. Kahru, R.A. Reynolds, J.D. Wieland and D. Stramski, 2000, Satellite Estimation Of Seasonal Variations In Organic Carbon To Chlorophyll-A Ratios In The Southern Ocean Oceans from Space Symposium. October 9 - 13, 2000, Venice, Italy

Reynolds, R.A., M. Kahru, J.D. Wieland, D. Stramski and B.G. Mitchell, 1998: An evaluation of SeaWiFS ocean color chlorophyll algorithms within the Southern Ocean, AGU, San Francisco.

Stramski, D., R.A. Reynolds, M. Kahru, J.D. Wieland and B.G. Mitchell 2000 Geographic distribution and seasonal variations in particulate organic carbon within the Southern Ocean as determined from satellite imagery of ocean color. AGU Ocean Sciences Meeting, San Antonio, TX

Chapter 14

SIMBIOS Normalized Water-Leaving Radiance Calibration and Validation: Sensor Response, Atmospheric Corrections, Stray Light and Sun Glint

James L. Mueller

Center for Hydro-Optics and Remote Sensing, San Diego State University, California

14.1 INTRODUCTION

This SIMBIOS contract supports acquisition of match up radiometric and bio-optical data for validation of SeaWiFS and other ocean color satellites, and evaluation of uncertainty budgets and protocols for *in situ* measurements of normalized water leaving radiances.

14.2 RESEARCH ACTIVITIES

Research activities during the third and final year of this contract break down into three areas:

1. Data Acquisition and Analysis: we supported, but did not participate in, one cruise in the Gulf of California (GOCAL 99B) under this contract. This work included pre-cruise radiometric calibrations, near real-time interpretative analysis of SeaWiFS imagery and communication of mesoscale front and eddy locations to the ship, and post-cruise data analysis for SeaBASS archival. GoCAL 99B was the final CHORS/CICESE/OSU collaborative cruise associated with the SIMBIOS project.

2. Ocean Optics Protocols for normalized water-leaving radiance measurements and analyses methods, and uncertainty budgets, were reviewed, evaluated and updated.

3. Modeling: A set of radiative transfer model experiments were undertaken to evaluate selected aspects of normalized remote-sensing reflectance uncertainties.

14.3 RESEARCH RESULTS

PRR radiometric profiles and phytoplankton pigment concentration data acquired during GoCAL 99B were analyzed and formatted for archival in SeaBASS. Analyses and archival preparation of data from GoCAL 98B and 99A were also completed during the period. Our manuscript describing bio-optical provinces of the Gulf of California, and a remote sensing algorithm for estimating euphotic zone depth, was revised and published (Cervantes-Duarte *et al.* 2000).

A comprehensive evaluation and update of progress in protocols for *in situ* determinations of Normalized Water-Leaving Radiance (or equivalently, Normalized Remote-Sensing Reflectance) was completed and published (Mueller 2000a, 2000b; Mueller *et al.* 2000). These topics included determinations of L_W and R_{RS} from both in-water (Mueller 2000b) and above-water (Mueller *et al.* 2000) radiometric measurements, and the normalization procedure to determine L_{WN} and R_{RSN} from the measured quantities, solar zenith angle and inherent optical properties parameterized by the method of Morel and Gentili (1996) (Mueller 2000a).

A supplemental radiative transfer modeling task was undertaken to estimate the uncertainty associated with the Morel and Gentili (1996) remote-sensing [Chl] parameterization of the inherent optical properties. This has been approached by comparing measured R_{RSN} (from in-water PRR profiles) with that calculated using measured IOP in the commercially available Hydrolight radiative transfer model for station data from the GoCAL cruises.

At the request of the SIMBIOS Project Office (SPO), the Principal Investigator accepted a high-priority task to completely and comprehensively revise the ocean optics protocols (Mueller and Austin 1995) to reflect the considerable progress made in many areas over the previous 5 years. The revised protocol document was completed and published in August (Fargion and Mueller 2000). The overall scope of this revision greatly exceeded the 3 L_{WN} chapters cited above. The additional work was supported by the SPO under a separate contract. The priority given to the overall protocol revision task necessarily delayed progress in the other research efforts under this contract, and accordingly, delivery schedule waivers were requested and approved by the SPO.

14.4 CONCLUSIONS

The research and results outline above complete work on the present SIMBIOS contract. The Principal Investigator's

future research efforts within the SIMBIOS program, under terms of a new contract with the SPO, will be devoted entirely to preparation and publication of annual revisions to Ocean Optics Protocols (Fargion and Mueller 2000). Each revision will reflect annual progress and improvements in ocean optical and bio-optical instrumentation, measurement methods and methods of data analysis. The protocol revisions will be drawn from a combination of peer-reviewed literature, workshop results, and collaborative written reviews reflecting realizations of community consensus on recent advances in these methods. Revision 3 to the protocols will be prepared and delivered to the SPO on 1 October 2001, for administrative review and publication by 1 December 2001. To allow this schedule, draft protocol materials received later than July 2001 will be automatically deferred and considered for publication in a later revision. It is anticipated that Revisions 4 and 5 will be prepared and delivered on a similar schedule in 2002 and 2003, respectively.

REFERENCES

Fargion G.S. and J.L. Mueller, 2000. Ocean Optics Protocols for Satellite Ocean Color Sensor Validation, Revision 2. *NASA/TM-2000-209966*. NASA Goddard Space Flight Center, Greenbelt, MD. 184pp.

Morel, A. and B. Gentili, 1996. Diffuse reflectance of oceanic waters. III. Implication of bidirectionality for the remote-sensing problem. *Appl. Opt.*, **35**(24), 4850-4862.

Mueller, J.L., 2000a. Overview of measurement and data analysis protocols. In: Fargion, G.S. and J.L Mueller, 2000. Ocean Optics Protocols for Satellite Ocean Color Sensor Validation, Revision 2. *NASA/TM-2000-209966*. NASA Goddard Space Flight Center, Greenbelt, MD. (Chapter 8) pp65 – 86.

Mueller. J.L., 2000b. In-water radiometric profile measurements and data analysis protocols. In: Fargion, G.S. and J.L Mueller, 2000. Ocean Optics Protocols for Satellite Ocean Color Sensor Validation, Revision 2. *NASA/TM-2000-209966.* NASA Goddard Space Flight Center, Greenbelt, MD. (Chapter 9) pp87-97.

Mueller, J.L., et al., 2000. Above-water radiance and remote sensing reflectance measurements and data analysis protocols. In: Fargion, G.S. and J.L Mueller, 2000. Ocean Optics Protocols for Satellite Ocean Color Sensor Validation, Revision 2. NASA/TM-2000-209966. NASA Goddard Space Flight Center, Greenbelt, MD. (Chapter 10) pp98-107.

This research was supported by the

SIMBIOS NASA contract # 97126

PEER REVIEWED PUBLICATIONS

Barnard, A.H., J.R.V. Zaneveld, W.S. Pegau, J.L Mueller, H. Maske, R. Lara-Lara, S. Alvarez-Borrego, and E. Valdez-Holquin. 1999: The determination of PAR levels from absorption coefficient profiles at 490 nm. Ciencias Marinas, in press.

Cervantes-Duarte, R., J. L. Mueller, C.C. Trees, H. Maske, S. Alvarez-Borrego and R. Lara-Lara, 2000. Euphotic depth, irradiance attenuation and remote sensing K490 in bio-optical provinces of the Gulf of California. *Ciencias Marinas*, **26(4)** ,533-560.

Mueller, J.L., J.R.V. Zaneveld, W.S. Pegau, E. Valdez, H. Maske, S. Alvarrez-Borrego, and R. Lara-Lara. 1997: Remote sensing reflectance: preliminary comparisons between in-water and above-water measurements, and estimates modelled from measured inherent optical properties. *SPIE*, **2963**, 502-513.

Zaneveld, J.R.V., W.S. Pegau, A.H. Barnard, J.L. Mueller, H. Maske, E. Valdez, R. Lara-Lara, and S. Alvarez-Borreo. 1997: Prediction of euphotic depths and diffuse attenuation coefficients from absorption profiles: A model based on comparison between vertical profiles of spectral absorption, spectral irradiance, and PAR. *SPIE*, **2963**, 585-590

PRESENTATIONS

Pegau, W.S., A.H. Barnard, J.R.V. Zaneveld, J.L. Mueller, H. Maske, R. Lara-Lara, S. Alvarez-Borrego, E. Valdez-Holguin, and R. Cervantes-Duarte, 1998: Optical variability in the Gulf of California. Ocean Optics XIV Conference Papers, Volume 2, Kailua-Kona, HI.

Chapter 15

Validation of Carbon Flux & Related Products for SIMBIOS: the CARIACO Continental Margin Time Series & the Orinoco River Plume

Frank Muller-Karger, Chuanmin Hu and John P. Akl
University of South Florida, Department of Marine Science, St. Petersburg, Florida

Ramon Varela
Fundacion La Salle de Ciencias Naturales, Punta de Piedras, Edo. Nueva Esparta, Venezuela

15.1 INTRODUCTION

Between 1997 and 2000, this SIMBIOS investigation collected bio-optical measurements in the Southeastern Caribbean Sea and the tropical western Atlantic to help understand the color of coastal and continental shelf waters. Specifically, bio-optical data were collected to complement an oceanographic time series maintained within the Cariaco Basin, a site affected by seasonal coastal upwelling. Bio-optical data were also collected within the plume of the Orinoco River during seasonal extremes in discharge. This program focused on providing data to the SeaWiFS and SIMBIOS Projects for validating SeaWiFS products. The data are unique in that they provide a substantial number of observations on repeated seasonal cycles for the SeaBASS bio-optical database.

An important aspect of this SIMBIOS investigation was a focus on proper interpretation of ocean color remote sensing data from coastal and continental shelf environments. With this goal in mind, ocean color satellite data from a variety and locations and from different satellite sensors were examined to understand spatial and temporal variability in pigment concentrations, and also to conduct an in-depth study of current atmospheric correction and bio-optical algorithms.

15.2 RESEARCH ACTIVITIES

Here we provide an update on activities during 1999-2000 and a summary of contributions made to SIMBIOS over the past three years. Background information on this SIMBIOS contract is provided in Muller-Karger (1999) and Muller-Karger et al. (1999).

The CARIACO Time Series

This SIMBIOS effort conducted monthly bio-optical observations at 10.5°N, 64.67°W within the Cariaco Basin (Figure 15.1) in the southeastern Caribbean Sea. This was part of a multidisciplinary program referred to as CARIACO (CArbon Retention In A Colored Ocean) that received support from the U.S. National Science Foundation and the Consejo Nacional de Investigaciones Cientificas y Tecnologicas (CONICIT) of Venezuela for oceanographic cruises and for investigations focusing on processes affecting particulate carbon flux to the bottom of the Cariaco Basin. Initial results from the CARIACO program are presented by Muller-Karger et al. (2000a, 2000b) and Thunell et al. (2000).

During each cruise, we collected a series of bio-optical measurements. In 1997 and 1998, we used the underwater profiling Biospherical Instruments MER2048 in conjunction with a MER2041 Deck Cell. Since mid-1998, we have used a PRR-600 profiler with matching deck cell. Above water measurements were made with a Photo Research Hyperspectral Colorimeter Model PR650. Derived products include Lw (Water-Leaving Radiance), Rrs (Remote-sensed reflectance) and K (attenuation coefficient). In addition, a full suite of measurements is made which includes: particulate material concentration and absorption coefficients, HPLC, fluorometric determinations of Chl concentration, pH, Alkalinity, primary productivity, DOC absorption and concentration, nutrients, sun photometry, oxygen, and salinity.

As of October 2000, data from 30 CARIACO cruises had been submitted to the SeaBASS archive. Figure 15.2 presents results of the time series, comparing in situ observations with chlorophyll-a estimates based on above-water reflectance measurements and using the bio-optical algorithms adopted by the SeaWiFS project (O'Reilly et al., 1998; O'Reilly et al., 2000).

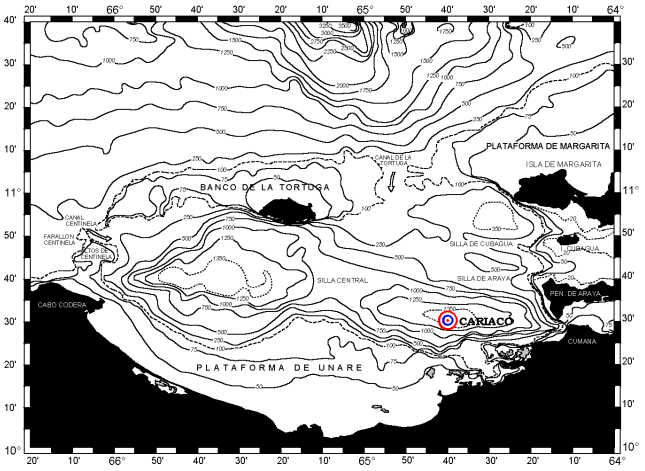

Figure 15.1. The Cariaco Basin: bathymetry and the location of the CARIACO time series station.

The Orinoco River Plume

Muller-Karger et al. (1989) and Muller-Karger and Varela (1990) describe a seasonal cycle in the spatial structure of near-surface pigment detected with Coastal Zone Color Scanner (CZCS) data collected over the eastern Caribbean Sea. In addition to describing the seasonal occurrence of large pigment patches associated with coastal upwelling, as seen in the Cariaco Basin, they discovered that the seasonally-expanding plume of the Orinoco River reached Puerto Rico around September-October and drifted westward, slowly losing its color signature. The Orinoco dispersed pigment over > 3x105 km2 of the Caribbean Sea. Clearly, while there are phytoplankton within the plume, the plume represents Case II waters in which colored dissolved organic matter (Yellow Substance) and suspended sediment lead to erroneous satellite-derived pigment products. The Orinoco River provides a good study region for extreme Case II waters which can easily be covered by satellite observations at a variety of spatial and temporal resolutions.

We carried out five cruises to the Orinoco Delta and plume under this SIMBIOS program. Stations were occupied north of Dragon's Mouth (the northern strait between Venezuela and Trinidad), within the Gulf of Paria, immediately off the delta of the Orinoco River south of Serpent's Mouth (the southern strait between Venezuela and Trinidad), and within several branches of the Orinoco Delta. Figure 4 shows station locations for the first four Orinoco River cruises. As of October 2000, data from five Orinoco River cruises had been submitted to the SeaBASS archive. An additional Orinoco cruise is scheduled for late October 2000.

Above-water spectral remote-sensing reflectance was measured including corrections for sky-radiance initially using a Photo Research Hyperspectral Colorimeter Model PR650, and starting in 1999 an Analytical Spectral Devices (ASD) spectrometer which extended the spectral range of observations, namely from 380 to 1,200 nm. We also conducted underwater measurements of remote sensing reflectance using submersible MER2048 and, since 1998, PRR-600 instrumentation (Biospherical Instr.). Some observations were conducted away from the coast, where the color of the plume is influenced by colored dissolved organic matter as well as phytoplankton, but where suspended terrestrial material is expected to be minimal. We also collected data very close to the coast where the plume is extremely turbid.

Figure 15.5 shows the variability obtained in the absorption coefficient for colored dissolved organic matter relative to variation in salinity during the first four cruises. These data will help us to understand the dependence of variability in absorption to geographical location and season.

The river plume data are being used by Joe Salisbury and Charles Vorosmarty at the University of New Hampshire for automated modeling of river water impact off the continent of South America, in a model linked to terrestrial hydrology.

SeaWiFS Data Calibration Efforts

Dr. Chuanmin Hu from our group forwarded a Gain/CalibrationTable study summary to Chuck McClain, which we believe was used in evaluating the new SeaWiFS calibration. Specifically, during January – May 1998 we found that the normalized water leaving radiance, nLw555, for clear water was frequently lower than 0.25 (not to mention the well-accepted value, 0.28, from Gordon and Clark). After studying several images very carefully, we found that the calibration table released at that time was probably inappropriate. We forwarded detailed analyses to the SeaWiFS Project outlining our results.

Algorithm development

Dr. Hu (Hu et al., 2000a, b) developed and implemented a turbid-water (case II) atmospheric correction procedure for ocean color satellite sensors. It uses a nearest-neighbor method to propagate the aerosol type derived over adjacent clear water to apply over turbid water. The advantage of this procedure over an iterative approach is that the dependence on the under-water optics is minimized, therefore it can be applied to unknown type of water or shallow water where bottom reflection may contribute to the sensor signal. The procedure is particularly useful for turbid coastal or shallow inland waters

Errors in SeaWiFS products caused by cirrus clouds, high altitude aerosols, or digitization-noise were analyzed by Hu et al. (2000c). The use of an alternative band in the atmospheric correction to avoid the O2 absorption lines can greatly reduce the errors. It was also found that the SeaWiFS mission goals, namely to estimate water-leaving radiance to within 5% uncertainly and chlorophyll to within 35% can't always be achieved merely because of digitization round-off

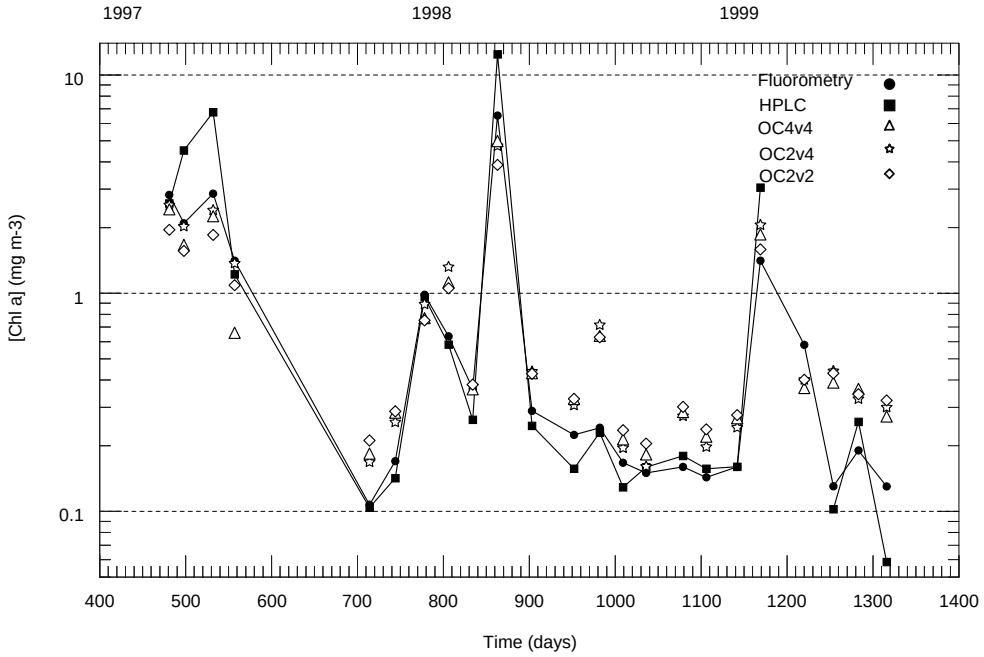

Temporal variation in [Chl a] at the CARIACO Station (Feb. 1997 - Jun. 1999). The values for fluorometry and HPLC were obtained at approximately 1 m depth while the values for the algorithms OC2v2, OC2v4, and OC4v4 were calculated from reflectance measurements above the surface.

Figure 15.2 Temporal variation in chlorophyll-a at the CARIACO station (February 1997-June 1999). The values for fluorometry and HPLC were obtained at approximately 1 m depth while the values for the OC algorithms were calculated from above-water reflectance measurements using O'Reilly et al. (2000)

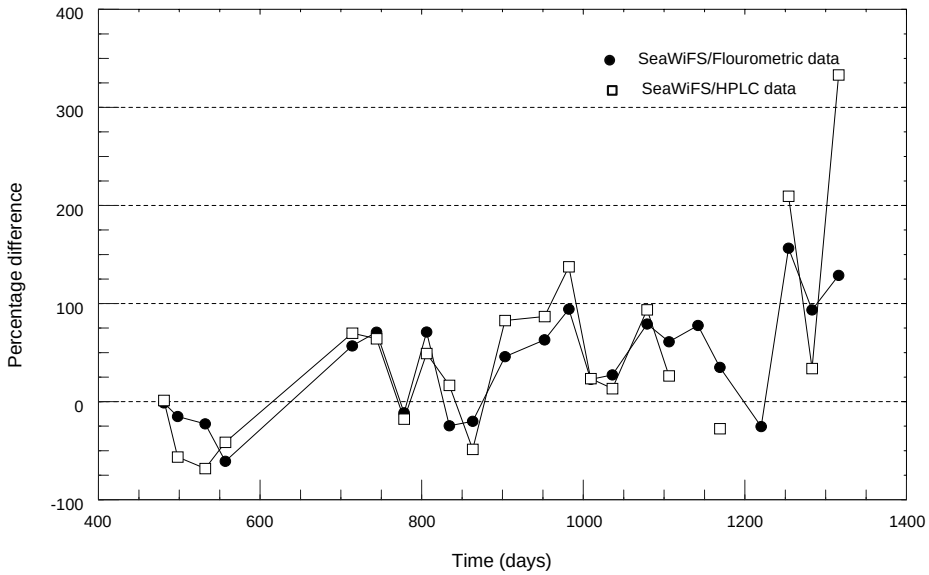

Percentage difference of [Chl a] derived from reflectance (OC4v4) with respect to in situ [Chl a] averaged over one optical depth for the CARIACO Station.

Figure 15.3 Temporal variation in the difference (%) between SeaWiFS-derived chlorophyll-a and in situ observations of chlorophyll-a at the CARIACO station (February 1997-June 1999).

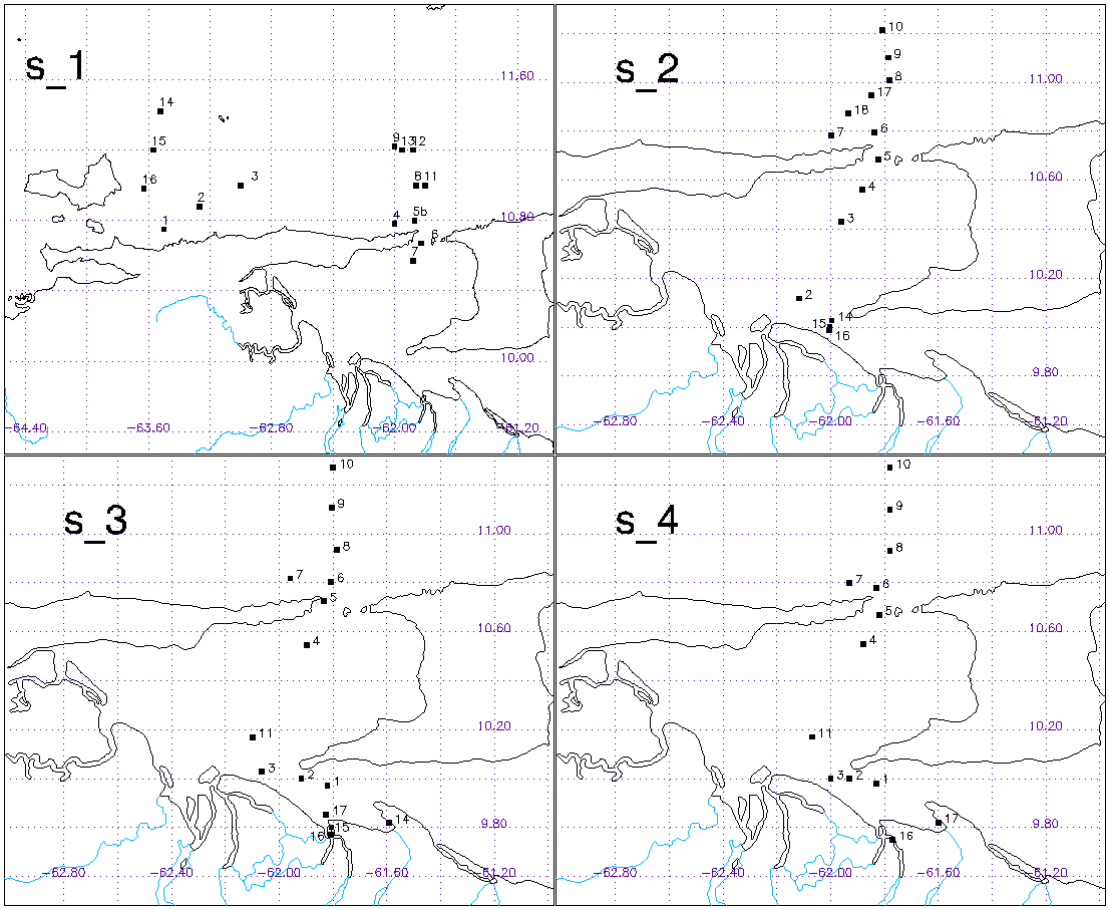

Figure 15.4 Cruise tracks for Orinoco Plume cruises 1-4, conducted 23-29 June, 1998 (S_1), 27-30 October, 1998 (S_2), 23-27 February, 1999 (S_3), and 26-31 October, 1999 (S_4).

and systematic noise. Use of an alternative band in the atmospheric correction or performing a 3x3 smoothing for the atmospheric-correction bands can greatly reduce this type of errors. The results are useful for data validation protocols.

We also developed and implemented a multi-platform approach for atmospheric correction of Landsat-like sensors using SeaWiFS/MODIS derived atmospheric parameters (Hu et al, 2000d). The procedure is useful for combining the high accuracy of atmospheric correction of ocean-color satellite and high spatial resolution of Landsat-like sensors to study coastal processes.

SeaWiFS data processing improvements

Our group implemented an extensive SeaWiFS batch processing system for use with IDL™and SeaDAS. We also implemented a series of convenient SeaWiFS data analysis tools based on IDL and IDL On the Net (ION™), to allow analyses over the world wide web.

We found several problems with SeaDAS and interacted with the SeaDAS Development Group to solve them. Specifically, we found bugs in the bL2map and histogram routines, as well as in the more recent implementation of selection menus for flag products, and pin-pointed a problem that led to a 'Windowing effect' in the level 2 processing of SeaWiFS data. Solutions were found for these problems.

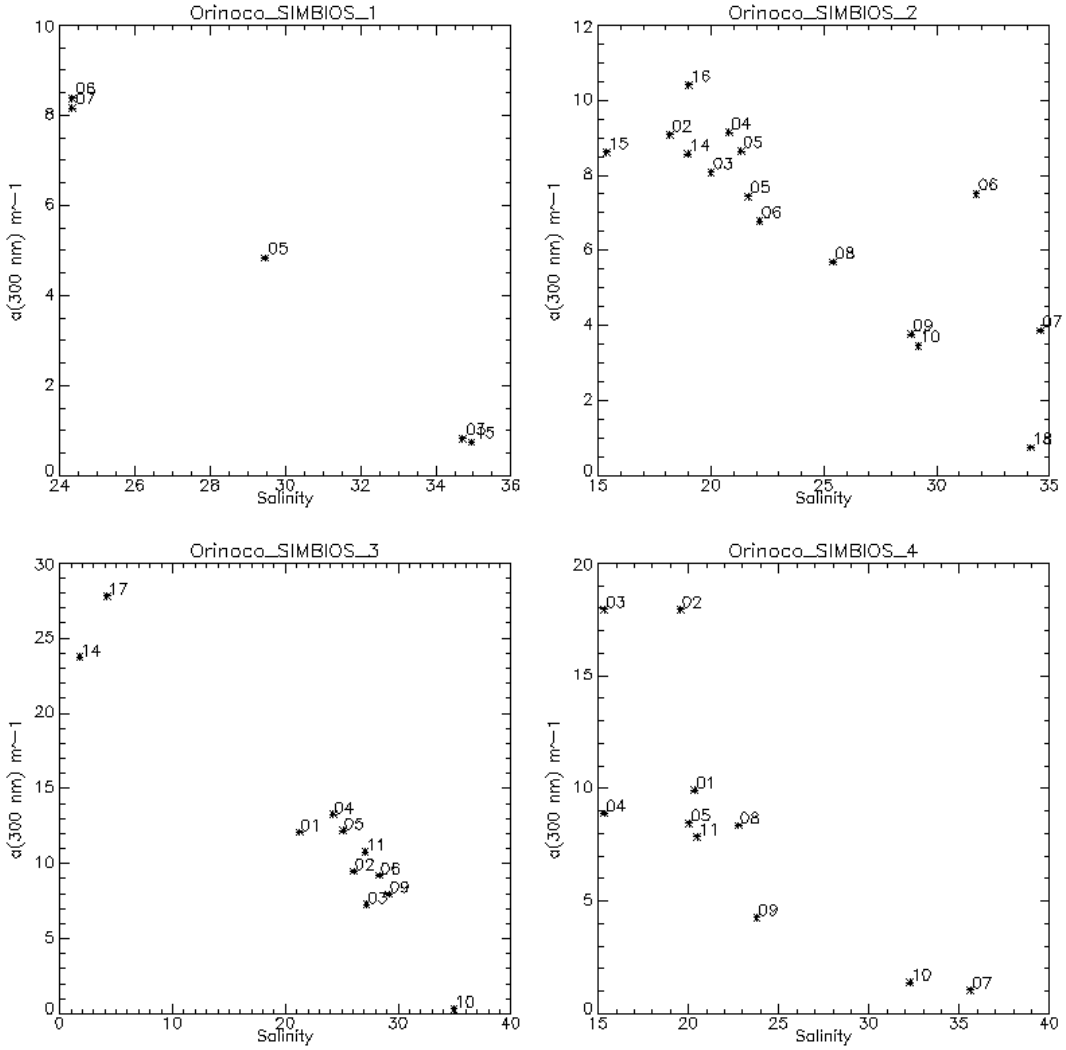

Figure 15.5. Relationship between the absorption coefficient for colored dissolved organic matter and salinity within the Orinoco Plume.

We also addressed the speckling problem found in processed SeaWiFS data. We suggested to Chuck McClain that a fine tune of the epsilon retrieval software may be necessary due to the high correlation between epsilon and chlorophyll.

Additional Field Campaigns and Data Validation

Participated in the Northeast Gulf of Mexico (NEGOM) program sponsored by the US Mineral Management Services. Eight 2-week cruises have been conducted in continental margin waters to the 1000-m isobath off Florida and Alabama. Extensive data sets were collected, among which included along-track flow-through chlorophyll and CDOM fluorescence, salinity and temperature, and sample collection and optical measurement at discrete stations (~50 for each cruise). Data analysis is still underway, while some preliminary results have been presented in a number of conferences and submitted to the International Journal of Remote Sensing.

Data Synthesis

We have generated an extensive list of publications based on our SIMBIOS and related research (see section labeled "Peer-Reviewed Publications" below. There will be additional publications based on the data collected via this SIMBIOS activity. The CARIACO station and Orinoco Plume data are central to the research of four graduate students, namely two Ph. D. and two Masters students.

ACKNOWLEDGEMENTS

This work was supported by the National Science Foundation (NSF Grant OCE 9216626), the National Aeronautics and Space Administration (NASA Grants NAG5-6448 and NAS5-97128), and the Consejo Nacional de Investigaciones Cientificas y Tecnologicas (CONICIT, Venezuela). Many other people have contributed substantially to the success of this program. We are indebted to the personnel of the Fundacion La Salle de Ciencias Naturales/Estacion de Investigaciones Marinas Isla Margarita (FLASA/EDIMAR) for their enthusiasm and professional support. In particular we thank FLASA's Director, Dr. Hermano Gines, for his confidence in our activities and the crew of the R/V Hermano Gines (FLASA) for their able support at sea. Field bio-optical measurements were conducted primarily by Natasha Rondon and John Akl of FLASA. They, and Yrene Astor and Ana Lucia Odriozola have processed the majority of the data to satisfy the seabass report formats. Jonathan Garcia (also at FLASA) has processed the samples for particulate and dissolved absorption coefficients. Juan Capelo and Javier Gutierrez (FLASA) have assisted with the primary production observations. Robert Thunell and Eric Tappa (U. South Carolina) maintain the sediment trapping program and process our particulate samples (POC, PON). Mary Scranton and Gordon Taylor (SUNY) conduct bacteria productivity studies. Dissolved Organic Carbon samples were processed by Ed Peltzer (formerly at the Woods Hole Oceanographic Institution and currently at the Monterrey Bay Aquarium Research Institute), and lately by David J. Hirschberg of State University of New York at Stony Brook.

REFERENCES

Hu, C., K. L. Carder, and F. E. Muller-Karger. 2000a: Atmospheric correction of SeaWIFS imagery over turbid coastal waters; a practical method. *Remote Sensing of Environment* **74**(2), 195-206.

Hu, C., K. L. Carder, and F. E. Muller-Karger. 2000b: Atmospheric correction of SeaWiFS imagery: assessment of the use of alternative bands. *Applied Optics*, **39**(21), 3573-3581.

Hu, C., K. L. Carder, F. E. Muller-Karger. 2000c: How precise are SeaWiFS ocean color estimates? Implications from digitization-noise errors. *Remote Sensing of Environment* (submitted)

Hu, C., K. L. Carder, and F. Muller-Karger. 2000d: A multi-platform approach to atmospheric correctionand calibration of LANDSAT-7/ETM= imagery over aquatic environments. *Remote Sensing of Environment.*, (Submitted)

Muller-Karger, F. E., C. R. McClain, T. R. Fisher, W. E. Esaias, and R. Varela. 1989: Pigment distribution in the Caribbean Sea: Observations from Space. *Progress in Oceanography*, **23**, 23-69.

Muller-Karger, F. E., and R. Varela. 1990: Influjo del Rio Orinoco en el Mar Caribe: observaciones con el CZCS desde el espacio. *Memoria. Sociedad de Ciencias Naturales La Salle. Caracas, Venezuela*. Tomo IL, numero **131-132**; Tomo L, numero **133-134**, 361-390.

Muller-Karger, F. E. 1999: Validation of Carbon Flux and Related Products for SIMBIOS: The CARIACO Continental Margin Time Series. SIMBIOS Project 1998 Annual Report. Edited by: C. R. McCLain and G. S. Fargion. NASA TM 1999-208645. Chapter 19. Pages 71-73.

Muller-Karger, F. E., C. Hu., and R. Varela. 1999: Validation of Carbon Flux and Related Products for SIMBIOS: The CARIACO Continental Margin Time Series and the Orinoco River Plume. SIMBIOS Project 1999 Annual Report. Edited by: C. R. McCLain and G. S. Fargion. NASA TM 1999-209486. Chapter 17. Pages 88-91.

Muller-Karger, F. E. R. Varela, R. Thunell, M. Scranton, R. Bohrer, G. Taylor, J. Capelo, Y. Astor, E. Tappa, T. Y. Ho, and J. J. Walsh. 2000a: The Annual Cycle of Primary Production in the Cariaco Basin: Implications for Vertical Export of Carbon Along a Continental Margin. *Journal of Geophysical Research*, (In press).

Muller-Karger, F., R. Varela, R. Thunell, M. Scranton, R. Bohrer, G. Taylor, J. Capelo, Y. Astor, E. Tappa, T.-Y. Ho, M. Iabichella, J. J. Walsh, and J. R. Diaz. 2000b: The CARIACO Project: Understanding the Link between the Ocean Surface and the Sinking Flux of Particulate Carbon in the Cariaco BasinEOS. *AGU Transactions*, (In press).

O'Reilly, J. E., S. Maritorena, B. G. Mitchell, D. A. Siegel, K. L. Carder, S. A. Garver, M. Kahru, and C. McClain. 1998: Ocean Color Chlorophyll Algorithms for SeaWiFS. *J. Geophys. Res.* **103** (C11), 24,937-24,953.

O'Reilly, J. E. and others. 2000: Ocean Chlorophyll-a Algorithms for SeaWiFS, OC2 and OC4: version 4. SeaWiFS Postlaunch Calibration and Validation Analyses, Part 3. Chapter 2. SeaWiFS Techinal Report. (Submitted).

Thunell, R., R. Varela, M. Llano, J. Collister, F. Muller-Karger, and R. Bohrer. 2000: Organic carbon flux in an anoxic water column: sediment trap results from the Cariaco Basin. *Limnology and Oceanography*. **45,** 300-308.

This research was supported by the

SIMBIOS NASA contract # 97128

PEER REVIEWED PUBLICATIONS

Del Castillo, C., F. Gilbes, P. Coble, and F. E. Muller-Karger. 2000: On the dispersal of riverine colored dissolved organic matter over the West Florida Shelf. *Limnology and Oceanography*. Vol. **45**, No. 6.

Hu, C., K. L. Carder, and F. E. Muller-Karger. 2000: Atmospheric correction of SeaWIFS imagery over turbid coastal waters; a practical method. *Remote Sensing of Environment*. **74**(2),195-206

Hu, C., K. L. Carder, and F. E. Muller-Karger. 2000: Atmospheric correction of SeaWiFS imagery: assessment of the use of alternative bands. *Applied Optics*, **39**(21),3573-3581.

Hu, C., K. L. Carder, and F. Muller-Karger. 1998: Preliminary algorithm to derive chlorophyll pigment concentration and DOM absorption in turbid coastal waters from SeaWiFS imagery. PORSEC Quingdao, China, Proceedings, 888-892.

Hu, C., K. L. Carder, and F. Muller-Karger. 2000: A multi-platform approach to atmospheric correctionand calibration of LANDSAT-7/ETM= imagery over aquatic environments. *Remote Sensing of Environment.* (Submitted).

Hu, C., K. L. Carder. 2000: Atmospheric correction of airborne sensors: comments on a scheme used for CASI. *Remote Sensing of Environment*. (Submitted).

Hu, C., K. L. Carder, F. E. Muller-Karger. 2000: How precise are SeaWiFS ocean color estimates? Implications from digitization-noise errors. *Remote Sensing of Environment,* (Submitted).

Hu, C., F. E. Muller-Karger, D. C. Biggs, K. L. Carder, B. Nababan, D. Nadeau, J. Vanderbloemen. 2000: Comparison of ship and satellite bio-optical measurements on the continental margin of the NE Gulf of Mexico. *International Journal of Remote Sensing*, (Submitted).

Hu,C. F. E. Muller-Karger, S. Andrefouet, K. L. Carder, 2000: A multi-platform approach to atmospheric correction and calibration of LANDSAT-7/ETM+ imagery over aquatic environments. *Remote Sensing of Environment*, (Submitted).

Melo Gonzalez, N.; Müller-Karger, F.E.; Cerdeira Estrada, S.; Pérez de los Reyes, R.; Victoria del Rio, I.; Cárdenas Perez, P.; Mitrani Arenal, I. 2000: Near-surface phytoplankton distribution in the western Intra-Americas Sea: The influence of El Niño and weather events. *Journal of Geophysical Research*, Vol. **105.** No. C6. 14029-14043.

Müller-Karger, F. E., and C. Fuentes-Yaco, 2000: Characteristics of Wind-Generated Rings in the eastern tropical Pacific Ocean. Journal of Geophysical Research. Vol 105. C1. 1271-1284.

Muller-Karger, F. E. 2000: The Spring 1998 NEGOM Cold Water Event: Remote Sensing Evidence for Upwelling and for Eastward Advection of Mississippi Water (or: How an Errant LC Anticyclone Took the NEGOM for a Spin*). Gulf of Mexico Science*, **1**. 55-67.

Muller-Karger, F. E. 2000: SMP workshop looks at role of continental margins in ocean carbon cycle. In*: U.S. JGOFS Newsletter*, Volume **10**, Number 4, 4-6.

Muller-Karger, F., R. Varela, R. Thunell, M. Scranton, R. Bohrer, G. Taylor, J. Capelo, Y. Astor, E. Tappa, T.-Y. Ho, M. Iabichella, J. J. Walsh, and J. R. Diaz, 2000: The CARIACO Project: Understanding the Link between the Ocean Surface and the Sinking Flux of Particulate Carbon in the Cariaco Basin. *EOS.* AGU Transactions. (In press)

Muller-Karger, F. E. R. Varela, R. Thunell, M. Scranton, R. Bohrer, G. Taylor, J. Capelo, Y. Astor, E. Tappa, T. Y. Ho, and J. J. Walsh, 2000: The Annual Cycle of Primary Production in the Cariaco Basin: Implications for Vertical Export of Carbon Along a Continental Margin. *Journal of Geophysical Research,* (In press)

Neumann, A., R. Doerffer, H. Krawczyk, M. Dowell, R. Arnone, C. Davis, M. Kishino, A. Tanaka, C. Hu, J. Campbell, and S. Sathyendranath, 2000: Algorithm for Case 2 waters", IOCCG. Remote sensing of ocean color in coastal, and other optically-complex, waters. Sathyendranath, S. (eds), *Reports of the International*

Ocean-Colour Coordinating Group, No. **3**, IOCCG, Dartmouth, Canada.

Perez, R., F. E. Muller-Karger, I. Victoria, N. Melo, S. Cerdeira. 1999: Cuban, Mexican, US Researchers Probing Mysteries of Yucatan Current. *EOS.* AGU Transactions. Volume **80,** No. 14, p. 153.

Perez, R., F. E. Muller-Karger, M. Merino, I. Victoria, N. Melo, S. Cerdeira. 1999: Cuban, Mexican, US researchers probing mysteries of Yucatan Current. *Earth In Space*. Vol. **12**, No. 1. p. 10-14.

Santamaría-del-Angel E., S. Alvarez-Borrego, R. Millan-Nuñez y F.E. Muller-Karger, 1999: On the weak effect of summer upwelling on the phytoplankton biomass of the Gulf of California. *Rev.Soc.Mex.Hist.Nat*., **49**, 207-212.

Thunell, R., R. Varela, M. Llano, J. Collister, F. Muller-Karger, and R. Bohrer. 2000: Organic carbon flux in an anoxic water column: sediment trap results from the Cariaco Basin. *Limnology and Oceanography*. **45**, 300-308.

Yao W., L.O. Hall, D.B. Goldgof, and F. Muller-Karger. 2000. Finding Green River in SeaWiFS Satellite Images. Proceedings of the International Conference on Pattern Recognition (ICPR'2000). September 3-8, 2000, Barcelona, Spain.

Zhang M., L. Hall, D. Goldgof, and F. E. Muller-Karger. 2000: Knowledge-guided Classification of Coastal Zone Color *International Journal of Pattern Recognition and Artificial Intelligence*, (In press).

Zhang, M., K. Carder, Z. Lee, F. E. Muller-Karger, and D. B. Goldgof. 1999: Noise Reduction and Atmospheric Correction for Coastal Applications of Landsat Thematic mapper Imagery. *Remote Sensing of the Environment*, **70**, 167-180.

Zhang, M., L. O. Hall, D. B. Goldgof, and F. E. Muller-Karger. 1997: Fuzzy Analysis of Satellite Images to Find Phytoplankton Blooms. *IEEE* International Conference on Systems, Man, and Cybernetics. Orlando, Florida.

Tang, D. L., I-H. Ni, D. R. Kester, and F. E. Müller-Karger, . 1999: Remote sensing observations of winter phytoplankton blooms southwest of the Luzon Strait in the South China Sea. *Marine Ecology Progress Series*, (in press).

Thunell, R. E. Tappa., R. Varela, M. Llano, Y. Astor, F. Muller-Karger, and R. Bohrer. 1999: Increased marine sediment suspension and fluxes following an earthquake. *Nature*, **398**, 233-236.

PRESENTATIONS

Carder, K., C. Hu, and A. Strub, 1999: Application of a semi-analytic SeaWiFS algorithm for chlorophyll-a and Gelbstoff, American Society of Limnology and Oceanography, Santa Fe, New Mexico.

Del Castillo, C. E., F. Gilbes, P. G. Coble, and F. E. Muller-Karger. 1998: Optical Characteristics of Dissolved Organic Matter During a Bloom on the West Florida Shelf. Ocean Optics. Hawaii.

Hu, C., K. L. Carder, and F. Muller-Karger, 1998: Preliminary algorith to derive chlorophyll pigment concentration and DOM absorption in turbid coastal waters from SeaWiFS imagery. PORSEC Quingdao, China, Proceedings, 888-892.

Hu, C., F. Muller-Karger, K. L. Carder, and Z. Lee, 1998: A method to derive optical properties over shallow waters using SeaWiFS. SPIE Meeting, Kona, Hawaii. Proceedings.

Hu, C., D. Biggs, D. Nadeau, and F. Muller-Karger, 1999: Riverine impact on the distribution of chlorophyll-a and colored dissolved organic matter (CDOM) in the Northeastern Gulf of Mexico (NEGOM), American Society of Limnology and Oceanography, Santa Fe, New Mexico.

Hu, C., K. L. Carder, F. E. Muller-Karger, 1999: Digitization errors in satellite ocean color data: implications based on SeaWiFS. *EOS*, Transactions, American Geophysical Union, **80**(49), 154.

Hu, C., F. E. Muller-Karger, D. C. Biggs, B. Nababan, D. Nadeau, 2000: Spatial and temporal variations of bio-optical properties in the Northeastern Gulf of Mexico: two year observations from ship and satellite, supplement to EOS, Transactions, *American Geophysical Union*, **80**(49), 33.

Perez, R., F. E. Muller-Karger, I. Victoria, N. Melo, S. Cerdeira. 1999. Cuban, Mexican, US Researchers Probing Mysteries of Yucatan Current. EOS. AGU Transactions. Volume **80**, No. 14, p. 153.

Chapter 16

The Bermuda Bio-Optics Program (BBOP)

David A. Siegel

ICESS, University of California at Santa Barbara, Santa Barbara, California

16.1 INTRODUCTION

The Bermuda BioOptics Project (BBOP) is a collaborative effort between the Institute for Computational Earth System Science (ICESS) at the University of California at Santa Barbara (UCSB) and the Bermuda Biological Station for Research (BBSR). This research program is designed to characterize light availability and utilization in the Sargasso Sea, and to provide an optical link by which biogeochemical observations may be used to evaluate bio-optical models for pigment concentration, primary production, and sinking particle fluxes from satellite-based ocean color sensors. The BBOP time-series was initiated in 1992, and is carried out in conjunction with the U.S. JGOFS Bermuda Atlantic Time-series Study (BATS) at the Bermuda Biological Station for Research. The BATS program itself has been observing biogeochemical processes (primary productivity, particle flux and elemental cycles) in the mesotrophic waters of the Sargasso Sea since 1988. Closely affiliated with BBOP and BATS is a separate NASA-funded study of the spatial variability of biogeochemical processes in the Sargasso Sea using high-resolution AVHRR and SeaWiFS data collected at Bermuda (N. Nelson, P.I.). The collaboration between BATS and BBOP measurements has resulted in a unique data set that addresses not only the SIMBIOS goals but also the broader issues of important factors controlling the carbon cycle.

16.2 RESEARCH ACTIVITIES

BBOP personnel participate on all BATS cruises, which are conducted monthly with additional cruises during the spring bloom period, January through May. Table 16.1 contains a list of data products collected by BBOP and/or BATS, which are relevant to SIMBIOS. The BBOP project collects continuous profiles of apparent optical properties (AOPs) in the upper 200m and deployments are planned to optimize match-ups with the BATS primary production incubations and with SeaWiFS overpasses. The primary optical measurements are downwelling vector irradiance and upwelling radiance, $E_d(z,t,\lambda)$ and $L_u(z,t,\lambda)$, respectively. Derived products include profiles of remote sensing reflectance ($R_{rs}(z,\lambda)$ and down- and upwelled attenuation coefficients ($K_d(z,\lambda)$, $K_u(z,\lambda)$), and are reported in near-real time with ~98% reliability. From 1992 until mid-2000, the primary profiling instrument has been a Biospherical MER2040 (sn8728/8733). Recently these were replaced by a free-falling Satlantic profiling radiometer system (SPMR/SMSR s/n 028) which is also UV-capable. The sampling package also includes a second mast-mounted radiometer with wavebands matching those on the underwater instrument for measuring incident downwelling vector irradiance, $E_d(0^+,t,\lambda)$.

In 1994, collection of bottle samples for fluorometric chlorophyll-*a* and inherent optical properties (IOPs) were added. Chlorophyll-*a* is collected once or twice daily during each cruise. Discrete samples for determining the absorption spectra of particulates, $a_{ph}(z,\lambda)$ and $a_d(z,\lambda)$, and CDOM ($a_g(z,\lambda)$) are collected according to Nelson *et al* (1998). Particulate absorption spectra are determined using the quantitative filter technique (Mitchell, 1990) and CDOM absorption according to Nelson et al (1998). Hyperspectral observations of above water $R_{rs}^{+}(\lambda)$ are collected using the Analytical Spectral Devices FieldSpec spectrometer (ASD, Boulder CO).

16.3 RESEARCH RESULTS

Careful attention to instrument behavior is crucial to assuring high quality time-series data, and the diversity of instruments used by BBOP during the past year has lead to new challenges in instrument calibration and intercomparison. To date, the largest source of calibration error that we have found is variability between individual calibration lamps and different calibration of the same lamp. Since the radiometers used in our projects have been remarkably stable, we have been able to observe the 1% variability between calibration lamps stated by the manufacturer (O'Brien *et al* in press). Thus, we have concluded that calibration coefficients are best calculated from a long-term average of several calibrations using several different lamps. Following the procedures that have proved fruitful with our Biospherical radiometers, we have embarked on a detailed description of the calibration behavior of our SPMR systems. Our recently purchased NIST-calibrated lamp should reduce inter-calibration variability by a significant amount. Our calibration facility regularly conducts informal comparisons between manufacturers' calibrations and our own and has achieved good agreement. For example, a recent check of the

calibration of a BBSR SPMR/SMSR (s/n 028) yielded results within 2% of the calibration done 3 months earlier by the manufacturer (D. Menzies, pers. comm.). In addition, the field comparisons between this Satlantic radiometer and MER 8728/8733 have been quite good (Fig. 16.1), even though these instruments were calibrated at different facilities.

The Sargasso Sea near Bermuda is mesotrophic, characterized by both eutrophic and oligotrophic conditions during different times of the year. Low chlorophyll-*a* stocks and primary production rates prevail for the most of the year, although there is a short spring bloom characterized by somewhat higher concentrations and rates. The accepted mechanisms of nutrient supply have accounted for less than half of the annual nutrient flux required to fuel these blooms. Using evidence from BATS-CTD surveys, moored instruments, satellite altimetry and eddy-resolving model simulations, Siegel, et al (1999) and McGillicuddy et al (1998) illustrated the importance of mesoscale eddies to new production in the Sargasso Sea. They demonstrated that eddy pumping and entrainment into the mixed layer during winter convection are the two dominant mechanisms transporting new nutrients into the euphotic zone at BATS. Smaller contributions are made by mixing in the thermocline and wind-driven transport, effectively balancing geochemical estimates of annual new production.

The problems associated with modeling integrated primary production and effective quantum yield (ϕ_c, mol C Ein^{-1}) in the Sargasso Sea have been illustrated using site-specific and previously published global models and a 6-year time series of BBOP and BATS data (Sorensen and Siegel in press, Siegel *et al* in press). The low predictive capability of published models using a variety of parameters demonstrates that we have yet to develop a predictive understanding of the important photophysiological, ecological and methodological processes controlling primary production. In addition, the assumptions of steady state and balanced growth required by production models are not easily met by the "snapshot" nature of optical or satellite measurements, and boundaries must be placed on how empirical models for integrated primary production are developed, validated and applied to satellite ocean color data sets. Although the values of ϕ_c were highly variable over time, few parameters correlated consistently and rationally with ϕ_c. One parameter with an interesting negative correlation was the concentration of photoprotective carotenoids and xanthophylls. The concentration of photoprotective carotenoids relative to chlorophyll is an indicator of phytoplankton species composition with implications for light absorption which may be related to systematic changes in ϕ_c values.

Phytoplankton fluorescence has been proposed as a means of assessing biomass and primary production rates in laboratory, *in situ*, and in satellite based investigations. A time series of the quantum yield of phytoplankton fluorescence (ϕ_f) from BBOP was used to predict depth-dependent and depth-integrated primary production rates (Westberry and Siegel, in prep). Preliminary results give fluorescence quantum yields (ϕ_f) similar to previous studies (1 to 5%), and ratios of ϕ_c/ϕ_f that vary from ~ 0 to 5 atoms carbon fixed per quanta fluoresced. The predictions of integrated primary productivity have been marginally successful (r^2 <= 50%), although they are comparable with results from global models for this region. Improvements have been hindered by weak statistical relationships with other physical and biological parameters. Seasonal variations in ϕ_f showed maximum values in the surface layer during summer months and lower, more uniform values throughout the winter when deep mixing occurs. Episodic changes in ϕ_f during the summer were associated with shoaling of isopycnals and may be attributed to the 'eddy pumping' mechanism. These results suggest that determinations of ϕ_f may be useful for assessing the nutritional status of phytoplankton populations.

The time-series of CDOM measurements (now in its sixth year) has revealed significant inter-annual fluctuations in the 'background' concentration of CDOM upon which the previously described annual cycle of CDOM is superimposed (Fig. 16.2, Nelson *et al.* 1998). Periods of low background CDOM concentration and high CDOM spectral slope appear to lag behind periods of high-salinity anomalies at the BATS site, which may suggest a role for CDOM as a semi-conservative tracer of surface water masses. This time series has also confirmed previous inferences made from BBOP AOP profiles (e.g. Siegel and Michaels 1996), including a seasonal time-scale for the bleaching rates of CDOM. Preliminary results of another collaborative study (NSF-funded) suggest that the higher concentration of CDOM in surface waters during winter and spring offsets the lower seasonal light availability relative to the summer, leading to similar summer/winter-spring photochemical reaction rates (Nelson and Carlson in prep). Our study of the sources and sinks of CDOM in the Sargasso Sea (also collaborative) suggests an important role for zooplankton and microbial community in the annual cycle of CDOM.

The importance of CD(O)M to light penetration the Sargasso Sea is also evident in the absorbance profiles collected with the WET Labs ac9 at the BATS station from 1994-1997 (Fig. 16.2, Brody *et al.* in prep). The seasonal patterns in absorbance observed with the ac9 were consistent with other optical descriptions of the Sargasso Sea (Siegel *et al* 1995b, Siegel and Michaels 1996, Nelson *et al* 1998). During the winters when the water column was well mixed, absorbance is approximately uniform throughout the water column. During periods of spring and summer stratification, values at the surface and at depth were lower (e.g. less than 0.01 m^{-1} at 440nm) and a seasonal maximum was observed near 100m. These maxima were coincident with chlorophyll peaks. The lower absorbance values at the surface during the summer have been observed in several studies, and have been hypothesized to be the result of decreased phytoplankton stocks after nutrient depletion or due to bleaching (Siegel and Michaels 1996, Nelson *et al* 1998). A weak exponential relationship existed between Chl-*a* and a_{440} in the surface layer

and near the chlorophyll max (r^2 = 0.58 and 0.50, respectively, n=248). Below 150m, published models did not fit the data at all, and usually underestimated observed absorbance. If the data were subsampled to include only data points in which CDM was known to be low and uniform (i.e., in the surface layer during winter-early spring), the fit could be improved to about 80%. During the fall, when absorbance by CDM has been observed to be highest (Nelson, *et al* 1998), the chlorophyll-based model underestimated absorbance throughout the water column. Our ac9 data set supports the suggestion that simple chlorophyll-based models are inappropriate for the open ocean, and leave the optical definition of Case I waters open to question.

REFERENCES

Brody, E.A., D.A. Siegel , M.C. O'Brien, S. Wolfe, J.R. Morrison and N.B. Nelson, in prep: Variability of *in situ* inherent optical properties in the Sargasso Sea. For Limnol. Oceanogr.

Mitchell, B.G., 1990: Algorithms for determining the absorption coefficient for aquatic particles using the quantitative filter technique. Ocean Optics X, Proceedings of S.P.I.E., **1302**, 137-142.

McGillicuddy Jr., D.J., A.R. Robinson, D.A. Siegel, H.W. Jannasch, R. Johnson, T.D. Dickey, J. McNeil, A.F. Michaels and A.H. Knap, 1998: Influence of mesoscale eddies on new production in the Sargasso Sea. *Nature*, **394**, 63-265.

Nelson N.B. and C. Carlson (in prep). Microbial production of chromophoric dissolved organic matter in the Sargasso Sea.

Nelson, N.B., D.A. Siegel, and A.F. Michaels, 1998: Seasonal dynamics of colored dissolved material in the Sargasso Sea, *Deep Sea Research I,* **45**, 931-957.

Siegel, D.A., E. Fields and D.J. McGillicuddy, Jr., 1999: Mesoscale motions, satellite altimetry and new production in the Sargasso Sea. *Journal of Geophysical Research*, **104**, 13359-13379.

Siegel, D.A., T.K. Westberry, M.C. O'Brien, N.B. Nelson, A.F. Michaels, J.R. Morrison, E.A. Caporelli, J.C. Sorensen, S.A. Garver, E.A. Brody, J. Ubante and M.A. Hammer, in press: The Bermuda BioOptics Project: Bio-optical modeling of primary production from space-sensible variables. In press Deep Sea Research II.

Sorensen J. and D.A Siegel, in press. Variability and models of the effective quantum yield of carbon assimilation in the Sargasso Sea. In press *Deep Sea Research II*.

Westberry TK. and D.A. Siegel (in prep). Solar-stimulated fluorescence and primary production in the Sargasso Sea.

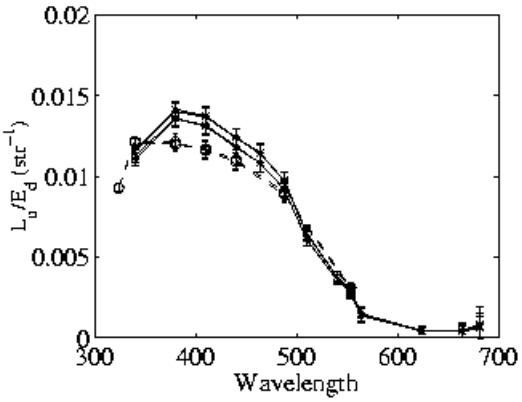

Figure 16.1 Comparison of average reflectance (L_u/E_d) in the top 20m from the BBOP Biospherical MER-2040 s/n 8733 (×), and the BBSR Satlantic SPMR s/n 028 (○), during February 2000.

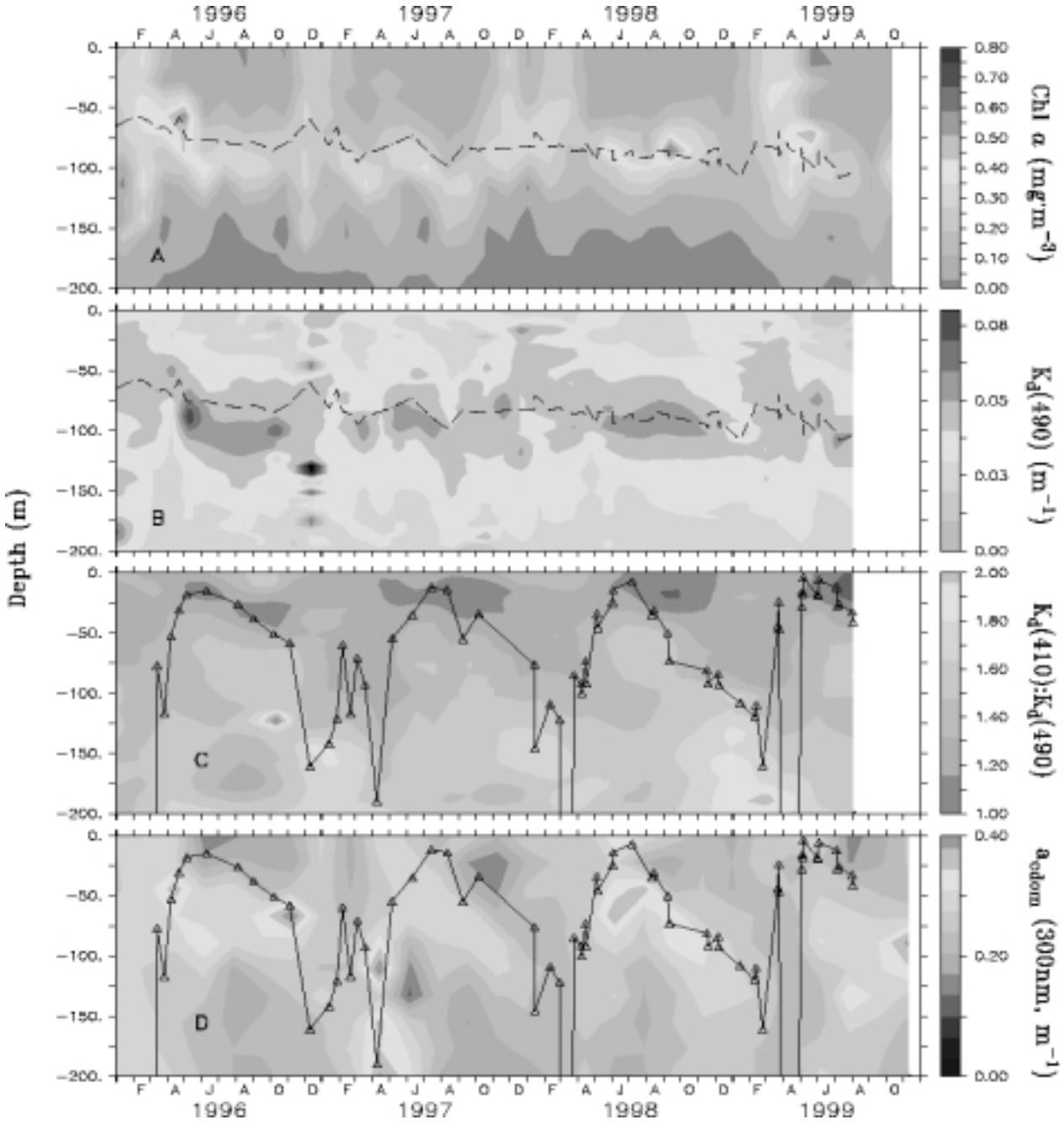

Figure 16.2 Bio-optical properties of the BATS site, 1996-1999. A: chlorophyll *a* concentration, showing the permanent subsurface chlorophyll maximum layer and the spring bloom, with depth of 1% light penetration (dotted line). B: Diffuse attenuation coefficient (K_d, m^{-1}) at 490 nm, an apparent optical property closely related to particulate light absorption, also with $Z_{1\%PAR}$ (note the similarity in distribution to chlorophyll *a*). C: Ratio of K_d(410 nm) to K_d(443 nm), highlighting the optical implications of changes in CDM (colored dissolved and detrital matter) distribution. D: Absorption coefficient of CDOM (colored dissolved organic matter, a subset of CDM) at 300 nm, from spectroscopic measurements of filtered seawater samples; panels C and D also show mixed-layer depth.

TABLE 16.1. A partial list of measurements made by BBOP & BATS

BBOP

Direct Measurements:

$E_d(z,\lambda)$	Downwelling vector irradiance (410,441,465,488,510,520,555,565,589,625,665 & 683 nm)
$E_d(0^+,\lambda)$	Incident irradiance (340,390,410,441,465,488,520,545,565,589,625,665 & 683 & 350-1050 nm)
$L_u(z,\lambda)$	Upwelling radiance (410,441,465,488,510,520,555,565,589,625,665 & 683 nm)
$a_{tp}(\lambda)$	Particulate absorption spectrum by QFT
$a_d(\lambda)$	Detrital particle absorption spectrum by MeOH extraction
$a_{ys}(\lambda)$	Colored dissolved absorption spectrum
$E_o(z,\lambda)$	Scalar irradiance at 441 and 488 nm
$F_f(z)$	Natural chlorophyll fluorescence using a broadband upwelled radiance sensor
chl-fl(z)	Chlorophyll fluorescence with a SeaTech fluorometer
c(z,660)	Beam attenuation coefficient at 660 nm with SeaTech 25 cm transmissometer
T(z) & S(z)	Temperature and conductivity with SeaBird probes
chl-a(z)	Discrete chlorophyll *a* determinations via Turner fluorometry (for next day delivery)

Primary Derived Products:

$L_{wN}(\lambda)$	Normalized water leaving radiance (410,441,465,488,510,520,555,565,589,625,665 & 683 nm)
$R_{RS}(0^-,\lambda)$	In-water remote sensing reflectance (410,441,465,488,510,520,555,565,589,625,665 & 683nm)
$R_{RS}(0^+,\lambda)$	Above-water remote sensing reflectance (350 to 1050 nm)
$a_{ph}(\lambda)$	Phytoplankton absorption spectrum (= $a_p(\lambda)$ - $a_{det}(\lambda)$)
$K_d(z,\lambda)$	Attenuation coefficient for $E_d(z,\lambda)$ (410,441,465,488,510,520,555,565,589,625,665 & 683 nm)
$K_L(z,\lambda)$	Attenuation coefficient for $L_u(z,\lambda)$ (410,441,465,488,510,520,555,565,589,625,665 & 683 nm)
<PAR(z)>	Daily mean photosynthetically available radiation at depths of the *in situ* C^{14} incubations
$b(z,\lambda)$	Spectral scattering coefficient (= $c(z,\lambda)$ - $a(z,\lambda)$)

U.S. JGOFS BATS (NSF) and Related Biogeochemistry Sampling Programs

Primary Production (*in situ* ^{14}C incubation)
Phytoplankton pigments (fluorometric & HPLC)
CO_2 system (alkalinity, TCO_2 and pCO_2)
Dissolved oxygen (continuous & discrete)
POC & PON (POP infrequently)
Full water column, WOCE-standard CTD profile
Phytoplankton abundance by flow cytometry
Validation spatial cruises (5 days, 4cruises/year)
Sinking flux (sediment trap array)
Nutrients (NO_3+NO_2, SiO_4, PO_4)
Continuous atmosphere & surface pCO_2
Zooplankton biomass & grazing
DOC & DON (DOP infrequently)
Bacterial abundance and rates
Coccolithophore abundance
Deep ocean sediment sinking rates

This research was supported by the

SIMBIOS NASA contract # 97125

PEER REVIEWED PUBLICATIONS

Dickey, T., S. Zedler, D. Frye, H. Jannasch, D. Manov, D. Sigurdson, J. D. McNeil, L. Dobeck, X. Yu, T. Gilboy, C. Bravo, S. C. Doney, D.A. Siegel and N. Nelson: Physical and biogeochemical variability from hours to years at the Bermuda Testbed Mooring: June 1994 - March 1998. *Deep Sea Research, Part II.*

Dickey, T., D. Frye, J. McNeil, D. Manov, N. Nelson, D. Sigurdson, H. Jannasch, D. Siegel, T. Michaels and R. Johnson, 1998: Upper ocean response to Hurricane Felix as measured by the Bermuda Testbed Mooring. Monthly *Weather Review,* **126**, *1195-1201.*

Dickey, T., D. Frye, H. Jannasch, E. Boyle, D. Manov, D. Sigurdson, J. McNeil, M. Stramska, T. Michaels, N. Nelson, D. Siegel, G. Chang and J. Woo, 1998: Preliminary results from the Bermuda testbed mooring program. *Deep Sea Research* I, **45**, 771-794.

Garver, S.A., and D.A. Siegel, 1997: Inherent optical property inversion of ocean color spectra and its biogeochemical interpretation: I. Time series from the Sargasso Sea. *Journal of Geophysical Research*., **102**, 18,607-18,625.

McGillicuddy, Jr., D.J., A.R. Robinson, D.A. Siegel, H.W. Jannasch, R. Johnson, T.D. Dickey, J. McNeil, A.F. Michaels and A.H. Knap, 1998: Influence of mesoscale eddies on new production in the Sargasso Sea. *Nature*, **394**, 263-265.

McGillicuddy, Jr., D.J., R.J. Johnson, D.A. Siegel, A.F. Michaels, N. Bates and A.H. Knap, 1999: Mesoscale variability of ocean biogeochemistry in the Sargasso Sea. *Journal of Geophysical Research*, **104**, 13381-13394.

Nelson, N.B., D.A. Siegel, and A.F. Michaels, 1998: Seasonal dynamics of colored dissolved material in the Sargasso Sea. *Deep Sea Research* I, **45**, 931-957.

Nelson, N.B., N.R. Bates, D.A. Siegel, and A.F. Michaels; Spatial variability of the CO_2 sink in the Sargasso Sea. *Deep-Sea Research, Part II*.

O'Reilly, J.J., S. Maritorena, D.A. Siegel et al: Ocean Color Chlorophyll *a* Algorithms for SeaWiFS,OC2 and OC4: Version 4. NASA Tech. Memo., SeaWiFS Postlaunch Calibration and Validation Analyses, Vol. 3, Chap. 2.

O'Reilly, J., S. Maritorena, B.G. Mitchell, D.A. Siegel, K.L. Carder, M. Kahru, S.A. Garver, C.R. McClain, 1998: Ocean color algorithms for SeaWiFS. *Journal of Geophysical Research*, 103, 24,937-24,953.

Siegel, D.A, and W.G. Deuser, 1997: Trajectories of sinking particles in the Sargasso Sea: Modeling of statistical funnels above deep-ocean sediment traps. *Deep-Sea Research, I* , 44, 1,519-1,541.

Siegel, D.A., E. Fields and D.J. McGillicuddy, Jr., 1999: Mesoscale motions, satellite altimetry and new production in the Sargasso Sea. *Journal of Geophysical Research*, **104**, 13359-13379.

Accepted

Sorensen, J.C., and D.A. Siegel, 1999: Variability and models of the effective quantum yield of carbon assimilation in the Sargasso Sea, Accepted for publication in *Deep Sea Research, II.*

Submitted

Behrenfeld, M.J., E. Marañon, D.A. Siegel and S.B. Hooker: Modeling oceanic primary production: Photoacclimation and nutrient effects on light-saturated photosynthesis. Submitted to Limnology and Oceanography.

Siegel, D.A., S. Maritorena, N.B. Nelson, D.A., Hansell and M. Lorenzi-Kayser. Global Distribution of Colored Dissolved Organic Matter. Submitted to Global Biogeochemical Cycles.

Toole, D.A., D.A. Siegel, D.W. Menzies, M.J. Neumann and R.C. Smith, 1999: Remote sensing reflectance determinations in coastal environments - Impacts of instrumental characteristics and environmental variability. In review in *Applied Optics*.

Siegel, D.A., M.C. O'Brien, T.K. Westberry, N.B. Nelson, A.F. Michaels, J.R. Morrison, E.A. Caporelli, J.C. Sorensen, S.A. Garver, E.A. Brody, J. Ubante and M.A. Hammer, 1999: The Bermuda BioOptics Project: Bio-optical modeling of primary production from space-sensible variables. Submitted to *Deep Sea Research, II*.

Siegel, D.A., D.M. Karl and A.F. Michaels: Interpretations of biogeochemical processes from the U.S. JGOFS Bermuda and Hawaii time series sites. *Deep-Sea Research, Part II*.

Siegel, D.A., T.K. Westberry, M.C. O'Brien, N.B. Nelson, A.F. Michaels, J.R. Morrison, A. Scott, E.A. Caporelli, J.C. Sorensen, S. Maritorena, S.A. Garver, E.A. Brody, J. Ubante & M.A. Hammer: Bio-Optical Modeling of Primary Production on Regional Scales: The Bermuda BioOptics Project. *Deep-Sea Research, Part II*.

Siegel, D.A., M. Wang, S. Maritorena and W. Robinson. 2000. Atmospheric correction of satellite ocean color imagery: the black pixel assumption. Applied Optics, 39, 3582-2591.

OTHER PUBLICATIONS

O'Brien, M.C., D.W. Menzies, D.A. Siegel and R.C. Smith, 1999, Calibration History of Several Marine Environmental Radiometers. SeaWiFS Post Launch Technical Report Series, NASA Tech. Memo. 1999-206892. In press.

PRESENTATIONS

Brody, E.A., D.A. Siegel, M.C. O'Brien, E.A. Caporelli and N.B. Nelson. 1997: Temporal patterns of IOPs in the Sargasso Sea. Presented at the 1997 ALSO Aquatic Sciences Meeting. Sante Fe.

Fields, E.A., D.A. Siegel and D.J. McGillicuddy, 1998: Mesoscale motions, satellite altimetry and biogeochemical processes in the Sargasso Sea. Presented at the AGU Ocean Sciences Meeting. San Diego, *Trans. Amer, Geophys. Union, Eos*, **79**, no. 1, OS22D-9.

Garver, S.A., and D.A. Siegel, 1997: Global Application of a nonlinear inherent optical property inversion model. Presented at the 1997 ALSO Aquatic Sciences Meeting. Sante Fe.

Michaels, A.F., D.A. Siegel, R. Johnson, N. Nelson, N. Bates and A. Knap, 1998: Hydrostation S, the Bermuda Atlantic Time-series Study and decadal variability in the Sargasso Sea. Presented at the AGU Ocean Sciences Meeting. San Diego. *Trans. Amer, Geophys. Union, Eos*, **79**, no. 1, OS21I-4.

Nelson, N.B., C.A. Carlson, N.L. Krupp, and D.A. Siegel, 1997: Dynamics of chromophoric dissolved organic material (CDOM) in the Sargasso Sea. Presented at the 1997 ALSO Aquatic Sciences Meeting. Sante Fe.

Nelson, N.B., D.A. Siegel and J.A. Yoder, 2000: The spring bloom in the Sargasso Sea: Spatial pattern and relationship to winter mixing Talk and abstract presented at the 2000 AGU Ocean Sciences Meeting (OS12M-10), January 2000, San Antonio TX.

O'Brien, M.C., D. Menzies, D.A. Siegel and R.C. Smith, 1998: Long-term calibration history of several marine environmental radiometers. Presented at the AGU Ocean Sciences Meeting. San Diego.. *Trans. Amer, Geophys. Union, Eos*, 79, no. 1, OS32A-2.

Peterson, A.R, D.A. Siegel, S.A. Maritorena and S.A. Garver, 1999: Optimal tuning of semi-analytical ocean color algorithms for the global ocean. Presented at the 1999 ASLO Aquatic Sciences Meeting, Sante Fe.

Scott, A. J. and N.B. Nelson, 2000: Light energy available for photochemistry in the Sargasso Sea, August 1999. Poster presented at the 2000 AGU Ocean Sciences Meeting (OS31A-11), January 2000, San Antonio TX.

Shih ,A.S., D.A. Siegel, N.B. Nelson, M.C. O'Brien and S.A. Garver, 1998: Modeling of optical property characteristics: Analyses of observations from the Sargasso Sea. Presented at the AGU Ocean Sciences Meeting. San Diego, *Trans. Amer, Geophys. Union, Eos*, 79, no. 1, OS12B-9.

Siegel, D.A, E. Fields, D.J. McGillicuddy and A.F. Michaels, 1997: Mesoscale motions, satellite altimetry and biogeochemical processes in the Sargasso Sea. Presented at the 1997 ALSO Aquatic Sciences Meeting, Sante Fe.

Siegel, D.A., 1998: Spectral data assimilation for merging satellite ocean color imagery, Presented at the Ocean Optics XIV Meeting, Kona HI.

Siegel, D.A., 1999: Orthothogonal views of the global ocean biosphere using SeaWiFS. Presented at the 1999 ASLO Aquatic Sciences Meeting, Sante Fe.

Siegel, D.A., M. Lorenzi-Kaiser, and S. Maritorena, 1999: Alternative views of the global ocean biosphere using SeaWiFS. Opening Science Address, SeaWiFS Science Team Meeting, Moss Landing, CA, May 1999.

Siegel, D., J. Yoder, S. Doney, N. Nelson, M. Kennelly, M. Lorenzi-Kaiser, 1999: Satellite Views of the North Atlantic Spring Bloom, To be presented at 1999 AGU Fall Meeting.

Westberry, T.K., D.A. Siegel, N.B. Nelson and M.C. O'Brien, 1999: Regional modeling of primary production in the Sargasso Sea. Presented at the 1999 ASLO Aquatic Sciences Meeting, Sante Fe.

Westberry, T.K., D.A. Siegel, 2000: Solar-stimulated fluorescence variability in the Sargasso Sea. Poster and abstract presented at the 2000 AGU Ocean Sciences Meeting (OS22B-02), January 2000, San Antonio TX.

Chapter 17

Spectral Data Assimilation for Merging Satellite Ocean Color Imagery

David A. Siegel and Stéphane Maritorena

ICESS, University of California at Santa Barbara, Santa Barbara, California

17.1 INTRODUCTION

The Sensor Intercomparison and Merger for Biological and Interdisciplinary Oceanic Studies (SIMBIOS) project was initiated "to develop a methodology and operational capability to combine data products from various ocean color missions in a manner that ensures the best possible global coverage and best exploits the complementary missions of the sensors" (GSFC ocean color group, 1995). While the merging of data from multiple sources has already been implemented for SST (e.g. Reynolds & Smith, 1994), altimetry (e.g. Le Traon & Ogor, 1998) or clouds (Rossow & Schiffer, 1991), this is a new topic in ocean color science.

Merging ocean color data has obvious advantage in terms of spatial and temporal coverage of the global ocean (see Gregg et al., 1998; Gregg and Woodward, 1998) but data merging should also result in new, more diverse and improved data products with lower uncertainties. The merging of ocean color satellite data is generally considered at the level of the global gridded products, i.e. NASA Level-3 (IOCCG, 1999) and, more specifically, for the merging of chlorophyll *a* concentration data, [Chl]. This approach limits computational issues and deals with a unique, simple quantity, [Chl].

However, ocean color data merging can also be conducted at the level of water-leaving radiances, $L_{wN}(\lambda)$, using either empirical or semi-analytical algorithms. Although more challenging, this latter approach is potentially extremely powerful as it can achieve good consistency in the final data products and can take advantage of both the specificities and differences of each source of data. The demonstration of the feasibility of such approach is the main objective of our SIMBIOS work.

Here, we use a semi-analytical algorithm (Garver & Siegel, 1997; Maritorena et al., 2000) to merge Rrs (or, equivalently, L_{wN}) data from different sources to estimate [Chl]. The model also allows for the retrieval of other quantities such as the combined absorption of colored detrital particulate and dissolved organic matter at 443 nm, $a_{cdm}(443)$ and the particulate backscattering, $b_{bp}(443)$.

The model is designed to deal with the uncertainties associated with each source of input data and to allow the calculation of uncertainty estimates of the retrieved products. Examples are illustrated using the SeaWiFS matchup data set (Bailey et al., 2000). An example of the benefit of using data sources with different wavebands is also presented.

17.2 RESEARCH ACTIVITIES

The UCSB IOP Inversion Model for Ocean Color

Over the past years, our group has developed and validated a semi-analytical, inherent optical property (IOP) inversion model for ocean color that can be applied to satellite ocean color data (Garver and Siegel, 1997; Maritorena et al., 2000). The functional relationship between $L_{wN}(\lambda)$ and the backscattering to absorption ratio is taken from Gordon *et al.* (1988) and the IOP spectra, $a(\lambda)$ and $b_b(\lambda)$, are partitioned into relevant components of seawater backscatter, $b_{bw}(\lambda)$ and absorption, $a_w(\lambda)$, particulate backscatter, $b_{bp}(\lambda)$, phytoplankton absorption. $a_{ph}(\lambda)$, and the combined of dissolved and detrital particulate absorption coefficients, $a_{cdm}(\lambda)$. Values of $b_{bw}(\lambda)$ and $a_w(\lambda)$ are assumed to be known (e.g., Smith and Baker, 1981; Pope and Fry, 1997).

The contributions to total absorption by detrital particulates and dissolved materials are lumped together into a single term, $a_{cdm}(\lambda)$, as these factors are essentially indistinguishable (Carder *et al.*, 1991, Nelson *et al.*, 1998). Each of the non-water terms are parameterized as a constant spectral shape scaled by an unknown magnitude. These magnitudes, namely the chlorophyll *a* concentration ([Chl]), the CDM absorption coefficient ($a_{cdm}(\lambda_o)$), and the particulate backscatter coefficient (b_{bp} (λ_o)), for $a_{ph}(\lambda)$, $a_{cdm}(\lambda)$, and $b_{bp}(\lambda)$ respectively, are the unknowns in the model. The reference wavelength (λ_o) is 443 nm. A complete formulation of the model is as follows:

$$\hat{L}_{wN}(\lambda) = \frac{t\,F_0}{m^2} \sum_{i=1}^{2} gi \left(\frac{b_{bw}(\lambda) + b_{bp}(\lambda_0)(\lambda/\lambda_0)^{-n}}{b_{bw}(\lambda) + b_{bp}(\lambda_0)(\lambda/\lambda_0)^{-n} + a_w(\lambda) + [Chl]a^*_{ph}(\lambda,[Chl]) + a_{cdm}(\lambda_0)\exp(-S(\lambda-\lambda_0))} \right)^i \quad (17.1)$$

where S is the spectral decay constant for CDM absorption (Bricaud *et al*. 1981, Green & Blough, 1994), n is power law exponent for particulate backscattering coefficient, t is the sea-air transmission factor, F_0 is the extraterrestrial solar irradiance and m is the index of refraction of the water. By determining $L_{wN}(\lambda)$ (or $Rrs(\lambda)$) for more than 3 wavelengths, non-linear least-squares techniques can be used to solve for the unknowns in equation (17.1). For later purposes, the equation 19.1 can be stated as $\hat{L}_{wN}(\lambda;\mathbf{\Theta};\mathbf{\Psi})$ where $\mathbf{\Theta}$ is the vector for the retrieved parameters ($\mathbf{\Theta}$ = [[Chl], $a_{cdm}(\lambda_O)$ and $b_{bp}(\lambda_O)$), $\mathbf{\Psi}$ is the vector of the model parameters ($\mathbf{\Psi}$ = [a^*_p $h(\lambda_1)$ ... a^*_p $h(\lambda_N)$ S n]). The parameters to retrieve, $\mathbf{\Theta}$, are obtained by minimizing a cost function we defined to be the mean square difference between modeled and measured data, or

$$CF = \frac{1}{(N\lambda - 1)} \sum_{i=1}^{N\lambda} [\hat{L}_{wN}(\lambda_i;\mathbf{\Theta};\mathbf{\Psi}) - L_{wN}(\lambda_i)]^2 \quad (17.2)$$

where $N\lambda$ is the number of wavelengths available and $L_{wN}(\lambda_i)$ is the measured normalized water-leaving radiance for wavelength i. For the merging of data from several sources, the cost function can be summed over the various data sources (see below). Several numerical methods exist to solve eq. 17.1 using the cost function in eq. 17.2. In its present state, the model uses a nonlinear Levenberg-Marquardt fitting procedure. One advantage of this method is that it can take into account the uncertainties associated with the data injected in the model.

Global Optimization of the UCSB IOP Inversion Model Using Simulated Annealing

In its initial development, the various terms forming a and b_b in the UCSB model were based on formulations and coefficients taken from the literature. These initial versions of the model were reasonably good but, as revealed during SeaBAM (O'Reilly et al., 1998), they were not performing as well as some other models or empirical algorithms. Improving the overall performance of the UCSB IOP model was thus a necessary step before it could be used for data merging. For this purpose, we have developed a procedure based on the simulated annealing technique (Press *et al*., 1992) that optimizes the vector of parameters, $\mathbf{\Psi}$, in the UCSB IOP model so it returns the best possible retrievals under most situations. This is not a trivial task because of the high non-linearity of model (eq. 17.1) and the large number of (potentially interacting) parameters for which optimal values need to be determined. The method has first been tested successfully on synthetic data (Peterson *et al*., 1999). We have then developed a "semi-real" data set (i.e. actual [Chl] and Rrs measurements and theoretically derived $a_{cdm}(443)$ and $b_{bp}(443)$ using an "improved" version of the SeaBAM data containing diffuse attenuation coefficient data (K_d)) which we used in the optimization procedure. The [Chl] retrievals generated by the model after the optimization are excellent (Maritorena *et al*., 2000), with performance as good as those of the SeaWiFS operational algorithm (Figure 17.1).

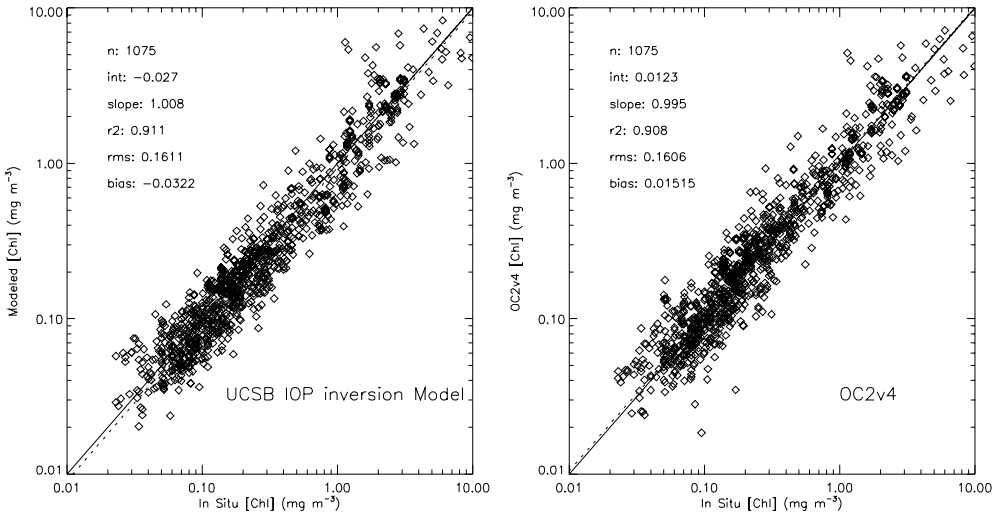

Figure 17.1 Chlorophyll retrievals using an "improved" SeaBAM data set. Left panel : [Chl] retrievals using the optimized UCSB IOP inversion model as a function of in situ [Chl]. Right panel: [Chl]retrievals using OC2v4 algorithm.

Results for the other retrieved variables ($a_{cdm}(443)$ and $b_{bp}(443)$) are also very good although these results still need to be fully validated against actual in situ measurements.

The SeaWiFS Matchup Data Set

To develop, test and demonstrate the feasibility of our approach for data merging, we used the SeaWiFS matchup data set which is assembled and maintained by the SeaWiFS project (Bailey et al., 2000). This data set contains nearly simultaneous in situ and SeaWiFS measurements at the same location. The data set we used contains 126 stations from various optical provinces and chlorophyll concentrations ranging from ~0.04 to ~5 mg m^{-3}. Figure 17.2a shows the [Chl] retrievals from the UCSB IOP model when using the SeaWiFS Rrs data from the matchup data set. While most of the points are reasonably close to the 1:1 line several of them are strongly underestimated by the model. For some stations, the model returned either a negative [Chl] or failed to converge during the non-linear fitting process. These low estimates and failures are likely a consequence of the sensitivity of the model to any kind of "noise" in the data, and particularly in the short wavelengths bands. Sensitivity to noise is a typical problem with semi-analytical algorithms. Data merging along with the weighting of the data according to their estimated level of uncertainty, can correct for these problems.

Merging the In-situ Data and SeaWiFS Data.

Whether the UCSB IOP model uses one or several sources of data, it solves for the unknowns by minimizing, in the nonlinear fit, the cost function described in eq. 17.2. Under this simple scheme, the in situ and SeaWiFS data from the matchup set can be used together, as input to the model. The results of this in situ and SeaWiFS data merging are illustrated in figure 17.2b. Compared to the results with the SeaWiFS data alone (fig. 17.2a), the statistical results are clearly improved (better slope, better R^2, smaller bias) with the merged data. Data merging also results in fewer negative or non-converging retrievals (1 over 126 stations) but for the sake of comparison with non-merged data these new points were not included in the analysis.

With the merged data, the statistical results are clearly better (better slope, better R^2, smaller bias, higher number of stations successfully processed) than with the SeaWiFS data alone. In this example, both sources of data were given the same weight in the merging process, that is each source of data had a similar influence in the minimization of the cost function. This approach is fine when the uncertainties associated with each of the data sources are of the same order of magnitude. In other cases, a weighting of the input data is recommended.

Weighting of the Input Data by their Uncertainty Level

The cost function used in the UCSB IOP model (eq. 17.2) can actually account for the uncertainties associated with the input data by dividing the difference between model and observed quantities by the uncertainty estimate for the observation (e.g., Press *et al*. 1992), as

$$CF = \sum_{i=1}^{N_{sat}} \sum_{j=1}^{N_{\lambda\text{-}i}} \left(\frac{\hat{L}_{wN}(\lambda_j, \Theta, \Psi) - L_{wN\text{-}i}(\lambda_j)}{\sigma_i(\lambda_j)} \right)^2 \qquad (17.3)$$

where $N_{\lambda i}$ are the number of wavebands for data source i, N_{sat} is the number of observing platforms providing data, $L_{wN\text{-}i}(\lambda_j)$ is the observed L_{wN} for band j of data source i, $\hat{L}_{wN}(\lambda;\Theta;\Psi)$ is the modeled L_{wN} and $\sigma_i(\lambda_j)$ is the uncertainty level for band j from source i. The uncertainty weighting in equation 3 insures that the best observations have a higher weight in the inversion for the retrieval vector, $\hat{\theta}$.

Following the work of Hooker & Maritorena (2000), the level of uncertainty for in situ data should be close to 5% for the the visible bands. Assuming a 20% uncertainty in Rrs in each of the SeaWiFS visible bands leads to the [Chl] retrievals presented in figure 19.3. The overall benefit of the weighting by the uncertainty level is obvious with an improvement of all statistics.

In the case study presented here, the uncertainties in the input data were set to the same value for all the wavebands (and all the stations) of a particular data source but each band and each station can actually handle specific settings. For example, at short wavelengths in satellite data (e.g. the 412 nm band) where perturbation from atmospheric correction can be important (see e.g. Siegel et al., 2000), it is reasonable to assume a larger level of uncertainty than in other bands and thus to limit the influence of these perturbations in the inversion of the model. Assessing the level of uncertainty for each band of a specific spaceborne sensor is not a straightforward problem. Vicarious calibrations and intercomparison studies conducted in the frame of the SIMBIOS Project will likely provide the necessary information on the accuracy of the sensors bands.

Uncertainties in Data Products

The UCSB IOP inversion model provides uncertainty estimates for its outputs using a linear approximation to the calculation of non-linear regression inference regions (Bates & Watts, 1988).

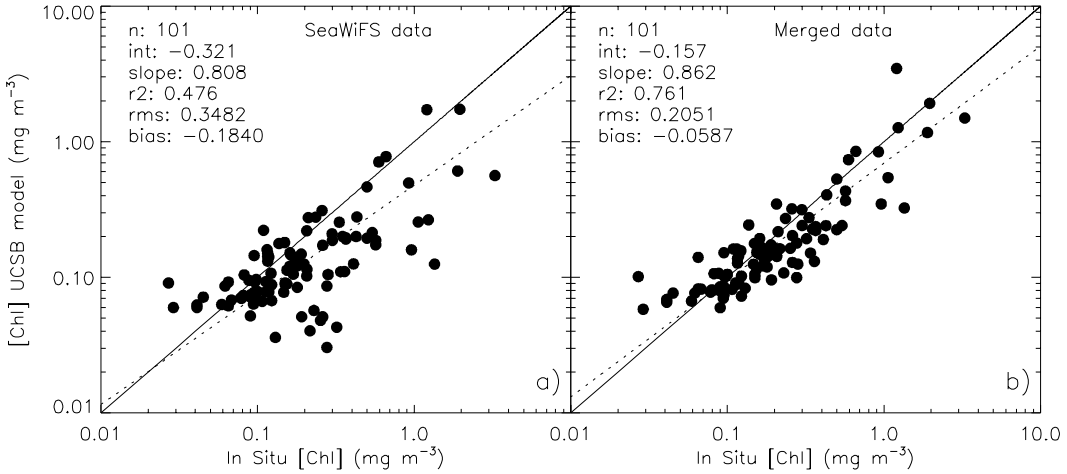

Figure 17.2. (a) Chlorophyll retrievals using the UCSB IOP model with the SeaWIFS data from the matchup data set as a function of in situ [Chl]. The 1:1 (solid) and regression (dotted) lines are also plotted. (b) Chlorophyll retrievals from the UCSB IOP model using both the SeaWIFS and in situ Rrs data from the matchup data set as a function of in situ [Chl].

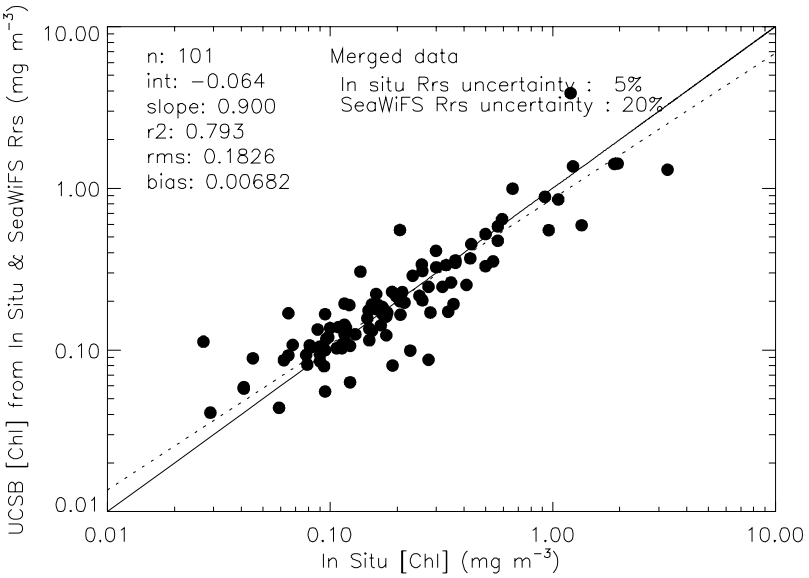

Figure 17.3. [Chl] retrievals from the UCSB IOP model using both SeaWiFS and in situ Rrs data with assumed levels of uncertainty of 20% and 5%, respectively. The 1:1 (solid) and regression (dotted) lines are also plotted.

This approach can also be used when merging data. The standard error for each estimate is given by the square root of the total mean square error between observed Rrs and modeled Rrs (using the retrieved IOPs, i.e. forward model) multiplied by the corresponding diagonal element of the inverted Z matrix where Z = transpose(V)*V and V is the matrix of partial derivatives of the UCSB IOP model for the wavelengths of a particular Rrs spectrum. In the linear approximation, this latter term corresponds to the ratio of the parameter plane area to that of the expectation plane (Bates and Watts, 1988) :

$$se(i) = \sqrt{mse * inverse(transpose(V) * V)[i, i]}$$

Uncertainties (standard errors) in [Chl] retrievals are plotted on figure 17.4a when using the SeaWiFS data alone and the same stations are plotted when merged with in situ data (fig. 17.4b; assuming a 5% uncertainty at all wavelengths

for in situ Rrs data and 20% for SeaWIFS). In Figure 17.4a, uncertainties are generally large, sometimes of same order of magnitude (or larger !) than the estimated [Chl]. Uncertainties are much reduced with the merged data although a few stations (6 over 101) still show high levels of uncertainty in their estimated [Chl].

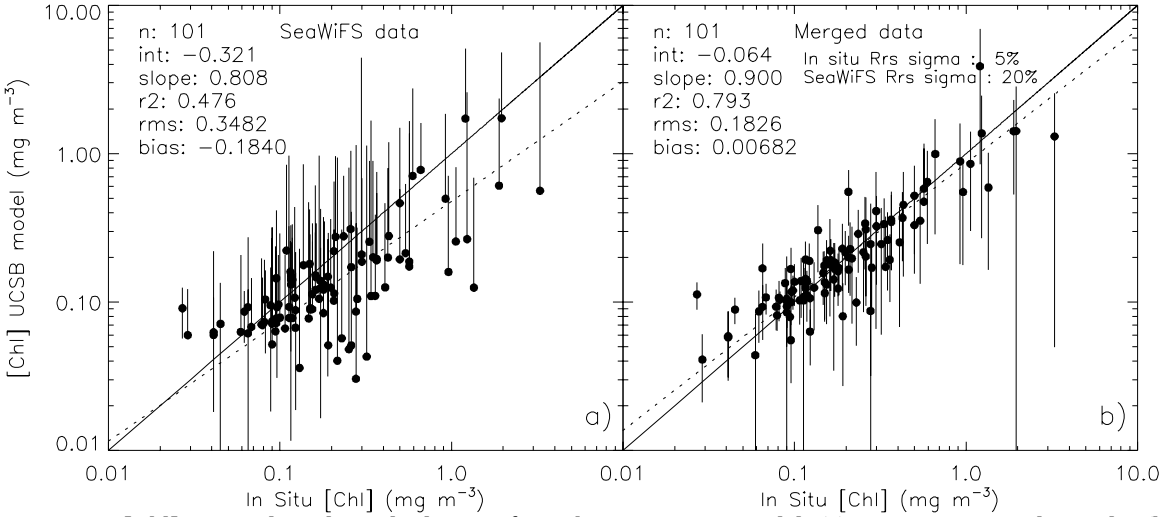

Figure 17.4. [Chl] retrievals and standard errors from the UCSB IOP model. (a) using SeaWiFS data only. (b) using SeaWiFS and in situ Rrs data from the matchup data set (assuming the same level of uncertainty in the data sources than in figure 17.3). When the standard error is greater than the estimated [Chl], the lower error bar is not plotted.

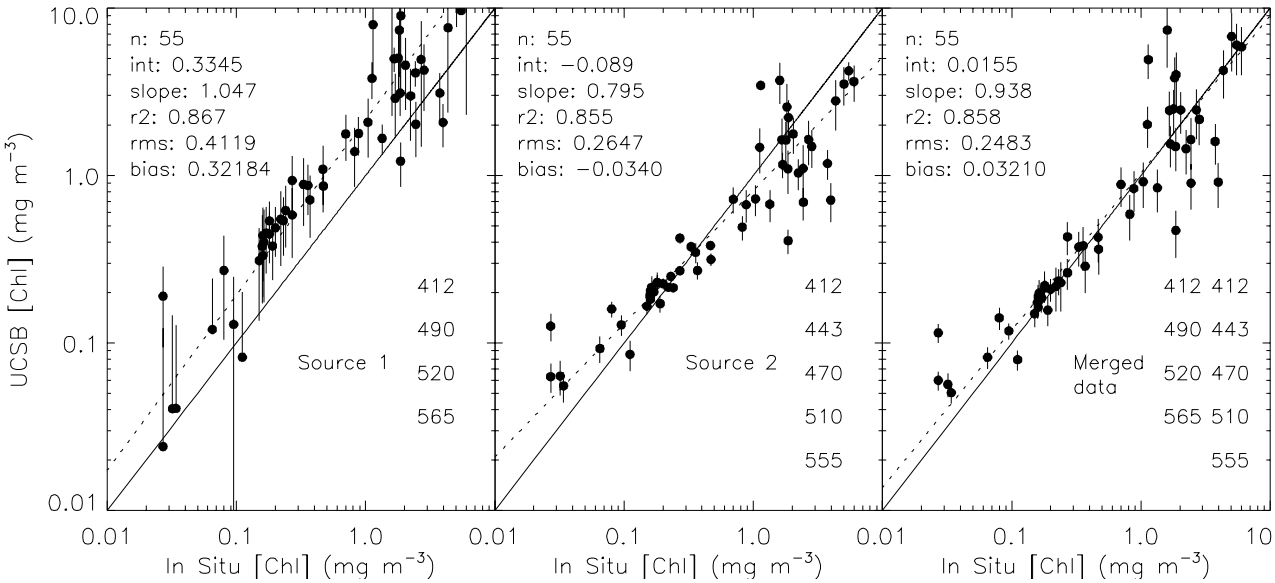

Figure 17.5 Estimated [Chl] and standard errors from the UCSB IOP model. Left panel : using a data source with Rrs at 412, 490, 520 and 565nm. Center panel : using a data source with Rrs at 412, 443, 470, 510 and 555nm. Right panel : using the merged data. When the standard error is greater than the estimated [Chl], the lower error bar is not plotted.

Merging data with different bands

Because we used the SeaWiFS matchup data set to develop and test our approach of data merging, the previous examples were based on the use of data sources with the same bands (the 5 first SeaWiFS bands). The UCSB IOP inversion model is however designed to handle data sources having different bands. This is an important aspect as the various ocean color

sensors to be used within the next decade will have different bands. The potential benefits of using data sources with different bands can be illustrated by the merging of 2 sets of in situ data with different bands using the UCSB model. To do so, the Rrs data collected with an in situ radiometer during a recent cruise were split into 2 different files , one containing the 412, 490, 520 and 565nm channels (source 1) and the second receiving the 412, 443, 470, 510 and 555 nm data (source 2). The results (for [Chl]) using each of the data sets separately and merged are shown on figure 19.5. The results with source 1 only clearly show a good slope and R^2 but the bias is important in the estimated [Chl] and the uncertainties are sometimes high. With the data from source 2, the results are better although the slope of the regression between the estimated and measured [Chl] is relatively far from 1.0. With the merged data, all statistical parameters are improved with a good slope, high R^2, small bias and reduced uncertainties.

17.3 CONCLUSIONS

In this study, we have shown the feasibility of using an ocean color semi-analytical algorithm to merge ocean color radiometric data from different sources to estimate the concentration of chlorophyll *a*. Data merging leads to better, more accurate retrievals with lower uncertainties. The merging procedure we have developed also deals with uncertainties associated with the input data and, provided that these uncertainties are known with sufficient accuracy, uses them to weight the contribution of each source of data in the merging process. This allows more weight to be given to the "best" data when inverting the model to derive the estimated [Chl] and IOPs. The model also calculates the uncertainties for each of the retrieved parameters.

Using in situ and SeaWiFS data, we have shown some of the benefits that can be expected from data merging. We have also shown how the use of data sources with different bands can improve the overall results of the merging. The same benefits should result from the merging of data from 2 or more satellite. We are planning on testing our procedure to merge SeaWiFS and MODIS data in a near future. To merge different satellite data we will also develop a BRDF correction scheme (in collaboration with A. Morel) to take the geometry of the data sources into account. We also plan on improving several aspects of the model itself. The major improvement we are currently working on is a "bandless" formulation for absorption that will allow the model to work with virtually any possible wavebands. In this report we have mostly documented the results for the [Chl] estimated by the model while other variables (i.e. $a_{cdm}(443)$ and $b_{bp}(443)$) are also retrieved. These other quantities are important for the ocean color science (see Siegel et al., 2000) and data merging should also result in increased accuracy of these data products.

REFRENCES

Bailey, S.W., C.R.McClain, P.J. Werdelland B.D. Schieber. 2000: Normalized Water-Leaving Radiance and Chlorophylla Match-Up Analyses SeaWiFS Postlaunch Technical Report Series Vol. 10, NASA Tech. Memo. 2000-206892, S.B. Hooker and E.R. Firestone, Eds., NASA Goddard Space Flight Center, Greenbelt, Maryland, (In press).

Bates, D.M., and D.G. Watts, 1988: *Nonlinear Regression Analysis and its Applications.* Wily, 365 pp.

Bennett, A.F., 1992: *Inverse Methods in Physical Oceanography*, Cambridge, 453 pp.

Bricaud, A., A. Morel and L. Prieur, 1981: Absorption by dissolved organic matter in the sea (yellow substance) in the UV and visible domains. *Limnology and Oceanography*, **26**, 43-53.

Bricaud, A., M. Babin, A. Morel and H. Claustre. 1995: Variability in the chlorophyll-specific absorption coefficients of natural phytoplankton: analysis and parameterization, *J. Geophys. Res*., **100**(C7): 13321-13332.

Bricaud, A, A. Morel, M. Babin, K. Allali, H. Claustre. 1998: Variations of light absorption by suspended particles with chlorophyll a concentration in oceanic (case 1) waters: Analysis and implications for bio-optical models. *J. Geophys. Res.*, **103**, (C13) 31033-31044.

Carder, K.L., S.K. Hawes, K.A. Baker, R.C. Smith, R.G. Steward, and B.G. Mitchell, 1991: Reflectance model for quantifying chlorophyll *a* in the presence of productivity degradation products. *J. Geophys. Res.*, **96**, 20,599-20,611.

Garver, S.A., and D.A. Siegel, 1997: Inherent optical property inversion of ocean color spectra and its biogeochemical interpretation: I. Time series from the Sargasso Sea. *J. Geophys. Res.*, **102**, 18,607-18,625.

Gordon, H.R., O.B. Brown, R.H. Evans, J.W. Brown, R.C. Smith, K.S. Baker, and D.K. Clark. 1988: A semi-analytic radiance model of ocean color. *J. Geophys. Res.*, **93**, 10,909-10,924.

Green S.A., Blough N.V. 1994: Optical-absorption and fluorescence properties of chromophoric dissolved organic-matter in natural-waters. *Limnol. Oceanogr*, **39**: (8), 1903-1916.

Hooker S.B. and S. Maritorena. 2000: An Evaluation of Oceanographic Radiometers and Deployment Methodologies. *J. Atmos. Ocean. Tech.,* **17**(6) : 811-830.

Gregg, WW; Esaias, WE; Feldman, GC; Frouin, R; Hooker, SB; McClain, CR; and Woodward, RH. 1998: Coverage opportunities for global ocean color in a multimission era. IEEE Transactions On Geoscience And Remote Sensing, 36 :1620-1627.

Gregg, WW and Woodward, 2000: RH. Improvements in coverage frequency of ocean color: Combining data from SeaWiFS and MODIS. *IEEE* Transactions On Geoscience And Remote Sensing, **36**, 1350-1353.

IOCCG. 1999: Status and Plans for Satellite Ocean-Colour Missions: Considerations for Complementary Missions. Yoder, J.A. (ed.), Reports of the International Ocean-Colour Coordinating Group, No. 2, IOCCG, Darmouth, Canada, 43pp.

Le Traon, P.Y. and F. Ogor, 1998: ERS-1/2 orbit improvement using TOPEX/POSEIDON: The 2cm challenge. *J. Geophys. Res.*, **103**, 8045-8057.

Maritorena, S., D.A. Siegel, A.R. Peterson and M. Lorenzi-Kayser, 2000: Tuning of a pseudo-analytical ocean color algorithm for studies at global scales. Talk and abstract presented at the 2000 AGU Ocean Sciences Meeting (OS12M-05), San Antonio Texas.

Morel A. and S. Maritorena, 2000: Bio-optical properties of oceanic waters : a reappraisal. In Press *J. Geophys. Res.*

Nelson, N.B., Siegel D.A. and Michaels A.F. 1998. Seasonal dynamics of colored dissolved material in the Sargasso Sea. *Deep-Sea Res.* I, **45**: (6), 931-957.

O'Reilly, J., S. Maritorena, B.G. Mitchell, D.A. Siegel, K.L. Carder, M. Kahru, S.A. Garver, C.R. McClain, 1998: Ocean color algorithms for SeaWiFS. *J. Geophys. Res.*, **103**, 24,937-24,953.

Parker, R.L., 1994; *Geophysical Inverse Theory*, Princeton Univ. Press, 386 pp.

Peterson, A.R, D.A. Siegel, S.A. Maritorena and S.A. Garver, 1999: Optimal tuning of semi-analytical ocean color algorithms for the global ocean. Presented at the 1999 ASLO Aquatic Sciences Meeting, Sante Fe, NM, Feb. 1999.

Pope, R.M., and E.S. Fry, 1997: Absorption spectrum (380-700 nm) of pure water. 2. Integrating cavity measurements. *Applied Optics*, **36**, 8710-8723.

Press W.H., S.A. Teukolsky, W.T. Vettering and B.P. Flannery, 1992: *Numerical Recipes in C: The Art of Scientific Computing, 2nd edition.* Cambridge University Press, 994 pp.

Reynolds, R.W., and T.M. Smith, 1994: Improved global sea surface temperature analyses using optimum interpolation. *J. Climate*, **7**, 929-948.

Rossow, W.B., and R.A. Schiffer, 1991: ISCCP cloud data products. *Bull. Amer. Met. Soc.*, **72**, 2-20.

Siegel D. A., S. Maritorena, N. B. Nelson, D.A. Hansell and M. Lorenzi-Kayser, 2000: Global Distribution of Colored Dissolved Organic Materials. *Global Biogeochemical Cycles*, (Submitted).

Siegel, D.A., M. Wang, S. Maritorena and W. Robinson. 2000: Atmospheric correction of satellite ocean color imagery: the black pixel assumption. *Applied Optics*, 39 , 3582 - 3591.

Smith, R.C., and K.S. Baker, 1981: Optical properties of the clearest natural waters. *Applied Optics*, **20**, 177-184.

This research was supported by the

SIMBIOS NASA contract # 98083

PEER REVIEWED PUBLICATIONS

Hooker S.B. and S. Maritorena. 2000. An Evaluation of Oceanographic Radiometers and Deployment Methodologies. *J. Atmos. Ocean. Tech.,* **17**(6): 811-830.

Maritorena, S., A. Morel and B. Gentili. Determination of the fluorescence quantum yield by oceanic phytoplankton in their natural habitat. *Applied Optics* (In Press).

Morel A. and S. Maritorena. Bio-optical properties of oceanic waters : a reappraisal. *J. Geophys. Res.* (In Press).

Siegel, D.A., M. Wang, S. Maritorena and W. Robinson. 2000. Atmospheric correction of satellite ocean color imagery: the black pixel assumption. *Applied Optics*, **39** : 3582 - 3591.

Siegel, D.A., 1998: Spectral data assimilation for merging satellite ocean color imagery. Extended abstract published on the CD proceedings from *Ocean Optics XIV*.

PRESENTATIONS

Maritorena, S., D.A. Siegel, A.R. Peterson & M. Lorenzi-Kayser, 2000: Tuning of a pseudo-analytical ocean color algorithm for studies at global scales. AGU Ocean Sciences Meeting (OS12M-05), San Antonio.

Peterson, A.R, D.A. Siegel, S.A. Maritorena and S.A. Garver, 1999: Optimal tuning of semi-analytical ocean color algorithms for the global ocean. ASLO Aquatic Sciences Meeting, Sante Fe.

Siegel, D.A., 1998: Spectral data assimilation for merging satellite ocean color imagery, Ocean Optics XIV meeting, Kona. Extended abstract published on the CD proceedings from Ocean Optics XIV.

Siegel, D.A., 1999: Orthothogonal views of the global ocean biosphere using SeaWiFS. *ASLO* Aquatic Sciences Meeting, Sante Fe.

Chapter 18

SIMBIOS Data Product and Algorithm Validation with Emphasis on the Biogeochemical and Inherent Optical Properties

J. Ronald V. Zaneveld, W. Scott Pegau, and Andrew H. Barnard

College of Oceanic and Atmospheric Sciences, Oregon State University, Corvallis, Oregon

18.1 INTRODUCTION

The purpose of our component of the SIMBIOS program is to address and quantify the relative accuracy of the various ocean color remote sensing products by means of product and algorithm validation. In order to accomplish these goals, we have been collaborating in an international research program in the Gulf of California designed to examine the spatial and temporal bio-optical variability in this region. In addition, we participated in various cruises of opportunity to supplement our validation data set. Our long-term objectives are to; a) collect optical and biochemical data in oceanic and coastal regions of interest, b) provide collected data to the SeaBASS database, the SIMBIOS project office, and other interested users, c) maintain and update instrumentation and data archiving and dissemination systems, and d) determine spatial and temporal error fields for the biological and geophysical data products from the various ocean color missions.

18.2 RESEARCH ACTIVITIES

Over the past 6 years we have been involved in a multi-national research effort focused on determining the physical and biogeochemical variability in the Gulf of California. This research is done in coordination with Drs. J. Mueller and C. Trees from San Diego State University (SDSU), Drs. S Alvarez Borrego, R. Lara-Lara, G. Gaxiola and H. Maske from the Centro de Investigacion Cientifica y de Educacion Superor de Ensenada (CICESE), Ensenada, Mexico, and Dr. E. Valdez from the University of Sonora, Hermosillo, Mexico. Our component has been to measure the inherent optical properties (IOP; the absorption, scattering, and attenuation characteristics of the water and the materials suspended and dissolved therein) and apparent optical properties (AOP; the radiometric parameters of the submarine daylight field) as well as the traditional CTD parameters on vertical scales less than 0.5 m.

During the three-year contract period, we have participated in 9 field campaigns, collecting an extensive amount of radiometric, inherent optical property, aerosol optical thickness, and physical data (Table 18.1). The field campaigns included cruises offshore of Oregon, 5 Gulf of California cruises (Figure 1), a cruise with Dr. Francisco Chavez (MBARI), a cruise of opportunity with Drs. Vivian Montecino (University of Chile) and Giovanni Daneri (University of Vaparaiso), and the MODIS validation cruise off Southern California, the West coast of the Baja peninsula in Mexico, and the Gulf of California (MOCE5). We have maintained and utilized the optical absorption/attenuation profiling system that is part of the SIMBIOS instrument pool. We also maintained 3 water filtration systems as a part of the SIMBIOS equipment pool. Recently, we have developed a self-recording small inherent optical property, CTD and radiometer profiling system for small boat operations. In the past year we have worked extensively on building an inline optical sampling system to be deployed on a commercial ferry in the Gulf of California.

Two sampling platforms were typically used during these cruises; a SLOW Descent Rate Optical Profiler (SLOWDROP) to measure the inherent optical properties as well as the physical parameters, and a profiling radiometer system to measure the downwelling irradiance and upwelling radiance. Typically, SLOWDROP and radiometer profiles are made within an hour of each other at the same location.

The SLOWDROP platform is free-falling and slightly negatively buoyant providing 10-20 cm scale vertical resolution. A typical instrument configuration includes a SeaBird SBE-25 CTD for measuring physical parameters, a fluorometer, and two WETLabs ac-9 (9 wavelength absorption and attenuation meters) for measuring the particulate and dissolved components of the IOP. In 1998, a HOBI Labs

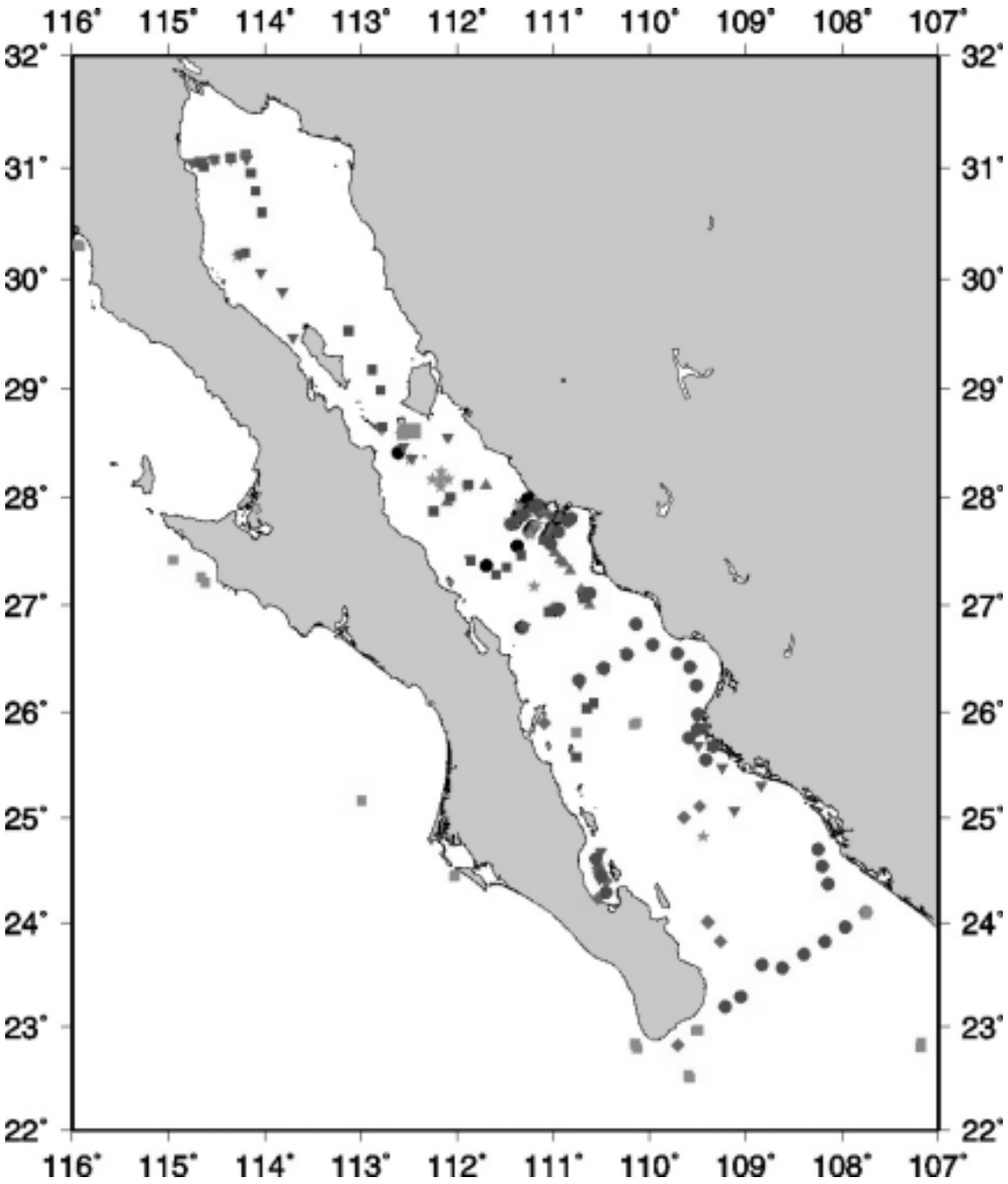

Figure 18.1. Map of the Gulf of California with sampling locations from the 8 cruises conducted.

Hydroscat-6 was added to the platform to measure the spectral backscattering coefficient. CTD and IOP data are collected simultaneously during a single profile using a WETLabs MODAPS system for data collection and integration. Calibrations of the ac-9 instruments were performed several times during the contract period. Field calibrations of the ac-9 meters were typically done once per sampling day using a clean water standard produced using a Barnstead nanopure water system according to the SIMBIOS protocols for this instrument.

A Satlantic Inc. SPMR system was used to measure profiles of the apparent optical properties including downwelling irradiance and upwelling radiance at 412, 444, 490, 533, 555, 590, and 684 nm. The Satlantic radiometer is calibrated at SDSU by Drs. Mueller and Pegau following NIST protocols and calibrated twice a year by Satlantic Inc. The optical filters on this radiometer were upgraded by the manufacturer (Satlantic) over the past year.

One meter binned profiles of all of the data, were provided to the SeaBASS database within 90 days of completion of each cruise. Also provided are the calibration histories of the ac-9's and the radiometer, as well as a detailed logbook of the cruise activities. The dates of each SIMBIOS-supported cruise and the number of profiles made using each system are listed in Table 18.1. Figure 18.1 shows the station locations sampled during each cruise within the Gulf of California.

Currently, we are receiving all of the SeaWiFS HRPT Level 1A data for the West Coast of North America including the Gulf of California from the DAAC. This data has been archived and processed to various levels for use in the validation of ocean color products.

We have maintained an optical profiling system for use in the SIMBIOS instrument pool. The system contains 2 hyperspectral absorption and attenuation meters (WETLabs Histars), a CTD (SeaBird Electronics 25), a data acquisition system (WETLabs MODAPS+), cage, and necessary cabling. A full time technician was hired to accompany this system, to assist users in deployment and operation and to process the data. We also maintained 3 deionizing water filtration systems (Barnstead Nanopure) which are for use by the SIMBIOS authorized users. These systems are used to produce a clean water standard for ac-9 and HiStar field calibrations.

We conducted two ac9 workshops designed to train technicians and scientists how to operate the instruments and interpret the data, and to compare techniques used by various groups. In attendance were 40 people representing 5 European programs, NASA, NRL, NavOc, NDBC, and numerous research groups. We found that most programs followed the same operating protocols with a few minor exceptions. Many of these exceptions will be written into future operating protocols. The group recommended testing the use of a longer reference wavelength in the ac9. Those tests are underway at OSU.

We have also been involved in a collaborative effort with Drs. Knut Stamnes and Bingquan Chen at the Stevens Institute of Technology investigating atmospheric correction of SeaWiFS imagery.

18.3 RESEARCH RESULTS

Data collected in the Gulf of California as well as other locations were used to examine the spectral relationships between the inherent optical properties in Barnard et al. (1998a). The results of this research were used to compare and contrast the inherent optical properties observed in the Gulf of California (Pegau et al. 1998). In the shallow northwest region of the Gulf, Case II waters are consistently observed due to the resuspension of sediments. In the central portion of the Gulf, the largest variability in optical properties is associated with coastal upwelling. Away from the coasts the spectral optical properties are fairly constant.

Validation of the normalized water leaving radiance measured by SeaWiFS in the Gulf of California during the 1997 and spring 1998 cruises was examined in Barnard et al. (1998b). The results of this research indicated that atmospheric correction was problematic, often causing negative water leaving radiance at 412 nm.

In coordination with our SeaWiFS funding, we have undertaken the development of a new remote sensing algorithm involving the triple ratio of the remote sensing reflectance. The results of this work were presented at the 1998 Ocean Sciences meeting at San Diego, CA in a presentation titled "A nearly backscattering independent algorithm for the retrieval of spectral absorption from remote-sensing reflectence" by J. R. V. Zaneveld, A. H. Barnard, and W. S. Pegau. This work was subsequently published in Applied Optics (Barnard et al., 1999a).

We have also compared the in situ radiance with the upwelling radiance resolved by the OCTS sensor off the northeastern U.S. coast. The results of this work were presented at the 1998 Ocean Sciences meeting in a talk titled "Bio-optical maps derived from ocean color imagery using a nearly backscattering independent algorithm" by A. H. Barnard, J. R. V. Zaneveld, and W. S. Pegau.

A detailed analysis of the spectral characteristics of the absorption, attenuation, and scattering data collected in the Gulf of California over the past 5 years has been completed (Pegau, et al., 1998; 1999; 2000). In situ data collected in the Gulf of California during

two separate research cruises, were used in an investigation into the validation of SeaWiFS satellite measurements (Barnard, et al., 1998). Radiometric data collected during a recent cruise in the Gulf of California were used to validate the normalized water leaving radiance estimated by the SeaWiFS satellite. The results of this work show that the blue wavelengths are greatly underestimated by the SeaWiFS sensor possibly due to inaccurate atmospheric correction (Figure 18.2).

In order to correctly invert the remotely sensed reflectance to obtain the optical properties, we developed a method for the appropriate depth averaging of remotely sensed optical parameters (Zaneveld, et al., 1998). This method was used to investigate the influence of vertical structure on the remotely sensed signal. The results of this work were presented at the ASLO Aquatic Sciences meeting in Santa Fe, NM, February 1-5, 1999, titled "Assessing a key implicit assumption in ocean color remote sensing algorithms: Optical homogeneity" (Barnard, et al, 1999b).

Based on the consistent relationships resolved by an earlier study (Barnard, et al, 1998), we developed a method to obtain closure between the inherent optical properties and remotely sensed reflectance measurements (Barnard, et al., 1999a). The results of this model showed that inversion of the remotely sensed reflectance to obtain the absorption coefficient is possible if the spectral relationships of the absorption coefficient are known. A recent model that resulted from this research was the determination of photosynthetically available radiation light levels using profiles of the absorption coefficient (Barnard, et al.,1999c).

As a result of our participation in the MODIS validation cruise, we have been working with Dr. Dennis Clark of NOA to achieve closure between his IOP and AOP measurements.

REFERENCES

Barnard, A. H., W. S. Pegau, and J. R. V. Zaneveld, 1998a: Global relationships of the inherent optical properties of the oceans, *J. Geophys. Res*., **103**, 24,955-24,968.

Barnard, A. H., J. R. V. Zaneveld, J. L. Mueller, W. S. Pegau, and C. Trees, 1998b: SeaWiFS ocean color in the Gulf of California: Variability, validation, and algorithm development, Ocean Optics XIV Conference Papers, Kailua-Kona, HI, November 10-13.

Barnard, A.H., J.R.V. Zaneveld, and W.S. Pegau. 1999a: Remotely sensed reflectance and the absorption coefficient: Closure and inversion. *Applied Optics*, **38**, 5108-5117.

Barnard, A.H., J.R.V. Zaneveld, W.S. Pegau, and T.J. Cowles. 1999b: Assessing a key implicit assumption in ocean color remote sensing: Optical homogeneity. ASLO Aquatic Sciences meeting, Santa Fe,.

Barnard, A.H., J.R.V. Zaneveld, W.S. Pegau, J.L Mueller, H. Maske, R. Lara-Lara, S. Alvarez-Borrego, and E. Valdez-Holquin. 1999c: The determination of PAR levels from absorption coefficient profiles at 490 nm. *Ciencias Marinas.* **25**(4), 487-507.

Pegau, W.S., A.H. Barnard, J.R.V. Zaneveld, J.L. Mueller, H. Maske, R. Lara-Lara, S. Alvarez-Borrego, E. Valdez-Holguin, and R. Cervantes-Duarte. 1998: Optical variability in the Gulf of California. Ocean Optics XIV Conference Papers, Volume 2, Kailua-Kona, Hawaii.

Pegau, W.S., J.R.V. Zaneveld, A.H. Barnard, H. Maske, S. Alvarez-Borrego, R. Lara-Lara, R. Cervantes-Duarte. 1999: Inherent optical properties in the Gulf of California. *Ciencias Marinas.* **25**(4), 469-485.

Zaneveld, J.R.V., A.H. Barnard, W.S. Pegau, and E. Boss. 1998: An investigation into the appropriate depth average of remotely sensed optical parameters. Ocean Optics XIV Conference Papers, Volume 2, Kailua-Kona, Hawaii.

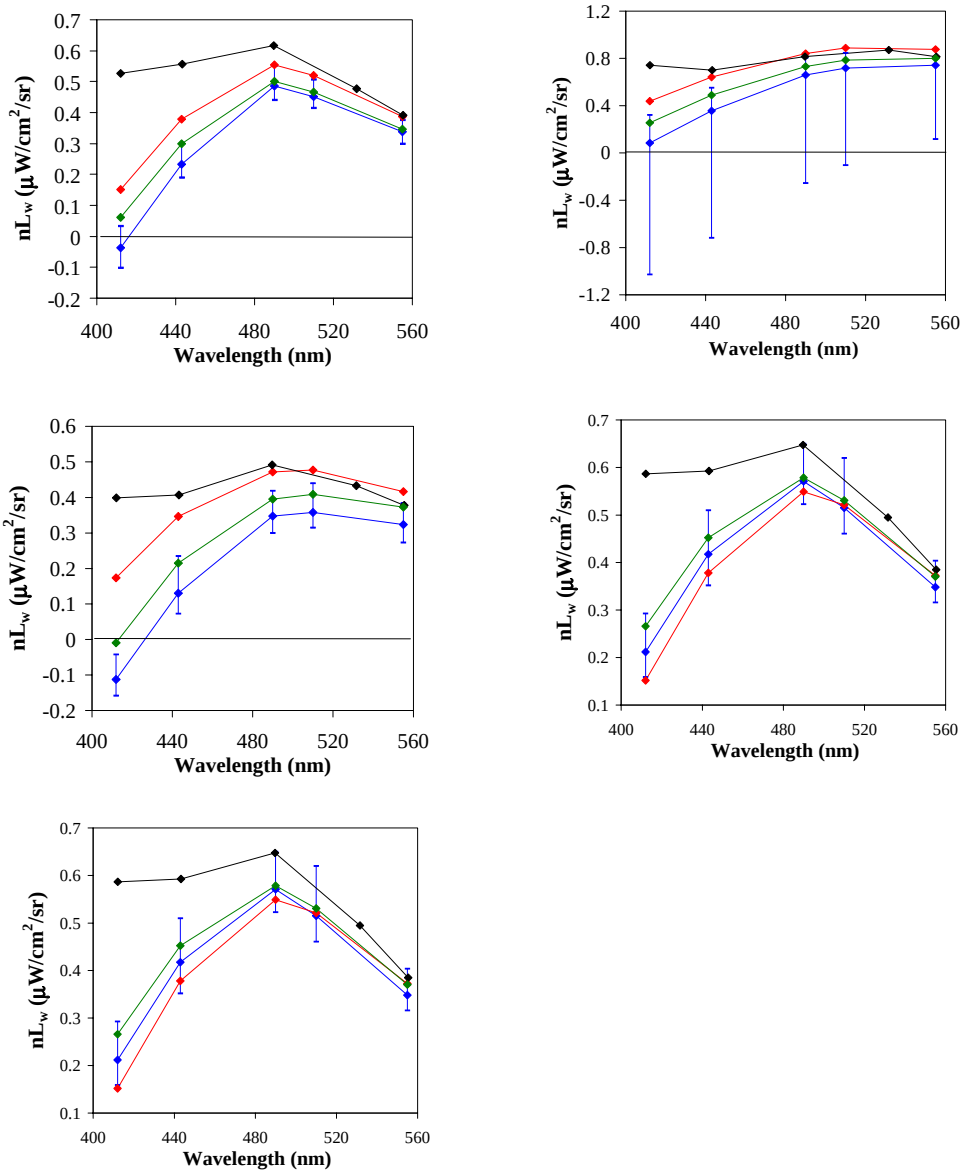

Figure 18.2 - Spectral comparison of the normalized water leaving radiance measured *in situ* (black) and as determined by SeaWiFS using the Gordon and Wang (blue), Siegel (green) and Stumpf (red) atmospheric correction algorithms for 5 days of match-up data in the Gulf of California (April 21, 24, 26, 28, and 30, 1999).

Table 18.1 - Dates and number of profiles made during each of the SIMBIOS cruises. The first two listed cruises were not supported by SIMBIOS, but the data has been submitted to SeaBASS. In additionally discrete samples for pigment analyses were taken, and sun photometer readings were obtained.

Cruise Name	Dates	# IOP profiles	# AOP profiles
Gulf Of California 1995 fall	11/25/95 to 12/6/95	28	69
Gulf Of California 1996 fall	10/30/96 to 11/7/96	25	25
Gulf Of California 1997 fall	10/16/97 to 10/29/97	39	24
Offshore Oregon 1997	9/6/97 to 9/18/97	150	0
Gulf of California 1998 spring	3/6/98 to 3/16/98	31	11
Gulf of California 1998 fall	11/27/98 to 12/7/98	36	19
Coastal California	5/22/99 to 5/27/99	6	0
Coastal Chile	7/4/99 to 7/17/99	22	22
Gulf of California 1999 spring	4/21/99 to 5/1/99	40	19
Gulf of California 1999 fall	10/29/99 to 11/7/99	37	23
Modis validation cruise (MOCE5)	10/1/99 to 10/21/99	48	(carried out by other researchers)

This research was supported by the

SIMBIOS NASA contract # 97129

PEER REVIEWED PUBLICATIONS

Barnard, A.H., W.S. Pegau, and J.R.V. Zaneveld. 1998: Global relationships in the Inherent Optical Properties of the oceans. *J. Geophys. Res.*, **103**:24,955-24,968.

Barnard, A.H., J.R.V. Zaneveld, and W.S. Pegau, 1999: Remotely sensed reflectance and the absorption coefficient: Closure and inversion. *Applied Optics*, (In press).

Barnard, A.H., J.R.V. Zaneveld, W.S. Pegau, J.L Mueller, H. Maske, R. Lara-Lara, S. Alvarez-Borrego, and E. Valdez-Holquin, 1999: The determination of PAR levels from absorption coefficient profiles at 490 nm. *Ciencias Marinas*. (In press).

Pegau, W.S., J.R.V. Zaneveld, A.H. Barnard, H. Maske, S. Alvarez-Borrego, R. Lara-Lara, R. Cervantes-Duarte. 1999: Inherent optical properties in the Gulf of California, *Ciencias Marinas*. (In press).

Zaneveld, J.R.V and W.S. Pegau. 1998: A model for the reflectance of thin layers, fronts, and internal waves and its inversion. *Oceanography*. 11: 44-47.

PRESENTATIONS

Barnard, A.H., J.R.V. Zaneveld, and W.S. Pegau, 1997: Comparison of inherent optical properties across a variety of oceanic regimes for application to remote sensing. ALSO Aquatic Sciences, Sante Fe.

Barnard, A.H., J.R.V. Zaneveld, and W.S. Pegau, 1998: Bio-optical maps derived from ocean color imagery using a backscattering independent algorithm. AGU/ASLO 1998 Ocean Sciences Meeting, San Diego.

Barnard A.H., J.R.V. Zaneveld, and W.S. Pegau, 1998: SeaWiFS ocean color in the Gulf of California: Validation. *Ocean Optics XIV* Conference Papers, Volume 2, Kailua-Kona, HI.

Barnard, A. H., J. R. V. Zaneveld, W. S. Pegau, and T. J. Cowles. 1999: Assessing a key implicit assumption in ocean color remote sensing algorithms: Optical homogeneity. ASLO Aquatic Sciences Meeting, Sante Fe.

Mueller, J.L., J.R.V. Zaneveld, W.S. Pegau, E. Valdez, H. Maske, S. Alvarrez-Borrego, and R. Lara-Lara. 1997: Remote sensing reflectance: preliminary comparisons between in-water and above-water measurements, and estimates modelled from measured inherent optical properties. *SPIE*, 2963: 502-513.

Pegau, W.S., A.H. Barnard, J.R.V. Zaneveld, J.L. Mueller, H. Maske, R. Lara-Lara, S. Alvarez-Borrego, E. Valdez-Holguin, and R. Cervantes-Duarte. 1998: Optical variability in the Gulf of California. *Ocean Optics XIV Conference* Papers, Volume 2, Kailua-Kona, HI.

Zaneveld, J.R.V., W.S. Pegau, A.H. Barnard, J.L. Mueller, H. Maske, E. Valdez, R. Lara-Lara, and S. Alvarez-Borreo. 1997: Prediction of euphotic depths and diffuse attenuation coefficients from absorption profiles: A model based on comparison between vertical profiles of spectral absorption, spectral irradiance, and PAR. *SPIE*, 2963: 585-590.

Zaneveld, J.R.V, A.H. Barnard, and W.S. Pegau. 1998: A nearly backscattering independent algorithm for the retrieval of spectral absorption from remote-sensing reflectance. AGU/ASLO 1998 Ocean Sciences Meeting, San Diego.

Zaneveld, J.R.V., A.H. Barnard, W.S. Pegau, and E. Boss. 1998: An investigation into the appropriate depth average of remotely sensed optical parameters. *Ocean Optics XIV* Conference Papers, Volume 2, Kailua-Kona, HI.

Chapter 19

Aerosol Optical Properties over the Oceans: Summary and Interpretation of Shadow-Band Radiometer Data from Six Cruises

Mark A. Miller, R. M. Reynolds and Mary Jane Bartholomew
Brookhaven National Laboratory Upton, New York

19.1 INTRODUCTION

The aerosol scattering component of the total radiance measured at the detectors of ocean color satellites is determined with atmospheric correction algorithms. These algorithms are based on aerosol optical thickness measurements made in two channels that lie in the near-infrared portion of the electromagnetic spectrum. The aerosol properties in the near-infrared region are used because there is no significant contribution to the satellite-measured radiance from the underlying ocean surface in that spectral region. In the visible wavelength bands, the spectrum of radiation scattered from the turbid atmosphere is convolved with the spectrum of radiation scattered from the surface layers of the ocean. The radiance contribution made by aerosols in the visible bands is determined from the near-infrared measurements through the use of aerosol models and radiation transfer codes. Selection of appropriate aerosol models from the near-infrared measurements is a fundamental challenge.

There are several challenges with respect to the development, improvement, and evaluation of satellite ocean-color atmospheric correction algorithms. A common thread among these challenges is the lack of over-ocean aerosol data. Until recently, one of the most important limitations has been the lack of techniques and instruments to make aerosol measurements at sea. There has been steady progress in this area over the past five years, and there are several new and promising devices and techniques for data collection. The development of new instruments and the collection of more aerosol data from over the world's oceans have brought the realization that aerosol measurements that can be directly compared with aerosol measurements from ocean color satellite measurements are difficult to obtain. There are two problems that limit these types of comparisons: the cloudiness of the atmosphere over the world's oceans and the limitations of the techniques and instruments used to collect aerosol data from ships. To address the latter, we have developed a new type of shipboard sun photometer.

There are two primary types of sun photometer used to measure the aerosol optical depth: narrow field-of-view radiometers aimed at the solar disk and rotating shadow-band radiometers. Shadow-band radiometers are wide-field-of-view radiometers that employ an occulting apparatus to add directional capabilities. Just as narrow-field-of-view radiometers must be accurately aimed, a serious drawback for measurements on ships at sea, conventional shadow-band radiometers also require exact orientation. Fast-Rotating Shadow-band Radiometers (FRSRs) are a hybrid form of the original shadow-band radiometer design, but do not have a rigid requirement for orientation. Thus, it is possible to use a slightly modified version of the land-based FRSR on ships. As compared to land-based FRSRs, shipboard FRSRs require much faster rotation of the occulting arm, faster-response silicon detectors, higher data sampling rates, and more sophisticated data analysis.

As part of our NASA SIMBIOS contract and with additional support from the Department of Energy's (DOE) Atmospheric Radiation Measurement (ARM) Program, we developed and deployed a new instrument during the past two years: the shipboard Fast-Rotating Shadow-band Spectral Radiometer (FRSR; Reynolds et al., 1999). This instrument makes continuous, semi-automated shipboard measurements of the direct-normal, diffuse, and global irradiance in seven channels (415 nm, 500 nm, ~610 nm, ~660 nm, ~862 nm, 936 nm, and broadband) and does not require a mechanically stabilized platform, thereby making it cost effective and reliable. The FRSR can operate continuously for months on a ship and can be monitored by someone with minimal training. The FRSR is part of a Portable Radiation Package (PRP), which also contains broadband solar and IR Eppley radiometers. The PRP has been deployed extensively during the past two years, traversing parts of all three oceans, and has demonstrated stable calibration. It has moved from proof-of-concept to a nearly operational instrument.

The shipboard FRSR measures spectral global and diffuse irradiance with 2-minute resolution. These data are combined with information about the pitch, roll, and heading of the ship to calculate the 2-minute spectral direct-normal irradiance. From these data, the aerosol optical thickness can be computed during clear periods using the Langley regression technique, or continuously if high quality extraterrestrial calibration coefficients are known. In addition, the diffuse irradiance measured by the FRSR can be used to evaluate

fractional cloudiness, thereby providing a means to test cloud-filtering algorithms used in satellite ocean color retrievals.

Our strategy for collecting relevant aerosol data from over the oceans has evolved over the past three years. As a benchmark of our progress, we (our group at the Brookhaven National Laboratory) believe that we have at least doubled the number of shipboard aerosol measurements over the world's oceans, and possibly tripled it. We have collected aerosol data from all three oceans and the database is growing rapidly. Coincidentally, our ability to correctly interpret these aerosol measurements is being refined. In this report, we present summary results from six separate deployments of the FRSR. We also discuss our data processing strategy, especially our uncertainty analyses, and comment on plans for the coming three years.

19.3 RESEARCH ACTIVITIES

Evaluating Ocean Color Atmospheric Correction Algorithms

An aerosol correction algorithm was developed by Gordon (1978), applied to the problem of phytoplankton pigment retrieval by Gordon and Clark (1981), and used in the CZCS by Gordon et al. (1980). Mathematically, the atmospheric correction parameters, $\varepsilon(\lambda_i,\lambda_j)$, for the Gordon scheme are given by

$$\varepsilon(\lambda_i,\lambda_j)=\frac{\omega_a(\lambda_i)\tau_a(\lambda_i)p_a(\theta,\theta_0,\lambda_i)}{\omega_a(\lambda_j)\tau_a(\lambda_j)p_a(\theta,\theta_0,\lambda_j)}, \qquad (19.1)$$

where $\omega_a(\lambda_i)$ is the aerosol single scattering albedo, $\tau_a(\lambda)$ is the aerosol optical thickness, and $p(\theta,\theta_0,\lambda_i)$ is the aerosol scattering phase function. The Gordon technique is to model $\varepsilon(\lambda_i,\lambda_j)$ using a power-law relationship defined as

$$\varepsilon(\lambda_i,\lambda_j)=\left(\frac{\lambda_i}{\lambda_j}\right)^{-n}. \qquad (19.2)$$

The coefficient n is determined for two wavelengths in the near infrared and used to select an aerosol model. From this model, radiation transfer codes are used to estimate the satellite radiance contribution of the aerosol in the visible wavelengths (Gordon and Wang, 1994). Evaluation of this atmospheric correction scheme therefore involves collection of shipboard data from which the characteristics of $\varepsilon(\lambda_i,\lambda_j)$ may be determined for a wide variety of aerosol conditions.

What have we learned in the past two years that is relevant to the measurement of $\varepsilon(\lambda_i,\lambda_j)$ over the oceans? One important finding is that the FRSR can measure $\tau_a(\lambda)$ to an accuracy of 0.02-0.03 on a relatively large ship (>200 feet) in typical sea-states. Our accuracy estimates are based on comparisons with manually operated sun photometers and at-sea Langley calibrations, however, as we will demonstrate subsequently, the uncertainty in $\tau_a(\lambda)$ varies from observation to observation and must be computed independently for each measurement.

Theoretically, most of the variability in $\varepsilon(\lambda_i,\lambda_j)$ is attributable to $\tau_a(\lambda)$ and caused by different aerosol loadings, although significant variability can also be present due to the wavelength dependence of $p(\theta,\theta_0,\lambda_i)$. A critical question is therefore: can the FRSR measure $\tau_a(\lambda)$ with the accuracy required to meet the specification for $\Delta\varepsilon(\leq 0.08)$ required for the 5% limit on water-leaving radiance? Error analysis suggests that the FRSR meets this criterion under many conditions, although difficulty is experienced in relatively clean air masses. We are thus encouraged to proceed, keeping in mind that the variability due to $p(\theta,\theta_0,\lambda_i)$ remains unknown due to the lack of a technique from which to measure it continuously over water.

Frsr Data Analysis Database Summary

Seminal to the analysis of data from the shipboard FRSRs is a proper understanding of the uncertainty (error propagation) in measurements. This uncertainty is manifested in three forms: pure uncertainty due to instrument noise and design; uncertainty in the shadow-band technique (particularly in shadow identification in cloudy conditions); and uncertainty in the application of Beer's law to determine $\tau_a(\lambda)$ when the instrument being employed for this purpose generates noise. The first two sources of uncertainty can be effectively quantified and minimized, while the last varies widely from measurement-to-measurement and must be computed for each data point. We have recently written a NASA TM concerning the analysis of uncertainty and repeat the variance equations for $\tau_a(\lambda)$ and α, the Angstrom exponent for a brief discussion. These variance equations are given by

$$\sigma^2_{\tau_\lambda}=\left(\frac{1}{m}\right)^2\left[\left(\frac{\sigma_{I_{\lambda 0}}}{I_{\lambda 0}}\right)^2+\left(\frac{\sigma_{I_{\lambda N}}}{I_{\lambda N}}\right)^2\right] \qquad (19.3)$$

$$\sigma^2_{\alpha}=\alpha\left[\left(\frac{\sigma_{\tau_{\lambda 1}}}{\tau_{\lambda 1}}\right)^2+\left(\frac{\sigma_{\tau_{\lambda 2}}}{\tau_{\lambda 2}}\right)^2\right]^{1/2} \qquad (19.4)$$

where m is the air mass and I_λ is the direct-normal irradiance. The subscripts 0 and N indicate the extra-terrestrial value and the measured value, respectively, and the subscripts 1 and 2 indicate the two wavelengths used in the calculation of the Angstrom exponent. These variance equations provide a means to evaluate σ^2 for each individual measurement, thereby permitting a running assessment of the quality of the aerosol measurements. The variance equations also permit the data to be filtered according to the uncertainty in $\tau_a(\lambda)$, α, or both variables. It should also be noted that the uncertainty in the Angstrom exponent is inversely proportional to τ_a, so constraints on σ_α^2 will naturally favor observations with large optical thickness.

19.4 RESEARCH RESULTS

There are currently seven PRPs with their resident FRSRs. They are typically deployed on medium to large ships making lengthy voyages, preferably months, or on any ship that is traveling to a unique part of the world's oceans. Data are collected continuously from the instrument using a laptop computer, recorded on CD or disk, and shipped to BNL for analysis. Calibration of the FRSRs is done at regular intervals (six months to one year) by transporting the instruments to Mauna Loa and deploying them for a period of two weeks to one month. Spot calibrations are performed during the cruise when meteorological conditions permit, but these calibrations are used primarily to diagnose drift in the laminated interference filters for the various channels. The procedure used to compute the spectral direct-normal irradiance with the FRSR is discussed in Reynolds et al. (1999) and not repeated here.

We have performed extensive comparisons of FRSR data with coincident data collected with other sun photometers (see Reynolds et al., 1999). These comparisons show that the shipboard FRSRs can measure $\tau_a(\lambda)$ with accuracy that is at least as good as hand-held and platform-stabilized narrow-beam sun photometers. It is also noteworthy that the FRSR measures the diffuse component of irradiance, which can be used to evaluate the sky state at the time of the observation.

Results for six deployments of the FRSR summarized in this report are presented in Table 19.1. These cruises cover portions of all three oceans and represent a wide range of aerosol conditions. The six cruises include a total of 42,577 two-minute observations (1419 hours/~177 separate days) from the FRSRs collected in sky conditions that allow a shadow to be identified when the solar disk occulting arm passes over the detectors. From these observations, 15,275 (509 hours, or 35% of total observations) passed a cloud filter that selects measurements that are not influenced by clouds between the solar disk and the FRSR detectors. The uncertainty of each individual cloud-filtered measurement of $\tau_a(\lambda)$ and α [i.e. σ_τ^2 and σ_α^2] was computed and observations were accepted if $\sigma_\tau^2(\lambda) \le 0.03$ and $\sigma_\alpha^2(\lambda) \le 0.3$, a stringent requirement. Only 682 observations (56 hours, or 4.4% of the cloud filtered observations) passed the uncertainty filter.

Data that passed the uncertainty bounds are presented in Figure 19.1, which shows $\tau(865)$ plotted against $\alpha(865,\lambda)$ for all six cruises. In this figure, $\alpha(865,\lambda)$ was computed using only the data from the two wavelengths, rather than as a fit to all the data. The latter method provides less detail. Figure 19.1 shows that the data from various parts of the oceans contain complex relationships in the $\tau(865)$, $\alpha(865,\lambda)$ phase space. The data points in the upper right hand portion of the phase spaces (separated with a dashed line) were collected in regions of biomass burning off the coast of Africa and over the Indian Ocean, as revealed by chemical analysis of the aerosol.

Excluding these regions of biomass burning, the $\tau(865)$, $\alpha(865,415)$ and $\tau(865)$, $\alpha(865,610)$ phase spaces show less differentiation between various regions of the oceans than the $\tau(865)$, $\alpha(865,500)$ and $\tau(865)$, $\alpha(865,660)$ phase spaces. The $\tau(865)$, $\alpha(865,660)$ phase space shows the sharpest differentiation between various regions of the oceans and shows large variability between the five sources of data from the Pacific Ocean [$\alpha(865,500)$ varies from –2 to 2].

Table 19.1. FRSR deployments

Platform	Experiment	Location	Other AOT data	Duration
R/V Ron Brown	Aerosols99	Atlantic Ocean	Microtops, SIMBAD, lidar	1 month
	INDOEX	Indian Ocean	Microtops,SIMBAD,PREDE, lidar	1 months
R/V Ron Brown	Nauru99	Tropical W. Pacific	Microtops, lidar	1 months
R/V Mirai	Nauru99	Tropical W. Pacific	Microtops	1.5 months
Island of Nauru	Nauru99	Tropical W. Pacific	Full complement	2 months
R/V Melville	SIMBIOS	Gulf of California	Full complement	1 month
R/V Polar Star	U. Miami	Australia-Mexico-US		2 months

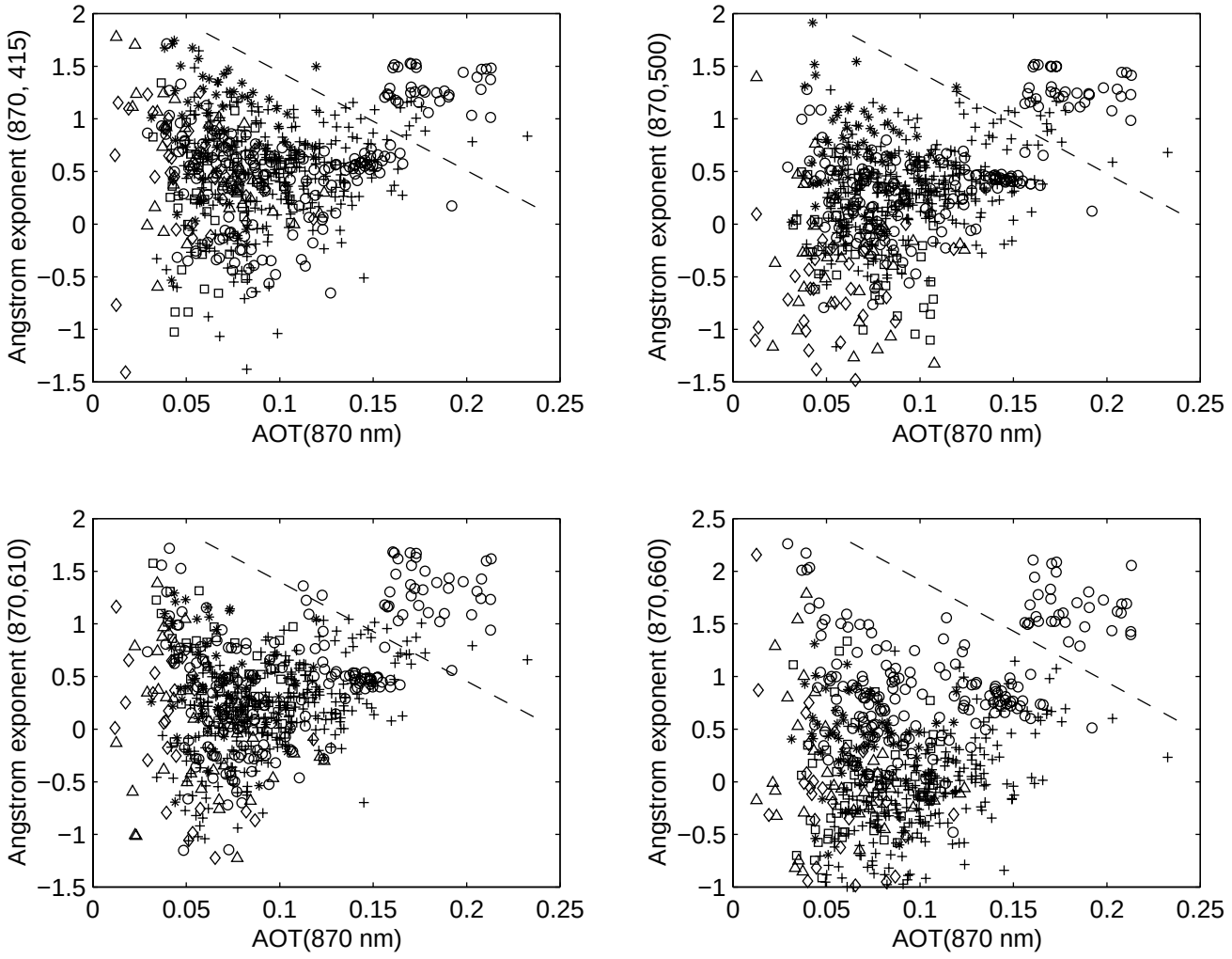

Figure 19.1. Plots of $\tau(865)$ versus $\alpha(865,\lambda)$ for the six cruises. Atlantic and Indian Ocean transects (Aerosols99/INDOEX) are shown as circles and a Pacific transect (Polar Star) as plus symbols. Data from the Tropical Western Pacific (Nauru99) are shown as squares, triangles, and diamonds, and data from the Gulf of California and California coastal waters are indicated with stars. The dashed line distinguishes aerosol associated with biomass burning (upper right corner of phase space). Note the change in the Angstrom scale for $\alpha(870,660)$.

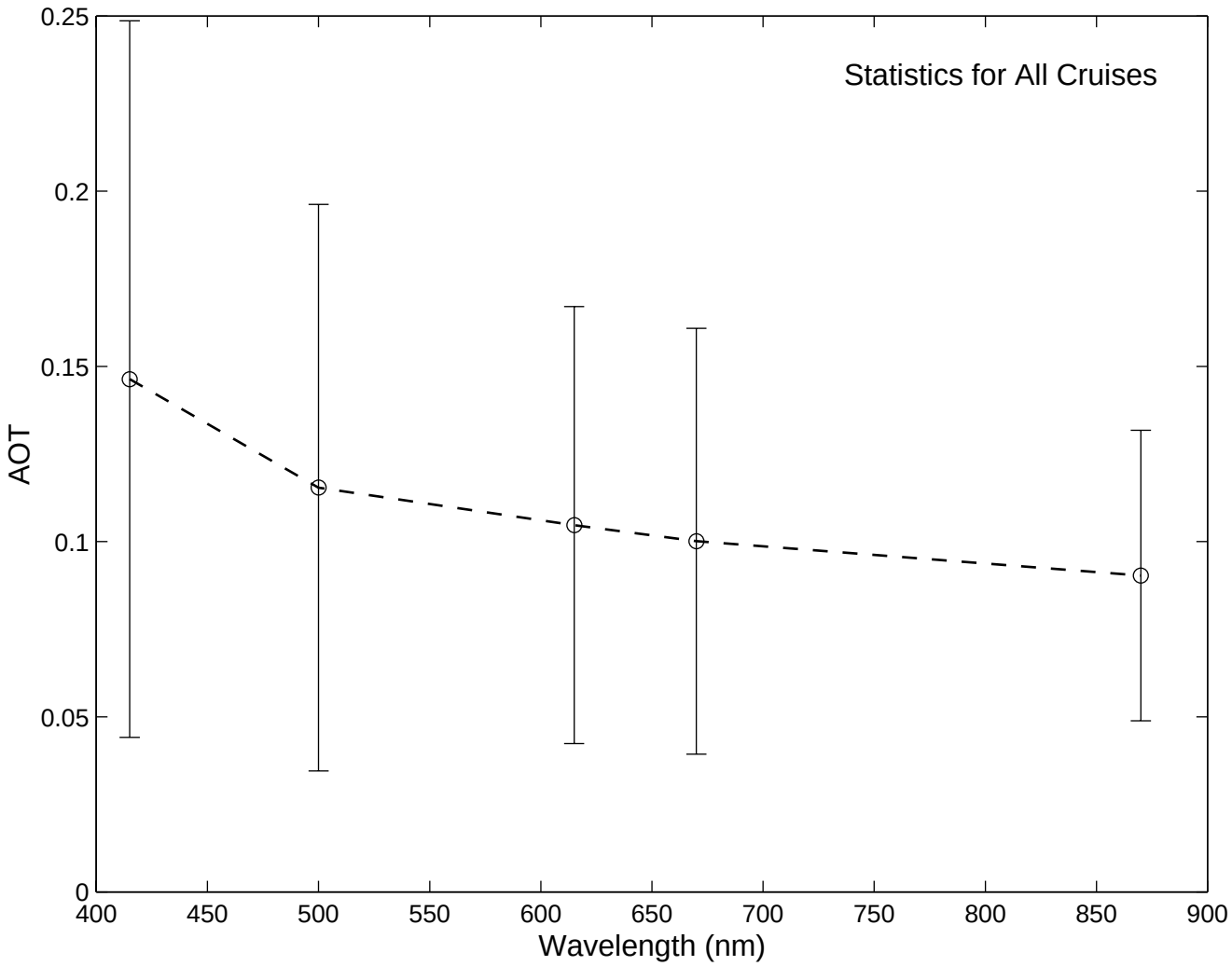

Figure 19.2. Composite of aerosol optical thickness versus wavelength for all six cruises that pass the cloud and uncertainty filters. Means are indicated with circles and the standard deviations as error bars.

A conspicuous feature of the phase plots is the presence of negative and near-zero two-wavelength Angstrom exponents in the data from every cruise, a feature that has been linked through chemical analysis to the occurrence of sea-salt aerosol. The singular exception to this rule is $\alpha(865,660)$ in the Atlantic and Indian Oceans where almost all Angstrom exponents are positive in this wavelength range, regardless of the type of aerosol that is present (i.e. sea-salt or biomass burning). We view this observation with caution, however, since filter degradation at 660 nm is a known problem for the type of detectors used in the FRSR. Moreover, coincident data from hand-held sun photometers do not validate this conclusion.

Statistics for the aerosol optical properties summarized in this report are presented in Figures 19.2 and 19.3. Figure 19.2 shows the mean and standard deviation as a function of wavelength for all data passing the stringent uncertainty filter outlined in the previous paragraph. It should be emphasized that the standard deviations represent the variation in the aerosol optical thickness values over the ocean rather than instrument uncertainty, which has been minimized by the filtering technique. The large standard deviations, particularly in the visible wavelengths, are a fundamental problem when correcting satellite ocean color for atmospheric aerosol scattering. We assume that the lower bound on the standard deviations roughly represents typical aerosol conditions in clean air masses far removed from continental sources, while the upper bounds represent conditions in polluted air.

The mean and standard deviation of the data passing the uncertainty filter sorted by ocean are presented in Figure 3(*a-c*). The experiments during which these ocean-segregated data were collected are Aerosols99 (Atlantic Ocean), INDOEX (Indian Ocean), and Polar Star Cruise (Pacific Ocean). Cruise trajectories suggest that the data collected over the Atlantic Ocean should have less continental influence, relative to the Pacific and Indian Ocean Cruises, an idea reinforced by the generally lower aerosol optical thickness observed in the

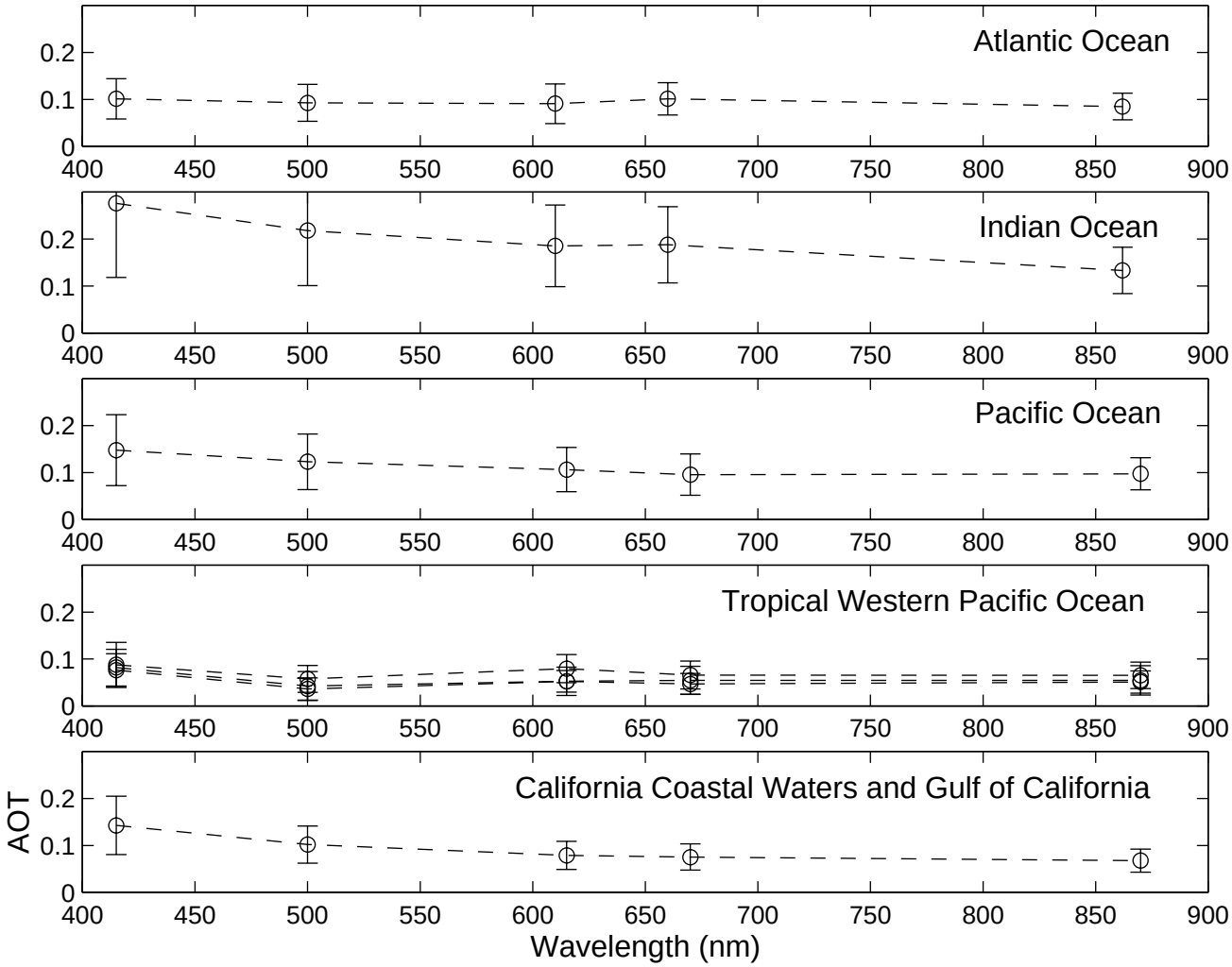

Figure 19.3. Means (circles) and standard deviations (error bars) for all data collected in the region specified in the upper right hand corner of the plot.

visible wavelengths. The Angstrom exponents for these Atlantic data are nearly zero, a characteristic that we will demonstrate for other parts of the ocean devoid of continental influence. Data from the Indian Ocean suggest aerosol optical thickness values that are nearly double the values found over the Pacific and Atlantic. The Indian Ocean data also exhibit extreme variability.

Additional data from sub-regions of the Pacific Ocean collected during regional cruises and an island deployment of the FRSR are shown in Figure 19.3 (*d-f*). The sub-regions are the Tropical Western Pacific (Nauru99, three platforms) and the California coast and Gulf of California (SIMBIOS Melville Cruise). Data from the Tropical Western Pacific indicate low optical thickness, little variability, and Angstrom exponents near zero or negative for all channels. As discussed above, data from the Atlantic Ocean also indicate Angstrom exponents near zero, although the optical thickness is somewhat larger than in the Tropical Western Pacific. Composite data from a Pacific transect (the Polar Star cruise) are similar in optical structure to the data taken from the California Coast (the Melville cruise), but also contain lower bounds that include the optical structure of the Tropical Western Pacific. We therefore conclude that the data from the Polar Star Cruise that transects the Pacific Ocean appear to faithfully represent the variety of conditions that may be observed.

19.5 CONLUSIONS

The analysis of the data from the six cruises presented here is ongoing and data from additional deployments are being processed. Nonetheless, some conclusions can be drawn from this analysis. First, aerosol optical thickness data subject to stringent uncertainty bounds suggest that the Angstrom exponent in clean oceanic air masses far removed

from continental sources is nearly zero. This result suggests that there is no mechanism present in the marine boundary layer that can produce sea-salt particles as small as the particles contained in polluted air masses. This is not surprising, since sea-salt is deliquescent and humidity is high. It is interesting to note that aerosol data collected over the Atlantic Ocean have systematically higher aerosol optical thickness than their counterparts over the Tropical Western Pacific. This observation may be explained by the smaller area of the Atlantic Ocean, relative to the Pacific, and Trade Winds in the Tropical Western Pacific. Trade winds may permit long over-ocean trajectories for air masses arriving in the Tropical Western Pacific. While dry deposition of continental aerosol may naturally cleanse the air mass, the presence of sporadic tropical convection may act as an additional source of aerosol deposition.

The air mass observed over the Indian Ocean was highly polluted. On the downside, this observation suggests that the atmospheric correction for ocean color measurements will be large over this region. On the upside, this may be the only region that truly fits the requirements for the current atmospheric correction algorithm. We make this contention on the basis of Figure 19.3 because it suggests that the Angstrom exponent in the near infrared does not differ significantly from region to region, despite significant differences in aerosol optical impacts in the visible. We surmise that the current atmospheric correction algorithm should perform well in highly polluted air masses, which is the good news. In contrast, we suggest that the current atmospheric correction algorithm is destined to fail in relatively clean air masses, or polluted air masses that possess the characteristics shown in Figure 3c. Because of this optical structure, which appears to be present over relatively large areas of ocean, we endorse the development of a new atmospheric correction scheme based on climatology, perhaps supplemented by aerosol transport models. Another approach may be to incorporate additional data to help select an appropriate aerosol model, since $\alpha(870,765)$ shows little information leading to an accurate specification of

$$\tau(870, wavelengths < 765).$$

It can be argued that the correction factor will be small in clean air masses, so the fact that the current algorithm may not perform well under these conditions may be considered tolerable. To the contrary, we argue that the area of the oceans covered by relatively clean air is likely to be much larger than that covered by polluted air, so slight errors in the correction scheme are greatly compounded in the context of global estimates.

REFERENCES

Gordon, H.R. 1978: Removal of atmospheric effects from satellite imagery of the oceans. *Applied Optics*, **17**, 1631-1636.

Gordon, H.R., D.K. Clark, J.L. Mueller, and W.A. Hovis 1980: Phytoplankton pigments derived from the Nimbus-7 CZCS: initial comparisons with surface measurements. *Science*, **210**, 63-66.

Gordon, H.R., and D.K. Clark 1981: Clear water radiances for atmospheric correction of coastal zone color scanner imagery, *Applied Optics*, **20**, 4175-4180.

Gordon, H.R. and M.Wang 1994: Retrieval of water-leaving radiance and aerosol optical thickness over the oceans with SeaWiFS: a preliminary algorithm. *Applied Optics*, **33**, 443-452.

Reynolds, M.R., M.A. Miller, and M.J. Bartholomew, 1999: A fast-rotating, spectral shadowband radiometer for marine applications, *J. Atmos. Ocean. Tech.*, (in press).

This research was supported by the

SIMBIOS NASA interagency agreement # 97888

PEER REVIEWED PUBLICATION

Benkovitz, C.M., M.A. Miller, S.E. Schwartz, and O. Kwon, 2000: The influence of atmospheric dynamics on the distribution and loading of SO2 and sulfate over the North Atlantic and Europe, *G3* (electronic publication), submitted.

Frouin, R., B. Holben, M.A. Miller, C. Pietras, E. Ainsworth, J. Porter, and K.Voss, 2000; Sun photometer and sky radiance measurements and data analysis protocols. Chapter 11; Ocean optics protocols for satellite ocean color sensor validation, revision 2; *NASA Tech. Memo*. 2000-20996, edited by G.S. Gargion and J.L. Mueller.

Pietras, C.M., M.A. Miller, E.Ainsworth, R.Frouin, B.Holben, and K.Voss, 2000: Calibration of sun photometers and

sky radiance sensors; in Chapter 5; Ocean optics protocols for satellite ocean color sensor validation, revision 2; *NASA Tech. Memo*. 2000-20996, edited by G.S. Gargion and J.L. Mueller.

Porter, J.N., M.A. Miller, C. Motell, and C.Pietras, 2000: Use of hand-held sun photometers for measurements of aerosol optical thickness at sea. Submitted to *J. Atmos. Ocean. Tech*.(in press).

Reynolds, R.M., M.A. Miller, and M.J. Bartholomew, 2000: Design, operation, and calibration of a shipboard fast-rotating shadowband spectral radiometer. Submitted to *J. Atmos. Ocean. Tech*.(in press)

Reynolds, R.M., M.A. Miller, and M.J. Bartholomew, 2000: A fast-rotating, spectral shadowband radiometer for marine applications, *J. Atmos. Ocean. Tech*., (in press)

Voss, K.J., E.J. Welton, P.K. Quinn, R. Frouin, M.A. Miller, and R.M. Reynolds, 2000: Aerosol optical depth measurements during the Aerosols99 experiment, *J. Geophys. Research*, (accepted).

Quinn, P.K., D.J. Coffman, T.S. Bates, T.L. Miller, J.E. Johnson, E.J. Welton, C. Neusüss, M.A.Miller, and Sheridan, P 2000: Aerosol Optical Properties during INDOEX 1999: Means,Variability, and Controlling Factors, *J. Geophys. Research*, (submitted).

PRESENTATIONS

Benkovitz, C.M., M.A. Miller, S.E. Schwartz , and R.C. Easter, 2000: Effects of Sulfur Emissions from Popocatepelt Volcano on the Central U.S. in June 1997; AGU Fall Meeting

Miller, M.A., R. M. Reynolds, and M.J. Bartholomew, 1999: Aerosol optical thickness and diffuse irradiance measurements during INDOEX, AGU Meeting.

Reynolds, R.M. and M.A. Miller, 1999: Instrument demonstration at the 9th Annual ARM Science Team Meeting, San Antonio, Texas.

Chapter 20

Measurements of Aerosol, Ocean and Sky Properties at the HOT Site in the Central Pacific.

John N. Porter and Ricardo Letelier

Hawaii Institute of Geophysics and Planetology, University of Hawaii, Honolulu, Hawaii

20.1 INTRODUCTION

Monthly cruises have been made to the HOT site (~100 km north of Oahu) since October 1988. The goal of these cruises is to make hydrography, chemistry, and biology observations (PI: Dave Karl and Roger Lucas). Measurements are typically made at a near coastal station (Kahe) on the first day to test the equipment and to obtain coastal shallow water (~1500m) observations. The second and third days are spent at the HOT site. On the morning of the fourth day, measurements are made at the HOT site and noontime measurements are made at the Hale-Aloha station near the mooring before returning to port by early the next morning. The locations of the three stations are:

- Kahe (21.34^o N, 158.27^o W)
- HOT (22.75^o N, 158.0^{o}W)
- Hale-ALOHA buoy (22.43^{o}N, 158.0^{o}W).

The routine HOT measurements are available during the summer following the year of the observations. The 1998 measurements will therefore become available during the summer of 1999. The data sets can be obtained at the National Oceanographic Data Center (NODC) or from the HOT web site http://kahana.soest.hawaii.edu/hot/hot_jgofs.html.

20.2 RESARCH ACTIVITIES

Microtops Sun Photometer Measurements

Beginning with the HOT89 cruise, aerosol optical depth measurements were made with two Microtops sun photometers. Calibration, proper measurement protocols and data analysis of the Microtops measurements were our initial concerns. The difficulty in making measurements at sea from a moving platform raised serious questions about the quality of the data. It was found that under rough conditions, it was difficult to point at the sun resulting in many measurements being biased towards larger optical depths. In order to minimize this bias, a large number of sun photometer measurements (~25) should be taken in a short period of time and the higher values should be discarded in post processing. Under rough ocean conditions, it is also best to shorten the Microtops sun photometer-sampling period (less than 5 sec.) and save only a single value (no averaging). It was also is found that the Microtops should be turned off frequently to correct for zero drift caused by temperature effects. Further discussion of the use of Microtops sun photometers on ships is given in Porter et al., 2000. A similar version of this approach is now being used by the SIMBIOS group efforts with their large collection of Microtops sun photometer data.

Calibration for our Microtops were maintained by routine Langley plot calibrations at the Mauna Loa Observatory. This was found to be more accurate than the cross calibration approach used by the SIMBIOS program (Porter at al., 2000). Although this involves additional effort, it also allowed us to test the Microtops under different conditions. It was also found that, even at a clean site like the Mauna Loa observatory, the more calibrations performed the better and outliers must be removed.

A time series of aerosol optical depth measurements made on the HOT cruises are shown in Figure 23.1 for 380 nm. An annual cycle is clearly present with a maximum during springtime, which is consistent with Asian transport. At longer wavelengths (up to 1020 nm) the annual cycle is less evident suggesting the springtime Asian transport during 1998 brought significant accumulation mode aerosol to the Central Pacific, which is most likely due to anthropogenic pollution. A similar feature is seen in the SeaWifs images processed for the HOT region for a portion of the same time period. This is shown in figure 23.2 which shows the ratio of aerosol scattered light at two wavelengths (780 and 860 nm) (eps_78). Larger ratio values correspond to smaller aerosol and smaller values to larger aerosol. Similar to the aerosol optical depth measurements, the eps_78 suggest a seasonal cycle of smaller aerosol over the HOT site during the springtime.

Aerosol optical depth measurements were made at 380, 440, 500, 675, 870 and 1020 nm, column integrated water vapor and ozone concentrations were also derived. These measurements have been submitted to the SeaBASS archive.

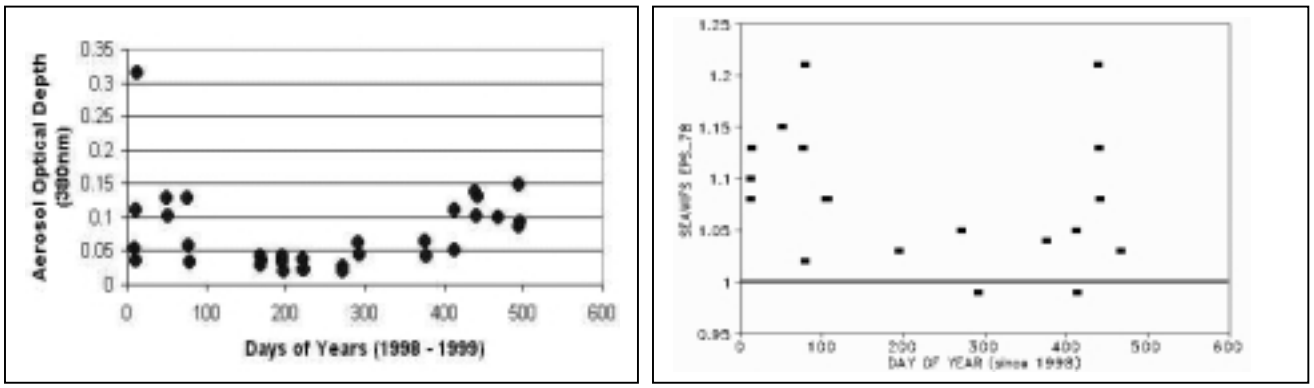

Figure 20.1. Left panel shows time series of aerosol optical depth (380 nm) at the HOT site. Right panel shows eps_78 derived from SeaWifs for the HOT site.

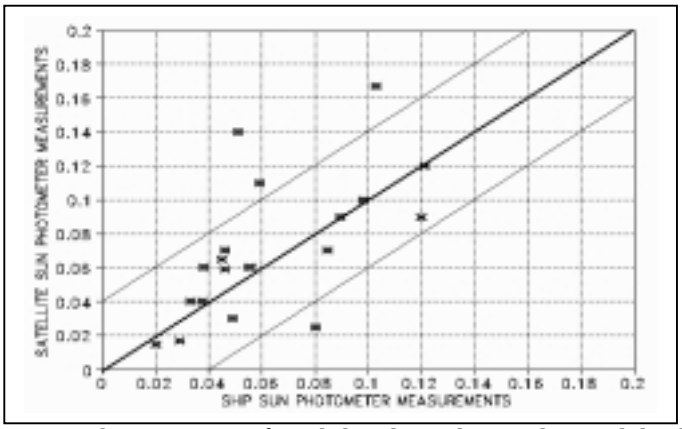

Figure 20.2. Comparison between Seawifs and ship derived aerosol optical depths (870 nm).

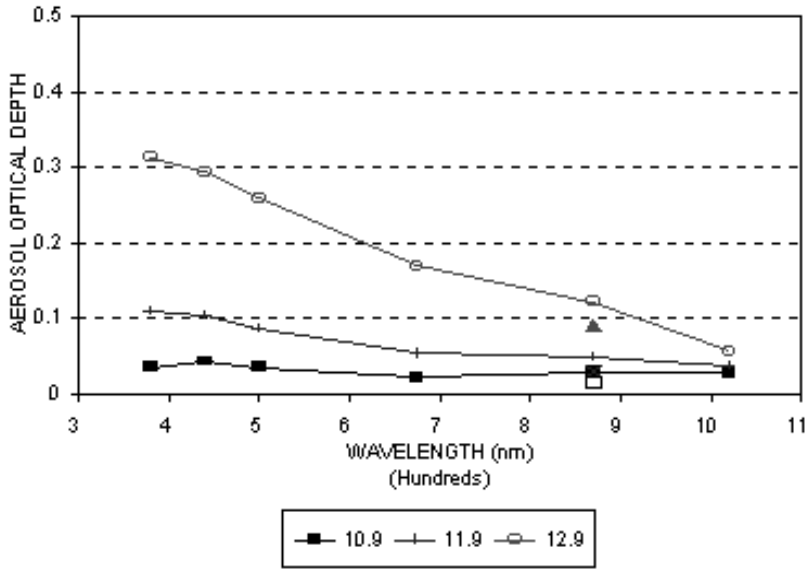

Figure 20.3. The figure shows the spectral dependence of the aerosol optical measured on January 10-12, 1998 at the HOT site.

Some comparisons between ship and satellite optical depths are shown in figure 20.2. The best comparisons are shown as blocks and the x values are cases where ship and satellite were close but not exactly the same. In general the agreement is within 0.03 but several outliers are present. These outliers usually typically occur with flat spectral optical depths, which may be dust. We have investigated the possibility of deriving aerosol size distributions from the

spectral information in the aerosol optical depths (Lienert et al., 2000; Porter et al., 2000). As an example of this inversion process, Fig. 20.3 shows a set of aerosol optical depth measurements made on HOT 89 cruise. On day 10 the aerosol was typical marine aerosol with a flat spectral shape. By day 12 it had changes to volcanic aerosol with a strong spectral shape, which is typical when the accumulation mode dominate as in city pollution. These two days illustrate polluted versus marine conditions. Figures 23.4 and 20.5 show the inversion results from the optical depths collected on day 10 and 12. It can be seen that for day 10 the various aerosol size distributions which were derived were approximately the same but that for day 12 they are all over the place. This means that when coarse mode aerosol are present the aerosol optical depths up to 1 um are not sufficient to constrain the measurements. We are now working on a more empirical approach (lookup table) to estimate the coarse mode based on realistic aerosol models (Porter and Clarke, 1997).

In-Water Optics Measurements

As part of this SIMBIOS effort, routine optical measurements have been made at each of the HOT stations. Measurements are made simultaneously with a PRR (Profiling Reflectance Radiometer) and a TSRB (Tethered Spectral Radiometer Buoy). These instruments provide measurements in the visible wavelength range of downwelling irradiance and upwelling radiance at the sea surface and at depth. These measurements have been made since the HOT89 cruise (January 1998) by Karl et al. and are processed by R. Letelier and J. Bartlett. Deployment and calibration procedures follow the recommended protocols for SeaWiFS calibration and validation. Immediately following each monthly HOT cruise, the PRR data are processed and submitted to SeaBASS. The processed PRR and TSRB data are also available online for use by the scientific community http://picasso.oce.orst.edu/ORSOO. This web site also provides details of the measurement locations, instrumentation, and deployment procedures. The optical data resulting from this ongoing effort will aid in the interpretation of the temporal and spatial variability of the constituents of Hawaiian waters.

Sky Radiometer

We have recently begun using a manual radiometer to measure sky radiance from ship and aircraft platforms. The goal is to collect spectral radiance measurements from scattering angles of 3-25°. The spectral measurements are then used in the inversion process described above to better restrict the aerosol possibilities. One example of these measurements is shown in Fig. 20.6.

Measurements of the Aerosol Scattering and Absorbing Coefficients and the Aerosol Phase Function

During 1998 a prototype polar nephelometer was built to measure the aerosol phase function (Porter et al., Hilo Ocean Optics meeting in 1998). Two new improved versions have been built. Measurements are made at three wavelengths (1064, 532, 355 nm) and include the aerosol scattering coefficient and aerosol phase function from ~3 to 177°. An example from our ground based version is shown in Figure 23.7 for marine aerosol.

As part of this effort a soot absorption photometer was also acquired. Measurements on several HOT cruises during the spring time had absorption values of $1x10^{-5}$ m^{-1} which is surprisingly high and further suggest Asian transport to the Central Pacific. During selected future HOT cruises we will be making measurements of the aerosol scattering and absorption coefficients. This should help to better understand the aerosol properties of the Central Pacific.

Marine Shadowband Radiometer

During the past three years we have been working on a custom marine shadowband radiometer which will save aerosol optical depths and downwelling irradiance at many wavelengths. This system uses a gimbaled cosine response detector and a rotating shadowband arm which shadows the detector. A temperature controlled CVI Laser spectrometer is used to collect the light which is saved on a portable computer. The system has been tested on several cruises and the gimbal works well. A new improved cosine response collector has been built and is now being tested. Although the system is not yet complete, we anticipate it will be soon and will be used on future cruises.

Modeling Efforts

We have several topics we are looking at using modeling efforts. These include algorithms to derive information on the aerosol type from sun photometer measurements, studies of the surface reflection problem, and satellite retrievals of aerosol type and the wavelength dependence of aerosol radiance.

In order to study these effects we have developed an atmospheric Monte Carlo model. This code has been compared successfully with the Nakajima RTRN algorithm for a Lambertian surface. A Cox and Munk model modified for whitecaps will be used for the final calculations.

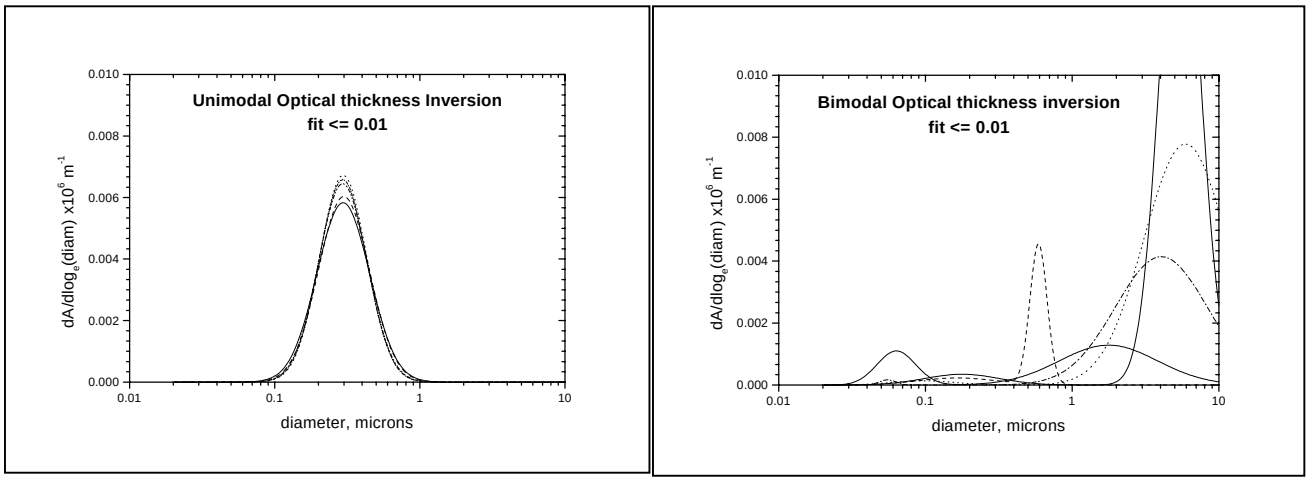

Figure 20.4. Left panel shows the aerosol distributions derived from sun photometer measurements made on day 12 in Fig. 11.

Figure 20.5. Right panel shows the aerosol distributions derived from sun photometer measurements made of day 10 in Fig. 11.

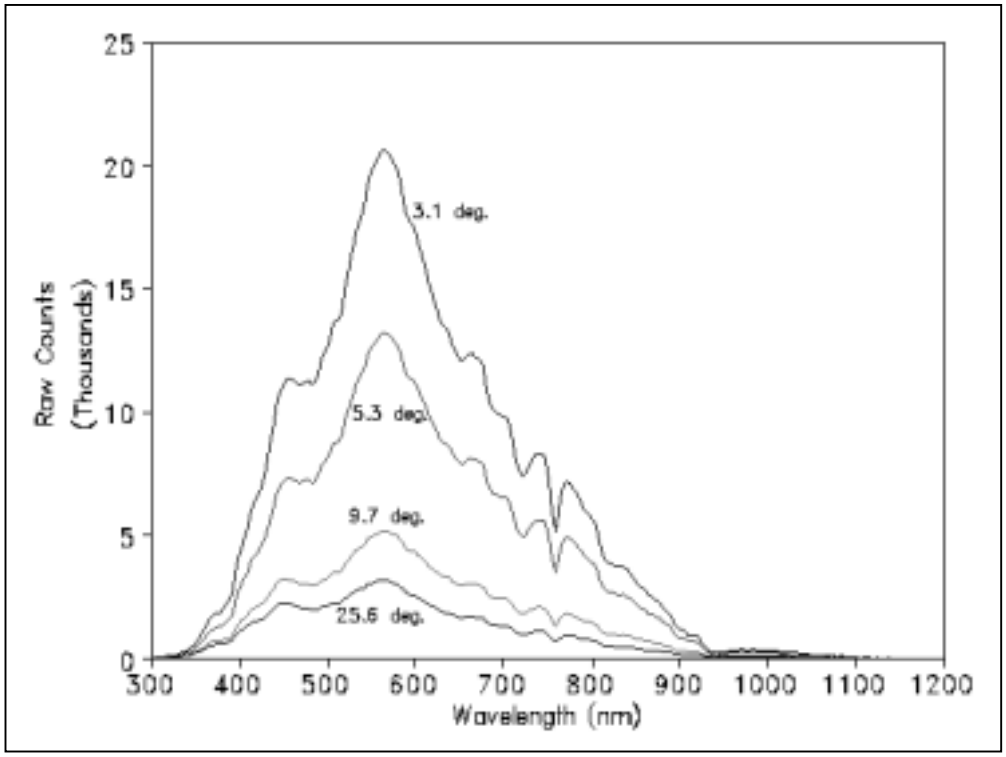

Figure 20.6. Spectral sky radiance measurements made on a HOT cruise from a manual sky radiometer. Measurements shown here are for 3.1, 5.3, 9.7, and 25.6° from the sun.

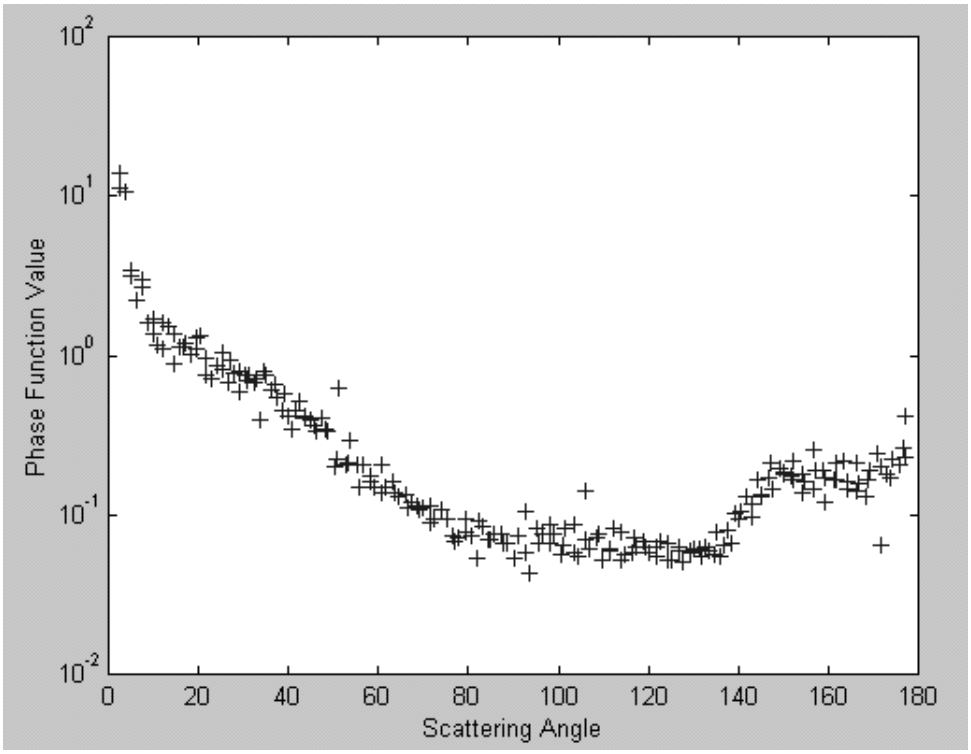

Figure 20.7 Aerosol phase function measurements made at Bellows Beach with our ground based polar nephelometer. Here five separate scans are layed on top of each other showing the measurements are reproducible. During the measurements marine sea spray was dominant but pollution from Asia was also present.

REFERENCES

Lienert, B.R., J.N. Porter, and S.K. Sharma, 2000: Repetitive Genetic Inversion of Optical Extinction Data, *Applied Optics* (submitted).

Porter, J., Clarke, A., 1997: An Aerosol Size Distribution Model Based on In-Situ Measurements. *J. Geophy. Res*., **102,** 6035-6045.

Porter, John N., Tom F. Cooney and Craig Motell, 1998: Coastal aerosol phase function measurements with a custom polar nephelometer. *Ocean Optics XIV* Conference, Kona, Hawaii.

Porter, J.N., Lienert, B., S.K. Sharma, 2000: Using the Horizontal and Slant Lidar Calibration Methods To Obtain Aerosol Scattering Coefficients From A Coastal Lidar In Hawaii. *Journal of Atmospheric and Oceanic Technology* (in press).

Porter, J, Miller, M., Pietras, C., 2000: Use of the MicroTops Sunphotometer On Ships. *Journal of Atmospheric and Oceanic Technology* (accepted).

Porter, J. N., A.D. Clarke, and B. R. Lienert, 2000: Aircraft/Surface Derived Aerosol Optical Properties Near Hawaii For Satellite Validation, *SPIE* Remote Sensing of the Atmosphere, Environment and Space, Sendai, Japan.

This research was supported by the

SIMBIOS NASA interagency agreement # 97136

PEER REVIEWED PUBLICATION

Porter, J., Clarke, A., 1997: An Aerosol Size Distribution Model Based on In-Situ Measurements. *J. Geophy. Res*., **102,** 6035-6045.

Porter, J.N., Lienert, B., S.K. Sharma, 2000: Using the Horizontal and Slant Lidar Calibration Methods To Obtain Aerosol Scattering Coefficients From A Coastal Lidar In Hawaii. *Journal of Atmospheric and Oceanic Technology* (in press).

Porter, J, Miller, M., Pietras, C., 2000: Use of the MicroTops Sunphotometer On Ships. *Journal of Atmospheric and Oceanic Technology* (accepted).

Lienert, B.R., J.N. Porter, and S.K. Sharma, 2000: Repetitive Genetic Inversion of Optical Extinction Data, *Applied Optics* (submitted).

OTHER PUBLICATIONS

Porter, John N., Tom F. Cooney and Craig Motell, 1998: Coastal aerosol phase function measurements with a custom polar nephelometer. *Ocean Optics XIV* Conference, Kona, Hawaii.

Porter, J. N., A.D. Clarke, and B. R. Lienert, 2000: Aircraft/Surface Derived Aerosol Optical Properties Near Hawaii For Satellite Validation, *SPIE* Remote Sensing of the Atmosphere, Environment and Space, Sendai, Japan.

.

Chapter 21

Assessment of the Contribution of the Atmosphere to Uncertainties in Normalized Water-Leaving Radiance: A Combined Modeling and Data Analysis Approach.

Knut Stamnes, Wei Li and Bingquan Chen

Department of Physics and Engineering Physics, Stevens Institute of Technology, New Jersey

21.1 INTRODUCTION

Our research for the SIMBIOS program has been focused on modeling and simulation studies as well as the development of atmospheric correction algorithms. Based on our original proposal and discussions at the SIMBIOS team meetings and workshops, the objectives of our research can be summarized as follows: (i) Use our radiative transfer model for the coupled atmosphere-ocean system to simulate the radiation field at arbitrary levels and in any desired direction in the atmosphere and ocean so as to provide a firm connection between the signal received by the satellite sensor and by a sensor looking down into the water column just above the surface and just below it. (ii) Use the simulations to quantify the influence of atmospheric aerosols on the water-leaving radiance, and to quantify the error in the water-leaving radiance as a function of uncertainties in the aerosol optical properties, mass loading and vertical extent. (iii) Use the model simulations in conjunction with validation measurements taken by other SIMBIOS investigators (for satellite overpasses) to assess our understanding of the radiative transfer process in the coupled atmosphere-ocean column, and to examine the extent to which the model provides a realistic prediction of simultaneously measured in situ water-leaving radiance and the radiance received by the satellite sensor. (iv) Modify and improve an existing atmospheric correction algorithm, based on the work above, as needed by constructing new look-up tables that include scattering by ocean particles. (v) Carry out approaches to developing an atmospheric correction algorithm for ocean color imagery with strongly absorbing aerosols.

21. 2 RESEARCH ACTIVITIES

We have carried out studies aimed at examining the accuracy of methods employed for computing aerosol optical properties. Accurate aerosol optical properties are critically important for atmospheric correction as well as for development of algorithms to retrieve aerosol optical properties and chlorophyll concentration.

Algorithm Development

We have developed a new algorithm for simultaneous retrieval of the chlorophyll concentration [C] and the aerosol optical properties [τ_a(865) and model]. We have used synthetic data to test the basic soundness of our algorithm. Work on processing of satellite data and comparing our results with those from Gordon and Wang's algorithm and Siegel's algorithm is in progress.

Collaborations

Collaborations with other PIs in the SIMBIOS Program and collaborations with other investigators in ocean optics and atmospheric correction: (a) We have had close collaborations with Dr. S.-C. Tsay at NASA GSFC on this study. (b) We have been collaborating with Drs. J.J. Stamnes and O. Frette at University of Bergen, Norway on the problems of atmospheric correction as well as bio-optical models appropriate for use in open ocean and coastal waters. (c) We have been collaborating with Dr. Menghua Wang at SIMBIOS Project Office on resolving the aerosol issue.

21.3 RESEARCH RESULTS

We have compared the following two methods in computing aerosol optical properties: (i) Method 1 (Shettle and Fenn, 1979): (a) An effective refractive index is generated for a multi-component aerosol population: i.e. the multi-component aerosol model is reduced to a single component with an effective refractive index. (b) The optical properties of the aerosols are computed based on this single-component aerosol model with its effective refractive index. (ii) Method 2 (Tsay and Stephens, 1990): (a) For a multi-component aerosol, the optical properties of each aerosol component are computed separately. (b) The optical properties of the aerosols are computed as the concentration-weighted-average of the optical properties of each aerosol component. Comparisons between methods 1 and 2 for

computing TOA reflectances indicate that the difference is more than 10%, which is larger than the total contribution by the ocean. Thus, this error or uncertainty is significant and must be corrected.

Removing the aerosol contribution from the measured TOA radiance is the most important issue in atmospheric correction. Accurate removal of the aerosol contribution requires: (i) access to accurate aerosol optical properties; (ii) a critical re-examination of the adequacy of current aerosol models. Accurate computation of aerosol optical properties is critically important for atmospheric correction and ocean chlorophyll retrieval. Further studies are required to establish which method (Shettle and Fenn, or Tsay and Stephens, or other) is adequate for computing aerosol optical properties. More data on aerosol optical properties and their variability over the world's oceans are needed for testing and validation of theoretical approaches.

Algorithm Development

We have developed a new algorithm for simultaneous retrieval of the chlorophyll concentration and the aerosol optical properties based on a radiative transfer model for the coupled atmosphere-ocean system that includes rigorous multiple scattering computations. The algorithm is described in the figure 24.1: "Flowchart: Simultaneous retrieval of aerosol optical properties and chlorophyll concentration". Our new approach does not employ the *black-pixel assumption*. It relies on channels at λ = 490, 555, 765, and 865 nm, and on an iterative method for simultaneous retrieval of the chlorophyll concentration [C] and the aerosol optical properties [τ_a(865) and model]. This algorithm can be applied to non-absorbing, weakly-absorbing as well as strongly-absorbing aerosols.

ACKNOWLEDGMENTS

This work was supported by the National Aeronautics and Space Administration (NASA) under the contract NAS5-97138.

This research was supported by the

SIMBIOS NASA contract # 97138

PEER REVIEWED PUBLICATIONS

Bingquan Chen, Knut Stamnes, Banghua Yan, Oyvind Frette, and Jakob J. Stamnes, 1998: Water-leaving radiance in the NIR spectral region and its effects on atmospheric correction of ocean color imagery. *Journal of Advanced Marine Science and Technology Society*, Vol. **4**, No. 2, 329-338.

PRESENTATIONS

Yan, Banghua, Knut Stamnes, and Bingquan Chen, 1999: A Generalized Algorithm for Atmospheric Correction of the Ocean Color Imagery: Feasibility Simulation. AGU 1999 Spring Meeting in Boston.

Knut Stamnes, Wei Li, and Bingquan Chen, 2000: A simple inversion algorithm for simultaneous retrieval of aerosol optical properties and chlorophyll concentration. Workshop on Hyperspectral Imaging held at University of Puerto Rico, Mayaguez, September 8-9, 2000.

Knut Stamnes, Banghua Yan, Wei Li, Bingquan Chen, Jakob J. Stamnes, and Si-Chee Tsay, 2000: Atmospheric correction for strongly absorbing aerosols. Ocean Optics XV, Monaco, October 16-20, 2000.

Flowchart: Simultaneous retrieval of aerosol optical properties and chlorophyll concentration

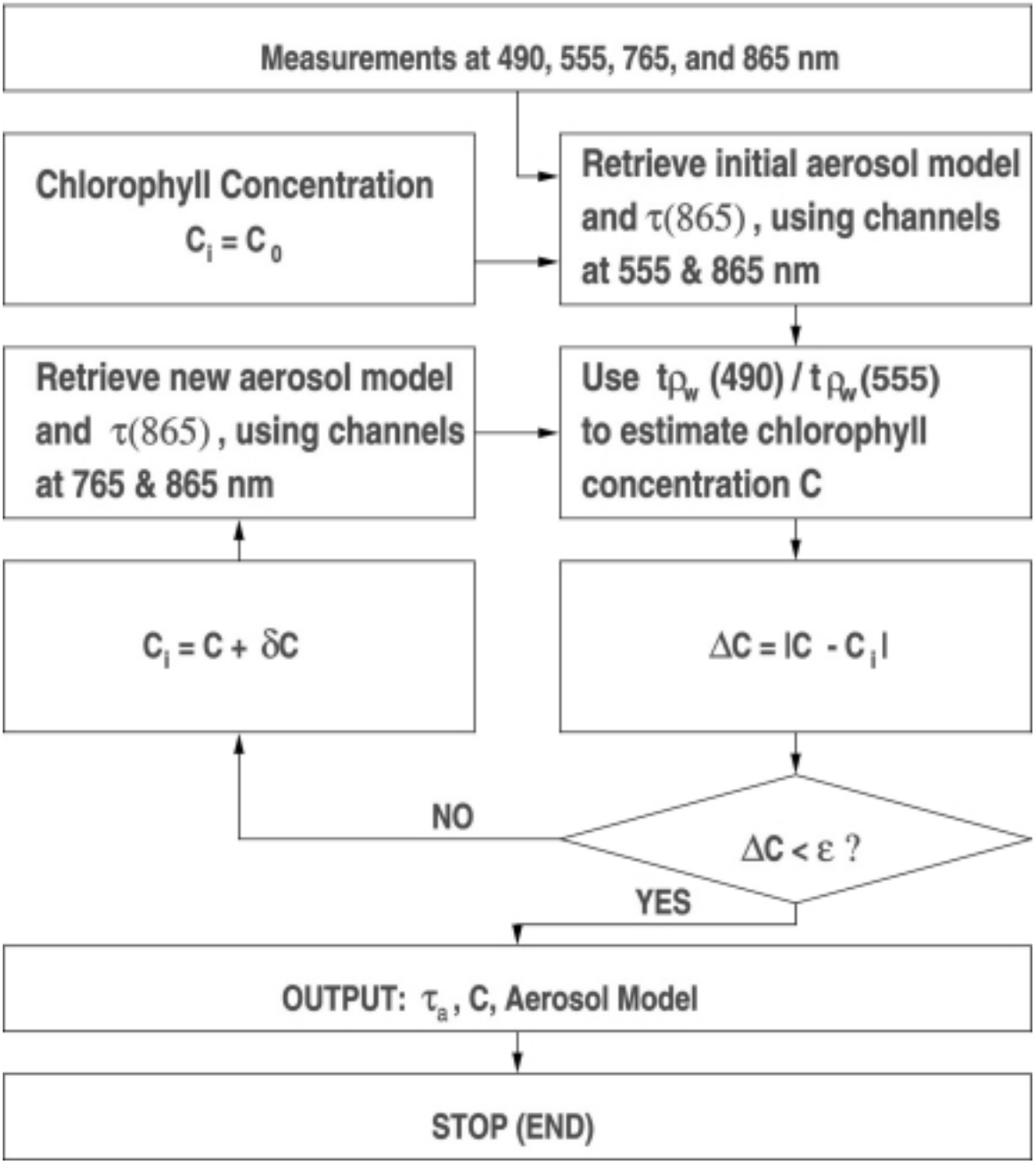

Chapter 22

SOURCES OF VARIABILITY IN CHLOROPHYLL ANALYSIS BY FLUOROMETRY AND BY HIGH PERFORMANCE LIQUID CHROMATOGRAPHY

Laurie VanHeukelem, Crystal S. Thomas and Patricia M. Glibert

Horn Point Laboratory, University of Maryland Center for Environmental Science, Cambridge, Maryland

22.1 INTRODUCTION

The need for accurate determination of chlorophyll *a* (chl *a*) is of interest for numerous reasons. From the need for ground-truth data for remote sensing to pigment detection for laboratory experimentation, it is essential to know the accuracy of the analyses and the factors potentially contributing to variability and error. Numerous methods and instrument techniques are currently employed in the analyses of chl *a*. These methods range from spectrophotometric quantification, to fluorometric analysis and determination by high performance liquid chromatography (HPLC; Parsons et al., 1984; Clesceri et al. 1998; Jeffrey et al. 1999). Even within the application of HPLC techniques, methods vary (e.g. Goericke and Repeta 1993, Mantoura and Llewellyn 1983, Wright et al. 1991, VanHeukelem and Thomas in press). Here we provide the results of a comparison among methods and provide some guidance for improving the accuracy of these analyses.

These results are based on a round-robin conducted among numerous investigators, including several in the SIMBIOS and HyCODE Programs. Our purpose here is not to present the full results of the laboratory intercalibration; those results will be presented elsewhere. Rather, here we highlight some of the major factors that may contribute to the variability observed. Specifically, we aim to assess the comparability of chl *a* analyses performed by fluorometry and HPLC, and we identify several factors in the analyses which may contribute disproportionately to this variability.

Experimental Design

There were three aspects to this study that are analyzed here. The first is a comparison of standards of pure chl *a* analyzed by the participant laboratories using fluorometry and HPLC. The second aspect examines the effect of the difference between instrumental approaches when the standards of chl *a* have a variable, but known, contribution of divinyl chl *a* (DV chl *a*). Finally, analysis of chlorophyll on laboratory-prepared and field-collected filters were compared using varying extraction protocols or injection techniques prior to pigment separation and detection. All instruments were calibrated with the same set of standards prior to the above tests.

Preparation of the Stock Solutions

The chl *a* stock solution was prepared by dissolving chl *a* granules (Fluka 25730) in 90% acetone and initially determining the stock concentrations by spectrophotometric analysis (Clesceri et al. 1998). A Hitachi U-3100 spectrophotometer, with 2 nm bandwith, was employed. Absorbances between 0.1 and 1.0 were read using an extinction coefficient of 87.67 at 664nm. The absorbance accuracy of this instrument was verified using National Institute of Standards and Technology traceable neutral density filters (Starna cells RM-N1N35N and RM-1N2N3N).

For distribution to the various participants, standards of 5 calibration levels were prepared. All dilutions were made using Class A volumetric glassware and gas-tight glass syringes. The accuracy and precision of the pipettes and syringes were assessed prior to use. For distribution, solutions were dispensed into amber glass vials with Teflon-lined screw caps. Sufficient chl *a* standard was dispensed to allow each investigator to analyze in replicate by each method.

Extraction Procedures

For the analysis of samples on filters, two approaches were used. For one set of analyses, the same extraction procedures were employed by all participants. Samples were extracted in 90% actetone (5 ml added to filters for HPLC analysis, and 10 ml to filters for fluorometric analysis). Filters were allowed to soak for 3 to 4 hrs in the dark (-15^{o}C), after which the extract was filtered through a Teflon HPLC syringe cartridge filter (Scientific Resources Inc. 44525). Total extraction volumes took into account the average contribution of the water retained by the GF/F filters (145 µl for a 25 mm GF/F filter and 500 µl for a 47 mm GF/F filter). Hence, for the filters analyzed by fluorometry, the extraction volume of

10.145 ml was employed, while for the filters analyzed by HPLC, either 5.145 ml or 5.500 ml was used, depending on filter diameter. For the second set of analyses, participants employed their own protocols for sample extraction (see below).

Fluorometric Analyses

All participating laboratories analyzed the distributed standards using methods based on Parsons et al. (1984). There were differences among instruments employed, which will be described in more detail in a future report.

HPLC Methods

The methods used by participating laboratories varied widely with respect to instrumentation as well as sample preparation for HPLC analysis (Table 1). With most pigment HPLC methods, the sample extract is mixed with buffer (or water) prior to injection. Fully automated HPLC's can perform this step automatically. Vials containing sample extract, and separate vials containing buffer (or water), are placed in the auto-sampler compartment and an automated sequence combines the buffer with sample immediately prior to the analysis of each sample. Some autosamplers are refrigerated. Sample vials may reside in an auto-sampler compartment from 1 to 24 hr. An alternate method employs an auto-sampler compartment and an automatic injector programmed to inject a specific volume from each sample vial, but the auto-injector cannot mix sample with buffer prior to analysis. In this case, the analyst must individually combine each sample with buffer at the beginning of a sequence of analyses, which in turn results in samples residing in the autosampler for variable lengths of time after being mixed. Finally, when autosamplers are not available, manual mixing of sample extract with buffer and the manual injection of the mixture into the instrument is used.

The method of separation and detection also varied among laboratories. Investigators used HPLC instruments from either Hewlett-Packard, Dionex, Waters, or Beckman. A summary of the columns used and published mobile phases employed are summarized in Table 1.

22.2 RESULTS

Comparison of Fluorometry and HPLC Analysis for a Pure chl a Standard

The variation between the concentration as reported by participants and the concentration of chl *a*, as initially formulated and calibrated spectrophotometrically, ranged from –0.4 to 11.3% for fluorometric analyses (Fig. 22.1A). When the same standard was analyzed by HPLC (all methods), the total difference between reported and formulated values ranged from –30.6% and 26.4% (Fig.22.1A). A closer inspection, however, of the variability associated with the HPLC results indicates that accuracy was highly coupled with HPLC injection mode. The fully automated mode of injection resulted in significantly reduced variability. The differences between reported and formulated values for this standard analyzed on instruments with fully automated injection modes was –0.23% to 1.7% (Fig. 22.1A).

Comparison of Fluorometry and HPLC Analysis for a Mixed chl a Standard

Chl *a*-like products (chl *a* allomers epimers, chlorophyllide *a* (chlide *a*) and DV chl *a*) respond similarly to chl *a* in a fluorometer. However, because of different separation and reporting practices in the use of HPLC, weaker agreement would be expected when comparing results from HPLC in which samples contain varying amounts of chl *a* products. For the standard distributed that contained equal proportions of chl *a* and DV chl *a*, the chl *a* concentration reported by participants employing fluorometric techniques differed from the formulated value (sum of chl *a* and DV chl *a*) by –9.4% to 14.6% (Fig. 22.1B). This variation was slightly higher than that seen with the discrete pure chl *a* standard. At least one participant in this study chromatographically separated DV chl from chl *a* in their HPLC analyses, and hence reported individual values for each chl component. Other participants did not employ separation techniques that permitted the chromatographic separation of chl *a* from DV chl *a*. Thus, in their analysis of the mixed standard containing both chl *a* and DV chl *a*, only one peak was seen and reported. The values reported by these laboratories differed from the formulated value by –10% to 100% (Fig. 22.1B). When comparisons are limited to data resulting only from instruments in the fully automated mode, the error reduced to a range from –3.5 % to 16.1% (Fig. 22.1B).

There was some variation in the detector settings used by participants in the HPLC analysis of chl *a*. This also resulted in some degree of variability in the ability to accurately report total chl *a*, in the presence of DV chl *a* and when chl *a* was used as the calibrant (Fig. 22.2). For those laboratories using a detector setting of 436 (4 nm bandwidth) or 665 (20 nm bandwidth), the total chl *a* values reported varied by no more than 5% from the formulated value. At other wavelengths or bandwidths, the DV chl *a* response was much greater than the chl *a* response, therefore the selection of these wavelengths resulted in and overestimation of total chl *a*. A wavelength of 440 nm incurred the greatest error in the comparison here (Fig. 22.2).

Comparison of Fluorometry and HPLC Analysis for Laboratory-prepared Filters

Sample filters, with a mean consensus HPLC value of 1025 ng chl *a* per filter and a simple suite of pigments, were analyzed by all participants. These samples did not contain

chlide *a*, which can strongly affect fluorometer values and cause poor agreement between fluorometer and HPLC if not accounted for in the HPLC total chl *a* value. Additionally, the same extraction protocol was used by all laboratories and the chl *a* calibration among laboratories and between fluorometer and HPLC was standardized. Here, the fluorometer values ranged from 110 to 120% of the mean consensus HPLC value (Fig. 22.3). The range seen with HPLC values was 73.7 to 121%, including all injection modes, but 96 to 105% if the values from the manual mode of injection are excluded.

Effects Of Differing Extraction Procedures For Field-Collected Filters

In order to assess the effect of varying extraction protocols on the analysis of chl *a* by both fluorometry and HPLC, it was first necessary to establish the agreement that could be achieved within one laboratory when the identical extraction method was used. This analysis, undertaken for field samples representing a wide range of concentrations and containing a broad spectrum of pigments, revealed a strong relationship between fluorometric and HPLC values (Fig. 22.4); the maximum variation observed was $\pm$ 14% (Fig. 22.5).

Such a level of agreement, however, when varying extraction protocols are employed, would not be expected. In routine analysis, all participants used a different extraction procedure for filters in HPLC analysis than for filters in fluorometric analysis. Typically, the extraction volumes for filters used in HPLC analysis were significantly lower than those used for fluorometric analysis. Mode of filter disruption (if used) also varied. Finally, the contribution of water retained by the GF/F filter to the total extraction volume was sometimes not accounted for.

When all data are analyzed in which participants used their respective extraction protocols, the values determined by fluorometry ranged from 62% to 142% of the values determined by HPLC (Fig. 22.5). The larger discrepancies here, relative to the same comparison for samples in which extraction was standardized, are not surprising for several reasons. In addition to the differences in extraction procedure and manner in which extraction volume was determined, these results also reflect variability associated with differences in HPLC injection modes, chlide *a* reporting practices, and the ability to resolve (or report) DV chl *a*.

22.3 CONCLUSIONS

Previous intercalibration studies and methods comparisons have yielded insights into improved analytical performance for analysis of chl and other pigments (Latasa et al. 1996; Bidigare and Trees 2000; Trees et al. 2000, Hooker et al. in press). Our findings extend these previous efforts. There were three major findings from this study. First, for the analysis of a pure chl *a* standard, fluorometric results were within 11% of the formulated value while fully automated HPLC analyses were within 2% of the formulated value. Second, variability in sample composition, such as the contribution of DV chl *a*, can increase variability with both fluorometric and HPLC analyses. Third, variability in chl *a* analysis is further increased when effects of variable extraction procedures of material on filters and variable modes of injection and data reporting are incorporated in the comparison.

Effects Of Variability In Sample Composition

The best agreement between fluorometric and HPLC analyses will be attained when all chl *a* products measured by HPLC are accurately quantified and then summed. This analysis requires a careful choice of wavelength on the detector setting to avoid the potential for overestimation of total chl *a* when DV chl *a* is present (Goericke and Repeta 1993, Latasa et al. 1996, Bidigare and Trees 2000).

Effects Of Extraction Procedures

The most accurate analysis of chl *a* will be derived when careful attention is given to extraction protocols. Due to the extremely small volumes of extraction solvent used, small differences in extraction volume, or variability in water retention by the filter may have a large impact on the final calculated value.

Effects Of HPLC Injection Mode

Although the most accurate analysis of chl *a* requires modern, automated equipment, improvement in accuracy can be attained for manual mixed injection systems. As has been previously recognized (e.g. Mantoura et al. 1997), variability increases substantially when samples are premixed, then loaded on the autosampler. By maintaining a constant time interval between mixing and injecting, variability can be reduced.

Implications

These findings demonstrated that the most accurate results were obtained from good instrumentation. A combination of high quality instrumentation and good laboratory practices resulted in reduced discrepancy in reported values relative to formulated values for either instrumental approach. Attention to detector settings and injection protocols are important to reduced variability. While some sources of variability can only be reduced with improved instrumentation, other sources of variability in reported results can be reduced through mathematical corrections. Taking the results from one set of reported values derived from field analyses, the impacts of these corrections can be shown (Fig. 22.6). In this case, the data were derived from samples collected on 47 mm GF/F filters, to which 5 ml of 90%

acetone was added for extraction. As originally reported, water content contributed by the filters was not accounted for. Measured water retention by filters of this diameter is approximately 500 µl. Thus, the reported value was underestimated on average by 10% due to this factor alone. Furthermore, these samples were shown (in separate analyses) to have substantial concentrations of chlide *a*. By determining the contribution of chlide *a* to total chl *a* in this case, further improvements in accuracy were attained. These corrections resulted in final values that were, on average, 95% of the values independently determined. In summary, attention to extraction and injection methods, as well as to reporting practices when chl products are present, will reduce the variability associated with chl detection by various methods and will improve the accuracy of chl *a* results.

ACKNOWLEDGEMENTS

This work was supported by the SIMBIOS Project and the Office of Naval Research. We thank Dr. Giulietta S. Fargion and the NASA SIMBIOS Project, Goddard Space Flight Center, for support as well. The willingness to help in this endeavor extended by participants from SIMBIOS laboratories and others is greatly appreciated. This is a contribution from the University of Maryland Center for Environmental Science.

REFERENCES

Bidigare, R.R. and C.C. Trees. 2000: HPLC phytoplankton piugments: sampling, laboratory methods, and quality assurance procedures. Ch. 13, In G.C. Fargion and J.L. Mueller (eds), Ocean optics protocols for satellite ocean color sensor validation, rev. 2. NASA Technical Memorandum –2000-209966.

Clesceri, L.S., A.E. Greenberg, and A.D. Easton (eds). 1992: Part 10000, Biological Examination, Section 10200H. In Standard Methods for the examination of water and wastewater, 20th ed. Baltimore (MD): American Public Health Assoc, American Water Works Association, Water Environment Federation.

Goericke, R. and D.J. Repeta. 1993: Chlorophylls *a* and *b* and divinyl chlorophylls in the open subtropical North Atlantic Ocean. *Mar. Ecol. Prog. Ser.,* **10**, 307-313.

Hooker, S.B., H. Claustre, J. Ras, L. Van Heukelem, C. Targa, and R. Barlow, 2000: The first SeaWifS HPLC analysis round-robin experiment (SeaHARRE-1). Vol. 14 of SeaWifS Postlaunch Technical Report Series. Hooker, S.B. and E.R. Firestone (eds). NASA Technical Memorandum 104566 (in press).

Jeffrey, S.W., R.F.C. Mantoura, and S.W. Wright. (Eds.) 1997: Phytoplankton pigments in oceanography: Guidelines to modern methods. Vol. 10, Monographs on oceanographic methodology, Paris: UNESCO Publishing, 661 pp.

Jeffrey, S.W., S.W. Wright, and M. Zapata. 1999: Recent advances in HPLC pigment anlaysis of phytoplankton. *Mar. Freshwater Res.* , **50**, 879-896.

Latasa, M., R.R. Bidigare, M.E. Ondrusek, M.C. Kennicutt II. 1996: HPLC analysis of algal pigments: A comparison exercise among laboratories and recommendations for improved analytical performance. *Mar. Chem.* , **51**, 315-324.

Mantoura, R.F.C., R.G. Barlow, and E.J.H. Head. 1997: Simple isocractic HPLC methods for chlorophylls and their degradations products. In Jeffrey, S.W., R.F.C. Mantoura, and S.W. Wright (eds). Phytoplankton pigments in oceanography: guidelines to modern methods. Vol. 10, Monographs on oceanographic methodology. UNESCO Publishing. 307-326.

Mantoura, R.F.C. and C.A. Llewellyn. 1983: The rapid determination of algal chlorophyll and carotenoid pigments and their breakdown products in natural waters by reverse-phase high-performance liquid chromatography. *Anal. Chim. Acta,* **151**, 297-314.

Parsons, T.R., Y. Maita, and C.M. Lalli. 1984: A manual of chemical and biological methods for seawater analysis. Pergamon Press, New York. 173 pp.

Trees, C.C., D.K. Clark, R.R. Bidigare, M.E. Ondrusek and J.L. Mueller. 2000: Accessory pigments versus chlorophyll *a* concentrations within the euphotic zone: a ubiquitous relationship. *Limnol. Oceanogr.*, **45**, 1130-1143.

Van Heukelem, L. and C.S. Thomas. 2000: Computer-assisted high-performance liquid chromatography method development with applications to the isolation and analysis of phytoplankton pigments. *J. Chromatogr. A,* (in press).

Wright, S.W., S.W. Jeffrey, R.F.C. Mantoura, C.A. Llewellyn, T. Bjornland, D. Repeta and N. Welschmeyer. 1991: Improved HPLC method for the analysis of chlorophylls and carotenoids from marine phytoplankton. *Mar. Ecol. Prog. Ser.*, **77**, 186-196.

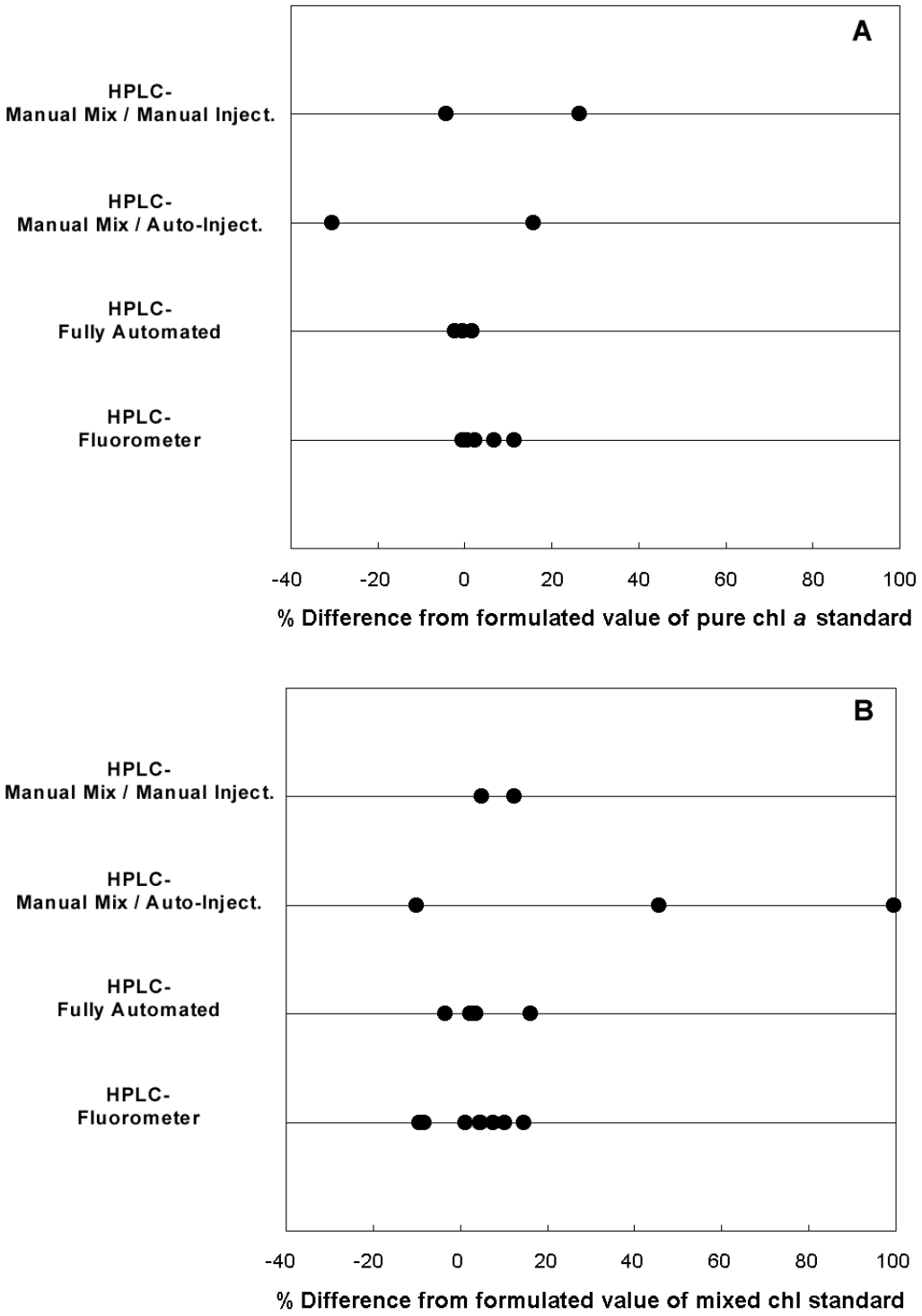

Figure 22.1 Accuracy associated with the analysis of prepared, identical chl *a* standards analyzed by participants using their own analytical methods. In all cases, chl *a* was used as the calibrant. The percent differences between the values reported by each participant and the values as formulated are shown for a standard containing only chl *a* in (A) and for a standard containing equal portions of DV chl *a* and chl *a* in (B). Data is sorted by mode of analysis. In (A) each data point represents the mean of triplicate analyses. Average variability for fluorometric analyses was 1.5%, for HPLC fully automated analyses 0.8%, for manual mix/ auto-inject analyses 14.2% and for manual mix/ manual inject analyses 7.3%.

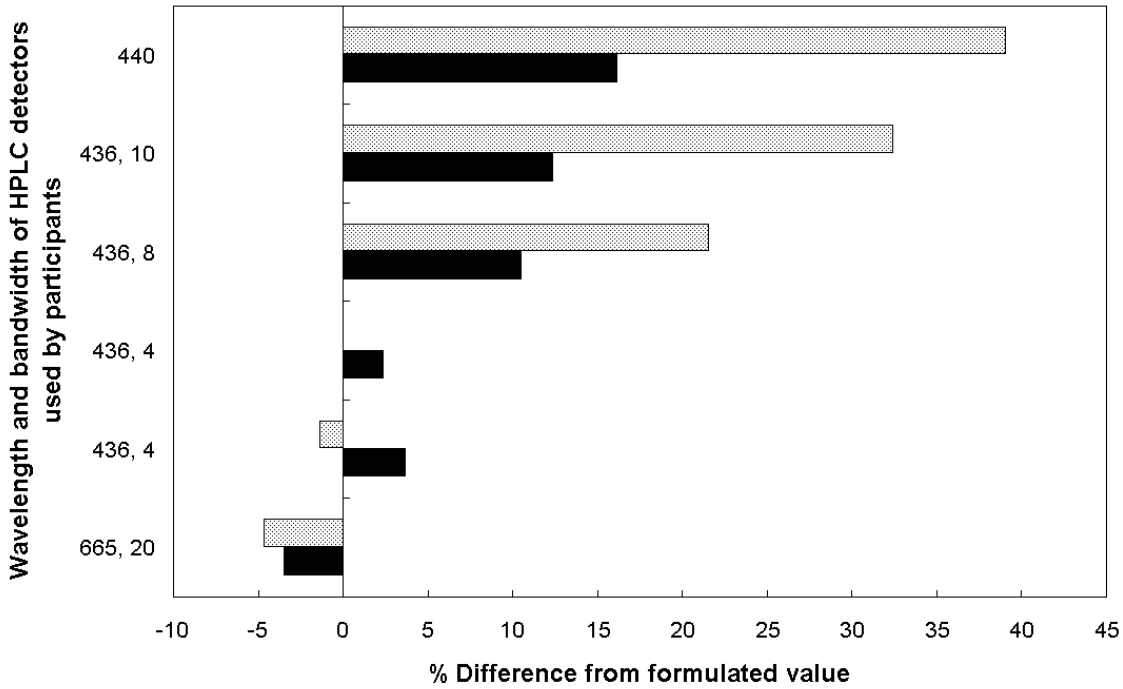

Figure 22.2. Errors in the HPLC analysis of DV chl *a* when chl *a* was used as the calibrant. Error varies with wavelength and bandwidth used. Standards containing only DV chl *a* (stippled bar) and equal portions of chl *a* and DV chl *a* (solid bar) were used. Only data from laboratories which demonstrated error of ≤ 4% in the analysis of chl *a* alone were included.

Table 22.1. Injection and analysis configuration for participants employing HPLC in the detection of chl *a*.

Injection Mode	Number of participants	Type of column employed	Reference for mobile phase employed
Fully automated, refrigerated autosampler	4	C_{18} (2 investigators) C_8 (1 investigator) C_8 (1 investigator)	Mantoura and Llewellyn (1983) Van Heukelem and Thomas (in press) Goericke and Repeta (1993)
Fully automated, non-refrigerated autosampler	1	C_{18}	Wright et al. (1991)
Manual mix/auto-injection, Non-refrigerated	2	C_{18}	Wright et al. (1991)
Manual mix/ manual injection	1 1	C_8 C_{18}	Van Heukelem and Thomas (in press) Wright et al. (1991)

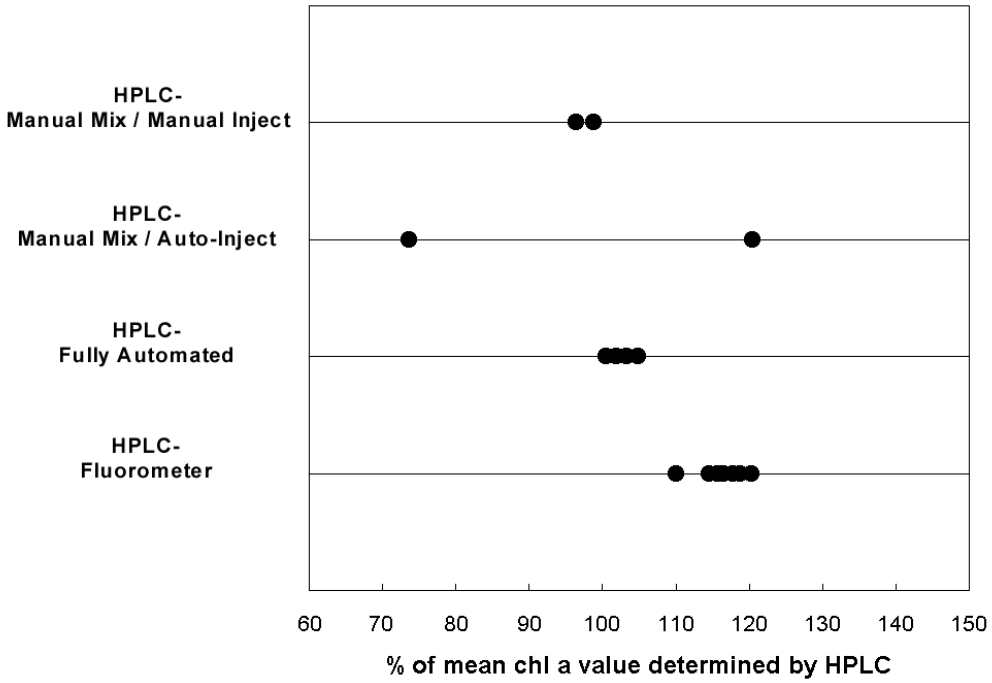

Figure 22.3. Agreement among laboratories and between fluorometer and HPLC in the analysis of replicate laboratory-prepared filters. All laboratories used their own analytical methods but employed the same procedure for extracting filters. Chl *a* values reported by individual laboratories are expressed as the % of the mean consensus HPLC value. Data are sorted by mode of analysis. Each point represents the mean of 2 analyses (with the exception of two data points).

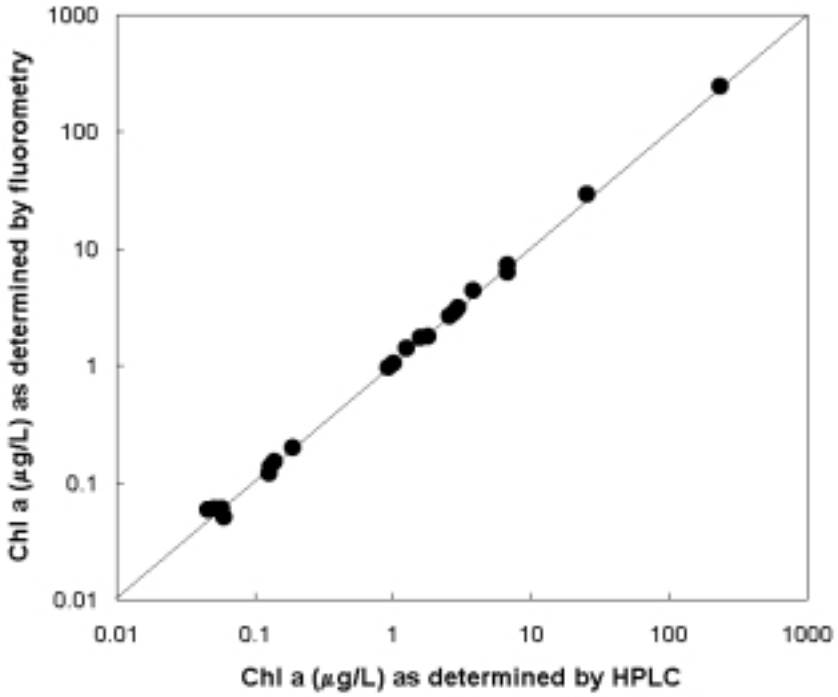

Figure 22.4. Results of replicate field sample filters of varying concentration analyzed by HPLC and fluorometer by one laboratory. The same extraction procedure was employed for filters used for HPLC analysis as those used for fluorometric analysis. In all but four cases, each point compares mean of three replicate filters analyzed by fluorometry and mean mean of three replicate filters analyzed by HPLC. For reference, the 1:1 line is drawn.

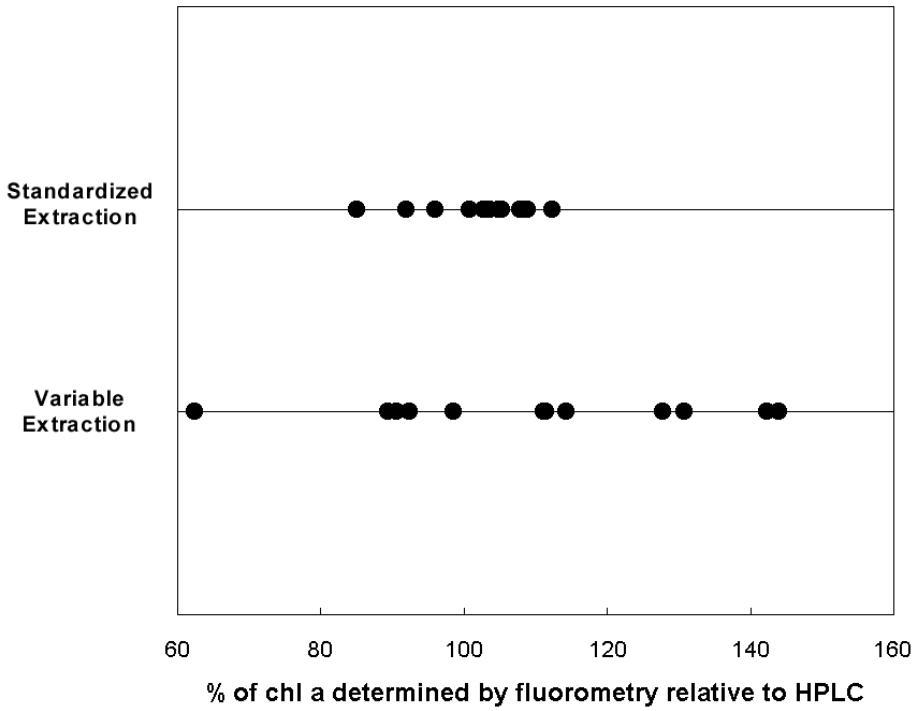

Figure 22.5. Agreement between replicate field samples of varying concentration analyzed by HPLC and fluorometry. Results of filters extracted for and analyzed on the fluorometer are compared to results of filters extracted for and analyzed on the HPLC. In the top line, all filters were extracted using the same procedure and all analyses were performed by one laboratory (Standardized Extraction). In the bottom line, results were reported by various laboratories employing their own methods for extraction, analysis and reporting (Variable Extraction). Each point compares the mean of three filters analyzed by fluorometry and the mean of three filters analyzed by HPLC.

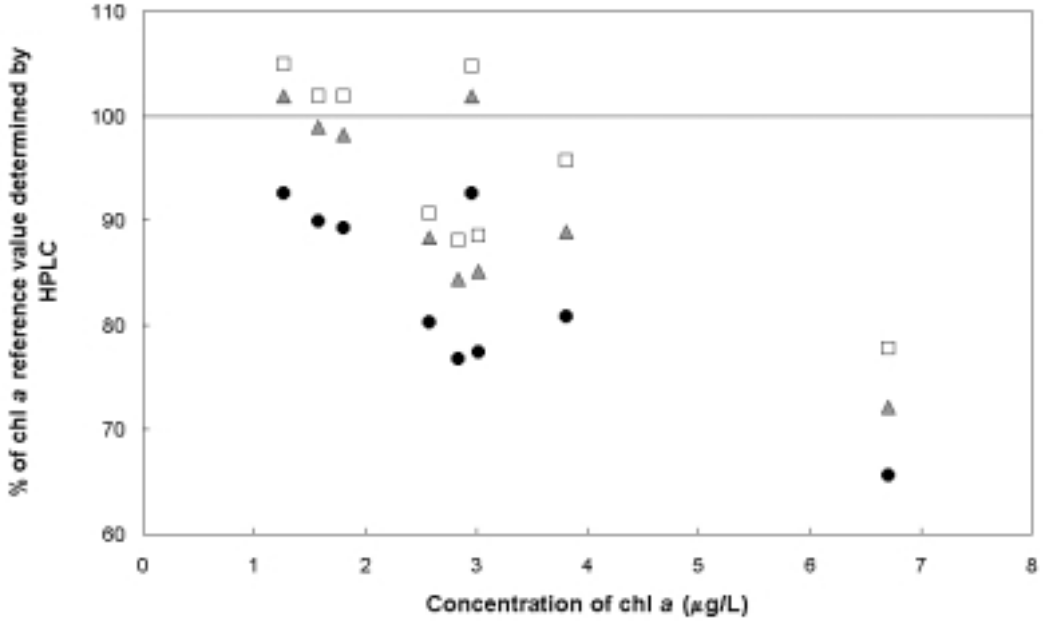

Figure 22.6. An example illustrating the ability to correct errors associated with HPLC reporting practices. Data derived from field collected filters of one participant are presented as percent of the HPLC total chl *a* values for the same sites derived by a reference laboratory. Agreement between the participants data and the reference laboratory's HPLC data is shown for (•) the data as reported, (Δ) the data corrected for extraction volume (water retained in the filter had not been accounted for in the total extraction volume) and ( ) the data corrected for extraction volumes and contribution of chlide *a* to the total HPLC chl *a* value. Each data point compares the mean of three replicate filters analyzed for each site by the participant to the mean of three replicate filters analyzed by the reference laboratory.

Chapter 23

Validation of the Water-Leaving Radiance Data Product

Oleg V. Kopelevich, Vladimir I. Burenkov, Svetlana V. Ershova, Sergey V. Sheberstov, Marina A. Evdoshenko, Genrik S. Karabashev and Constantine A. Pavlov

Ocean Optics Laboratory, P.P.Shirshov Institute of Oceanology, Moscow, Russia

23.1 INTRODUCTION

The project accomplishments made by SIO RAS group during the period of 1997-2000 are described below. The goal of this research was to assess an accuracy of data products derived from satellite ocean color data including an accuracy of the atmospheric correction algorithms for variety of meteorological and oceanological conditions and of the bio-optical algorithms for different water cases. A combined approach was used which included a direct comparison of the values of water-leaving radiance and chlorophyll concentration derived from satellite and *in situ* measured data as well as numerical simulation and theoretical analysis.

23.2 RESEARCH ACTIVITIES

New Instrumentation

Two new instruments have been constructed for field studies: a floating spectroradiometer and a portable monitor photometer (Artemiev et al. 2000a, Kopelevich 1999a). The floating spectroradiometer measures the continuous spectral distributions of downwelling irradiance just above sea surface and of upwelling radiance just beneath sea surface in the spectral range 390-700 nm with spectral resolution 2.5 nm. Measurements beneath sea surface allow to eliminate effects of sun glints and sky light reflected at surface; they are performed at a distance about 30-50 m from ship to avoid influence of ship shadow. The monitor photometer was designed to check calibration of irradiance at 554 nm and measure continuously the surface irradiance at this wavelength during spectral measurements by the spectroradiometer. The radiometric accuracy of the floating spectroradiometer and the monitor photometer is respectively 5% and 3%.

The calibration was conducted by different ways including laboratory calibration with a standard lamp and field calibration with Sun as a standard light source (Sun-shadow method);also intercalibration of the floating spectroradiometer and the submersible radiometer MER-2040 was carried out during *Akvanavt'97* cruise (Artemiev et al. 2000b, Kopelevich 1999a).

Field Measurements

Three series of field measurements have been carried out:

- in the Black and Aegean Seas, October 6-24, 1997 (Artemiev et al. 2000b, Kopelevich 1999a);
- in the eastern part of the Barents Sea in August-September 1998 (Burenkov et al. 2001, Kopelevich 1999a);
- in the eastern part of the Black Sea, September 14-25, 2000.

The latter was performed at nine drift stations of R/V *Kvant-1* in coastal zone of the Black Sea near Gelendjick (Table 23.1). The field studies included measurements of the spectral upwelling radiance and surface irradiance by the floating spectroradiometer and of vertical profiles of the beam attenuation coefficient by a submersible transmissometer as well as sampling and conservation of water samples for determination of chlorophyll concentration. Two of stations in Table 23.1 marked by asterisk were performed concurrently with SeaWiFS measurement at clear-sky conditions and can be included in the match-up data set; other stations will be used only for validation of the bio-optical algorithms.

The total number of stations with measurements of the spectral upwelling radiance and surface irradiance by the floating spectroradiometer and chlorophyll determinations in 1997-2000 is 36; twelve of them under clear-sky conditions can be included in SeaWiFS match-up data set, three of them in the match-up data set for MOS-IRS.

Numerical Simulation

Numerical simulation was performed for modeling the atmospheric correction and bio-optical algorithms, evaluation of their error in different situations, and elucidation of reasons for the occurrence of the errors. The new computer code has been devised. The atmosphere-ocean system is considered as a system of plane-parallel layers with the sea surface treated as a separate layer. The operators of transmittance and downward and upward reflectivities for the layers are linked between them by the recursion relations. The computer code executes an expansion of all the operators in a Fourier cosine

series over the azimuth angle, discretization over the zenith angle, solving the algebraic linear equations resulting from the above discretization, and computing radiances and irradiances. Solution of the problem for a single uniform layer can be found by using both the modified discrete ordinate (DISORT) and Monte Carlo techniques, and the solutions found by different techniques can be compared.

The following quantities were computed for SeaWiFS spectral bands at 412, 443, 490, 510, 555, 670, 765, and 865 nm and different solar and viewing zenith angles θ_0 and θ:

- upwelling radiances $L_t(\theta, \theta_0)$ at the top-of-the-atmosphere;
- contribution $L_R(\theta, \theta_0)$ arising from Rayleigh scattering;
- contribution $L_a(\theta, \theta_0)$ arising from aerosol scattering (including the interaction between Rayleigh and aerosol scattering);
- contribution $L_W(\theta, \theta_0)$ arising from backscattering out of the water;
- upwelling radiances $L_u(\theta, \theta_0, 0^-)$ and $L_u(\theta, \theta_0, 0^+)$ respectively just beneath and above the sea surface;
- upwelling irradiances $E_u(\theta_0, 0^-)$ just beneath the sea surface;
- downwelling irradiances $E_d(\theta_0, 0^-)$ and $E_d(\theta_0, 0^+)$ just beneath and above the sea surface.

The computations were made for two contrasting cases: the Philippine Sea with very clear water and the Barents Sea with high concentrations of yellow substance and suspended matter. The subsurface quantities were calculated with seawater optical characteristics either directly *in situ* measured in the Philippine Sea or retrieved from the spectral values of subsurface radiance reflectance in the Barents Sea; the flat sea surface and the three-layer atmosphere were asssumed (Kopelevich et al. 1998).

23.3 RESEARCH RESULTS

Validation of the Atmospheric Correction Algorithm.

The SeaWiFS atmospheric correction algorithm was validated by direct comparison of the $L_{WN}(\lambda_i)$ and $\tau_a(\lambda_i)$ values derived from SeaWiFS data and from *in situ* measurements. For the Black and Aegean Seas the agreement was quite satisfactory for the $L_{WN}(\lambda_i)$ and τ_a (Burenkov et al. 1999, Kopelevich 1999a). For the Barents Sea (Table 23.2) the SeaWiFS atmospheric correction algorithm resulted to negative *Lwn* values at 412 and 443 nm; it underestimated the *Lwn* values at 490 nm by 26-71%, and gave rather reasonable values of *Lwn* only at 510 and 555 nm. As for chlorophyll concentration, the SeaWiFS operational algorithm overestimated its values by the factor of 35-50 (Table 2); the most part of this error was due to the bio-optical algorithm which could overestimate chlorophyll concentration more than twenty times ((Burenkov et al. 2001, Kopelevich 1999b). The overcorrection of atmospheric effects for the Barents Sea can be explained by two reasons: first, the assumption of zero water-leaving radiance in the near-infrared (NIR) is not correct in turbid waters of the Barents Sea, and second, increasing error in atmospheric correction under condition of large solar zenith angle (about 60^o).

We found negative *Lwn412* values not only in the Barents Sea where they were quite common, but also in oligotrophic waters of the Eastern Mediterranean where the assumption of zero NIR water reflectance was valid (Kopelevich 1999b). Our analysis showed that results of the atmospheric correction depend on the scan angle. Comparison between the *Lwn* values derived at small (less than 20^o) and large (greater than 30^0) scan angles for different spectral bands in the Eastern Mediterranean showed that the spatially averaged *Lwn* values calculated at the small scan angle were higher than the ones at the large scan angle.

To check an error which can arise from anisotropy of angular distribution of the water-leaving radiance $L_u(\theta, 0^+)$, the results of our numerical simulation were used. Figure 23.1 shows examples of angular distributions of the upwelling radiances $L_u(\theta, 0^-)$ just beneath the sea surface (dashed lines) and $L_u(\theta, 0^+)$ just above the sea surface (solid lines) for five SeaWiFS spectral bands and the solar zenith angles θ_0=20^o and 40^o calculated for the Philippine Sea. It is seen that the angular distributions of $L_u(\theta, 0^-)$ have well-defined anisotropy whereas it is much less pronounced for the angular distributions of $L_u(\theta, 0^+)$. The reason of such correction of the angular distribution of the upwelling radiance by the sea surface is the angular dependence of the reflection coefficient which is increased with the viewing angle θ. The anisotropy grows with the solar zenith angle θ_0: the ratio of $L_u(60^o, 0^+)/L_u(0^o, 0^+)$ is equal to 1.02-1.08 for $\theta_0 = 20^o$ and 1.11-1.18 for $\theta_0 = 60^o$. The obtained results show that the anisotropy of angular distribution of the water-leaving radiance $L_u(\theta, 0^+)$ can not explain the observed errors in atmospheric correction; their reason is most likely to be a wrong choice of the aerosol optical model under observation at large scan angles.

The another manifestation of errors in atmospheric correction was a false mesoscale structure of the Lwn spatial distribution (Kopelevich 1999b). Our analysis showed that such structure was connected with inefficiency of elimination of cloud effects and could be resulted from scattering by edges of clouds or stray light within the SeaWiFS sensor or from high cirrus clouds.

Validation of the Bio-optical Algorithms

Most of our stations can be related to Case 2 waters, and the SeaWiFS operational algorithm overestimated chlorophyll concentration. It has been demonstrated that the ratio β between the absorption coefficients of yellow substance and phytoplankton pigments at 440 nm can be used as an indicator of validity of the SeaWiFS bio-optical algorithm (Burenkov et al. 1999, Kopelevich 1999b). This empirical algorithm is only

Figure 23.1. Angular distributions of water-leaving radiance just beneath (dashed line) and above (solid line) the sea surface: the left figures – solar zenith angle 20^0 , the right ones- 40^0.

Table 23.1. The information on the stations in the Black Sea, September 14-25, 2000.

Date	Station	Coordinates (degrees) at the measurement moments	Local time	Difference with GMT, h
09/14/00	1*	44.506 N, 37.837 E	13:50 – 14:20	+4
09/17/00	2	44.485 N, 37.932 E	13:10 – 13:40	+4
09/17/00	3	44.520 N, 37.963 E	15:00 – 15:30	+4
09/17/00	4	44.528 N, 37.973 E	16:10 – 16:30	+4
09/18/00	5	44.526 N, 37.994 E	11:40 – 12:05	+4
09/18/00	6	44.500 N, 37.975 E	12:30 – 13:00	+4
09/18/00	7*	44.462 N, 37.964 E	13:50 – 14:25	+4
09/23/00	8	44.491 N, 37.943 E	13:50 – 14:30	+4
09/25/00	9	44.485 N, 37.967 E	13:50 – 14:30	+4

Table 23.2 The values of the water-leaving radiances ($W \cdot m^{-2} \cdot \mu^{-1} \cdot sr^{-1}$), aerosol optical thickness τ_a^{865}, and chlorophyll concentration ($mg \cdot m^{-3}$) for two stations in the Barents Sea measured and derived from SeaWiFS data; Δ, % is the relative discrepancy between derived and measured data.

λ, nm	St.1112			St.1131		
	L_{WN} SeaWiFS	L_{WN} measured	Δ	L_{WN} SeaWiFS	L_{WN} measured	Δ
412	-0.66	0.088	-	-0.671	0.145	-
443	-0.226	0.18	-	-0.255	0.225	-
490	0.288	0.387	-26%	0.151	0.350	-71%
510	0.430	0.472	-9%	0.224	0.336	-33%
555	0.686	0.681	+0.8%	0.181	0.243	-25%
τ_a^{865}	0.050	0.045	+11%	0.065	0.055	+18%
• . . , $mg \cdot m^3$	20.7	0.42	+50 times	3.3	0.09	+35 times

Table 23.3. Comparison between chlorophyll-a concentrations ($mg \cdot m^{-3}$) measured and retrieved by SIO RAS and operational SeaWiFS algorithms at different stations in the Barents Sea. Δ, % is the relative error; β is the ratio between the absorption coefficients of yellow substance and phytoplankton pigments at 440 nm.

St.	Coordinates	Chl measured	Chl SIORAS	Δ SIORAS	Chl SeaWiFS	Δ SeaWiFS	β
1088	70.42 N, 47.58E	0.16	0.24	52	0.63	300	8.2
1090	70.18N, 52.42E	0.50	0.56	12	3.3	540	14.9
1095	68.97N, 58.47E	0.79	0.34	57	9.9	1200	20.9
1112	69.09N, 58.29E	0.42	0.46	9	9.5	2170	35.9
1123	69.50N, 57.25E	0.38	0.55	45	4.8	1160	22.9
1126	69.67N, 57.24E	0.18	0.114	37	2.7	1390	25.5
1131	69.77 N, 56.28 E	0.091	0.038	58	1.01	1010	14.7
1157	70.54N, 52.79E	0.25	0.14	43	1.09	340	8.7
1174	69.25N, 41.00E	1.39	0.92	34	1.0	28	1.6
1183	71.50N, 41.00E	0.38	0.38	0.5	0.81	113	3.2
1196	74.75N, 41.00E	0.13	0.14	8	0.28	115	4.1
1209	78.00 N, 41.00E	0.16	0.17	3	0.25	56	3.0
1281	76.00N, 42.27E	0.27	0.38	40	0.44	63	3.2

applicable to Case 1 waters and assumes an existence of definite relationship between the absorption by phytoplankton pigments and absorption by yellow sunstance. According to results of our analysis, the SeaWiFS algorithm overestimates chlorophyll concentration if the ratio β exceeds the critical value which is about 2. In the Black and Aegean Seas where the β values are 2.6-5.9 the SeaWiFS algorithm overestimates the chlorophyll concentration about twice. The refined results for the Barents Sea are presented in Table 23.3. As it is seen, in the Pechora Basin (St. 1090-1157), which is under strong influence of the Pechora river discharge, the β values are 8.7-35.9, and the SeaWiFS algorithm overestimates the chlorophyll concentration by a factor of 4.4-22.7.

The semianalytic algorithm based on an analytic formula for the water radiance reflectance and low-parametric models for seawater absorption and backscattering coefficients has been developed. As it is seen from Table 23.3, it provides a reasonable agreement between the calculated and measured chlorophyll concentration: relative errors are equal to 9-57% for stations in the Pechora Basin and 0.5-52% for other stations; for stations in the Black and Aegean Seas the errors were within 2-33% (Burenkov et al. 1999, Kopelevich 1999b).

The semianalytic algorithm allows to retrieve not only chlorophyll concentration but also the yellow substance absorption and particle backscattering coefficients under assumption that their spectral dependencies are known. In this case we have three unknowns a_g, b_{bp} and c_a and five equations (with SeaWiFS spectral bands 412, 443, 490, 510, and 555 nm) to find these unknowns. Our sensitivity studies have showed that a correct choice of the slope parameters S and n of spectral dependencies of the yellow substance absorption and particle backscattering coefficients (especially of the former) is of critical importance in the retrieval of a_g, b_{bp} and c_a. in the Barents Sea waters with high concentrations of yellow substance and suspended matter. A special procedure to assess regional S-values, using results of the field studies, has been developed, and the relationship between the S-parameter and the band ratio r (412)/r (490) has been found (Burenkov et al. 2001). The mean error in determining the S-parameter is equal to ~0.001 nm^{-1}; and our analysis showed that effect of this error on the error in chlorophyll concentration depends on the β-ratio between the absorption coefficients of yellow substance and phytoplankton pigments. The errors in chlorophyll concentration are within 18-40% if

$\beta < 5$, but the errors increase for higher values of β (Burenkov et al. 2001).

Our studies showed that the semianalytic algorithm can solve the problem of Case 2 waters but it places much more severe requirements to atmospheric correction than the SeaWiFS operational algorithm, and improvement of atmospheric correction for Case 2 waters is of paramount importance.

REFERENCES

Artemiev, V.A., Burenkov, V.I., Vortman, M.I., Grigoriev, A.V., Kopelevich, O.V., and Khrapko, A.N., 2000a: Sea-truth measurements of ocean color: a new floating spectroradiometer and its metrology. *Oceanology*, **40**, 139-145. Translated from *Okeanologiya*, 40, No.1, 2000, pp.148-155.

Artemiev, V.A., Burenkov, V.I., Woznyak, S.V., Grigoriev, A.V., Daretsky, M., Demidov, A., Kopelevich, O.V., Frantsuzov, O.N., and Khrapko, A.N., 2000b: Sea-truth measurements of ocean color: Field studies in the Black and Aegean Seas. *Oceanology*, **40**, 177-182. Translated from *Okeanologiya*, 40, No.2, 2000, pp.192-198.

Burenkov V.I., Kopelevich O.V., Sheberstov S.V., Ershova S.V., Evdoshenko M.A., 1999: Bio-optical characteristics retrieved from satellite ocean color data. *The Eastern Mediterranean as a Laboratory Basin for the Assessment of Contrasting Ecosystems.* P.Malanotte-Rizzoli and V.N.Eremeev (eds), Kluwer Academic Publishers, Netherlands. P. 313-326.

Burenkov V.I., Kopelevich O.V., Sheberstov S.V., and Vedernikov, V.I., 2000: Sea-truth measurements of ocean color: Validation of the SeaWiFS satellite scanner data. *Oceanology*, 40, 329-334. Translated from *Okeanologiya*, **40**, No.3, 2000, pp.357-362.

Burenkov, V.I., Vedernikov, V.I., Ershova, S.V., Kopelevich, O.V., and Sheberstov, S.V., 2001: Use of SeaWiFS data for assessment of bio-optical characteristics of the Barents Sea. *Oceanology* (in press).

Kopelevich, O.V., D.B. Rogozkin, and S.V. Sheberstov, 1998: Results of application of the new atmospheric correction method to the Pacific ocean color simulated data set. 1998. *Proceedings of PORSEC'98-Qingdao, July 28-31, Qingdao, China*, **1,** 54-58.

Kopelevich, O.V., 1999a: Validation of the water-leaving radiance data product. NASA/TM-1999-208645, 88-93.

Kopelevich, O.V., 1999b: Validation of the water-leaving radiance data product. NASA/TM-1999-209486, 121-126.

GLOSSARY

ACE	Aerosol Characterization Experiment
ADEOS	Advanced Earth Observation Satellite
AERONET	Aerosol Robotic Network
AM-1	Not a acronym, used to designate the morning platform of EOS
AOP	Apparent Optical Properties
AOT	Aerosol Optical Thickness
APV	Autonomous Profiling Vehicle
ARGOS	Not an acronym, but the name given to the data collection and location system on the NOAA Operational Satellites.
ASCII	American Standard Code for Information Interchange
AVHRR	Advanced Very High Resolution Radiometer
AVIRIS	Advanced Visible and Infrared Imaging Spectrometer
BATS	Bermuda Atlantic Time-series Study
BBOP	Bermuda Bio-Optics Profiler
BBSR	Bermuda Biological Station for Research
BNL	Brookhaven National Laboratory
BTM	Bermuda Test Mooring
Cal/Val	Calibration and Validation
CalCOFI	California Cooperative Oceanic Fisheries Investigation
CALVAL	Calibration Validation
CARICO	Carbon Retention in a Colored Ocean
Case-1	Water whose reflectance is determined by absorption.
Case-2	Water whose reflectance is significantly influenced by scattering.
CCD	Charge-Coupled Device
CDOM	Chromophoric Dissolved Organic Matter
CHN	Carbon, Hydrogen and Nitrogen
CHORS	Center for Hydro-Optics and Remote Sensing
CICESE	Centro de Investigation Cientifica y de Edcacion Superior de Ensenada
CIMEL	The name of a sun photometer manufacturer
CNES	Centre National d'Edudes Spatialle
CONICIT	Consejo Nacional de Investigaciones Cientifica y Technologicas (Venezuela)
CRAM	Conditional Relaxation Analysis Method
CTD	Conductivity-Temperature-Depth
CZCS	Coastal Zone Color Scanner
DAAC	Distributed Active Archive Center
DLR	Deutshe Forshungsanstalt f r Luft-und Raumfarhrt (German Aerospace Center)
DMF	Dimethylformamide
DOC	Dissolved Organic Carbon
DoD	Department of Defense
DOE	Department of Energy
ECOHAB	Ecology of Harmful Algal Blooms
EEZ	Exclusive Economic Zone
EORC	Earth Observation Research Center
EOS	Earth Observing System
FFP	Firm-Fixed Price
FOV	Field of View
ftp	File transfer protocol
FWHM	Full Width Half Maximum
GAC	Global Area Coverage, coarse resolution satellite data with a nominal ground resolution at nadir of approximately 4 Km
GB	Gigabyte, or about one billion bytes
GF/F	Not an acronym, but a specific type of glass fiber manufactured by Whatman.
GLI	Global Imager
GoCal	Gulf of California
GPS	Global Positioning System
GSFC	Goddard Space Flight Center
HIVE	High-Latitude Intercomparison and Validation Experiment
HOBI	Hydro-Optics, Biology and Instrumentation
HOT	Hawaii Ocean Time series
HPLC	High Performance Liquid Chromatography
HQ	Headquarters
HRPT	High Resolution Picture Transmission
ICESS	Institute for Computational Earth Science System
IDL	Interactive Data Language
INDOEX	Indian Ocean Experiment
IOCCG	International Ocean Color Coordinating Group
IOP	Inherent Optical Properties
IR	Infrared
IRS	Indian Remote Sensing Satellite
ISCCP	International Satellite Cloud Climatology Project
ISPO	Interim SIMBIOS Project Office
JGOFS	Joint Global Ocean Flux Study
JPL	Jet Propulsion Laboratory
LAC	Local Area Coverage, fine resolution satellite data with a nominal ground resolution at nadir of approximately 1Km
LIDAR	Light Detection and Ranging Instrument
LED	Light Emitting Dicode
LOA	Laboratorie d'Optique Atmospherique
MARMAP	Marine Resources Monitoring, Assessment and Prediction
MBARI	Monterey Bay Aquarium Research Institute
MB	Megabyte, or about one million bytes
MER	Multispectral Environmental Radiometer
MERIS	Medium Resolution Imaging Spectrometer
MFRSSR	Marine Fast Rotating Shadow-band Spectral Radiometer
MISR	Multi-angle Imaging SpectroRadiometer
MOBY	Marine Optical Buoy

MODAPS	Modular Ocean Data and Power System
MODIS	Moderate Resolution Imaging Spectroradiometer
MOS	Modular Optoelectronic Scanner
MSL12	Multi-Sensor level-1B to level-2 code
MTPE	Mission to Planet Earth
NASA	National Aeronautics and Space Administration
NASDA	National Space Development Agency of Japan
NAVOCEANO	Naval Oceanographic Office
NDBC	National Data Buoy Center
NIMBUS	Not an acronym, but a series of NASA experimental weather satellites containing a wide variety of atmosphere, ice, and ocean sensors.
NIST	National Institute of Standards and Technology
NOAA	National Oceanic and Atmospheric Administration
NODC	National Oceanographic Data Center
NOPP	NIMBUS Observation Processing System
NRA	NASA Research Announcement
NSF	National Science Foundation
NSPO	National Space Program Office
NTOU	National Taiwan Ocean University
OCI	Ocean Color Imager
OCTS	Ocean Color and Temperature Sensor
ONR	Office of Naval Research
ORCA	Optical Research Consortium of the Arctic
OSC	Orbital Sciences Corporation
OSU	Oregon State University
PAR	Photosynthetically Available Radiation
PHILLS	Hyperspectral Imager for Low Light Spectroscopy
PI	Principal Investigator
PM-1	Not a acronym, used to designate the afternoon platform of EOS
POLDER	Polarization Detecting Environmental Radiometer (France)
PRR	Profiling Reflectance Radiometer
R&D	Research and Development
R/V	Research Vessel
ROCSAT	Republic of China (Taiwan) Satellite platform for the OCI sensor.
RR	Round-Robin
SAB	South Atlantic Bight
SBE	Sea-Bird Electronics
SCOR	Scientific Committee on Oceanic Research
SDDC	Science Data Distribution Center
SeaOPS	SeaWiFS Optical Profiling System
SeaBAM	SeaWiFS Bio-optical Algorithms Mini-workshop
SeaBASS	SeaWiFS Bio-optical Archive and Storage System
SeaDAS	SeaWiFs Data Analysis System
SeaWiFS	Sea-viewing Wide Field-of-view Sensor
SIMBAD	The name of a sun photometer
SIMBIOS	Sensor Intercomparison and Merger for Biological and Interdisciplinary Oceanic Studies
SIO	Scripps Institution of Oceanography
SGI	Silicon Graphics, Inc.
SIRREX	SeaWiFS Intercalibration Round-Robin Experiment
SLOWDROP	Slow Descendent Rate Optical Profiler
SMSR	SeaWiFS Multispectral Surface Reference
SOOP	Ship of Opportunity Program
SOW	Statement of Work
SPMR	SeaWiFS Profiling Multi-channel Radiometer
SQM	SeaWiFS Quality Monitor
ST	Science Team
TB	Terabytes
TOA	Top of the Atmosphere
TOMS	Total Ozone Mapping Spectrometer
TOTO	Tongue of the Ocean
TSM	Total Suspended Matter
TSRB-II	Tethered Spectral Radiometer Buoy - II
XBT	Expendable Bathythermograph